Analysis of the role of VapBC-type toxin-antitoxin modules in growth, stress tolerance and drug tolerance in mycobacteria

Bintou Ahmadou Ahidjo

A thesis submitted to the Faculty of Science, University of the Witwatersrand, Johannesburg, in fulfillment of the requirements for the degree of Doctor of Philosophy.

January 2011.

"Somehow I can't believe that there are any heights that can't be scaled by a man who knows the secrets of making dreams come true. This special secret, it seems to me, can be summarized in four Cs. They are curiosity, confidence, courage, and constancy."

- Walt Disney -

Declaration

I declare that this thesis is my own unaided work. It is being submitted for the degree of Doctor of Philosophy at the University of the Witwatersrand, Johannesburg. It has not been submitted for any degree or examination at any other university.

A-Bintou

_____   _10th May 2011_____

Bintou Ahmadou Ahidjo   Date

Dedication

I dedicate this work to my parents **Awa Denise** and **Ahmadou Ahidjo Sali**,

and

Barack Hussein Obama. I may never meet this man, but his story is my story and the story of everyone who has a dream that does not seem achievable. He has inspired me beyond my wildest imagination and has shown me that if you put your mind to it you can and will achieve anything.

Abstract

Forty seven of the toxin-antitoxin modules in the genome of *Mycobacterium tuberculosis* belong to the VapBC family in which the VapC toxin is a member of the PIN-domain protein family associated with nuclease activity. The role of VapBCs in the physiology of *M. tuberculosis* and the cellular function(s) served by their expansion are unknown but is the subject of intense investigation as a result of the evidence suggesting an association between TA-module function and stress adaptation as well as phenotypic drug tolerance in certain organisms. In this study, the function of ten *vapBC* modules from *M. tuberculosis* and the single *vapBC* from *M. smegmatis* was investigated. Of the *vapC*s assessed, Rv0549c, Rv0595c, Rv2549c and Rv2829c were growth inhibitory when conditionally expressed under the control of a tetracycline (Tet)-regulated promoter in both *M. smegmatis* and *M. tuberculosis*, with Rv0549c being less toxic than the others. The toxicity of Rv2549c in *M. smegmatis* correlated with the level of protein expressed, suggesting that in order for toxicity to be observed, the VapC level must exceed a certain threshold. Low levels of protein expression were demonstrated for Rv2456 following induction, which may account for the lack of toxicity observed for this, and the remaining 'non-toxic' VapCs. In addition, given that Rv3320c was toxic in both *M. smegmatis* and *M. tuberculosis* only when expressed in the absence of the Tet repressor, protein expression levels, rather than differences in (nuclease) activity appeared to be the principal determinant of VapC toxicity in this assay system. VapC toxicity was neutralized by co-expression of the cognate *vapB* antitoxin from both an operon with the toxin, as well as from a different chromosomal locus. However, non-cognate antitoxins could not abrogate VapC toxicity, thus demonstrating a specificity of interaction between VapCs and their cognate VapBs. Deletion of selected *vapBC* genes did not affect mycobacterial growth *in vitro* or mycobacterial stress adaptation, but rendered it more susceptible to growth inhibition following toxic VapC expression. However, toxicity of 'non-toxic' VapCs was not increased in deletion mutant strains, even when the mutation eliminated the cognate VapB, presumably due to insufficient levels of VapC expression in this genetic background. Interestingly, low levels of VapC appeared

to result in increased ofloxacin tolerance, thus making it likely that lower levels of VapCs that are induced as a result of stochastic and/or environmentally-induced *vapBC* expression might have a significant effect on the physiology of mycobacteria. The above-mentioned findings suggest that the *vapBC* family may provide an abundant source of nuclease activity in *M. tuberculosis*, which can vary as a function of regulated expression of individual modules, and the rates/mechanisms of antitoxin degradation. Such activity is likely to have a profound impact on the physiology of *M. tuberculosis*.

Acknowledgements

I would like to thank my supervisor **Professor Valerie Mizrahi** who took a chance on me. Val, more than the science you taught me, your passion and dedication has been really inspiring. The skills you have instilled in me can and will only make me a better scientist. I am eternally grateful to you for having shown me that I can remain true to myself even as I pursue my dreams. You remain a great inspiration and role model.

From my co-supervisor **Dr Bhavna Gordhan**, I have learnt to balance both my personal and professional lives. Bhav, you have been an absolutely extraordinary teacher and mentor. It is largely because of you that I did not quit and that I still remain in love with science. I will never be able to thank you enough. Knowing you has most certainly shaped me into a better person.

There is a Nigerian proverb that says "it takes a village to raise a child". As such I would also like to acknowledge:

Garth Abrahams who's ability to turn a mountain into a molehill has literally been life-saving. I would not have been able to do it without you. **Diane Kuhnert**, who started the TA project in the lab; **Edith Machowski** who generated the flag-tagged constructs; **Bavesh Kana** my dear friend, master of RT-PCRs and emperor of Rpfs; and **Digby Warner**, all of whose discussions, advice and assistance have been invaluable; to my Nandos and Seattle hot chocolate buddies: **Atica Moosa** and **Monique Williams**, it is true that there is nothing good friends and food won't fix! Finally, to all the members of the MMRU (past and present) for your never-ending support – Thank you.

I would like to thank **Drs Sabine Ehrt** and **Dirk Schnappinger** (Weil Cornell Medical College, NY, USA) for providing pSE100, pMC1s and pMC2m; **Professor Gregory Cook** (University of Otago, New Zealand) for providing a

Publications from this thesis

Bintou Ahmadou Ahidjo, Diane Kuhnert, Edith E. Machowski, Bhavna G. Gordhan, Garth L. Abrahams and Valerie Mizrahi. Nuclease-Like VapC toxins from *Mycobacterium tuberculosis* differentially inhibit mycobacterial growth and are specifically neutralized by their cognate VapB antitoxins. Submitted.

Table of Contents

List of Figures

List of Tables

1. Introduction

1.1 Tuberculosis, chemotherapy and drug-resistance

Mycobacterium tuberculosis causes one of the most debilitating human diseases, tuberculosis (TB). This contagious and air-borne bacillus infects over 2 billion people worldwide. In 2008 alone, 9.4 million new cases were reported and 1.8 million people died from TB (302). While it remains true that these recent statistics indicate a drop in the global incidence rate from 143 cases per 100,000 in 2004 to 139 per 100,000 in 2008, the advent of the Human Immunodeficiency Virus (HIV) and poor socio-economic conditions in developing countries, which incidentally have the highest TB incidence and mortality rates, continue to make this disease a global health crisis (302).

This pandemic is particularly daunting when one considers that TB is a curable disease. In the late 1990's, the World Health Organization (WHO) introduced the DOTS (Directly Observed Therapy - Short Course) program which has been implemented worldwide (302). This strategy recommends combination therapy consisting of an intense 2 month treatment phase with the first-line drugs isoniazid, rifampicin, ethambutol and pyrazinamide; followed by a 4 month continuation phase of isoniazid and rifampicin (302). This intense chemotherapy often leads to patient non-compliance, which can result in the emergence and spread of strains of *M. tuberculosis* that are resistant to first-line drugs, thus the development of multidrug-resistant tuberculosis (MDR-TB), a form of TB that is resistant to the two most powerful anti-TB drugs isoniazid and rifampicin (68). MDR-TB is treatable using the second-line drugs pyrazinamide, ethionamide, cycloserine, any of the injectables (kanamycin, amikacin or capreomycin) and one of the fluoroquinolones (ciprofloxacin and ofloxacin) (302). This treatment is however expensive, can last for up to two years and can be quite toxic to patients (68).

In 2006, the Centres for Disease Control and Prevention (CDC) together with the WHO, genotyped *M. tuberculosis* strains collected in the years 2000 - 2004 from an international network of TB laboratories worldwide (6). Of the

drug-resistant strains, 2% of isolates, which they referred to as extensively drug resistant (XDR), were found to be resistant to at least three classes of second line drugs used in the 4-18 month continuation phase of TB treatment (6). With the paucity of information from Africa, and the lack of availability of HIV co-infection data, Gandhi and colleagues embarked on surveillance of *M. tuberculosis* isolates obtained from patients in a provincial district hospital of Msinga, a rural sub-district of KwaZulu Natal (South Africa), where approximately 40% of patients are infected with HIV. Of the 475 culture-positive TB patients tested, 53 were diagnosed as having XDR-TB, and of these, 44 patients were also seropositive for HIV. Alarmingly, within 16 days of diagnosis, 52 of the 53 XDR-TB patients had died (67). This was an immediate cause for concern. As a result, two other South African researchers set out to determine the evolution of the XDR F15/LAM4/KZN *M. tuberculosis* strain associated with this outbreak (225). Their analysis revealed that the first XDR strain of *M. tuberculosis* actually appeared in South Africa in 2001. This prompted them to hypothesize that the introduction of DOTS without performance of antibiotic susceptibility testing or drug resistance surveillance, may have played a major role in the evolution and transmissibility of the F15/LAM4/KZN *M. tuberculosis* strain, since patients with MDR-TB were still treated with the prescribed standard first line drug-regimen and so, only one or two drugs were successfully acting against the infecting bacteria (225). This was subsequently addressed by Calver and colleagues who documented a step-wise acquisition of drug-resistance as well as re-infection of patients with an MDR strain of *M. tuberculosis* despite strict adherence to the DOTS program (30). More recently, findings by Cohen and colleagues from autopsies of patients who died at the public Edendale Hospital in KwaZulu Natal (South Africa), indicate that not only did late diagnosis of TB lead to demise of the patients, but 16% of patients on TB treatment for the first time were harbouring MDR strains of *M. tuberculosis*, thereby confirming that first-time infections can be caused by drug-resistant strains circulating within a community (45).

As Charles Darwin would have predicted, it was only a matter of time before a strain of *M. tuberculosis* resistant to all second-line drugs emerged. In

2009, the first report of totally drug-resistant (TDR) strains came out of Iran (288). With most of these drug-resistant strains genotyped as members of the Beijing, Haarlem and EAI super families (288), the TB epidemic has become even more alarming given that members of the Beijing super-family have been associated with increased ability to cause and spread disease, drug resistance as well as co-infection with HIV (35, 64, 114, 133).

Drug-resistant strains of *M. tuberculosis* have been shown to arise as a result of sequential accumulation of chromosomal mutations (231), with rifampicin and isoniazid resistance being associated with a conditional cost of fitness dependent on the nature of the drug-resistance-conferring mutations, as well as the *M. tuberculosis* strain family (20, 85, 86, 180). While data are not yet available with regards to fitness cost and transmissibility of TDR strains of *M. tuberculosis*, whole-genome sequencing of MDR and XDR strains obtained from HIV-positive patients in KwaZulu Natal (South Africa), at the Broad Institute (Cambridge, Massachusetts, USA), revealed 22 novel mutations unique to the drug-resistant strains. Analysis of the 12 mutations not present in highly-repetitive genome regions, revealed that these mutations were specific to the KZN strains and did not confer any fitness advantage to the strain (191). Despite this finding, the emergence of drug-resistant *M. tuberculosis* strains remains extremely worrisome, not only because *M. tuberculosis* strains associated with high-fitness costs do cause disease in HIV-positive patients, but also because TB disease phenotype has been linked significantly to both *M. tuberculosis* and human genotypes (13, 30, 34, 75, 88, 191, 200, 288).

1.2 *Mycobacterium tuberculosis* – a pathogen's success story

One of the key attributes of a successful persistent pathogen is the ability to survive within an infecting host over long periods of time, whilst still retaining the ability to cause disease. Pathogens such as *Salmonella enterica* serovar Typhi, successfully persist in their human hosts by secreting effectors that control and diminish the response of the host's immune system during infection and also allow for subsequent colonization of the gallbladder – an organ not monitored by the immune system, which then serves as a reservoir of viable bacteria (274).

M. tuberculosis, on the other hand, thwarts the host immune response by forming a niche within the immune system where it uses specific mechanisms to counteract the stresses imposed by the host (274). Briefly, upon inhalation of *M. tuberculosis*, the aerosolized bacteria are phagocytosed by the host's alveolar macrophages. Within this primary site of infection known as the Ghon focus, the non-activated immature macrophages allow mycobacterial replication. These actively replicating bacteria recruit mobile monocyte-derived macrophages and other immune cells, forming lesions known as granulomas. These granulomas are then surrounded by lymphocytes, and eventually become calcified to form the Ghon complex. Whilst the Ghon complex can undergo caseous necrosis resulting in dissemination of tubercle bacilli into the lungs to cause acute *M. tuberculosis* infection, the bacilli within the granulomas of old pulmonary tissues and the Ghon complex establish an equilibrium with the host immune system to create a reservoir of viable bacteria, thereby allowing the bacilli to persist in the human host for decades in a state of latent infection. It is important to note that this chronic stage of infection, known as latent TB infection (LTBI), is characterised not only by low bacterial counts but it is also devoid of clinical symptoms (23, 48, 218, 274, 291, 298).

Whilst factors such as mycobacterial and human phenotypes, smoking, diabetes, malnutrition and residence in high-density locations increase the risk of TB infection, HIV co-infection has been the greatest risk factor for the progression of the TB epidemic, despite the introduction of highly active antiretroviral therapy (HAART) (67). One of the reasons for this is the immune reconstitution inflammatory syndrome (IRIS). This is a clinical deterioration of HAART-treated patients, despite satisfactory control of viral replication and improvements in the CD_4+ lymphocyte counts, which leads to inflammatory responses towards previously diagnosed or persisting pathogens (255). In the case of *M. tuberculosis*, TB-IRIS may present either paradoxically - where patients receiving and responding to TB treatment prior to initiation of antiretroviral therapy (ART) succumb to worsening TB symptoms once on HIV treatment; or as ART-associated TB - where patients neither diagnosed nor treated for TB prior to initiation of ART develop TB (185). This TB/HIV co-infection continues to be a

4

huge cause of concern, since one third of the world's population is estimated to be infected with *M. tuberculosis* and the HIV-positive population which reached 33.4 million in December 2008 - 20% more than reported in 2000 (93, 269, 279), is continuing to rise, and has thus increased the pool of possible TB cases worldwide.

It has been widely accepted, albeit not proven, that during the LTBI, the bacilli are dormant *i.e.* the bacteria are viable but have decreased metabolic activity and are not undergoing replication. *M. tuberculosis* possesses many mechanisms, including mycobacterial cell wall modifications, the ability to change its metabolism to survive on different carbon sources, DNA maintenance and repair, induction of the intrinsic apoptotic pathway of macrophages, as well as upregulation of genes involved in stress-regulation, which allow it to persist within the human host (36, 51, 71, 125, 188, 189, 218, 241, 252, 267, 297, 299). This successful intracellular persistent pathogen also retains its ability to cause post-primary or reactivation of disease, despite the stresses imposed by innate and adaptive host immune responses, and the hostile environments encountered by the bacilli within granulomas - where factors such as nutrient and oxygen starvation limit growth (18, 36, 53, 71, 136, 284, 290, 292, 297, 298).

While it has been conjectured that the bacilli are dormant during LTBI, recent findings that *M. tuberculosis* replicates throughout chronic infection in mice (99), and the wide range of pathologies associated with latent infection in humans, have shed further light on the phenomenon of mycobacterial "dormancy" during LTBI. It has been postulated that instead of presenting as either active disease where the bacilli are replicating, or latent disease where the bacilli are dormant, *M. tuberculosis* infection actually occurs as a continuous spectrum based on elicited host immune responses (16). In this model, the bacilli reside within different microenvironments within the host tissue, and it is the nature of these microenvironments that dictate whether the bacilli replicate, remain dormant, reactivate, or whether they are eradicated by the host (16). Hence, insight into the heterogeneous population of bacilli in the various lesions of the human host would be extremely valuable towards winning the war against TB.

1.3 *Mycobacterium tuberculosis* – winning the war

As part of a global effort to eradicate TB, the WHO has implemented a program known as the "Global Plan to Stop TB 2006-2015" (7), which aims at reducing the 1990 prevalence of TB by 50% by the year 2015 and the eventual eradication of the disease by 2050 (303). This multifaceted program entails i) expanding and improving the DOTS program, so that supervised standardised treatment and effective drug management is implemented; ii) increasing TB/HIV collaborations, preventing and managing drug resistant *M. tuberculosis* strains and addressing the poor socio-economic conditions of the most vulnerable populations; iii) strengthening the primary health care sector; iv) engaging all communities (TB patients, care providers as well as the affected communities) to endorse the implementation and adherence of International Standards of Tuberculosis Care (ISTC); and v) promoting the development of novel and more effective TB diagnostic tools as well as therapies (303).

In line with this, Salomon and colleagues, using a mathematical model, predicted that while the DOTS program would greatly reduce the incidence, prevalence and mortality of TB, implementation of shorter drug regimens would increase this decline in incidence and mortality by 2 - 3 fold (244). With no new antibiotics introduced for the treatment of TB since the discovery of rifampicin in 1967, a number of drug development programs have recently been implemented for the identification and characterization of novel drug targets against *M. tuberculosis* (240). From these initiatives, six new lead compounds with novel modes of action have been discovered in recent years, and four previously existing drugs are being redeveloped to be more efficacious against *M. tuberculosis* (171).

1.3.1 Drugs repurposed for use in TB

The four previously existing drugs being repurposed for TB treatment belong to three classes of antimicrobial agents. Rifapentine, a bacterial RNA polymerase inhibitor, which is more effective than rifampicin *in vitro* and has a longer serum half-life, would be an ideal replacement candidate for the latter. This drug is currently in Phase II clinical trials to assess if it could be given once or

twice weekly as a replacement for the daily intake of the first-line antibiotic rifampicin (171, 242).

The second drug, linezolid, is a member of the oxazolidinones. These compounds bind to the 50S ribosomal subunit inhibiting the subsequent formation of the 70S ribosome, thereby effectively inhibiting protein synthesis (15, 171). Although linezolid, which is currently in phase II clinical trials, is associated with high toxicity levels, this drug has been successfully used off-label for the treatment of MDR- and XDR-TB (15, 171, 242).

Gatifloxacin and moxifloxacin, which are members of the fluoroquinolone family of drugs - and thus target the bacterial DNA gyrase, have proven to be more effective than the current second-line drugs ofloxacin and ciprofloxacin in the treatment of TB. Currently, phase III clinical trials are underway to ascertain whether these drugs can be used to shorten first-line therapy to 4 months by replacement of ethambutol or isoniazid (171, 242).

1.3.2 Drugs developed specifically for TB

Six new compounds, specifically identified for TB treatment, are currently being characterised. Three of these are are currently in Phase I clinical trials. The first, PNU-100480 is an oxazolidinone that exhibits greater activity than linezolid against *M. tuberculosis* in a murine model (171, 242); the second drug AZD-5847, also an oxazolidinone compound, is active against drug-resistant forms of *M. tuberculosis* (171); and SQ-109 on the other hand, is an ethylenediamine with an unknown target(s) that interacts synergistically with isoniazid and rifampicin against *M. tuberculosis* in a murine model (15, 171, 242).

The new drugs developed specifically for TB that are currently in Phase II trials are TMC-207, OPC-67683 and PA-824. TMC-207, a member of the diarylquinoline class of compounds, is an ATP synthase inhibitor that has shown great efficacy against susceptible and resistant *M. tuberculosis* strains both *in vitro* and *in vivo* (15, 171, 242). PA-824 and OPC-67683, on the other hand, belong to the nitroimidazole class of antibiotics. These compounds have been shown to exhibit high potency against replicating and dormant bacilli through generation of

reactive chemical species upon bioreduction of their nitroimidazole pharmacophore. PA-824 has been demonstrated to kill drug-resistant *M. tuberculosis*, as well as dormant bacilli under hypoxic conditions, and OPC-67683 is highly efficacious against susceptible and resistant *M. tuberculosis* strains *in vitro* and *in vivo* (15, 171, 242).

It is remarkable that TMC-207, moxifloxacin and the nitroimidazoles, which target replicating and non-replicating bacilli, have also enabled the development of various models for testing the efficacy of new TB drugs under stressful conditions encountered within the host *e.g.* under conditions of hypoxia in the presence and absence of reactive nitrogen intermediates, (15, 128, 171, 242, 243). Despite the lack of experimental evidence, it is widely assumed that these non-replicating bacilli are responsible for the long duration of TB treatment, and relapse after successful chemotherapy. Since one of the primary goals of improved TB treatment is the implementation of shorter drug regimens (244), these models will be greatly beneficial in identifying non-replicating bacilli which arise from treatment of *M. tuberculosis* with new drug candidates and/or regimens. Insight into these recalcitrant *M. tuberculosis* populations is of extreme importance, since elucidation of genes involved in this phenomenon as well as their molecular mechanisms of action, would allow for more efficacious TB treatment.

1.4 Role of biofilms in infectious diseases

Biofilms, which are structured layers or matrices of microbial communities that adhere to either biological or non-biological surfaces, are responsible for many chronic human infections such as cystic fibrosis, and catheter related infections (109, 165). These biofilm matrices, caused either by bacteria, fungi, mixed species or mixed genera populations, are particularly noteworthy as organisms in this niche have the ability to avoid elimination by antimicrobial agents as well as the host immune system (109, 110). It has been postulated that biofilms are recalcitrant to elimination from a host for three main reasons. Firstly, the biofilm matrix provides a barrier that protects the communities within it from attack by large antimicrobial compounds, thus diluting the latter to sub-lethal concentrations which have no effect on the cells within the matrix (109, 110, 165).

Secondly, the different gradients within the biofilm create acidic, anoxic and nutrient depleted zones resulting in starved dormant cells. As such, antimicrobials that target rapidly replicating organisms e.g. β-lactams which act against gram-positive bacteria, are no longer functional (109, 110, 165). The third reason biofilms are refractory to elimination is the presence of cells within the microbial community known as persisters. It has been suggested that although antimicrobial agents and the host immune system do eventually eliminate most of the microbial cells within the biofilm, they do not eradicate the dormant multidrug tolerant cells known as persisters, which are described in detail in Section 1.5 (165). As a result, once treatment is halted and levels of antimicrobial agents diminish, these persisters resume active replication and re-colonize the biofilm thus causing infection relapse (109, 110, 165).

In 2007, *M. tuberculosis* bacilli present as clusters within the distinct acellular rim of primary granulomas, were hypothesized to be part of a biofilm (163). While biofilm formation had been documented in the saprophytic *M. smegmatis* (182, 205, 232) and the pathogenic *M. avium* (33, 182) relatives of *M. tuberculosis*, it was only in 2008 that *M. tuberculosis* was actually shown to have the ability to form biofilms *in vitro* (206). The emergence of a *M. tuberculosis* biofilm is stimulated by environments rich in carbon dioxide with low oxygen tensions and the presence of zinc and iron. Secretion of free mycolic acids as well as the presence of glycopeptidolipids in mycobacteria is also imperative in the formation of these highly structured matrices (33, 182, 205, 207, 232). *M. tuberculosis* biofilms, which are made of bacteria physiologically different from actively replicating bacilli in culture, have been shown to harbor persister cells that are intractable to elimination by isoniazid and rifampicin (206). This, coupled with the fact that persisters have been implicated in the ability of *M. tuberculosis* to evade elimination by the new antitubercular drugs moxifloxacin and PA-824 (162, 203, 278), makes the knowledge of these dormant multidrug tolerant cells crucial in the fight against TB. So, what exactly are persisters and how are they formed within a population?

1.5 Persistence – an epigenetic phenomenon

Nearly seven decades ago, Joseph Bigger first reported the observation that the bactericidal antibiotics do not completely eradicate bacteria within a culture (19). He demonstrated that despite lysis of *Staphylococcus pyogenes* by penicillin, the surviving bacterial sub-population was not penicillin-resistant. Interestingly these survivors were revealed to be penicillin-tolerant rather than penicillin-resistant, since subsequent addition of penicillin resulted in cell lysis (19). This phenomenon, which occurs due to the fact that over time the rate of killing by antibiotics declines thereby allowing a population of bacteria to survive, is an epigenetic one referred to as persistence (164). The explanation put forward for this phenomenon of non-inherited antibiotic resistance is that the surviving bacterial sub-population of approximately 1×10^{-6} of the original population of bacteria is not undergoing active replication during exposure to the antibiotic (56, 157, 164).

A number of biological mechanisms have been demonstrated to account for the cessation of replication. In the 'deterministic' or environmentally controlled mechanism of persister formation, bacteria cease to replicate when they encounter one or more conditions/ environments, such as hypoxia, nutrient depletion, genotoxic stress, and/or antibiotic exposure, that can trigger growth arrest. A classic example of a deterministic mechanism of persistence is the halt in replication upon over-expression of DpiA (187). This effector of the DpiBA two-component signal transduction system, which regulates transcription as well as DNA replication and segregation, interrupts DNA replication and induces the SOS response - a DNA repair system that enables the bypass of errors during DNA replication - resulting in inhibition of *Escherichia coli* cell division. To further corroborate this finding, inactivation of penicillin binding protein 3 by β-lactam antibiotics was demonstrated to increase expression of the *dpiBA* operon, which in turn initiates the *E. coli* SOS response thereby stopping bacterial cell division (187).

In the alternate, 'stochastic' mechanism of persistence, persistence is not as a result of arrest in replication due to a physiological response to a stress

condition, but is rather a reflection of heterogeneous bacterial populations which have yet to begin replication (12). Forty years after Bigger's discovery, Harry Moyed - as part of an attempt to understand the persistence phenomenon, identified a *hipA7* mutant allele of the *hipA* gene that conferred increased levels of persisters, up to 1000-fold more than wild-type *E. coli*, upon treatment with ampicillin (193). Using direct observations and optical microscopy of single *E. coli* cells harboring this *hipA7* mutant allele, Balaban and colleagues discovered the existence of two types of persisters: type I and type II (12). Type I persisters were initially believed to consist of a pre-existing population of non-replicating cells generated in response to a trigger during stationary phase. These persisters exhibit an extended lag phase upon inoculation into fresh media from stationary phase, as well as a slight spontaneous switching rate from normal to persister cells in exponential phase (12). Type II persisters on the other hand consist of slow growing bacterial cells that do not originate from passage through stationary phase, but are continuously generated during growth of the culture. Unlike type I persisters whose cell numbers are directly proportional to the size of the inoculum from stationary phase cells, the number of type II persister cells is determined by the total number of cells in the culture (12).

1.5.1 Physiology of bacterial persisters

In an attempt to understand the physiology of bacterial persisters, Shah and colleagues undertook the task to isolate these cells (254). They hypothesized that because persister cells are not undergoing active replication, these could be isolated from the general cell population based on their low translation levels. Using an *E. coli* strain expressing degradable green fluorescent protein (GFP) under the control a ribosomal promoter, the authors could successfully separate dim persister cells from the bright green growing population of the culture using fluorescent activated cell sorting (FACS), since expression of GFP could only occur during cell growth. They demonstrated that the gene expression profile of these persisters was vastly different from cells obtained during exponential and stationary phases of growth. In addition, possibly because of this difference, the

persisters were more tolerant, by 20-fold, to ofloxacin, an antibiotic known to kill both replicating and non-replicating cells (254).

Two years later, Gefen and colleagues studied single cell induction dynamics of *E. coli* persisters using microfluidic devices and detection by fluorescence (94). They observed that while persisters are physiologically different from the replicating cells in a population, protein production within persisters was surprisingly similar to replicating cells, albeit for a short period of time, with persisters fully forming only subsequent to this window period. This demonstrated that type I persisters are not formed during stationary phase as was initially believed (12), but rather form upon exit from stationary phase. As expected, fully formed persisters were tolerant to antibiotics and treatment of bacteria with antibiotics during the short period prior to persister formation drastically reduced the number of persisters in the culture. This suggested that treatment of bacteria with antibiotics during the period where persisters are similar to replicating cells might prevent formation of these persister cells (94).

Irrespective of the mechanism of persister formation however, the general accord until now has been that these cells, rather than occurring as a consequence of exposure to antibiotics, constitute a small slow-growing or dormant sub-population of cells (166). However, data from a recent study, suggests that the frequency of persisters in a given culture is not fixed at any given point in time, but varies depending on several factors including growth conditions (132). Using flow cytometry, Joers and colleagues observed different resuscitation kinetics when an equal number of *E. coli* cells from an identical stationary-phase culture was inoculated into different culture media (132). In addition, the variation in the kill kinetics of the bacteria in the different growth media upon treatment with antibiotics was attributable to the heterogeneous resuscitation kinetics of the population of cells (132).

More recently, the SOS response, which is activated when double-strand DNA breaks occur within a cell, has been implicated in the formation of persisters of *E. coli* upon treatment with the antibiotic ciprofloxacin (59). Dorr and colleagues determined that not only is persister formation within a population

dependent on the level of SOS induction, but the persister fraction formed upon treatment with ciprofloxacin is dependent on the antibiotic concentration as well as functional SOS response and double-strand DNA break pathways. However, the observation that mutants unable to produce ciprofloxacin-induced persisters, still generated persisters upon treatment with ampicillin and streptomycin, suggests that different persisters are formed in response to different antibiotics and that the stochastic mechanism of persistence is also responsible for the formation of persisters (59).

This adds on to previous observations (94, 132, 254), suggesting that while the physiology of persisters is markedly different to replicating cells, the frequency of persisters in any given population is dependent on the window period within which persisters are formed, and this, in turn, is dependent on factors such as growth media and antibiotic treatment. These findings raise the possibility that persisters may have very distinct physiologies depending on how and when they are formed, thus raising the likelihood that not all persisters are physiologically identical.

1.5.2 Molecular mechanisms of persister formation

The first attempt to elucidate the molecular mechanisms of persister formation was by Harris Moyed and Kevin Bertrand in 1983. In order to do this, they treated different mutagenized *E. coli* K-12 strains with ampicillin and isolated 10% of surviving populations as *E. coli* mutants with high persistence frequencies *i.e.* Hip mutants. After eliminating ampicillin-resistant mutants and mutants exhibiting either slow growth rates or no growth, four mutants were isolated: two from an *E. coli dapA* strain and two from a marked *E. coli* F⁻ strain. The two mutants HM7 and HM9 from the *E. coli* F⁻ strain were further characterized revealing mutations, *hipA7* and *hipA9* respectively, located within the *hipA* gene. This was the first demonstration of a genetic link to the high persistence frequency of approximately 1% of *E. coli* to ampicillin (193). Moyed and colleagues also convincingly demonstrated that a *hipA7* persister phenotype

was able to prevent cell death arising from stresses other than the inhibition of peptidoglycan synthesis by ampicillin (193, 251).

The *hipA* gene, a member of the *hipAB* toxin-antitoxin family [discussed in detail in Section 1.6], was observed to confer toxicity to *E. coli* (154, 155, 194). Korch and colleagues established that two mutations, G22S and D291A, which render *hipA7* non-toxic, are essential for the *hipA7* persistence phenotype (154). In addition, their findings that *relA* - a gene that synthesizes the stringent response regulator guanosine 3'-5'-bispyrophosphate (ppGpp), is required for the high persistence *hipA7* phenotype, has led to the hypothesis that expression of *hipA7* results in increased levels of ppGpp, which in turn allows the bacteria to cease replication and become antibiotic tolerant (154).

Besides *hipA*, members of a number of other toxin-antitoxin (TA) families have also been implicated in persister formation. Keren and colleagues observed that over-expression of RelE, a toxin of the *relBE* TA family that causes translation inhibition, also resulted in increased persister formation by up to 10,000 fold upon treatment with cefotaxime, tobramycin and ofloxacin (142). MazF, a member of the *mazEF* TA family also increased persisters upon treatment with kanamycin and gentamicin by up to 81-fold (113). In addition, whilst deletion of an SOS-inducible TA module (*tisAB/itsR*) decreased the number of persisters in an *E. coli* population by up to 100-fold upon treatment with ciprofloxacin, over-expression of the TisB toxin resulted in 100-fold more persisters in the presence of ciprofloxacin (60).

Given the evidence implicating TA modules in the formation of multidrug-tolerant persisters, Vazquez-Laslop and colleagues decided to establish whether only members of these families play a role in persister formation (286). They over-expressed HipA and MazF together with two unrelated proteins DnaJ, a molecular chaperone, and the *Salmonella enterica* PmrC. As a negative control, they included a component of homoserine kinase - ThrB. After protein induction of 1 - 2h, the cultures were treated with ampicillin (100µg/ml) and ciprofloxacin (0.4µg/ml) for 4h. At these antibiotic concentrations and for the time period exposed, resistant mutants are not formed hence ensuring that only normal cells

but not persister cells would be lysed. As expected, ThrB had no effect on persister formation and both HipA and MazF over-expression resulted in increased persister formation up to 10,000 fold. Interestingly, DnaJ as well as PmrC also resulted in increased levels of persisters although only up to 1000-fold (286).

In subsequent studies, over-expression of genes such as the 5-formyl-THF cyclo-ligase *yfgA*, the flavin mononucleotide phosphatase *yigB*, was also observed to yield a $\geq$ 0.5-$\log_{10}$ increase in persisters of an *E. coli* population in the presence of antibiotics such as ofloxacin (115). In addition, the alternate sigma factor *rpoS* has also been implicated in antibiotic tolerance of *Pseudomonas aeruginosa* during the stationary growth phase (197). All these observations clearly indicate that genes other than those of toxin-antitoxin families play a role in persister formation. As a result, bacterial molecular genetic tools such as transposon mutants and over-expression libraries were used to search for persistence genes.

1.5.2.1 Identification of molecular mechanisms of persister formation by use of transposon mutant libraries

In 2005, Hu and Coates screened 5000 *E. coli* transposon mutants for the reduced ability to grow on a lethal dose of kanamycin (100µg/ml) during the late stationary phase of growth. Of the nine kanamycin-sensitive mutants isolated, the KS639 mutant was analyzed in depth. This isolate, which was the most kanamycin-sensitive mutant with a 2-$\log_{10}$ more reduction in viability compared to the other mutants, was also highly sensitive to the antibiotics rifampicin, gentamicin and ciprofloxacin. The mutation of this strain mapped to the intragenic region between *aldB* - a gene involved in small carbon compound degradation, and *yiaW* - a gene of unknown function. Whilst deletion of *aldB* and *yiaW* had no effect on the number of persisters obtained after kanamycin treatment, deletion of their intragenic region resulted in a >1-$\log_{10}$ decrease in the viability of *E. coli* upon treatment with kanamycin both *in vitro* and *in vivo* (126).

Another *E. coli* transposon mutant library of over 11,000 clones was then used to identify genes implicated in the formation of ampicillin-tolerant persisters

(168). Li and Zhang screened for transposon mutants susceptible to 100µg/ml ampicillin. Of the susceptible mutants isolated, the JHU-313 mutant, which had an insertion within the *phoU* gene - a phosphate metabolism negative regulator, was further characterized. Besides being susceptible to ampicillin, the JHU-313 mutant was also ≥ 2-fold more susceptible to the antibiotics norfloxacin, tetracycline, trimethoprim and gentamicin. In addition, stresses such as starvation, oxidative and heat stresses as well as exposure to weak acids, energy metabolism inhibitors and acidic pH, resulted in decreased cell viability of this mutant. Whilst *phoU* is part of the PhoR-PhoB two-component signal transduction system that regulates gene expression during phosphate-limiting conditions, this gene was the only *bona fide* persister gene of the PhoR-PhoB two-component system, since none of the other members of the PhoR-PhoB affected the ability of *E. coli* to form persisters (168).

Although persister genes were identified by Hu & Coates (126) and Li & Zhang (168), the fact that both of these transposon mutant libraries were generated by random insertion mutagenesis prompted Hansen and colleagues to search for persistence genes using a more organized approach. As such, they generated a transposon mutant library of the already developed ordered *E. coli* Keio collection of 3985 strains, by removing the kanamycin resistance marker cassette to generate in frame single deletion mutants. The mutant library was then grown to stationary phase in the presence of 5µg/ml ofloxacin for 6h, since this antibiotic concentration allowed for survival of persister cells without generation of resistant mutants within the specified time-frame. The survivors were plated on 4µg/ml of the β-lactam amdinocillin in the presence of $MgSO_4$ to prevent ofloxacin carryover, as Mg^{2+} ions halt ofloxacin penetration. Although resistant mutants do emerge at this amdinocillin concentration, the frequency of mutation in a wild type control strain is 5×10^{-5} CFU/ml (colony forming units per ml), suggesting that under these conditions a transposon mutant with reduced persistence would either have fewer or no resistant mutants at all when compared to the wild type strain. Using this screen, 150 mutants which yielded few or no colonies were identified. After eliminating mutants that displayed reduced growth rates as well as increased sensitivity to the antibiotics used, they identified the following genes

16

as key for persister formation: the chaperone encoding genes *dnaJ* and *dnaK*, the diadenosine tetraphosphatase encoding gene *apaH*, the peptiyl-prolyl *cis-trans* isomerase encoding gene *surA*, the global regulator encoding genes *fis* and *hns*, the RpoS response regulator-encoding gene *hnr*, *dksA* which regulates rRNA transcription, the 5-formyl-THF cyclo-ligase-encoding gene *ygfA* and the flavin mononucleotide phosphatase-encoding gene *yigB* (115).

With all the large-scale screen searches for mechanisms of persister formation undertaken in *E. coli*, in 2009, De Groote and colleagues decided to identify persistence genes in *P. aeruginosa* – an opportunistic organism renowned for its ability to form biofilms (54). They generated a random insertion *P. aeruginosa* plasposon mutant library of 5000 mutants using the PA14 strain. These mutants were grown to stationary phase and then treated with 5µg/ml ofloxacin for 5h. The surviving cells after treatment, with this 10-fold MIC_{50} of ofloxacin, were inoculated into fresh media and the growth rates observed. Differences in the lag-phase of these isolates compared to that of the wild type strain were used to identify mutants with different persister fractions since these mutants would have longer or shorter lag-phases. Using this strategy, 126 mutants - all of which were confirmed to be genotypically ofloxacin-sensitive, were isolated. Of the nine mutants further characterized, four displayed longer lag-phases, and hence a smaller persister population, while five had shorter lag-phases and thus an increase in the persister population. Sequencing of the plasposon insertion sites revealed that disruptions of the genes encoding the putative DNA-helicase *dinG*, the putrescin aminotransferase *spuC*, the PA14 locus: PA14_17880 predicted to encode an acetyl-CoA acetyltransferase and the PA14 locus: PA14_66140 predicted to encode a conserved hypothetical protein; all reduce the number of persisters in a population. In contrast, disruptions of the genes encoding the alginate biosynthesis regulatory protein *algR*, the type IV pilus response regulator *pilH*, a putative fumarylacylacetoacetate hydrolase *ycgM*, the fused chorismate mutase-prephenate dehydratase *pheA* and the PA14 locus: PA14_13680 predicted to encode a short-chain dehydrogenase; increase the number of persisters in a *P. aeruginosa* population (54).

From all these mutagenesis data, it is interesting to note that most of the genes implicated in persistence play a major role in cell functioning and viability.

1.5.2.2 Identification of molecular mechanisms of persister formation by use of an expression library

In addition to transposon mutant libraries, an expression library was also used to identify genes responsible for persister formation in *E. coli* (266). Here, the library was constructed by cloning partially digested fragments of the genomic DNA into an expression vector. The expression library was then treated with 100µg/ml ampicillin to yield a 10^6 CFU/ml surviving persister population. As in the previous study, this antibiotic dosage was used because this high concentration ensures that only persisters survive. Plasmids were isolated from 6 clones obtained after antibiotic treatment, and one of these clones which contained the *yzgL* and *glpD* genes was further characterized. Over-expression of the glycerol-3-phosphate dehydrogenase *glpD* gene resulted in 10-fold more persisters upon treatment with ampicillin and ciprofloxacin when compared to the empty vector control. To further corroborate this finding, Spoering and colleagues generated an *E. coli glpD* mutant, and observed a decrease in viability of this strain in the presence of ciprofloxacin. Since *glpD* is involved in glycerol-3-phosphate metabolism, mutants of other members of this pathway were generated and tested for the ability to form persisters. Only two members involved in this pathway *i.e. glpABC* - a glycerol-3-phosphate dehydrogenase and *plsB* - a glycerol-3-phosphate dehydrogenase acetyltransferase were found to play a role in persister formation (266). This further corroborates the observations that genes targeting essential cellular processes affect persister formation.

1.5.3 Persistence in *M. tuberculosis*

In the pathogenic organism *M. tuberculosis*, numerous genes have been implicated in its ability to persist within a host, despite the adverse conditions encountered.

1.5.3.1 The mighty M. tuberculosis *proteasome*

One major approach *M. tuberculosis* uses to achieve persistence within the human host is by surviving the onslaught of reactive nitrogen and oxygen intermediates encountered within granulomas. In 2003, Darwin and colleagues, in an attempt to identify genes required for resistance to reactive nitrogen intermediates, screened a *M. tuberculosis* transposon mutant library for increased sensitivity to nitrite (53). Of the 10100 mutants screened, twelve were sensitive to nitric oxide, and of these, five had insertions within predicted proteasome encoding genes with two mutants containing insertions within *pafA* and three within *mpa*. Further characterization of these proteasome associated factors *pafA* and *mpa* mutants revealed an inability to grow in wild type and inducible nitric oxide synthase impaired (iNOS$^{-/-}$) macrophages. In addition, an *mpa* mutant also displayed a reduced ability to grow in mice. In mice lacking iNOS, which renders the animals susceptible to TB infections, the wild type *M. tuberculosis* strain completely colonized the mouse lung resulting in death as early as 9 weeks post-infection. In contrast, the *mpa* mutant exhibited markedly less colonization of the lung and did not affect viability of the mice even 37 weeks post-infection. These observations implicate the *M. tuberculosis* proteasome in the defense against reactive nitrogen intermediates (53).

Whilst eukaryotic proteasomes are responsible for oxidized protein degradation and bacterial proteolysis is carried out by the proteases ClpAP/XP, HslUV, FtsH and Lon, *M. tuberculosis* is unique as it possesses ClpAP/XP proteases as well as a proteasome which is comprised of the core subunits *prcA* and *prcB* genes. Just like with the proteasome associated factors *mpA* and *pafA*, deletion of the *prcA* and *prcB* subunits also resulted in impaired growth *in vitro*, reactive nitrogen intermediate hyper-susceptibility, and increased resistance to

oxidative stress (90). In addition, the *prcBA* operon was demonstrated to be essential for *in vivo* growth in mice as well as for during chronic TB infection (90). More recent data has also uncovered that the *M. tuberculosis* proteasome allows for mycobacterial survival within the host during nutrient starvation, independently of its ability to resist the action of reactive nitrogen intermediates (89).

1.5.3.2 How does M. tuberculosis *persist during chronic infections?*

One of the mechanisms used by *M. tuberculosis* to persist for prolonged periods of time within the human host is based on its ability to survive on different carbon sources such as fatty acids (184). To generate carbon and energy from fatty acids, bacteria make use of either the β-oxidation cycle where acetyl-CoA the first molecule in the Krebs cycle is generated, or the glyoxylate cycle where carbohydrates are synthesized. The isocitrate lyase (ICL) enzyme, which is required for catalysis of isocitrate to succinate and glyoxylate in the glyoxylate cycle, is encoded by two *M. tuberculosis* Erdman genes, denoted *icl1* and *icl2*. Whilst single deletion mutants of *icl1* and *icl2* could still enable *M. tuberculosis* growth on long-chain fatty acids, a double *icl1/icl2 M. tuberculosis* mutant could not survive on either short-chain or long-chain fatty acids (195). In addition, an *icl1* deletion mutant revealed that although this gene plays no role during acute TB infection, it is essential for chronic TB infection in mice (184). It was interesting to note that although the single *icl2* mutant did not affect the establishment of a murine TB infection, a *M. tuberculosis* mutant lacking both *icl* genes failed to establish acute TB infection, and hence was rapidly cleared from the lungs and spleens of the mice (195). Also, whilst only ICL1 was shown to be necessary for *M. tuberculosis* survival within murine activated and not non-activated macrophages (184), the double *icl1/icl2 M. tuberculosis* mutant could also not grow within non-activated macrophages (195). These key observations establish that both *icl* genes are required for *M. tuberculosis* growth and persistence during TB infections.

Interestingly, the stringent response was also shown to affect the ability of *M. tuberculosis* to survive in environments which are oxygen and nutrient limiting

in vitro and *in vivo* (226). The stringent response, which is induced in *E. coli* as a result of reduced levels of amino acids, nitrogen, carbon, phosphorus or fatty acids together with stresses such as DNA damage, is mediated by (p)ppGpp levels in the cell. This (p)ppGpp stringent response regulator can be synthesized and hydrolysed by *spoT* and *relA*. The only homologue of both *spoT* and *relA* present on the *M. tuberculosis* chromosome is encoded by the *Rv2583c* gene, also referred to as *rel$_{Mtb}$*. This gene was convincingly demonstrated to be responsible for the synthesis of (p)ppGpp during starvation of *M. tuberculosis* since no intracellular (p)ppGpp could be detected in a *rel$_{Mtb}$* deletion mutant and with complementation reversing this phenotype. In addition to *rel$_{Mtb}$* being necessitated for overcoming stresses such as heat, and growth in either minimal or rich synthetic liquid media *in vitro*, it was also required for survival during *in vitro* conditions of hypoxia, nutrient starvation and stationary phase growth (226). The Rel$_{Mtb}$ protein, which can both synthesize and hydrolyze (p)ppGpp, is also essential for growth in macrophages, and for sustaining TB infection in mice. Deletion of the *rel$_{Mtb}$* was observed not only to reduce the TB symptom of drastic weight loss, but it also changed the histopathology associated with a TB infection as reduced granuloma formation and foamy vacuoles within murine lung macrophages were observed. These findings, together with microarray analyses that reveal that *rel$_{Mtb}$* is essential for the down-regulation of essential genes during starvation, convincingly demonstrate that *rel$_{Mtb}$* is essential for persistence of *M. tuberculosis* during chronic TB infections (49, 226).

Another approach used by *M. tuberculosis* to persist within the human host is the use of a phosphate metabolism regulator. Deletion of both of the *E. coli phoU* phosphate metabolism regulator homologues present in *M. tuberculosis* - *phoY1* and *phoY2*, revealed that only *phoY2* was a *bona fide* persistence gene. This mutant exhibited increased sensitivity to the antimycobacterial drugs pyrazinamide and rifampicin, and also had a reduced ability of up to 30-fold to survive and persist *in vivo* in a mouse model (258).

All these observations have proven that *M. tuberculosis* is a formidable foe that possesses many mechanisms which allow for persistence during chronic

infection. However, whilst decreased growth rates and low metabolic activities of *M. tuberculosis* are thought to play a role in the failure of drug treatment, little is actually known about bacterial physiology during chemotherapy.

1.5.3.3 How does M. tuberculosis *persist during chemotherapy?*

In an attempt to understand *M. tuberculosis* physiology during chemotherapy, Dhar and McKinney set out to identify genetic mutations that would either decrease or increase *M. tuberculosis* persistence in isoniazid-treated mice (57). This antimycobacterial agent was chosen not only because *M. tuberculosis* persistence during isoniazid treatment has been reported in both murine and human hosts, but also because the efficiency of this drug is determined by the stage of infection, with it being more effective during acute infection. *M. tuberculosis* transposon mutants were generated by signature-tagged transposon mutagenesis and used to infect mice. After the acute stage of infection, half the mice were treated with isoniazid following which mutants were recovered after 6 weeks to test for persisters after early isoniazid treatment as well as after 12 weeks to determine the impact of prolonged isoniazid treatment. The 576 mutants recovered were then classified into three groups based on their ability to result in either: normal, reduced, or increased persistence after isoniazid treatment. One mutant from each group was then further characterized. For the mutant that displayed reduced persistence, a transposon insertion was identified within the *cydC* gene which is the last gene in the *cydABDC* operon, which has been implicated in aerobic respiration under microaerobic conditions (137, 257). Whilst growth and survival of this mutant was similar to wild type *M. tuberculosis* in untreated mice, these were severely impaired during isoniazid treatment but not rifampicin or pyrazinamide treatment. In contrast, a mutant that displayed increased persistence in the screen, displayed growth impairment in untreated mice but was not eliminated by isoniazid, rifampicin and pyrazinimide treatment. Whilst this appears to be common, not all mutants that displayed impaired growth in the absence of isoniazid were refractory to eradication by antimycobacterial drugs. Apart from suggesting that *M. tuberculosis* growth-impairing mutations in untreated mice can enhance persistence during treatment, and that INH-

persistence is dependent on the *cydDC* encoded ABC transporter, the authors' key finding was that the reduced or increased persistence phenotypes observed subsequent to isoniazid treatment appear to be dependent on the *in vivo* host - pathogen interaction(s) (57).

As these observations increase our ever - growing understanding into the molecular mechanisms of persister formation, what is obvious is that unlike antimicrobial resistance, where the bacteria develop point mutations to overcome the effect of the antibiotic, bacterial persistence is achieved using multiple mechanisms (Figure 1.1).
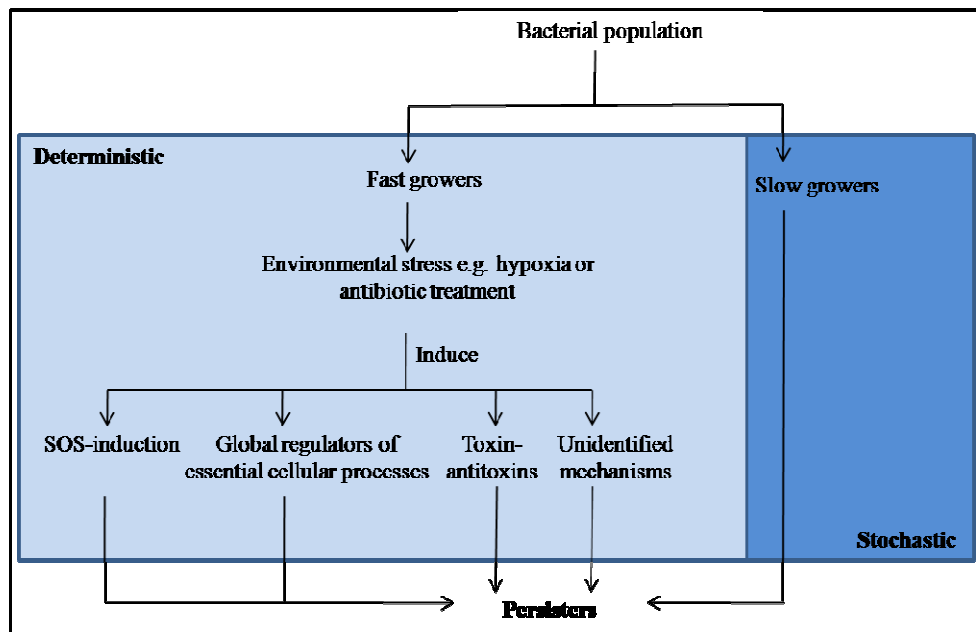
Figure 1.1: Schematic representation of the numerous mechanisms of persister formation.

1.5.4 Transcription profiling of persisters

Due to the fact that screens for bacterial mutants that are unable to form persisters have failed to yield a single "persister - less" mutant, it is likely that the mechanisms of persister formation are redundant (165). To further identify genes associated with persistence, the transcription profiles of persister cells have been examined (59, 60, 142, 254).

In 2004, Keren and colleagues, using the *E. coli hipA7* strain previously shown to produce persisters subsequent to ampicillin treatment (193), isolated an enriched persister fraction of the population after treatment with ampicillin (142). Analyses of the persister transcriptome profile revealed that approximately 300 genes were associated with persister cells. Further analysis of this cluster uncovered that these genes belonged to stress response regulatory pathways including the SOS, heat-, cold-, and phage shock pathways. In addition, genes responsible for macromolecular synthesis inhibition such as the translation inhibitor *rmf* and the replication inhibitor *umuDC*, as well as members of TA families such as *mazEF, relBE* which comprised about 2% of the persister genes, were identified (142).

Two years later, Shah and colleagues purified total RNA from their dim *E. coli* persister cells that were isolated as described in Section 1.5.1 (254), and analyzed the transcriptome by DNA microarray. The expression profile obtained revealed that about 420 genes were associated with persister formation. These genes, which were not upregulated in stationary phase *E. coli* cells, included metabolic genes such as the glycerol-3-phosphate dehydrogenase *glpD*, transcription regulation genes such as *marR*, phage shock genes as well as toxin-antitoxin genes such as *yoeB*, *relE* and *ygiU* (renamed *mqsR*). It is interesting to note that although *relE* and *mazF* were more highly expressed in the *hipA7* mutant allele strain (142), *mqsR* was the most highly expressed toxin gene in the wild type *E. coli* strain used by Shah and colleagues. This certainly raises the possibility that although persister formation occurs using similar mechanisms *i.e.* upregulation of stress response genes, macromolecular synthesis inhibitors as well as toxin - antitoxins, persisters formed under different conditions are not identical (254).

From these transcription profiles, what is abundantly clear is that in the state of persistence, where bacteria are able to survive hostile environments such as the presence of antibiotics, a notable number of genes that are differentially expressed are TA modules (96, 142, 164, 211, 254, 297). Taken together, all these observations about TA modules suggest that these are involved in persistence

24

through their toxin components. The toxins affect essential cellular processes required for bacterial growth, viability as well as survival, and thus enable the cell to enter a transient state of bacteriostasis refractory to elimination by antibiotics that target actively replicating cells.

1.6 Toxin - antitoxin modules

TA modules are small bicistronic genetic elements composed of two genes organized in an operon that encode a toxin and a cognate antitoxin. These loci, first discovered over two decades ago on bacterial plasmids, were initially shown to be responsible for post-segregational killing of bacteria (130). The phenomenon of post-segregational killing is one of the main approaches used by bacteria to prevent plasmid loss during cell division. In this instance, bacterial daughter cells which do not possess the plasmids containing a TA pair are killed due to the rapid degradation of the short-lived antitoxin. In the absence of this unstable cognate antitoxin to form a tight complex with the toxin, the latter which has a longer half-life accesses its cellular target ensuing in cell death (130).

TA loci have also been found on bacterial and archaeal chromosomes in multiple copies (10, 29, 211, 230). These chromosomal TA modules have been shown to reduce bacterial gene loss through stabilization of superintegrons thereby allowing unstable DNA regions to be retained within the genome (272). In addition, the absence of TA loci in obligate intracellular parasites such as *Rickettsia* and *Chlamydia,* which replicate in constant environmental conditions, suggests that chromosomal TA loci may also play a role in changing environments (96). Based on these observations as well as the implication of TA modules in persistence (Section 1.5), it has been postulated that TA modules could represent a general mechanism for the formation of persistent populations in the presence of antibiotics by inhibiting cell replication.

1.6.1 Transcriptional activation of TA modules

Deterministic and stochastic models have been proposed to account for the activation of TA loci. Two versions of the deterministic model, which occurs as a result of a signal, have been put forward. In the first version, environmental insults produce a signal that triggers a cellular protease such as Lon to degrade the less stable antitoxin, either in its free form or in association with the more stable toxin (96, 283). This action results in an increase in the amount of unpaired toxin in the cell which can either lead to bacteriostasis or cell death (Figure 1.2). In the second version of this model, environmental stress generates a signal that destabilizes the TA complex, consequently releasing the antitoxin which is then degraded by a cellular protease (96, 283).

Figure 1.2: A schematic representation of a TA operon, and its mode of activation. The broken arrow on the chromosome represents a promoter upstream of the operon, to which the TA complex binds to repress transcription of the operon. As proposed by the first deterministic mode of activation, cellular proteases degrade the less stable antitoxin either in its bound or unbound state, and the curved arrow represents the translational coupling of the toxin and antitoxin genes.

The stochastic model, on the other hand, proposes that activation of the TA locus occurs randomly in the absence of an external signal. Unlike in the deterministic model, where proteases such as Lon activate TA loci, in this model changes in intracellular rates of translation, brought about by amino acid starvation, directly result in TA loci activation. The reduced rate of translation of the antitoxin-encoding mRNA results in a reduction of the antitoxin, and a de-repression of the TA locus promoter. The ensuing increase in toxin activity is thought to be as a result of the increased transcription rate of the TA operon and the reduced antitoxin level in the cell (96).

1.6.2 Classification of TA modules

Members of the TA loci have been classified into three categories: type I, type II and type III TA loci, based on whether the antitoxin is an RNA or a protein molecule (76, 98).

1.6.2.1 Type I TA modules

Type I TA modules are comprised of *cis* or *trans* small RNA (sRNA) antitoxins that regulate toxin expression (82, 84, 98, 140). These modules which are widely distributed within the Enterobacteriaceae and Vibrionaceae families as well as the *Bacillus* and *Enterococcus* genera, have evolved by gene duplication (84). Type I toxins are hydrophobic membrane proteins generally smaller than 70 amino acids and their encoding genes are characterized by long stretches of intergenic regions from their neighbouring genes (82, 84, 98, 282). Chromosomal type I TA loci include Hok-Sok, RNAI (Fst)-RNAII, Ldr-Rd1, Ibs-Sib, ShoB-OhsC, TisB-IstR1, SymE-SymR, TpxA-RatA systems, as well as the newly identified *z3289/z3290*, the YhzE and YonT families (82, 84).

The Hok-Sok locus of *E. coli* was the first identified type I TA module (97). The Hok toxin is an approximately 50 amino acid membrane-associated protein that targets the cell membrane. Contrary to most TA loci, this locus comprises of three genes: the suppression of killing gene (*sok*), the modulation of killing gene (*mok*), and the host killing gene (*hok*). The *mok* gene overlaps with the *hok* gene and it is required for both expression and regulation of *hok* translation. Interestingly, the unstable *cis* Sok antitoxin with a 30s half-life inhibits *hok* translation indirectly by actually inhibiting *mok* translation. The Hok toxin, which results in bacterial cell death as a result of permanent bacterial cell membrane damage, is similar to holins which are proteins that cause pores within inner cell membranes of bacteria. Although the cellular target of Hok remains unknown, induction of this toxin has been observed to cause efflux of ATP and Mg^{2+}, influx of extracellular molecules and RNase I as well as collapse of membrane potential and cessation of respiration (82, 97, 98).

The unique Fst-RNAII locus, discovered in *Enterococcus faecalis* and *Bacillus subtilis*, consists of a 210 nucleotide (nt) RNAI or Fst toxin that is overlapped by 75 bp in its 3' end by the 65 nt RNAII antitoxin (219, 300). The *trans* RNAII antitoxin inhibits translation of Fst in the stable complex as well as ribosome - Fst binding (98). The Fst toxin encoded by the RNAI transcript is the smallest known toxin consisting of 33 amino acids. Whilst over-expression of Fst has been observed to cause inhibition of macromolecular synthesis and possibly result in persister formation, the loss of membrane integrity observed is due to defects in chromosomal segregation, thus suggesting that the primary target of Fst plays a role in chromosomal segregation (219, 301).

The Ldr-Rdl, Ibs-Sib, and ShoB-OhsC type I TA modules have all been discovered within repeat sequences of *E. coli*. The four long direct repeat (LDR) sequences, annotated LDR-A, -B, -C and -D, are approximately 500 bp tandem repeats that encode *ldrA*, *ldrB*, *ldrC* and *ldrD* genes whose 35 amino acid products are toxic to the bacterial cell. The unstable 60 nt *trans* sRNA *rdl* antitoxins control the translation of the Ldr toxins, and although all four LDR loci do not affect cell growth, morphology, mutation frequencies or nucleoid structures, over-expression of *ldrA, ldrB, ldrC* and *ldrD* result in bacterial death. Interestingly, *ldrD* over-expression results in condensation of the nucleoid structure and microarray data suggest that the LdrD actually affects purine metabolism (141).

The five homologous repeat elements termed s̲hort i̲ntergenic ab̲undant sequences (SIB) are also located in separate intergenic regions of *E. coli*. Although these toxins have not been fully characterized, all five Sib genes (*sibA, sibB, sibC, sibD* and *sibE*) encode the *sib* antitoxins as well as a toxic 18 - 19 amino acid hydrophobic protein called i̲nduction b̲rings s̲tasis (*ibs*), in a genomic organisation similar to the *ldR-rdl* TA module. Here the toxin is encoded by an open reading frame (ORF) opposite the antitoxin ORF, and the Sib sRNA antitoxins are complementary to both the ribosome binding sites and coding sequence of *ibs* (83).

The ShoB-OhsC TA module was identified within the *yfhL-acpS* intergenic region. While this locus appears unique to *E. coli* and *Shigella*, OhsC

behaves similarly to the other type I TA loci, as it regulates the toxic 26 amino acid ShoB protein downstream of it. Just as with Hok, over-expression of both IbsC and ShoB, is detrimental to the bacterial cell since the abundance of both proteins result in loss of cell membrane potential (83).

The TisAB-IstR1 locus of *E. coli* was the first type I TA module found to be regulated by the SOS response. This module, implicated in persister formation (Section 1.5.2), contains a LexA binding site (SOS box) within its promoter. It is predicted that only the toxin *i.e.* TisB, is upregulated upon SOS induction. The TisAB-IstR1 locus is unique in that it transcribes four different mRNAs: the constitutively transcribed *trans* IstR-1 antisense antitoxin that regulates the toxic *tisAB* mRNA, a LexA dependent IstR-2 transcript that does not regulate *tisAB*, a small RNA *tisA* as well as a *tisB* transcript. Although the two small *tisAB* transcripts are transcribed from different promoters they share the same terminator. *tisA* is an untranslated, unconserved reading frame that contains a binding site for both the IstR-1 antitoxin and the ribosome that allows for *tisB* translation. In fact, both the antitoxin and the ribosome compete for the site. As a result, upon binding of the antitoxin to the binding site, translation of *tisB* does not occur as RNase III cleaves the resulting RNA duplex. If however the ribosome attaches to the binding site, translation of *tisB* occurs. It has been proposed that upon translation of this 29 amino acid peptide, TisB binds to the inner membrane, causing loss of membrane potential. This, in turn, reduces cellular ATP levels, which results in decreased macromolecular synthesis and eventual bacteriostasis (82, 98, 280).

The second type I TA module regulated by the SOS response is the *E. coli* SymE-SymR locus. This module, which also contains an SOS box within its promoter, encodes a *cis* antisense RNA and a 113 amino acid SymE toxin. SymE over-expression results in mRNA cleavage, which reduces protein synthesis and ultimately leads to bacteriostasis. The expression of SymE is tightly regulated not only by SymR but also the LexA repressor and the Lon protease. It has been suggested that the cleavage of RNA by SymE allows it to contribute to the recycling of damaged RNAs during induction of the SOS response (82, 98, 140).

The TpxA-RatA locus was identified on the *Bacillus subtilis* chromosome (260). This type I TA module, like the Fst-RNAII, loci encodes a *trans* antisense RNA that overlaps the 3' end of the TxpA toxin by 75 nucleotides. Bioinformatic analysis of the TxpA toxin shows a predicted N-terminal membrane domain, and it has been proposed that the TpxA-RatA complex like with all other TA modules prevents translation of the 59 amino acid TpxA toxin and hence mRNA cleavage. In addition, TxpA has been hypothesized to be responsible for maintaining a *Bacillus subtilis* chromosomal region excised during spore formation (82, 84, 98).

Recently Basic Local Alignment Search Tool (BLAST) searches of numerous genomes demonstrated that type I TA loci were not acquired by horizontal gene transfer between organisms (84). In addition, these searches also uncovered three novel type I TA systems: *z3289/z3290*, the YhzE and YonT families. Although these have not yet been characterized, they are *bona fide* TA modules as the toxicity of the toxins encoded by these families have been shown to be abrogated by their cognate antitoxins (84).

While the function of these TA modules remains undeciphered, the differences observed thus far for the various type I systems (82, 84, 140, 282), suggests that different type I TA loci have distinct biological roles when integrated into bacterial chromosomes.

1.6.2.2 Type II TA modules

Type II TA modules, much like their plasmid-based counterparts, are comprised of operonic bicistronic toxin-antitoxin genes that are transcriptionally regulated and whose antitoxins encode unstable proteins instead of sRNA's (95, 96, 211, 282, 316). The type II antitoxins consist of two domain proteins: a C-terminus protein-protein interaction domain which binds to the toxin, as well as an N-terminus DNA-binding domain which binds the operator of the TA module thus resulting in transcription auto-repression of the whole module (174, 183, 263). Members of type II toxins and antitoxins can also be structurally and functionally different (174). While it was initially unclear whether the chromosomally located type II TA modules were functionally similar to those found on plasmids (10),

recent evidence suggests that once integrated into the bacterial chromosome, these modules assume new cellular roles as the type II TA families CcdAB, DinJ-YafQ, HigAB, HipBA, MazEF, MqsR-YgiT, ParDE, Phd-Doc, RelBE, VapC and YefM-YoeB affect a variety of cellular processes resulting in bacteriostasis or cell death (Table 1.1) (96, 282).

Table 1.1: Properties of type II TA chromosomal modules

TA locus	Toxin	Toxin cellular target	Cellular process targeted	Effect of toxin
ccdAB	CcdB	DNA gyrase	DNA replication	Cell death irreversible by addition of antitoxin
dinJ-yafQ	YafQ	mRNA bound ribosome	Protein translation and persister formation	Bacteriostasis and cell death
hicAB	HicA	Unknown	Protein translation	Bacteriostasis
higBA	HigB	Ribosome	Protein translation	Bacteriostasis
hipBA	HipA	EF-Tu translation factor	Protein translation and persister formation	Bacteriostasis and eventually cell death
mazEF	MazF	5'-NAC-3'site of single and double stranded RNA	Protein translation	Bacteriostasis / cell death
mqsRA	MqsR	Ribosome	Protein translation, biofilm and persister formation	Bacteriostasis
parDE	ParE	DNA gyrase	DNA replication	Cell death
phd-doc	Doc	Ribosome	Protein translation	Bacteriostasis
relBE	RelE	mRNA bound ribosome	Protein translation and persister formation	Bacteriostasis
vapBC	VapC	RNA	Protein translation	Bacteriostasis
yefM-yoeB	YoeB	mRNA bound ribosome	Protein translation and biofilm formation	Bacteriostasis

<u>The *mazEF* module</u>

In 1996, Engelberg-Kulka and colleagues first reported the *E. coli mazEF*, which encodes the MazE antitoxin and MazF toxin, as a *bona fide* type II TA module (2). This locus, identified as part of the *rel* operon, and downstream of *relA* (2, 248), has been one of the best characterized TA modules. A mutant lacking the *mazEF* locus was constructed in a *relA*$^+$ *E. coli* strain (73) since expression of *mazEF* is regulated by the ppGpp (2). A variety of stresses including amino acid starvation, inhibition of transcription and translation by antibiotics, DNA damage caused by thymine starvation, genotoxic and oxidative agents, as well as heat were demonstrated to induce transcription of the *mazEF* locus during exponential growth of the bacteria (118, 119, 248, 249). Upon transcription of the *E. coli mazEF*, the ClpXP proteases degrade the MazE antitoxin (42, 96, 147) and the MazF toxin, with its longer half-life, is freed from the C-terminus of MazE (309). The MazF protein is an endoribonuclease which cleaves the 5' end of the adenine residues within the consensus sequence, 5'-NAC-3' of single and double stranded RNA in a ribosome-independent manner, consequently halting protein translation (196). Whilst ectopic expression of MazF can result in bacteriostasis that is reversible upon expression of MazE (42, 72, 220), the reversal of toxicity is only possible within a short window period, after which an irreversible process leading eventually to bacterial cell death ensues (4, 148). However, because *mazEF*-mediated programmed cell death is an active process, MazE cannot reverse processes already affected by MazF (4, 148). Interestingly MazG, which is transcribed downstream of *mazEF*, has been observed to delay the "point of no return" upon which cidality of the bacterial cell occurs by reducing the levels of ppGpp in the cell which in turn represses transcription of *mazEF* thereby limiting the amount of MazF during amino acid starvation (106).

Recently, in an attempt to ascertain whether chromosomal TA modules play a role in bacterial stress management, Tsilibaris and colleagues used the Engelberg-Kulka MC4100*relA*$^+$Δ*mazEF E. coli* strain (73) as a host for generating an *E. coli* mutant lacking five TA systems, *mazEF*, *relBE*, *yefM-yoeB*, *chpB* and

dinJ-yafQ (276). Attempts to grow this MC4100*relA*$^+$Δ*mazEF* mutant on minimal media containing serine, methionine, and glycine were unsuccessful, thus suggesting that the mutant may have a *relA*$^-$ phenotype. Sequencing of the mutant revealed that the strain was actually *relA* and *mazG* deficient, and as such, Tsilibaris *et al.* generated a new *E. coli* mutant lacking the five targeted TA systems, whilst ensuring that their parental MC4100 strain remained *relA*$^+$ and had an intact *mazG*. Exposure of this new quintuple deletion mutant to a variety of stress conditions, including amino acid starvation, long term starvation, change in pH, heat and antibiotic treatment, did not affect the fitness of this *E. coli* mutant strain (276). These findings suggested that the observations made by the Engelberg-Kulka group were probably attributable to the absence of ppGpp and MazG in their mutant strain, and not to MazF. Subsequently however, the Engelberg-Kulka group rebutted these findings attributing the discrepancies to the density of the bacterial culture and not deficiencies in RelA and MazG (147).

The Engelberg-Kulka group also reported that *mazEF*-mediated programmed cell death, which acts in either a reactive oxygen species dependent or independent pathway, only occurs at high cell densities and requires an "extracellular death factor" (149, 150). This "extracellular death factor", characterized as a linear pentapeptide (Asn-Asn-Trp-Asn-Asn), acts as an autoinducer in the quorum-sensing *mazEF*-mediated cell death process to prevent further bacterial growth (147, 150, 151). While it was initially believed that the absence of the "extracellular death factor" in stationary-phase cultures was the reason for the sensitivity of logarithmically growing bacteria and not stationary-phase cultures to *mazEF*-mediated cell death, recent evidence has shown that the stationary-phase sigma factor σ^s is responsible for this phenomenon (149). It appears that the proteins induced by σ^s during stationary phase antagonize the proteins responsible for *mazEF*-mediated programmed cell death (149). It is also worth mentioning that although MazF leads to cidality of *E. coli*, it appears that MazF also results in the production of small proteins of less than 20kDa such as SoxR which are key for the survival of a sub-population of the bacteria (3).

The *relBE* module and its homologues

The second best characterized type II TA module, the *relBE* locus, was initially discovered in 1998 in *E. coli* (104). Upon activation of this module during amino acid starvation, Lon protease degrades the RelB antitoxin leading to increased levels of the toxic RelE which results in bacteriostasis (41). Interestingly, excess RelB in the cell promotes binding of this antitoxin to RelE and represses transcription of the operon (209). In contrast, excess RelE prevents proteolysis of RelB by Lon and promotes binding of RelB to the *rel* operator triggering transcription (208, 209). RelE acts by binding to ribosomes (87), where it cleaves sequence specific mRNA within the ribosomal A subunit rendering the ribosome inactive (221). A transfer messenger RNA (tmRNA) then attaches a protein degradation tag onto 3'- regions of these impaired mRNAs, resulting in the proteolysis of the truncated peptides and release of the ribosome. The decrease in the cellular tmRNA pool activates *relA* resulting in the production of ppGpp which reduces global protein translation rates and subsequently causes bacteriostasis (96). In addition to the RelB-reversible bacteriostasis caused by RelE (41, 104, 220), RelE toxin expression has also been shown to increase the number of persisters in a culture subsequent to antibiotic treatment with cefotaxime, ofloxacin and tobramycin (142).

E. coli also possesses two other *relBE* homologues, the *dinJ-yafQ* and *yefM-yoeB* loci (96). The *dinJ-yafQ* module encodes a toxic YafQ protein whose bacteriostatic effect is countered by the DinJ antitoxin (190). Upon activation of the module, Lon and ClpXP proteases degrade DinJ, thereby allowing the YafQ toxin to associate with ribosomes to initiate global translation inhibition. The toxin cleaves mRNA bound to the 50S subunit of the ribosome at the 5'AAA-G/A 3' site and prevents translation elongation which results in eventual bacteriostasis (228). Recently, the *dinJ-yafQ* module has been implicated in instigating bacterial cell death to achieve the threshold of dead cells required for biofilm formation (151). The YafQ toxin has also been shown to play a role in the formation of persisters tolerant to specific antibiotics within *E. coli* biofilms (116).

The other *relBE* homologue *yefM-yoeB* that encodes the YoeB toxin which forms a tight complex with the YefM antitoxin was discovered in *E. coli* (37). During overproduction of Lon, this protease specifically degrades YefM thus allowing the YoeB endoribonuclease to inhibit translation initiation in a ribosome-dependent fashion by associating with the 50S subunit of the ribosome to cleave translated mRNAs, thus resulting in bacteriostasis (40, 167, 201, 308, 311). Recently, this *yefM-yoeB* module has also been implicated in biofilm formation (143).

Other type II TA modules

The control of cell death (*ccdAB*) locus which is unique to Gram-negative bacteria encodes the CcdB toxin and CcdA antitoxin (1, 96). The toxin of this rare chromosomal locus acts as a DNA topoisomerase gyrase poison. To do so, CcdB binds the DNA gyrase in two manners. Firstly, it binds to the open conformation of DNA gyrase rendering it unable to bind and supercoil DNA, an essential prerequisite for DNA replication. CcdB also binds the DNA gyrase during its catalytic cycle when the gyrase binds to DNA. The resulting CcdB-gyrase-DNA complex forms a barrier preventing both DNA and RNA polymerases from traversing this block. This DNA gyrase poisoning leads to breaks in DNA and consequently induction of the SOS response which eventually results in death of the bacterial cell (11, 29, 52, 117).

The *parDE* locus encodes the toxic 9kDa ParE protein and a 12kDa ParD antitoxin (96, 131). This locus which was found within an *E. coli* prophage reinforces the notion that TA modules play a role in genome stabilization (111). In addition, this ParE toxin, just like CcdB, targets the DNA gyrase, inducing the SOS response and causing bacteriostasis, cell filamentation and eventual bacterial cell death (111, 131).

The *higBA* and *hicAB* operons are unique type II TA modules as these encode for the toxin upstream of the antitoxin (96, 211). Using bioinformatic analyses, the <u>Haemophilus</u> <u>i</u>nfluenza <u>c</u>ontiguous (*hicAB*) TA module was first proposed to be a *bona fide* TA operon whose HicA toxin binds and possibly

cleaves RNA (173). This was subsequently proven when induction of the HicA toxin resulted in bacteriostasis that was reversed by the HicB antitoxin (134). Transcription of this locus is induced via a Lon-dependent mechanism during amino acid and carbon starvation. Although the cellular HicA target remains unknown, over-expression of the 58 amino acid HicA protein leads to arrest of global translation rates as well as induction of mRNA cleavage ultimately resulting in bacteriostasis (134).

The host inhibition of growth (*higBA*) locus is also transcribed during amino acid starvation (38, 39). The HigB toxin is a Lon-dependent endoribonuclease associated with the 50S subunit of the ribosome, that cleaves translated mRNA at adenine-rich sites resulting in bacteriostasis of *Vibrio cholerae* and *E. coli* (27, 38, 39, 127).

The high persistence (*hipBA*) locus described in Section 1.5.1 encodes the *hipA* toxin and the *hipB* antitoxin. As mentioned previously, HipA, which has been implicated in persister formation in *E. coli* (74, 142, 154, 155), belongs to the phosphatidylinositol 3/4-kinase family (47). This toxin, whose serine kinase activity is crucial for persister formation, phosphorylates the EF-Tu translation factor, resulting in decreased macromolecular synthesis and eventually bacteriostasis (139, 142, 154, 155, 253). During prolonged conditions of stress however, HipA has been reported to initiate loss of cell viability (139).

The *phd-doc* TA locus, originally discovered on the plasmid prophage P1, is comprised of the antitoxin *phd* (prevents host death) and the toxin *doc* (death on curing) (120). Upon activation of the locus, ClpXP serine protease degrades the Phd antitoxin allowing the Doc toxin to associate with the 70S and 30S ribosomal subunits (161, 169). Whilst it has been suggested that this binding triggers bacteriostasis via activation of the *mazEF* module (120), over-expression of Doc alone has been shown to induce RelE (91). Although the MazF and RelE are not required for the activity of Doc, because both MazF and RelE are induced during cell stress, it is probable that the arrest of translation by Doc induces these ribonucleases as a fail-safe attempt by the bacteria to overcome this stress (91).

The motility quorum-sensing (*mqsRA*) TA locus encodes the MqsR toxin and MqsA antitoxin. The MqsR toxin, implicated in persister formation of *E. coli* (145, 254), has been observed to induce motility and biofilm formation through a two-component regulatory system (102, 138). This mRNA interferase, which cleaves RNA at GCU sites independently of translation (39, 305) is activated by the Lon protease during amino acid and carbon starvation resulting in bacteriostasis (39, 138, 305). The *mqsRA* operon has also been shown to repress activation of *cspD,* a gene implicated in persister formation by binding of its MqsA antitoxin (144, 145). As such, one probable mechanism of persister formation occurs when HipA activation results in upregulation of MqsR (138) through degradation of MqsA by the Lon protease which then allows for *cspD* transcription (144, 145). This suggests that MqsR, like RelE which can be induced by Doc, is part of a cascade of mechanisms used by the cell to overcome cellular stresses.

Finally, TA modules of the the virulence associated protein (*vapBC*) type, discovered initially in *Salmonella dublin*, are the most abundant of the TA loci (96). The *vapBC* operon, a homologue of which is absent in *E. coli*, encodes a VapC toxic toxin and a VapB antitoxin that abrogates VapC toxicity (50). The VapC toxin is unique because it belongs to the PIN-domain family of proteins that bear homology to the N-terminus of the pilin biogenesis protein and the RNase H nuclease domain (5, 186). Bioinformatic analyses of PIN domain proteins reveal that these consist of four conserved acidic residues, which are all in close proximity to each other thus allowing for the formation of a negatively charged cavity (8, 28). Based on this observation, these prokaryotic VapC toxins were initially thought to be metal-ion-dependent endoribonucleases that cleave mRNA-associated ribosomes in a manner similar to the eukoryotic RNA interference and nonsense-mediated RNA decay (5, 44, 96, 100). Although the VapC targets remain unknown, the auto-regulated *vapBC* TA modules regulate growth of bacteria during periods of stress such as amino acid starvation (50, 237, 304, 312). It is thought that dissociation of the VapB-VapC complex allows for the binding of the divalent metal ions - magnesium or manganese, to the negatively charged pocket of VapC thereby creating an active site for this ribonuclease to cleave free

RNA and thus inhibit protein translation (28, 46, 50, 186, 237, 304). Interestingly, although absent from the *E. coli* genome, overexpression of VapC in this organism has been shown to cleave mRNAs at translational stop codon sites between the second and third base resulting in translation inhibition. This is believed to result in activation of Lon which in turn degrades the YefM antitoxin, thus allowing for action of YoeB in *E. coli* (304). This suggests a possible role for VapC as part of a cascade of mechanisms used to overcome cellular stresses.

On the basis of all of the above-mentioned findings, what is abundantly clear is that TA modules play a significant and possible redundant role in stress-induced growth regulation with some modules appearing to directly or indirectly regulate other TA loci. They also appear to play a major role in chromosomal gene stabilization, biofilm formation, persister formation, programmed cell death and even pathogenesis of bacteria.

1.6.2.3 Type III TA modules

A novel TA system, the type III *toxIN* module was recently identified on a cryptic plasmid of *Erwinia carotovora* (76). This *bona fide* negatively autoregulated TA system encodes the RNA antitoxin *toxI* and a ToxN toxin, which is identical to the phage abortive infection, Abi, proteins. The *toxIN* module also allows for resistance to different bacteriophages and therefore may provide the bacteria with protection from mobile genetic elements (24, 76).

1.6.3 TA modules in mycobacteria

TA loci which have been discovered in the chromosomes of numerous bacteria and archaea are also found in mycobacterial genomes (96). Curiously, they appear to be found predominantly in mycobacteria that encounter changing environments. Bioinformatic analyses have revealed that only members of the *Mycobacterium tuberculosis* complex (MTBC) i.e. *M. tuberculosis*, *M. bovis*, *M. africanum* and their *M. canetti* progenitor, possess an unusually large number of ≥ 82 TA loci in their genomes (211, 230). It is interesting to note that, although not as many TA modules are present on the chromosomes of the non-MTBC mycobacterial relatives, a novel TA system Rv0909-Rv0910 has been identified in

all members of the *Mycobacterium* genus (230). Interestingly too, the closest MTBC relative - *M. marinum*, possesses only 2 TA modules on its chromosome, including the novel TA system Rv0909-Rv0910. This together with the fact that 37% of these loci were identified in the genomic islands acquired before speciation of the MTBC strongly indicates that these modules play a specific role in the physiology of these organisms (211, 230).

1.6.4 The TA modules of *M. tuberculosis*

M. tuberculosis possesses 88 putative TA loci including 1 *higBA*, 2 *parDE*, 3 *relBE*, 9 *mazEF*, 26 novel TA and 47 *vapBC* modules on its chromosome (230). Although the 2 *parDE* loci of *M. tuberculosis* have not been characterized, suffice to confirm that they are *bona fide* TA modules (108, 230), the sole *M. tuberculosis higBA* locus (Rv1955-Rv1956) (79) is part of an Rv1954A-Rv1957 operon (264) that encodes a HigA antitoxin that abrogates the toxic HigB toxin (108, 230). The HigA antitoxin appears to bind specifically to the ATATAGG(N_6)CCTATAT DNA binding motif, suggesting that this antitoxin only regulates its operon since this motif is unique to the promoter region of the Rv1954A-Rv1957 operon (79). The *higBA* operon has also been implicated in the survival of *M. tuberculosis* to various stresses including hypoxia and nutrient starvation (18, 230).

The *M. tuberculosis relBE* loci, typical of *relBE* homologue found in other organisms, encode a RelE toxin which causes mycobacterial growth inhibition, and RelB antitoxin which transcriptionally activates the *relBE* operon and abrogates RelE action via its C-terminus (152, 261). Whilst *M. tuberculosis relE* genes are induced *in vivo* during late macrophage infections and in mouse lungs, it is interesting to note that each individual *relE* is induced by specific bacterial stresses (152, 261). RelE1 and RelE2 were observed to be upregulated together with genes associated with nutrient starvation, while RelE3 was associated with genes that play a role in translation inhibition. These differences indicate that the RelE endoribonucleases may cleave target mRNAs at different sites. RelEs have also been observed to play a role in *M. tuberculosis* persister formation *in vitro* either through induction of persister formation or maintenance of persister cells,

with phenotypically different persister populations generated with each RelE (152, 261). These modules were found to be dispensable for *in vivo* growth and persister formation (152, 261) possibly as a result of functional redundancy within the family of *relBE* homologues in *M. tuberculosis* (307).

The other well characterized family of TA modules in *M. tuberculosis* is the *mazEF* family. Although not all nine MazFs were found to be toxic based on growth inhibition assays when ectopically expressed in the heterologous hosts *M. smegmatis* and *E. coli* (31, 230, 316), each of the characterized ribonucleases of this family have been shown to target sequence specific mRNAs. For example, Rv2801c degrades mRNA at the 5'-U$\downarrow$AC-3' sequence, Rv1102c at the 5'-U/CU$\downarrow$A/UCU/C-3' site, Rv1495c cuts within the pentad 5'-U$\downarrow$CGCU-3' mRNA sequence and Rv1991c targets 5'-U/CU$\downarrow$CCU-3' mRNA sites (314, 316). Microarray analyses have also suggested that like their *E. coli* counterparts, some of the *M. tuberculosis* MazFs are regulated by *relA* (18). Interestingly, recent data has revealed that heterologous expression of a *M. tuberculosis* MazF toxin, which was observed to induce bacteriostasis, also resulted in increased persister formation in *M. smegmatis* (113).

In an important recent study, 26 novel TA loci were identified on the *M. tuberculosis* chromosome (230). Four of these, including two which are absent in *M. tuberculosis* clinical isolates, were not tested for growth inhibitory properties. However, of the 22 remaining novel TA modules tested, only three were toxic to *M. smegmatis*. Although one of these is homologous to MazF and is believed to function in a similar manner, the other two novel toxins showed homology to neither of the TA families. Interestingly the Rv0910 toxin component of the Rv0909-Rv0910 operon found across all members of the *Mycobacterium* genus was one of the novel toxins that caused bacteriostasis in *M. smegmatis*. This novel toxin does not appear to target cellular translation and may represent a distinct mode of TA action in mycobacteria (230).

Most *M. tuberculosis* TA modules, however, belong to the *vapBC* family (10, 96, 211). Of the 47 members of this family identified so far in *M. tuberculosis* (230), only one VapC, Rv0627, has been structurally characterized (186). This

magnesium-dependent endoribonuclease, which was structurally analyzed in complex with the C-terminal end of its cognate VapB antitoxin, is a protein comprising of a core domain of four parallel β-sheets encompassed by five α-helices, and a clip structure domain that extends from the core domain and comprises two α-helices. This RNase H-like structure allows the four highly conserved acidic residues involved in divalent metal ion binding, characteristic of PIN domain proteins, to form the putative active site essential for ribonuclease activity (186).

Despite the fact that most of the VapCs appear to be dispensable for *in vitro* growth (159, 247), suggestions of functional and/or conditional differentiation within the VapC family has emerged from other studies, revealing that the toxins of this large *M. tuberculosis* TA family play a significant role for the survival and pathogenesis of this organism under certain stress conditions (Table 1.2).

Table 1.2: Properties of *M. tuberculosis* VapC proteins

VapC	*In vitro* essentiality (247)	Toxicity in *E. coli* (108)	Toxicity in *M. smegmatis* (186, 230)	Properties
Rv0065	No	Non-toxic	Non-toxic	Part of a genomic island (230)
Rv0240	No	-	Non-toxic	
Rv0277c	No	-	Toxic	Induced by SDS stress (179)
Rv0301	No	Non-toxic	Toxic	Exhibits RNase activity (230); Induced in the presence of diamide (178) and SDS stress (179). Protein identified in 30-d infected guinea pig lungs (156). Part of a genomic island (230)
Rv0549c	No	Non-toxic	Toxic	Induced by hypoxia (199, 230), SDS stress (179), during adaptation to nutrient starvation (112), during infection of human macrophages (65, 230), and in the presence of high concentrations of vancomycin (227).
Rv0582	No	-	Toxic	Induced by acid stress (78)
Rv0595c	No	Non- toxic	Non-toxic	Required for survival in nonhuman primate lungs (66); induced during adaptation to nutrient starvation (112), macrophage infection (268) and by SDS stress (179). Part of a genomic island (230).
Rv0598c	No	-	Non-toxic	Part of a genomic island (230)
Rv0609	No	-	Toxic	Part of a genomic island (230)
Rv0617	No	-	Non-toxic	
Rv0624	No	-	Toxic	
Rv0627	Yes	Non-toxic	Non-toxic	Structure determined in complex with C-terminal part of antitoxin (Rv0626) and biochemical evidence for ribonuclease activity (186).
Rv0656c	No	Non-toxic	Non-toxic	Part of a genomic island (230)
Rv0661c	No	Non-toxic	Non-toxic	Induced in SCID mice (273). Part of a genomic island (230)
Rv0665	No	Non-toxic	Non-toxic	Part of a genomic island (230)
Rv0749	No	-	Toxic	Induced in the presence of diamide (178) and by SDS stress (179). Part of a genomic

				island (230)
Rv0960	No	Non-toxic	Non-toxic	
Rv1114	No	-	Toxic	Induced in the presence of diamide (178)
Rv1242	No	-	Toxic	Repressed in sputum (92)
Rv1397c	No	Non-toxic	Non-toxic	Induced by SDS stress (179), and during nutrient starvation (18), but repressed in sputum (92). Part of a genomic island (230)
Rv1561	No	Toxic	Toxic	Exhibits RNase activity (230); and is induced in SCID mice (273)
Rv1720c	No	Non-toxic	Non-toxic	Induced in the presence of high concentrations of vancomycin (227) and in sputum (92)
Rv1838c	No	Non-toxic	Non-toxic	Induced in the presence of diamide (178) and by SDS stress (179)
Rv1953	No	Non-toxic	Non-toxic	C-terminally truncated and lacking part of the PIN domain. Induced during adaptation to nutrient starvation (18, 112)
Rv1962c	No	-	Toxic	Induced during macrophage infections (80). Part of a genomic island (230)
Rv1982c	-	-	Non-toxic	Part of a genomic island (230)
Rv2010	No	Non-toxic	Toxic	Induced during hypoxia (199) and in Balb/c mice (273), but repressed during nutrient starvation (18), adaptation to hypoxia (256) and in wild type H37Rv compared to a *phoP* mutant (296). Protein identified in 30-d infected guinea pig lungs (156).
Rv2103c	No	-	Toxic	Part of a genomic island (230)
Rv2231A	-	-	Non-toxic	
Rv2494	No	-	Non-toxic	Induced in the presence of diamide (178); Part of a genomic island (230)
Rv2527	No	Non-toxic	Non-toxic	Repressed by low iron (238) but induced by SDS stress (179)
Rv2530c	No	-	Toxic	
Rv2546	No	Non-toxic	Non-toxic	Induced in Balb/c mice (273) and during treatment with SRI#967, a compound exhibiting strong anti-mycobacterial properties (293)
Rv2548	No	Non-toxic	Toxic	Induced during hypoxia (199) and during macrophage infections (268), but repressed in sputum (92)

Rv2549c	No	Toxic	Non-toxic	Induced during macrophage infections (268) and in the presence of high iron concentrations (238).
Rv2596	-	-	Non-toxic	
Rv2602	No	-	Toxic	Induced in the presence of diamide (178); high concentrations of vancomycin (227) and by SDS stress (179)
Rv2757c	No	Non-toxic	Toxic	
Rv2759c	No	-	Non-toxic	Induced during nutrient starvation (18)
Rv2829c	-	Non-toxic	Toxic	Induced during macrophage infection (230), hypoxia (230, 256) and nutrient starvation (112). Protein identified in 30-d infected guinea pig lungs (156).
Rv2863	No	Non-toxic	Non-toxic	
Rv2872	No	-	Toxic	Part of a genomic island (230)
Rv3180c	No	-	-	Induced in sputum (92)
Rv3320c	No	-	Non-toxic	Repressed during hypoxia (256), by low iron (238) and nutrient starvation (18). Part of a genomic island (230).
Rv3384c	No	-	Toxic	Repressed in sputum (92)
Rv3408	No	-	Toxic	
Rv3697c	No	-	-	Induced during nutrient starvation (18)

-Unknown

1.7 Aim

In light of the observations in Sections 1.5 and 1.6 which suggest that TA modules play a role in genome stabilization, stress adaptation and phenotypic drug tolerance, this study aimed at understanding the individual and collective roles of selected VapBC modules in the stress physiology and drug tolerance of mycobacteria. This was achieved by assessing:

a) The growth inhibitory effects of VapCs in heterologous and native mycobacterial hosts;

b) The effect of *vapBC*-loss on the susceptibility of *vapC*-mediated toxicity

c) The requirements necessary for abrogation of VapC toxicity in mycobacteria;

d) The role of *vapBC*s in mycobacterial growth and survival; and

e) The role of *vapBC*s in the formation of phenotypic drug tolerant mycobacterial persister populations.

2. Materials and Methods

All DNA manipulations were performed according to standard protocols (246). The composition of culture media and solutions except otherwise stated are detailed in Appendix B.

2.1 General recombinant nucleic acid manipulations

2.1.1 <u>Bacterial strains, plasmids and culture conditions</u>

All bacterial strains and cloning vectors used in this study are listed in Table 2.1 and Table 2.2 respectively. Glycerol stocks of bacterial strains were prepared in 33.3% glycerol (v/v) and stored at -70°C.

Table 2.1: General bacterial strains

Bacterial Strain	Genotype	Reference
Esherichia coli DH5α	*supE44 ΔlacU169 hsdR17 recA1 endA1 gyrA96 thi-1 relA1*	Promega, Madison, WI
Mycobacterium smegmatis mc^{2}155	*High-frequency transformation mutant of M. smegmatis ATCC 607*	(265)
Mycobacterium tuberculosis H37Rv	*Virulent laboratory isolate ATCC 25618*	Laboratory collection

Table 2.2: Cloning vectors

Plasmid	Genotype	Reference
pGEM3Z(+)f	*E. coli* cloning vector; Amp^R	Promega
p2NIL	*E. coli* cloning vector; Km^R	(215)
pGOAL17	Plasmid carrying *lacZ* and *sacB* genes as a *Pac*I cassette; Amp^R	(215)
pGOAL19	Plasmid carrying *lacZ*, *sacB* and *hyg* genes as a *Pac*I cassette; Amp^R	(215)
pIJ963	Plasmid carrying *hyg* as a *Bam*HI-*Bgl*II cassette; Amp^R, Hyg^R	(22)
pOLYG	*E. coli*-Mycobacterium shuttle vector; Hyg^R	(204)
pGaa	pOLYG derivative carrying *M. smegmatis* acetamidase promoter (P$_{ami}$) from pAGAN11(213); Hyg^R	Digby Warner, MMRU
pSE100	*E. coli*-Mycobacterium shuttle vector carrying P$_{myc1}$*tetO*; Hyg^R	(70)
pSE0595c	pSE100 carrying Rv0595c under control of P$_{myc1}$*tetO* ; Hyg^R	Diane Kuhnert, MMRU
pMC1s	L5-based integration vector carrying P$_{smyc}$-*tetR*; Km^R	(70)
pMC2m	L5-based integration vector carrying P$_{imyc}$-*tetR*; Km^R	(107)
pTTP1B	Tweety-based integration vector; Amp^R, Km^R	(223)

a) E. coli *DH5α strains*

E. coli cells containing plasmids were grown in Luria-Bertani (LB) broth with the appropriate antibiotics at 37°C overnight, with vigorous shaking (Labcon Shaking Incubator) or at 30°C for 48h in the New Brunswick Scientific Innova 400 incubator shaker. For selection on solid media, *E. coli* containing plasmids were grown on Luria-Bertani agar (LA) containing the appropriate antibiotics at 37°C in the Incotherm Labotec Incubator overnight or at 30°C for 48h in the Heraeus Instrument Incubator. *E. coli* strains carrying large plasmids of ≥ 8000bp were grown at 30°C to avoid plasmid rearrangement.

For selection of *E. coli* cells containing plasmids, the following antibiotics at the indicated concentrations were used: 200µg/ml ampicillin (Amp), 200µg/ml hygromycin (Hyg), 50µg/ml kanamycin (Km) and 10µg/ml gentamycin (Gm). For counter selection of clones carrying *sacB,* 5% w/v sucrose was used. For confirmation of disruption of the *lac*Z- α cassette during cloning or identification of a clone containing the *lac*Z-α cassette 40µg/ml 5-bromo-4-chloro-3-indolyl- β-galactoside (X-gal) and 4µg/ml of its substrate isopropyl-beta-D-thiogalactopyranoside (IPTG) were used.

b) Mycobacterial strains

Mycobacterium smegmatis strains, unless otherwise stated, were grown in Middlebrook 7H9 media supplemented with 0.05% Tween or on Middlebrook 7H10 solid media supplemented with glucose salts (0.085 % NaCl, 0.2 % glucose) and 0.5% glycerol. *M. tuberculosis* strains were grown in Middlebrook 7H9 liquid media containing 0.05% Tween 80 or on Middlebrook 7H10 media, both of which were supplemented with 100ml oleic acid-albumin-dextrose-catalase (OADC) enrichment (Difco) per litre of media. All culturing of *M. tuberculosis* strains was performed in a Biosafety Level 3 laboratory, with manipulations performed in a Class II flow cabinet at a negative pressure of at least 160kPA.

For selection of strains containing plasmids, 50µg/ml Hyg and 25µg/ml Km were used. When gentamicin selection was required, 7H9 media were supplemented with 5µg/ml while on solid 7H10 media this was decreased to

2.5µg/ml. For induction of toxins, anhydrotetracycline (ATc, Sigma) at varying concentrations (0 - 200ng/ml) was used. For counter selection of clones carrying the *sacB* and *lac*Z-alpha cassettes*,* 2% w/v sucrose was included in plates containing 40µg/ml X-gal at a concentration of 40µg/ml and IPTG at 4µg/ml.

2.1.2 DNA extraction

a) Plasmid preparation from E. coli

Briefly, 1ml stationary phase aliquots of overnight *E. coli* cultures were transferred to 1.5ml microcentrifuge tubes. The cells were harvested by centrifugation at room temperature (16168 × g for 1 min) and resuspended in 100µl lysis solution I (50mM glucose, 25mM Tris-Cl pH 8.0, 10mM EDTA). To this suspension, 200µl solution II (1% SDS, 0.2M NaOH) was added and the cells were mixed by inversion and chilled on ice. After 5 min, 150µl neutralisation solution III (3M Potassium acetate, pH5.5) was added to the cells. The suspension was mixed vigorously and incubated on ice for 10 min. Cell debris was removed by centrifugation (16168 × g for 10 min), and the supernatant was transferred to a fresh microcentrifuge tube containing 2µl of 10µg/ml RNaseA, and incubated for 20 min at 42°C. Plasmid DNA was then precipitated by addition of 350µl isopropanol, incubation for 10 min at room temperature and centrifugation (16168 × g for 10 min). The DNA pellet was washed with 70% Ethanol and dried at 45°C in a vacuum centrifuge (SpeedVac, Savant, Farmingdale, NY, USA). The DNA was resuspended in 20 - 30µl sterile distilled water (sdH$_2$0).

For large scale DNA extractions, *E. coli* cultures were grown in 50ml LB, overnight with shaking, and cells were harvested by centrifugation in the Beckmann J2-21 centrifuge (3901 × g for 10 min). The DNA extraction method was as described above except that the solution volumes were increased by a factor of 10. The DNA was resuspended in a final volume of 300µl sdH$_2$O and then purified by addition of equal volumes of phenol: chloroform (1:1 v/v). The aqueous phase of the solution was added to an equal volume of chloroform: isoamyl alcohol (24:1 v/v) and centrifuged (16168 × g for 2 min). The plasmid DNA was then re-precipitated by addition of 1/10 volumes 5.3M sodium acetate

pH 5.2 and 2.5 × volumes 100% ethanol to the aqueous phase. The solution was incubated at -20°C for 1h and the precipitated DNA was collected by centrifugation (16168 × g for 20 min). The DNA pellet was further washed with ice-cold 70% ethanol to remove any residual salts, dried in a vacuum centrifuge and resuspended in 50 - 200µl sdH$_2$0.

b) Chromosomal extraction from mycobacteria

Mycobacterial chromosomal DNA was isolated using a modified cetyltrimethylammonium bromide (CTAB; ICN Biomedicals, Aurora, Ohio) method (160). Briefly, mycobacterial cells were harvested and resuspended in 500µl TE buffer (10mM Tris-HCl pH 8.0, and 1mM EDTA). The cells were heat killed (65°C for 10 min for *M. smegmatis* and 95°C for 5 min for *M. tuberculosis*), harvested by centrifugation (16168 × g for 5 min) and resuspended in 500µl TE buffer. To this 50µl lysozyme (10mg/ml) was added and incubated at 37°C overnight. A solution of 70µl 10% SDS and 6µl proteinase K (10mg/ml) was then added and the mixture incubated at 65°C for 2h. One hundred microlitres of a 5M solution of sodium chloride and 80µl pre-warmed CTAB/NaCl mix (10% CTAB made in 0.7M NaCl) was added to the sample and incubated at 65°C for a further 10 min. An equal volume of chloroform:isoamyl alcohol (24:1 v/v) was added to remove residual proteins. Subsequent to centrifugation (16168 × g for 10 min) the aqueous phase containing the DNA was precipitated by addition of 1/10 volume of 5.3M sodium acetate and 2.5 × volumes 100% ethanol, and incubation at -20°C for 1h. The DNA was then pelleted by centrifugation (16168 × g for 20 min), washed with ice-cold 70% ethanol, dried in a vacuum centrifuge and resuspended in sdH$_2$O.

2.1.3 <u>DNA manipulations</u>

a) Restriction enzyme digestions

All restriction enzymes were obtained from New England Biolabs, Inc., Roche Applied Science, or Amersham. Unless otherwise stated by the manufacturer, all digests were performed at 37°C with the appropriate buffer.

Plasmid DNA of up to 5µg was digested in 20µl reaction volumes for between 1 - 2h and up to 10µg mycobacterial chromosomal DNA was digested overnight in 50µl reaction volumes. DNA fragments were then separated on agarose gels using electrophoresis (See section 2.1.4).

b) Modification of 5' overhangs

5'-overhangs obtained subsequent to restriction digests were filled in when warranted using the DNA polymerase I, large (Klenow) fragment and dNTPs from Invitrogen as per manufacturer's instructions. The reaction mix was incubated on ice for 20 min and terminated by a phenol extraction.

c) Phosphorylation of DNA

Phosphorylation of blunt PCR products, to insert phosphates that allowed for ligation into the dephosphorylated vector, was performed using polynucleotide kinase (Roche Applied Science), as per the manufacturer's instructions for 30 min at 37°C. The reaction was stopped by separation on an agarose gel.

d) Dephosphorylation of 5'ends of plasmid DNA

Ensuing plasmid digestion, the 5'-phosphate of linearised vector DNA was removed by treatment with either Antarctic Alkaline Phosphatase (AAP) or Shrimp Alkaline Phosphatase (SAP), to prevent vector religation. Dephosphorylation was performed according to the manufacturer's instructions (Roche Applied Science) for 1h at 37°C after which the enzyme was heat inactivated for 20 min at 65°C.

e) Ligation reactions

DNA ligations were performed using either the Fast-Link^TM ligation kit (Epicentre ® Biotechnologies) or the T4 DNA Ligase (Roche Applied Science), as per instructions from the manufacturer. The ligation reactions were then used for transformations into *E. coli* DH5α cells (See section 2.1.6).

2.1.4 <u>Agarose gel electrophoresis</u>

General electrophoretic techniques were used to separate out DNA fragments (245, 246). For the separation of high molecular weight DNA fragments, 0.8% - 1% agarose gels, made in $1 \times$ TAE buffer (1mM EDTA, 40mM Tris-acetic acid pH8.5) were used. For low molecular weight DNA fragments of ≤1kb, 2% agarose gels were used.

All gels contained 0.5µg/ml ethidium bromide and the DNA samples were loaded with a tracking dye (0.025% bromophenol blue in 30% glycerol). Lambda DNA molecular weight markers (III, IV and V; Roche Applied Science) were used to assess DNA fragment sizes. The agarose gels were electrophoresed between 80 - 100V in a Mini-Sub Cell GT minigel horizontal submarine unit (BIO-RAD) and visualized under UV-light using the Gel Doc 2000 system (BIO-RAD).

2.1.5 <u>DNA fragment recovery from agarose gels and quantification</u>

The required DNA fragment was excised from the gel and purified using the Nucleospin kit (Macherey-Nagel) as per manufacturer's instructions. Briefly, the excised gel fragment was melted, loaded onto a provided column, and washed. The DNA was then eluted using pre-warmed sterile distilled water.

The DNA was quantified either on agarose gels by comparison to DNA molecular weight markers or on the NanoDrop ND-1000 Spectrophotometer (Thermo Scientific).

2.1.6 <u>Transformation of bacteria</u>

a) Chemical transformation of E. coli

E. coli DH5α chemically competent cells were used for transformation of plasmids. Rubidium chloride cells were prepared as detailed in the protocol obtained from Dr P Stolt. Briefly, 1ml of a stationary phase overnight culture was inoculated in 100ml LB and grown to an OD_{600} of between 0.48 - 0.55. The cells

were chilled on ice for 15 min and harvested (3901 × g for 5 min at 4°C). The pellets were resuspended in 20ml TfbI solution (30mM potassium acetate, 100mM rubidium chloride, 10mM calcium chloride, 50mM manganese chloride, and 15% v/v glycerol - pH 5.8), and chilled on ice for 15 min. The cells were re-harvested (3901 × g for 5 min at 4°C), resuspended in 2ml TfbII solution (10mM MOPS, 75mM calcium chloride, 10mM rubidium chloride and 15% v/v glycerol-pH 6.5) and 500µl aliquots were flash-frozen in ethanol and stored at -80°C until further use.

For transformations, *E. coli* DH5α competent cells were thawed on ice and 100µl cells used per transformation. Up to 1µg plasmid DNA was incubated with the cells on ice for 1h, heat-shocked for 90s at 42°C and chilled on ice for 2 min. Four volumes of 2TY was then added to rescue the cells at 37°C for 1h (245, 246). These were plated on LA media containing the appropriate antibiotics, and incubated 1 - 2 days at 37°C.

b) Electroduction of E. coli

Electrocompetent *E. coli* cells were used for electroductions. These cells were prepared as a modification of the protocol obtained from the BIO-RAD Gene Pulser manual. Briefly, 500µl of an overnight culture of *E. coli* DH5α was inoculated in 50ml 2TY broth and grown to an OD_{600} of 0.6 - 0.9. The cells were then chilled on ice for 20 min and harvested by centrifugation (3901 × g for 15 min at 4°C). The pellet was resuspended in 20ml ice-cold sterile distilled water and washed by centrifugation (3901 × g for 15 min at 4°C). A further wash step was performed in 10ml ice-cold sterile distilled water. The pellet was then resuspended in 2ml ice cold 10% glycerol and harvested (3901 × g for 10 min at 4°C). The resulting pellet was resuspended in 100µl ice-cold 10% glycerol.

For electroductions, a single *M. smegmatis* colony was dispersed in 20µl cold 10% glycerol and chilled on ice for 10 min. To this, 70µl of the electrocompetent *E. coli* DH5α was added and the suspension transferred to a 0.1cm electroporation cuvette. The cells were pulsed in an electroporator with the following conditions: 1.8kV, 25µF and 200Ω. The electroporated cells were

rescued for 1h at 37°C with 400μl 2TY. The cells were subsequently plated on LA media containing the appropriate antibiotics, and incubated 1 - 2 days at 37°C.

c) Transformation of mycobacteria by electroporation

All mycobacterial electroporations were carried out as previously described (103, 160), and these are briefly described below.

Electroporation into *Mycobacterium smegmatis*

One millilitre of a stationary phase *M. smegmatis* culture was inoculated in 100ml LB containing 0.05% Tween80 and grown to an OD_{600} of 0.4 - 0.7. The cells were harvested by centrifugation (2360 × g for 10 minutes at 4°C) and the pellet washed twice by gentle resuspension in 10ml ice-cold 10% glycerol and centrifugation at 2360 × g for 10 min at 4°C. The pellet was resuspended in 1ml ice-cold 10% glycerol and these competent cells were used immediately.

Up to 5μg plasmid DNA was added to 400μl *M. smegmatis* competent cells. This was transferred to a 0.2cm electroporation cuvette and pulsed using the following conditions: 2.5kV, 25μF and 1000Ω. The cells were rescued immediately with 800μl 2TY for at least 3h at 37°C. These were plated on Middlebrook 7H10 media containing the appropriate supplements and antibiotics, and incubated for 3 - 7 days at 37°C before scoring CFUs.

Electroporation into *Mycobacterium tuberculosis*

Electroporation into *M. tuberculosis* was performed in the same manner as with *M. smegmatis* with the following exceptions: a final concentration of 1.5% glycine was added to the *M. tuberculosis* cells 16h prior to harvesting; all manipulations were performed at room temperature and the plasmid DNA was UV-irradiated (100 mJ/cm^2) before electroporation into the cells. Subsequent to electroporation, the cells were rescued at 37°C overnight. The following day the cells were harvested, resuspended in fresh 7H9 media and spread on Middlebrook 7H10 media containing the appropriate supplements and antibiotics. The plates were incubated for at least 21 days at 37°C before scoring CFUs.

2.1.7 <u>Polymerase Chain Reaction (PCR)</u>

All preliminary and screening PCRs were performed using the Roche FastStart kit (Roche Applied Science), while for the amplification of fragments required for cloning, Phusion High-Fidelity DNA polymerase (Finnzymes) which has a low error rate of 4.4×10^{-7} was used. The reactions were performed as per manufacturer's instructions.

For reactions using the Roche FastStart Taq DNA polymerase, 20 - 50µl reactions were set up containing: $1 \times$ reaction buffer, up to 250ng plasmid or genomic DNA, 200µM of each dNTP, 0.5 - 1.0 µM of each primer, 1.5mM $MgCl_2$, $1 \times$ GC rich solution and 2U/50µl of the DNA polymerase. DNA amplification was performed using the following cycling parameters: denaturation at 94°C for 5 min; followed by 30 cycles of denaturation at 94°C for 60s, annealing for and an extension at 72°C for 60s; with a final extension at 72°C for 7 min.

For reactions using the Phusion High-Fidelity DNA polymerase (Finnzymes), 20 - 50µl reactions were set up to contain: $1 \times$ reaction buffer, up to 250ng plasmid or genomic DNA (gDNA), 200µM of each dNTP, 0.5 µM of each primer, 3% DMSO and 0.02U/µl of the DNA polymerase. DNA amplification was then performed using the following cycling parameters: denaturation at 98°C for 30s; followed by 25 - 35 cycles of denaturation at 98°C for 10s, annealing for 30s, and extension at 72°C for 30s/1kb; with a final extension at 72°C for 7 min.

For each amplification reaction, three control reactions (a no DNA control reaction; a reaction containing only the forward primer and one containing only the reverse primer) were included to elucidate the presence of genomic contamination and/or non-specific DNA amplification if present.

All polymerase chain reactions were performed using the MyCycler™ thermal cycler (BIO-RAD) or the PCR Express (Hybaid) machines with oligonucleotide primers (Sections 2.2, 2.3, 2.6 and 2.8) obtained from Inqaba Biotech Ltd.

2.1.8 <u>Sequencing</u>

Sequencing, which was outsourced to either the Department of Molecular and Cell Biology (University of Cape Town), Inqaba Biotech Ltd (South Africa) or the DNA Sequencing Facility of Stellenbosch University, was performed using the Big Dye terminator v3.1 Cycle Sequencing kit and Bioline Half Dye Mix. The EditSeq and SeqMan^{TM} modules of the Lasergene suite of programs were used to analyse the sequencing data.

2.1.9 <u>Southern blot analyses</u>

For the detection of specific DNA sequences within a complex DNA mixture, Southern blotting was performed using radioactively or non-radioactively labelled probes.

a) Electroblotting

Approximately 10µg of genomic DNA was digested overnight at 37°C with the appropriate restriction enzyme and the DNA fragments were separated on a 0.8% agarose gel at 80V. The DNA was initially depurinated by treating the agarose gel in a 0.25M HCl solution for 15 min, then denatured by soaking in a 0.5M NaOH/1.5M NaCl solution for 15 min and subsequently equilibrated in 1 × TBE buffer (Tris-Borate-EDTA pH 8.0, Sigma). The agarose gel was then overlayed with a Hybond^{TM} – N nitrocellulose membrane, sandwiched between two pre-soaked 3MM Whatmann filter papers, and two pre-soaked sponges. After ensuring no air bubbles were present, this "sandwich" was placed carefully in a TE 22 Mini Transphor cassette and the cassette transferred to a TE 22 Mini Transphor unit (Hoefer) containing 1 × TBE buffer. The DNA was then transferred to the nitrocellulose membrane (0.5A for 2h at 4°C), and cross-linked by irradiation at 1200mJ/cm^{2} in a UV Stratalinker 1800 (Stratagene).

b) Radioactive labelling and hybridization of probe

The random primed labelling kit (Roche Applied Science) was used to incorporate the [^{32}P]-dCTP radioactive isotope, as per manufacturer's protocol. The reaction was terminated by addition of 50µl TE buffer (pH 8.0) and the labelled probe was eluted by fractionation through two pre-equilibrated Sephadex G-25 columns. This ensured that unincorporated nucleotides were removed, as these bound to the columns. The eluted probe was then used immediately.

Subsequent to cross-linking the DNA onto nitrocellulose membranes, the membranes were pre-hybridised in pre-hybridisation solution (0.5% SDS, 6 × SSC, 5 × Denhardts and 50% deionised formamide) at 42°C with 10µg/ml heat-denatured salmon sperm DNA (Roche Applied Science) in Techne Hybridizer HB-1 roller bottles. After 2h, the radioactively labelled probe was denatured (95°C for 10 min), added to the pre-hybridisation buffer and hybridisation was allowed to occur overnight at 42°C. The membrane was subsequently washed twice with wash solution I (2 × SSC, 0.1% SDS), once with wash solution II (0.5 × SSC, 0.1% SDS), and once with wash solution III (0.1 × SSC, 0.1% SDS), with all four wash steps performed at 42°C for 15 min. Finally, the nitrocellulose membrane was washed with wash solution IV (0.1× SSC, 1% SDS) at 65°C for 30 min, and exposed to X-ray film at -80°C for 24 - 72h.

c) Non-radioactive labelling and hybridization of probe

For the non-radioactive labelling of probes, the alkali-labile digoxigenin (DIG)-dUTP was incorporated either by PCR or by random primed labelling, as per the manufacturer's instructions (Roche Applied Science).

Hybridisation of the probe to the membrane was implemented as detailed in the DNA High Prime DNA labelling and Detection Starter Kit II insert (Roche Applied Science). Briefly, the membrane was pre-hybridised with 12ml DIG Easy Hyb solution (1h at 52°C) in Hybaid HB-OV-BM roller bottles incubated in a hybridization oven (Hybaid Micro-4). The heat-denatured probe (95°C for 10 min) was added to the pre-hybridisation solution and hybridization was allowed to occur overnight at 52°C. The membrane was then washed twice with Solution I (2

× SSC, 0.1% SDS) at room temperature for 5 min and then once with Solution II (0.5 × SSC, 0.1% SDS) at 65°C for 30 min.

Following these stringency washes, the labeled DNA was detected as per the manufacturer's protocol (Roche Applied Science). Briefly, detection of the DIG-labelled hybrids was achieved by dephosphorylation of the CSPD substrate upon addition of a specific DIG alkaline phosphatase-conjugated antibody, which resulted in chemiluminescence at 477 nm. This enabled visualization on X-ray film after 30 min - 4h incubation at room temperature.

2.2 Construction of vectors for conditional expression of toxins and antitoxins in mycobacteria

2.2.1 Construction of toxin-expressing vectors

The toxins Rv2546, Rv2548, and Rv2549c were PCR amplified from *M. tuberculosis* H37Rv, and the toxin MSMEG_1284 was PCR amplified from *M.smegmatis* using the oligonucleotides listed in Table 2.3. A standardized concensus ribosome binding site (GGAAG/A) was incorporated to optimize the yield of the protein expressed. The PCR amplified toxins were cloned downstream of the $P_{myc1}tetO$ promoter-operator element of pSE100 to generate a toxin-expressing vector pSEvapC. The toxins Rv2546, Rv2548, and Rv2549c were expressed as *Bam*HI-*Hind*III fragments while MSMEG_1284 was cloned into the *Pvu*II site of pSE100. A pSE100 vector expressing the whole Rv2550c_49c operon was generated using the antitoxin specific primer Rv2550cF and the toxin primer Rv2549cR.

Table 2.3: Oligonucleotides used for generation of toxin expressing vectors[a]

Toxin	Primer	Sequence	Expected Size
Rv2546	Rv2546F	ACTG<u>GGATCC</u>**GGAAG**GTGATGGTGTTCTGCGTC	498bp
	Rv2546R	TGAT<u>AAGCTT</u>GGGTCACCTGAGTCCGCATG	
Rv2548	Rv2548F	ACTG<u>GGATCC</u>**GGAAG**GTCTGGCGTGAAGCTGAT	428bp
	Rv2548R	CGCG<u>AAGCTT</u>GCTGATGCCCCAGGGAGT	
Rv2549c	Rv2549cF	TGAT<u>GGATCC</u>**GGAAA**GCACGAATGATCTTC	500bp
	Rv2549cR	TGTA<u>AAGCTT</u>CAACGCAACGCAGCCCTGT	
Rv2550c	Rv2550cF	CGTA<u>GGATCC</u>GGAGGAACAGCATTATGCTAGTGG	746bp
MSMEG_1284	MSMEG_1284F	TTCT<u>AAGCTT</u>**GGAAG**GTCCTGATGGTTATCGAC	442bp
	MSMEG_1284R	CGAT<u>GGATCC</u>TGACCTGAATTCTGACCT	

[a]The highlighted sequence represents the incorporated ribosome binding sites and the underlined sequence represents incorporated restriction enzyme sites.

For regulated-toxin expression, all these constructs, unless otherwise stated, were co-electroporated in *M. smegmatis* or *M. tuberculosis* with either the intergrative *tetR*-containing plasmid pMC1s, whose tetracycline repressor is expressed under the control of the strong tetracycline promoter (P_{smyc}-*tetR*) or the intergrative *tetR*-containing plasmid pMC2m, whose tetracycline repressor is expressed under the control of the tetracycline promoter P_{imyc}-*tetR* of intermediate strength.

2.2.2 <u>Construction of vectors for uncoupled regulated expression of toxins and antitoxins</u>

a) Construction of the antitoxin expressing integrating vectors

The integrative pMC1s vector was digested with *Not*I and the 4kb vector backbone was re-ligated to generate the vector pMC1r. The vector pGaa was digested with *Pvu*II and *Cla*I, and the 4.4kb fragment, containing the acetamidase promoter, was then cloned into the *Pvu*II/*Cla*I site of pMC1r to generate the pMAP vector which integrates at the L5 tRNA[Gly] site of the mycobacterial chromosome.

The antitoxins Rv2550c, Rv0595c and Rv2830c were PCR amplified from genomic H37Rv DNA with the primer pairs Rv2550cF/Rv2550cR, 0596ACEfwd/0596ACErev and 2830ACEfwd/2830ACErev respectively (Table 2.4). The PCR products were digested with *EcoR*I and *Cla*I and then cloned into the *EcoR*I/*Cla*I site of pMAP to generate the vectors pMAP2550c, pMAP0595c and pMAP2830c respectively.

Table 2.4: Oligonucleotides used for generation of antitoxin expressing vectors[a]

Antitoxin	Primer	Sequence	Expected Size
Rv0596c	0596ACE fwd	TAGT<u>GAATTC</u>GTGAGGAATCGTAGCATGTCTGCTA	302bp
	0596ACE rev	TCAC<u>ATCGAT</u>TCATACGTTCACCACCGCACA	
Rv2550c	Rv2550c fwd	CGTA<u>GAATTC</u>GGAGGAACAGCATTATGCTAGTGG	314bp
	Rv2550c rev	GCCC<u>ATCGAT</u>TAAAGTGCAGCCCAGAA	
Rv2830c	2830ACE fwd	TACT<u>GAATTC</u>GTGAGGAAAGAAAAATGACCGCTACG	256bp
	2830ACE rev	TGCA<u>ATCGAT</u>ACTATGTCATGAAACGTTCCACG	

[a] The underlined sequence represents incorporated restriction enzyme sites.

b) Construction of the toxin expressing integrating vectors

To construct a toxin expressing integrating vector, it is imperative that the vector carries a different resistant cassette from the antitoxin expressing integrating vector. It is also essential that this vector should integrate at a different locus. As such, the Km-resistant Tweety vector pTT1B (223), which integrates at a tRNA^{Lys} gene distinct from the *attB* locus where the pMAP vector would integrate, was modified by replacing the Km-resistance cassette with a Gm-resistance cassette. This was done by digesting pTT1B with *Hind*III and re-ligation of the vector backbone to generate pTT1B*. The Gm-resistant plasmid pML10 (158) was digested with *Pst*I, and the 930bp fragment containing the Gm-resistance cassette was cloned into the *Pst*I site of pTT1B* to generate the vector pTTBG.

Another prerequisite for the toxin expressing integrating vector is that it must contain both a tetracyline repressor and the promoter-operator element $P_{myc1}tetO$ to allow for inducible toxin expression. To generate the plasmid with the tetracycline repressor, the integrative pMC1s vector was digested with *Not*I and the 1kb fragment containing the P_{smyc}-*tetR* was cloned into the *Sma*I site of pTTBG to produce pTTBGs. For incorporation of $P_{myc1}tetO$ and the toxin to pTTBG, the toxin expressing vectors pSE2549c, and pSE0595c were digested with *Spe*I/*Cla*I. The fragments containing the operator and toxins were cloned into the *Eco*RI site of pTTBGs thus generating the Gm-resistant toxin-expressing integrating vectors, pTTvapC.

Table 2.5: Cloning vectors used for the uncoupling system

Plasmid	Genotype	Reference
pTTP1BG	Derivative of pTTP1B with Km^R marker replaced by Gm^R marker from pML10 (158); Gm^R	Garth Abrahams, MMRU
pTTP1BGs	Derivative of pTTP1BG carrying P_{smyc}-*tetR* from pMC1s; Gm^R	This study
pTT2549c	pTTP1BGs derivative carrying $P_{myc1}tetO$::Rv2549c; Gm^R	This study
pTT0595c	pTTP1BGs derivative carrying $P_{myc1}tetO$::Rv0595c; Gm^R	This study
pMAP	Derivative of pMC1r carrying P_{ami} cloned as a 4.4-kb *Pvu*II/*Cla*I fragment from pGaa; Km^R	This study
pMAP2550c	Integration vector carrying P_{ami}::Rv2550c; Km^R	This study
pMAP2830c	Integration vector carrying P_{ami}::Rv2830c; Km^R	This study
pMAP0596c	Integration vector carrying P_{ami}::Rv0596c; Km^R	This study

For uncoupled regulated expression of both toxins and antitoxins, these constructs, unless otherwise stated, were co-electroporated in *M. smegmatis* in varying combinations as reported in Section 3.3.

2.3 Site-directed mutagenesis of a conserved aspartic acid residue of Rv2549c

A single D5A mutation was introduced in Rv2549c using the Megaprimer method (262). Briefly, the megaprimer was produced by PCR with Rv2549cR and the mutagenic F2*SDM primer CATGATCTTCGTC**GCC**ACGTCCTTCTGGG), using pSE2549c as the template DNA. For generation of pSE2549c[D5A] the

megaprimer and the F1_SDM primer (GCTAAGCAGAAGGCCATCC) were used in a second round of PCR, and the PCR product (Rv2549c^{D5A}) generated from the pSE2549c template DNA was then cloned into the *Bam*HI/ *Hind*III site of pSE100 to generate pSE2549cM.

2.4 Effect of toxin over-expression on mycobacterial growth and viability

2.4.1 Effect of constitutive ectopic toxin expression on mycobacteria

The effect of constitutive ectopic toxin expression on mycobacteria was assessed by electroporating the pSEvapC constructs in the absence of pMC1s and enumerating the number of transformants on 7H10 Middlebrook plates containing Hyg.

2.4.2 Effect of regulated toxin expression on mycobacteria

To assess regulated toxin expression, mycobacteria were first co-electroporated with the toxin-expressing vector and pMC1s or pMC2m, and transformants selected on 7H10 media containing Km and Hyg.

The effect of regulated toxin expression on *M. smegmatis* growth and viability was assessed on solid and liquid media. Briefly, for effect of toxin expression on solid media, *M. smegmatis* transformants were grown in 7H9 media containing Hyg and Km to late log-phase (OD$_{600}$ ~ 1). Ten-fold serial dilutions of the cultures were then spotted onto 7H10 plates containing varying concentrations of ATc (0 - 50ng/ml), and these were incubated at 37°C. Growth was assessed after 24h and 48h.

In liquid media, the effect of toxin expression was assessed by growing *M. smegmatis* transformants in 7H9 media containing Hyg and Km to early log-phase (OD$_{600}$ ~ 0.1 - 0.4), and diluting to OD$_{600}$ of 0.1 with fresh pre-warmed 7H9 antibiotic containing-media. The cultures were then split into two equal aliquots, one of which was treated with ATc at a concentration of 25ng/ml. Growth and viability was assessed by 2h OD$_{600}$ measurements and 4h CFU enumeration over a 25h period.

The effect of regulated toxin expression on *M. tuberculosis* was only assessed in liquid media. This was performed exactly as with *M. smegmatis* as described above, with the following exceptions: The cultures were diluted to an OD_{600} of 0.04 and left to grow overnight before splitting into two equal aliquots; growth and viability was assessed by 24h OD_{600} measurements and CFU enumerated over a period of 8 days.

2.5 Effect of regulated ectopic toxin expression on the drug tolerance of mycobacteria

Pre-cultures of H37Rv strains containing pMC1s together with pSE2829, pSE2546 and pSE2549c plasmids were inoculated in middlebrook 7H9 media containing Hyg and Km and grown with rolling overnight at 37°C. These cultures were split equally, and to one culture ATc at a concentration of 25ng/ml was added to induce toxin expression. After 24h incubation (rolling at 37°C), three equal aliquots were dispensed into separate receptacles. To the uninduced cultures, no antibiotics, 8µg/ml ofloxacin (10 × MIC), and 20µg/ml chloramphenicol (CM) + 8µg/ml ofloxacin after 1h of CM treatment were added to each aliquot. To the induced cultures, 8µg/ml ofloxacin and no antibiotics were added to each aliquot. The aliquots were incubated at 37°C for 7d and CFUs assessed by duplicate plating on 7H10 plates (See Figures 3.37 & 3.39 for schematic representation of assay).

2.6 Construction of knockout mycobacterial strains

Knockout mutant mycobacterial strains were generated by homologous recombination, as previously described (103). Briefly, suicide vectors p2Δ2545_50cKO and p2ΔSM1283_84KO, for the knockout of Rv2545-Rv2550c and MSMEG_1283-MSMEG_1284, were generated by PCR amplification of the upstream and downstream regions of the genes of interest from genomic H37Rv and *M. smegmatis* mc^{2}155 DNA respectively. Primers designed to amplify the upstream regions contained *Hind*III and *Bgl*II restriction sites, while the downstream amplification primers had *Bgl*II and *Asp*718 restrictions sites (Table 2.6). Each amplicon was cloned into the *Sma*I site of pGEM3Zf(+) vector and

sequenced before sub-cloning via 3-way cloning into the *Hind*III and *Asp*718 sites of p2NIL. The *hyg* resistance cassette from pIJ963 was cloned into the *Bgl*II site of p2NIL2545_50c to generate a marked deletion allele. The *lacZ-sacB* cassette from pGOAL17 (for the marked suicide vector p2NIL2545_50c::hyg) and pGOAL19 (unmarked suicide vector) were cloned into the *Pac*I site of p2NIL2545-50c and p2NIL1283-84 to create the marked suicide vector p2Δ2545_50cKO::hyg, and the unmarked suicide vectors p2Δ2545_50cKO and p2ΔSM1283_84KO respectively. These vectors were electroporated into H37Rv and mc^{2}155 (Section 2.1.6) and mutants Δ*Rv2545_Rv2550c* and Δ*MSMEG_1283-MSMEG_1284* were obtained by homologous recombination using a two step selection method as previously described by Gordhan and Parish (103).

Table 2.6: Oligonucleotides used for generation of knockout vectors[a]

Gene	Primer	Sequence	Expected Size	Deletion Size
Rv2545-Rv2550c upstream region	Forward	TGAT<u>AAGCTT</u>GATGACGATCTCGCGCAG	2052bp	2415bp
	Reverse	TAAT<u>AGATCT</u>GAGATATATGCATTGGA		
Rv2545-Rv2550c downstream region	Forward	ATGT<u>AGATCT</u>GCAGCCTTTTCACA	1776bp	
	Reverse	TTAT<u>GGTACC</u>AGGGACTATCAG		
MSMEG1283-MSMEG1284 Upstream region	Forward	TGAT<u>AAGCTT</u>GCTCATACGGCCAGGC	965bp	378bp
	Reverse	TAAT<u>AGATCT</u>CTGGCCAGCCGGTCGG		
MSMEG1283-MSMEG1284 Downstream region	Forward	CGCCG<u>AGATCT</u>GTGGTTGCATCGC	1099bp	
	Reverse	TGAT<u>GGTACC</u>GAGCAGTGGCTACTGG		

[a] The underlined sequence represents incorporated restriction sites.

2.7 Role of VapCs during mycobacterial stress

To determine whether VapCs play a role during mycobacterial stress, nitrosative, heat, genotoxic and cell wall stresses were applied to the *M. smegmatis* wild type and mutant Δ*MSMEG_1283-MSMEG_1284* strains.

The effect of cell wall stress was assessed as described by Vandal and colleagues (284). Briefly, 10μl of 10-fold dilution series of mid-log phase (OD_{600} ~ 0.6) cultures of wild type *M. smegmatis* and Δ*MSMEG_1283-MSMEG_1284* were spotted onto 7H10 plates containing 0.01% and 0.02% SDS. 7H10 plates with no SDS were used as controls.

The effect of nitrosative stress was assessed as described by Firmani and Riley (77). Briefly, mid-log phase cultures (OD_{600} ~ 0.6) were diluted 1:10 and incubated for 24h in 7H9 (pH 5.3) supplemented with sodium nitrite at concentrations up to 48mM. Mycobacterial survival was assessed by scoring CFU/ml on 7H10 plates after a 3-day incubation period at 37°C.

The effect of heat stress was assessed following a modified protocol from Stewart and co-workers (270). Briefly, 1ml of late log-phase cultures (OD_{600} ~ 0.8) were aliquoted in two eppendorf tubes. One was incubated at 37°C and the other at 45°C for 45h. CFUs were then scored for survival on 7H10 plates after 3d at 37°C.

For genotoxic stress, as previously decribed (192), mid-log phase cultures (OD_{600} ~ 0.6) were serially diluted and plated on 7H10 plates containing concentrations of mitomycin C ranging from 0mM to 0.1mM. CFUs were scored for survival after a 3-day incubation period at 37°C.

2.8 RNA Isolation and reverse transcription

RNA was isolated as a modification of the Downing and colleagues protocol (61). Briefly, 50ml logarithmic phase cultures were harvested at $2360 \times g$ for 20 min at room temperature. The pellets were resuspended in 1ml TRIzol (Gibco-BRL), and transferred to Lysing Matrix B tubes (Qbiogene). The cells were ribolysed three times for 20s at speed 6 using the Savant Fastprep FP120

ribolyser, with 2 min intervals between pulses when the cells were cooled on ice. The sample was then centrifuged at top speed for 45s, and the TRIzol solutions were transferred to a clean eppendorf. One hundred microlitres 1-bromo-3-chloropropane (BCP) was added to the solution for phase separation. The solution was inverted rapidly for 30s and centrifuged at top speed for 5 min. The aqueous phase containing the nucleic acids was transferred to a clean eppendorf tube and RNA was precipitated using the lithium chloride precipitation method as per manufacturer's instructions (Ambion).

Each RNA sample was then treated two to four times with Turbo DNase (Ambion) as per manufacturer's instructions to remove any contaminating DNA. The samples were then run on a 2% agarose gel containing 0.1% SDS to assess the quality of the purified RNA. The RNA was quantified using the NanoDrop ND-1000 Spectrophotometer (Thermo Scientific), and reverse transcription (RT) reactions were subsequently performed using the *C. therm.* Polymerase RT-PCR system (Roche) according to the manufacturer's instructions. Briefly, 50µl reactions were set up containing: 1 × reaction buffer, up to 1µg RNA, 25mM of each dNTP, 0.5µM of each primer, 7% DMSO, 5mM DTT, 20U RNase Inhibitor, and 2µl of the *C. therm* polymerase mixture. The RT reaction was performed by incubating the samples in a thermocycler equilibrated at 60°C for 30 min, and the primers used for RT-PCR analysis (Table 2.7) were designed using Primer 3 software (http://frodo.wi.mit.edu/cgi-bin/primer3/primer3_www.cgi). The DNA amplification was then performed using 2µl of the cDNA generated during the RT reaction. The cycling parameters used were as shown in Table 2.8.

Table 2.7: Oligonucleotides used to detect mRNA expression of toxins

Toxin	Primer	Sequence	Expected Size
Rv2546	Rv2546RTF	TATACCAGTCGGTGCCGAAA	143bp
	Rv2546RTR	ACACGATGGTGCCTGAAAGT	
Rv2549c	Rv2549cRTF	TCTTCCAGGTCGGCTGTTAC	138bp
	Rv2549cRTR	GATGACCTCCAACCATGTCC	
Rv2550c	Rv2550cRF1	CATGTGAAAAGGCTGCAGAT	218bp
	Rv2550cRR1	TGCTTTCCGTAAACCACGTC	
M. smegmatis sigA	MSM SigAF	GGGCGTGATGTCCATCTCCT	122bp
	MSM SigAR	GTATCCCGGTGCACATGGTC	

Table 2.8: Cycling Parameters used to amplify cDNA

Cycle	Cycling Condition	Number of cycles
1	94°C for 10 minutes	1
2	94°C for 30 seconds	14
	65°C (-0.5°C/cycle) for 30 seconds	
	72°C for 30 seconds	
3	94°C for 30 seconds	24
	57°C for 1 minute	
	72°C for 30 seconds	
4	Hold at 4°C	∞

2.9 Protein extraction, quantification and detection

For protein analyses, Rv2546, Rv2549c and Rv2549c^{D5A} were C-terminally tagged with a triple FLAG sequence by Dr Edith Machowski. Here, the gene of interest was amplified by PCR to incorporate the standardized consensus ribosome binding site (GGAAG/A) at the N-terminus in order to optimize the yield of expressed protein. The PCR amplification also incorporated a triple (3×) FLAG sequence (Asp-Tyr-Lys-Asp-His-Asp-Gly-Asp-Tyr-Lys-Asp-His-Asp-Ile-Asp-Tyr-Lys-Asp-Asp-Asp-Asp-Lys) at the C-terminus, followed by the native

stop codon. This amplicon was cloned into the *BamHI*/*Hind*III site of pSE100 under the control of the $P_{myc1}tetO$ promoter-operator element. The resulting FLAG-tagged construct, pSEvapC_FLAG, was co-electroporated with pMC1s into *M. smegmatis* to allow for conditional gene expression upon addition of ATc. The supernatants and pellets from whole-cell extracts of ATc-induced *vs*. uninduced *M. smegmatis* strains were run on SDS-PAGE gels, and blotted onto nitrocellulose membranes before detection of the FLAG-tagged fusion protein by an anti-FLAG antibody (Figure 3.17).

M. smegmatis cells containing triple FLAG-tagged VapC fusion proteins were grown in 50ml cultures to mid log-phase ($OD_{600} \sim 0.3 - 0.5$) and split in two equal 25ml volumes. One aliquot was treated with ATc (50ng/ml) and the other served as the uninduced control. After 3h induction, cells were harvested and resuspended in 250 µl of Bacterial Protein Extraction Reagent (B-PER II Reagent, Thermo Scientific) containing complete mini protease inhibitor cocktail (Roche). The cells were lysed three times for 20s at speed 6 using the Savant Fastprep FP120 ribolyser, with 5 min intervals between pulses when the cells were cooled on ice. The protein concentration of each sample was quantified using the Bradford Protein Assay as per the manufacturer's instructions (BIO-RAD).

Equal amounts of protein from supernatant and pellet fractions of the samples were resolved on SDS-PAGE gels and the proteins transferred to a PVDF membrane (Amersham). The membrane was incubated with the Anti-FLAG M2 antibody (Sigma) and the FLAG-tagged proteins were detected using the ProteoQwest[TM] chemiluminescent Western blotting kit (Sigma).

2.10 Minimal Inhibitory Concentration (MIC) determination

The role of *vapBC*s in mycobacterial drug susceptibility was determined in liquid medium using the broth microdilution method as previously described (58). Briefly, *M. smegmatis* wild type and Δ*MSMEG_1283-MSMEG_1284* cells were grown to an OD_{600} of 0.2 - 0.3 ($\sim 10^6$ CFU/ml). Before inoculation, the mycobacterial cells were diluted two fold ($\sim 10^4$ CFU/ml). Using the antibiotics rifampicin, ofloxacin, streptomycin and clofazimine, the assay was set up in 96-

well titre plates. The plates were visually read after 2 – 4 day incubation of 37°C, with the MIC scored as the lowest drug concentration that completely inhibited visible growth.

2.11 Statistics

The statistical significance of differences between data sets was calculated using the GraphPad QuickCalcs website: http://www.graphpad.com/quickcalcs/ttest1.cfm?Format=SD (accessed November 2010).

3. Results

3.1 VapC selection

As part of a study at the Molecular Mycobacteriology Research Unit (MMRU – University of the Witwatersrand, South Africa) to ascertain the significance of the massive expansion of *vapBC* modules in mycobacteria, a subset of 10 *vapBC* modules from *M. tuberculosis* and the sole *vapBC* module in *M. smegmatis*, *MSMEG_1283-MSMEG_1284*, were selected for investigation. The selection was guided, in part, by information on gene essentiality and transcriptional responsiveness of *vapBC* gene expression available at the time that the study was initiated (Table 3.1 and 3.2).

The vapCs *Rv2546*, *Rv2548* and *Rv2549c* were included as part of this subset since these genes are contained in a contiguous cluster on the *M. tuberculosis* chromosome (Figure 3.1). The remaining *Rv0549c*, *Rv2595c*, *Rv0627*, *Rv2010*, *Rv2829c* and *Rv3320c*, were selected after generation of a phylogenetic tree containing all 47 *M. tuberculosis* VapC proteins (Figure 3.2) in an attempt to ensure that a representative *vapC* from each cluster was included in the study.

Consistent with their designation as PIN domain proteins, most VapC proteins have the highly conserved Asp/Glu/Asp/Asp catalytic residues essential for ribonuclease activity (8, 14, 15, 22, 23). The *vapC Rv1953*, which encodes the Rv1953 protein that possesses only two conserved, active site acidic residues (Asp/Glu), was therefore included in the study as it was considered unlikely to possess nuclease function and, as such, could serve as a negative control (Figure 3.3).
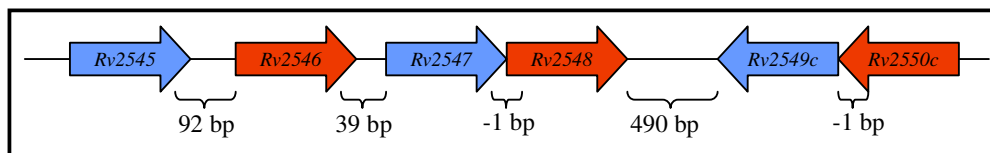
Figure 3.1: Diagrammatic representation of the contiguous gene cluster of Rv2545-Rv2550c on the *M. tuberculosis* chromosome. The blue arrows represent antitoxin genes, and the red arrows represent toxin genes. This figure is not drawn to scale.

Table 3.1: Properties of mycobacterial VapB antitoxins selected for study

VapB	*In vitro* essentiality (247)	Properties
Rv0550c	No	Induced by heat stress (270), during macrophage infections (230) and high concentrations of vancomycin (227)
Rv0596c	-	Induced in a *sigE* mutant after SDS stress (179)
Rv0626	-	Induced *in vivo* but not *in vitro* (273); repressed during infection of human macrophage-like cells (80); and structure of C-terminal region determined in complex with toxin Rv0627 (186)
Rv1952	No	Induced during phosphate starvation (235) and during macrophage infections (80)
Rv2009	No	Induced during human macrophage infections (65, 230), in SCID mice (273), after SDS stress (179) and during transition to hypoxia (230); but repressed during nutrient starvation (18), hypoxia (256), and in wild type H37Rv vs. a *phoP* mutant (296); Part of a genomic island (230)
Rv2545	No	Repressed at low pH *in vitro* (78); and a P19L polymorphism was identified in MDR strain of Mtb (129)
Rv2547	No	Induced during hypoxia (199, 230) and infection of macrophages (230, 268)
Rv2550c	No	Induced during macrophage infections (268), in Balb/c mice (273), in the presence of high iron concentrations (238) and SDS stress (179); but repressed by hypoxia (256) and in a *sigE* mutant after SDS stress (179)
Rv2830c	Yes	Induced during hypoxia (217), SDS stress (179) and during *in vitro* and *in vivo* growth (273)
Rv3321c	No	Induced in SCID mice (273) and during human macrophage infections (65)
MSMEG_1283	-	-

Table 3.2: Properties of mycobacterial VapC toxins selected for study

VapC	*In vitro* essentiality (247)	Toxicity in *E. coli* (108)	Toxicity in *M. smegmatis* (186, 230)	Properties
Rv0549c	No	Non-toxic	Toxic	Induced by hypoxia (199, 230), SDS stress (179), during adaptation to nutrient starvation (112), during infection of human macrophages (65, 230), and in the presence of high concentrations of vancomycin (227)
Rv0595c	No	Non-toxic	Non-toxic	Required for survival in nonhuman primate lungs (66); induced during adaptation to nutrient starvation (112), macrophage infection (268) and by SDS stress (179). Part of a genomic island (230).
Rv0627	Yes	Non-toxic	Non-toxic	Structure determined in complex with C-terminal part of antitoxin (Rv0626) and biochemical evidence for ribonuclease activity (186).
Rv1953	No	Non-toxic	Non-toxic	C-terminally truncated and lacking part of the PIN domain. Induced during adaptation to nutrient starvation (112)
Rv2010	No	Non-toxic	Toxic	Induced during hypoxia (199) and in Balb/c mice (273), but repressed during nutrient starvation (18), adaptation to hypoxia (256) and in wild type H37Rv compared to a *phoP* mutant (296). Protein identified in 30-d infected guinea pig lungs (156). Part of a genomic island (230).
Rv2546	No	Non-toxic	Non-toxic	Induced in Balb/c mice (273) and during treatment with SRI#967, a compound exhibiting strong anti-mycobacterial properties (293)
Rv2548	No	Non-toxic	Toxic	Induced during hypoxia (199) and macrophage infections (268), but repressed in sputum (92).
Rv2549c	No	Toxic	Non-toxic	Induced during macrophage infection (268) and in the presence of high iron concentrations (238).
Rv2829c	-	Non-toxic	Toxic	Induced during macrophage infection (230), hypoxia (230, 256) and nutrient starvation (112). Protein identified in 30-d infected guinea pig lungs (156).
Rv3320c	No	-	Non-toxic	Repressed during hypoxia (256) and nutrient starvation (18). Part of a genomic island (230).
MSMEG_1284			Toxic	

- Unknown

Figure 3.2: Phylogenetic tree of VapC proteins from mycobacteria. VapC proteins were aligned using ClustalW2 multiple sequence and alignment server (http://www.ebi.ac.uk/Tools/clustalw2/index.html). The tree was generated in Jalview 2.08.1 based on percentage identity between sequences. The arrows represent the 10 selected VapCs.

```
Conservation:                    95                                    8
MSMEG_1284    1  -----------MVIDTSALVAILTDEPDAELLEG-AVA--DDPVRTMSTASYLETAIVIESRFG------  50
Rv0627        1  ----VSTTPAAGVLDTSVFIATESGRQLDEAL--------IPDRVATTVVTLAELRVGVLAAAT-----T  53
Rv0595c       1  ------VNVRRALADTSVFIGIEATRFDPDRF--------AGYEWGVSVVTLGELRLGVLQASG-----P  51
Rv0549c       1  VRASPTSPPEQVVVDASAMVDLLARTSDRCSAVR-ARL--ARTAMHAPAHFDAEVLSALGRMQRA-GALT  66
Rv2549c       1  ---------MIFVDTSFWAALGNAGDARHGTAKRLWAS-KPPVVMTSNHVLGETWTLLNRRCG------  53
Rv2548        1  ----------VKLIDTTIAVDHLRGEPAAVLLAELIN--NGEEIAASELVRFELLAGVRES--------  50
Rv1953        1  ---------VTYVLDTNVVSALRVPGRHPAVAAWADSV--QVAEQFVVAITLAEIERGVIAKER----TD  55
Rv2010        1  -----------MIVDTSVWIAYLSTSESLASRWLADRIA-ADSTVIVPEVVMMELLIGKTDED-------  51
Rv3320c       1  ---------MRALLDVNVLLALLDRDHVDHERARAWITGQIERGWASCAITQNGFVRVISQPRYPSPISV  61
Rv2829c       1  --------MTTVLLDSHVAYWWSAEPQRLSMAASQAIE--HADELAVAAISWFELAWLAEQERI-----Q  55
Rv2546        1  ---------MVFCVDTSAWHHAARPEV---ARRWLAAL--SADQIGICDHVRLEILYSANSAT-------  49
Consensus_aa:    ...........hl.D.shhhsh.s....................hhhsshh..E...sh.p........
Consensus_ss:            eeeeehhhhhhhh     hhhhhhhhh      eee hhhhhhhhhhhh


Conservation:                                            8   6 8   6
MSMEG_1284   51  EPGGRELDLWLHRASVALVAV-DADQADAARLAYRRYGKGR--HRAGLNYGDCFSYALAKVSGQ-PLLFK  116
Rv0627       54  DIRAQRLATLESVADMETLPV-DDDAARMWARLRIHLAESG----RRVRINDLWIAAVAASRAL-PVITQ  117
Rv0595c      52  EAAARRLSTYQLAQRFEPLGI-DEAVSEAWALLVSKLRAAK----LRVPINDSWIAATAVAHGI-AILTQ  115
Rv0549c      67  VAYVDAALEELRQVPVTRHGL-SSLLAGAW---SRRD---------TLRLTDALYVELAETAGL-VLLTT  122
Rv2549c      54  HRAAVAAAAIRLSTVVRVEHV-TADLEEQAWEWLVRHDE------REYSFVDATSFAVMRKKGIQNAYAF  116
Rv2548       51  --ELAALEAFFS--AVVWTLV-TEDIARIGGRLARRYRSSH----RGIDDVDYLIAATAIVVDA-DLLTT  110
Rv1953       56  PTQSEHLRRWFD---DKVLRI-FVFARRGTNL-IMQPLAGH----IGYSLYSGISWF------------  103
Rv2010       52  --TAALRRRLLQ--RFAIEPLAPVRDAEDAAAIHRRCRRGG----DTVRSLIDCQVAAMALRIGV-AVAHR  113
Rv3320c      62  AHAIDLLARATHTRYHEFWSC-TVSILDSKVIDRSRLHS-------PKQVTDAYLLALAVAHDG-RFVTF  122
Rv2829c      56  LAIPVLSWLQQLAEHVRTVGI-TPSVAATAVALPSSF---------PGDPADRLIYATAIEHGW-RLVTK  114
Rv2546       50  --DYDALADELD--GLARIPV-GAETFTRACQVQRELAHVAGLHHRSVKIADLVIAAAAELSGT-IVWHY  113
Consensus_aa:    ......h..bb....h..h.l.ss.h.p.h..h...c............phsD.h.hhhA...s...hhh.
Consensus_ss:    hhhhhhhhhhhh     eee   hhhhhhhhhhhhhhhh           hhhhhhhhhhhhh   eeeee


Conservation:    6
MSMEG_1284  117  G-EAFRL---TD---VAAVH----------  129
Rv0627      118  D-DDFAA--LDG---AASVEIIRV------  135
Rv0595c     116  D-NDYAA--MPD---VEVITI---------  130
Rv0549c     123  D-ERLAR--AWP---SAHAIG---------  137
Rv2549c     117  D-GDFSA--AGF---VEVRPE---------  131
Rv2548      111  NVRHFPM--FPD---LQPPY----------  125
Rv1953           ----------------------------
Rv2010      114  D-RDYEA--IRT---HCGLRTEPLF-----  132
Rv3320c     123  D-QSIALTAVPGATKQHLATL---------  142
Rv2829c     115  D-RRLRS--HRH---PRPVTVW--------  130
Rv2546      114  D-ENYDR--VAA---ITGQPTEWIVPRGTL  137
Consensus_aa:    D.pph....h...................
Consensus_ss:       hhhh
```

Figure 3.3: Sequence alignment of the 11 VapCs encoded by the genes selected for study. VapC proteins were aligned using the PROMALS3D multiple sequence and structure alignment server (http://prodata.swmed.edu/promals3d/promals3d.php) (222). The circled residues represent the conserved catalytic residues essential for nuclease activity.

3.2 Differential growth inhibitory effects of VapC toxins in mycobacteria

The effect of the chosen VapC toxins in mycobacteria was assessed using an uncoupled conditional expression system which uses the antibiotic anhydrotetracycline (ATc) as an inducer. In this system, the gene of interest is under the control of an ATc-regulated $P_{myc1}tetO$ promoter-operator element carried on the episomal pSE100 plasmid, and a tetracycline repressor (*tetR*) located on an integrating plasmid is used to regulate the expression of the gene by varying the concentration of the inducer (70).

Briefly, when both the tetracycline repressor (TetR) and operator (*tetO*) are present in mycobacteria, the TetR binds to the *tetO* sequence and prevents expression of the gene of interest. However, upon addition of ATc, the antibiotic binds to the TetR resulting in a change in conformation of the TetR, leading to dissociation of TetR from *tetO* allowing for expression of the gene of interest (Figure 3.4). The modularity of this system also allows for assessment of gene function during constitutive or conditional expression in the absence and presence of TetR, respectively (Figure 3.5).
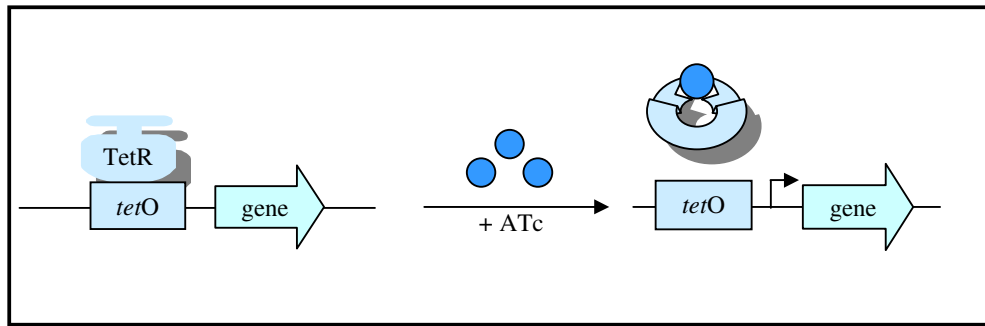
Figure 3.4: Mechanism for ATc conditional gene expression. Annotation: TetR: tetracycline repressor; *tetO*: tetracycline operator; ATc: anhydrotetracycline. The blue circles represent ATc molecules.
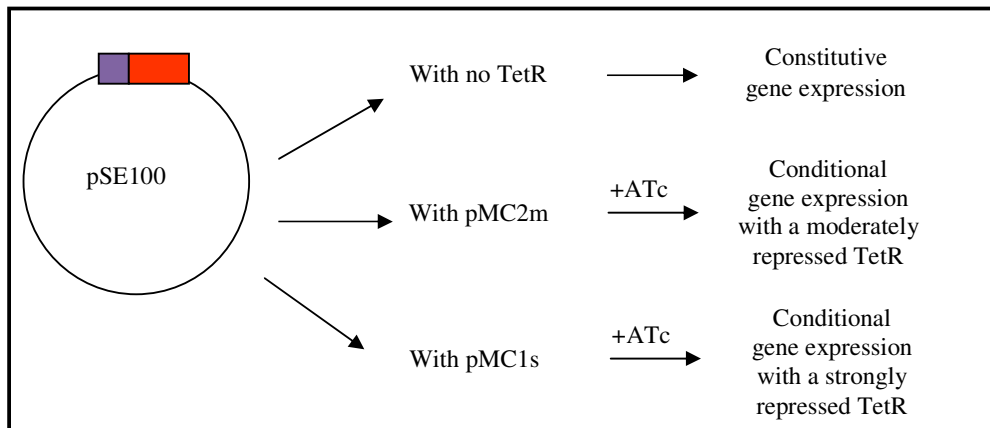
Figure 3.5: Schematic representation of the modularity of the ATc expression system used. Annotation: The purple box represents the $P_{myc1}tetO$ promoter-operator element and the red box represents the gene.

For the purposes of this study, the *vapC* genes were inserted downstream of the $P_{myc1}tetO$ promoter-operator element of pSE100 (Figure 3.6 & Section 3.2.1), and constitutive expression of these toxins was achieved by electroporating these constructs into mycobacteria in the absence of a TetR. Since there is some evidence to suggest that VapCs halt translation through mRNA cleavage (14, 15, 24, 25), the

physiological effect of each toxin was assessed by scoring transformation efficiencies. In this assay, low transformation efficiency would indicate VapC toxicity, whereas a transformation efficiency approximating that of the empty vector control would suggest a lack of VapC-mediated toxicity.

For conditional expression of VapCs on the other hand, the VapC constructs were co-electroporated into mycobacteria together with a TetR-encoding gene, which was either under the control of a strong mycobacterial promoter (P_{smyc}) as part of the L5-based integration vector pMC1s (70); or under the control of a mycobacterial promoter of intermediate strength (P_{imyc}) as part of the L5-based integration vector pMC2m (107) (Figure 3.6). In this configuration, addition of ATc would enable assessment of regulated expression of VapCs on the growth and viability of mycobacteria.

Figure 3.6: Schematic representation of the replicating vector pSE100 and the integrating vectors pMC1s and pMC2m. Annotation: rmBT1: transcriptional terminator; rmBT2: transcriptional terminator; Puv15: strong mycobacterial promoter; Ptb21: intermediate mycobacterial promoter; T4g32: *E. coli* transcriptional terminator; ColE1: origin of replication for *E. coli*; ori myc: origin of replication for mycobacteria; *hygR*: Hyg resistance cassette; *tetR*: tetracycline repressor gene.

3.2.1 Effect of constitutive ectopic VapC over-expression on the viability of wild type mycobacteria

M. smegmatis mc^{2}155 has been used widely as a model for studying mycobacterial physiology because it is a non-pathogenic, faster growing mycobacterium with a high transformation efficiency that is more easily genetically manipulated than its pathogenic relative *M. tuberculosis* (14, 198, 234, 259, 265, 277). Although its genome is nearly twice as large as that of *M. tuberculosis*, *M. smegmatis* has only one identifiable *vapBC* module on its chromosome (237), where the *vapB* is

homologous to Rv0623 and the *vapC* encodes a protein homologous to Rv0624 from *M. tuberculosis* (Figure 3.2). As such, *M. smegmatis* mc^{2}155 lacks *vapB* antitoxin homologues that could potentially counter the toxic effects of the *M. tuberculosis* VapCs under investigation in this study. These factors therefore suggested that *M. smegmatis* would be a useful host system to initially assess the toxicity or growth inhibitory effects of *M. tuberculosis* VapC proteins.

To determine the effect of the VapCs chosen for study on the viability of *M. smegmatis*, the *vapC* ORFs were amplified by PCR to incorporate a standardized consensus ribosome binding site (GGAAG/A). The amplicons were cloned into the *Bam*HI/*Hind*III (*Rv2546*, *Rv2548* and *Rv2549c*), *Bam*HI/*Pst*I (*Rv0549c*, *Rv0595c*, *Rv2829c* and *Rv1953*), *Pst*I/*Hind*III (*Rv0627*) or *Pvu*II (*MSMEG_1284*) sites of the episomal plasmid pSE100, under the control of the regulatory element, P$_{myc1}$*tetO*. The constructs pSE0549c, pSE0595c, pSE1953, pSE2010 and pSE2829c were generated by Dr. Diane Kuhnert, pSE0627 and pSE3320c were constructed by Dr. Garth Abrahams, whereas pSE2546, pSE2548, pSE2549c, and pSESM1284 were generated in this study.

All eleven constructs were electroporated into *M. smegmatis* without a corresponding *tetR*-encoding vector to allow for constitutive expression of the VapC proteins (Figure 3.5). As discussed above (Section 3.2), VapC toxicity was determined by scoring the transformation efficiency of the corresponding VapC expression vector. In this assay, a low transformation efficiency value is indicative of VapC toxicity whereas a high efficiency value suggests limited or no toxicity. The empty vector, pSE100, was used as negative control in this assay.

The results of this experiment revealed that pSE0549c, pSE0595c, pSE2549c, pSE2829c conferred toxicity to *M. smegmatis*, as evidenced by the fact that their transformation efficiencies were $\geq$ 3-log$_{10}$ lower than the empty vector control (Table 3.3). In accordance with the prediction that Rv1953 would lack ribonuclease activity and hence be non toxic to mycobacteria, the transformation efficiency of pSE1953 was indistinguishable from pSE100. However, it is interesting to note that the VapCs Rv0627, Rv2010, Rv2546, Rv2548 and MSMEG_1284 also appeared to have no growth inhibitory effects on *M. smegmatis*, as the transformation efficiencies of their

expression vectors were comparable to that of pSE100 (between 0.08- and 1.3-fold of the transformation efficiency of pSE100) (Table 3.3).

Table 3.3: Toxicity of VapCs in the *M. smegmatis* wild type strain as assessed by transformation efficiency of VapC expressing vectors

VapC	Plasmid	Transformation efficiency (CFU/µg)*
-	pSE100	2.7×10^4
Rv0549c	pSE0549c	63
Rv0595c	pSE0595c	8
Rv0627	pSE0627	2.4×10^4
Rv1953	pSE1953	2.6×10^4
Rv2010	pSE2010	2.1×10^3
Rv2546	pSE2546	3.5×10^4
Rv2548	pSE2548	2.0×10^4
Rv2549c	pSE2549c	11
Rv2829c	pSE2829c	15
Rv3320c	pSE3320c	1
MSMEG_1284	pSESM_1284	1.5×10^4

*These data represent the results from one of three independent experiments.

Interestingly, electroporation of pSE0549c into *M. smegmatis* resulted in the production of both normal-sized colonies as well as a background 'haze' of small colonies (Figure 3.7A). This phenomenon was not observed when *M. smegmatis* was electroporated with the vectors pSE0595c, pSE2549c and pSE2829, which carry toxic VapC-encoding genes: in these cases, normal *M. smegmatis* colony forming phenotypes were observed (Figure 3.7B).
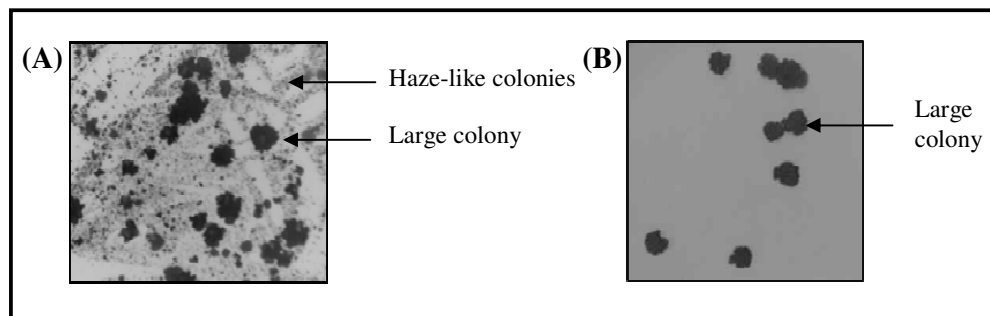
Figure 3.7: Phenotype of *M. smegmatis* upon constitutive ectopic over-expression of (A) Rv0549c and (B) Rv2549c.

Restriction analyses of plasmids recovered from the large colonies obtained by electroporation of *M. smegmatis* with pSE0549c showed rearrangement of the DNA (Figure 3.8A – left gel). This was not the case for the plasmids isolated from haze-like colonies, which appeared identical to the original plasmid (Figure 3.8A- right gel). However, when plasmid DNA was recovered from a haze-like colony and investigated further by sequence analysis, an 18bp deletion was observed within *Rv0549c*. These data, therefore, suggest that plasmids expressing toxic VapCs undergo either plasmid rearrangement or other types of mutation(s) to ensure that little or no toxic protein is produced, in a bid to ensure *M. smegmatis* cell survival.

This observation made it imperative to ascertain that the constructs expressing the apparently non-toxic VapCs were not rendered thus through mutation(s) or gross plasmid rearrangement. To this end, the plasmids expressing the non-toxic Rv0627, Rv2546, Rv2548 and MSMEG_1284 VapCs were recovered from the respective *M. smegmatis* transformants and analyzed. Restriction mapping together with sequencing of the promoter-operator regions of the toxin genes revealed that the plasmids pSE0627, pSE2546 pSE2548 and pSESM_1284 recovered post-electroporation were indistinguishable from the original constructs used for electroporations (Figure 3.8B, C, D & E). Taken together, these data therefore suggest that whilst Rv0627, Rv2546, Rv2548, MSMEG_1284 are non-toxic to *M. smegmatis* and undergo no plasmid alterations, plasmids expressing toxic VapCs are rearranged in such a manner as to reduce/ eliminate VapC toxicity.

(A)

pSE0549c
6047 bps

(B

pSE0627
6025 bps

C)

pSE2546
5993 bps
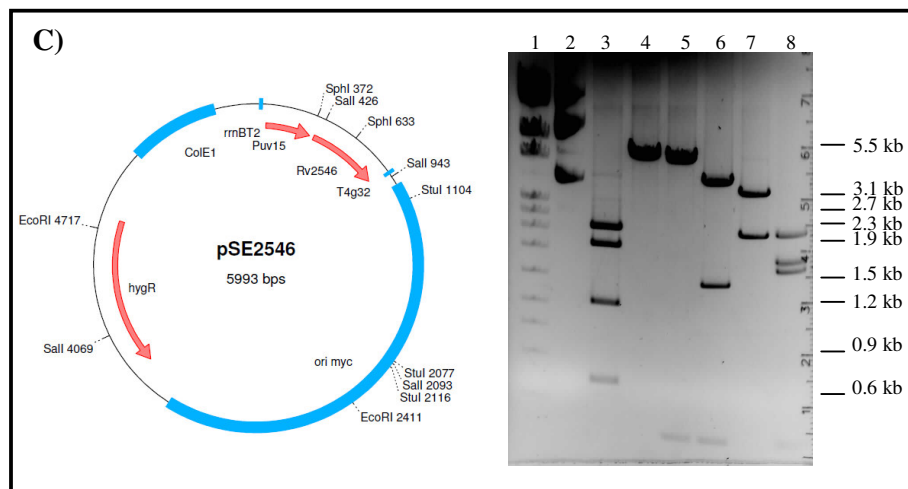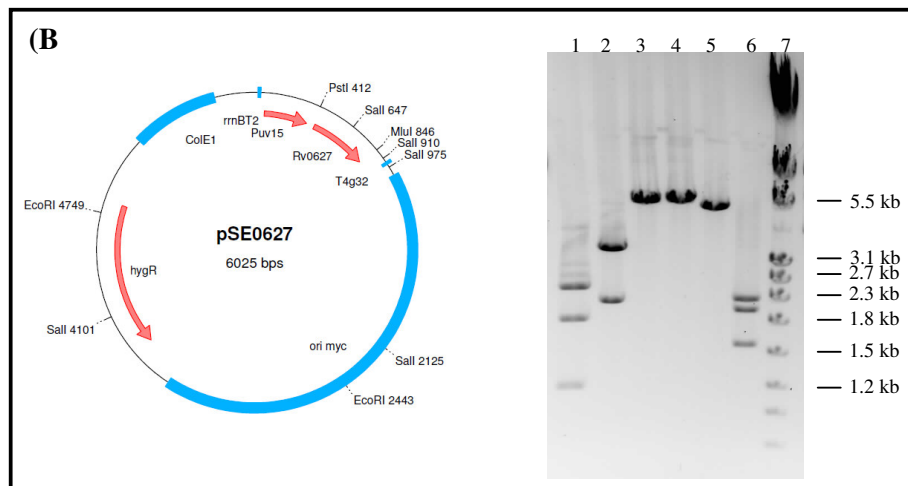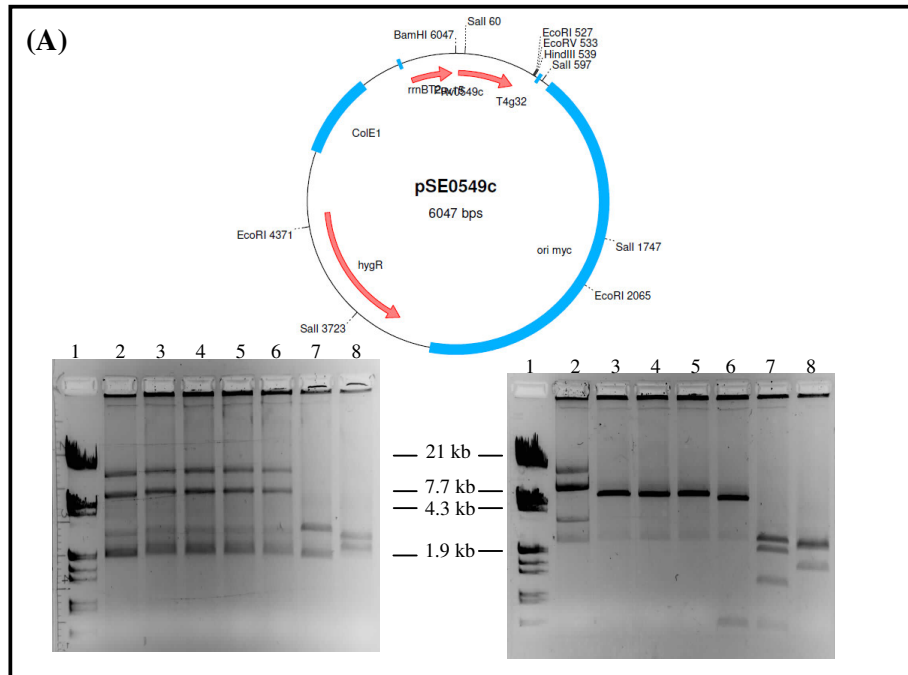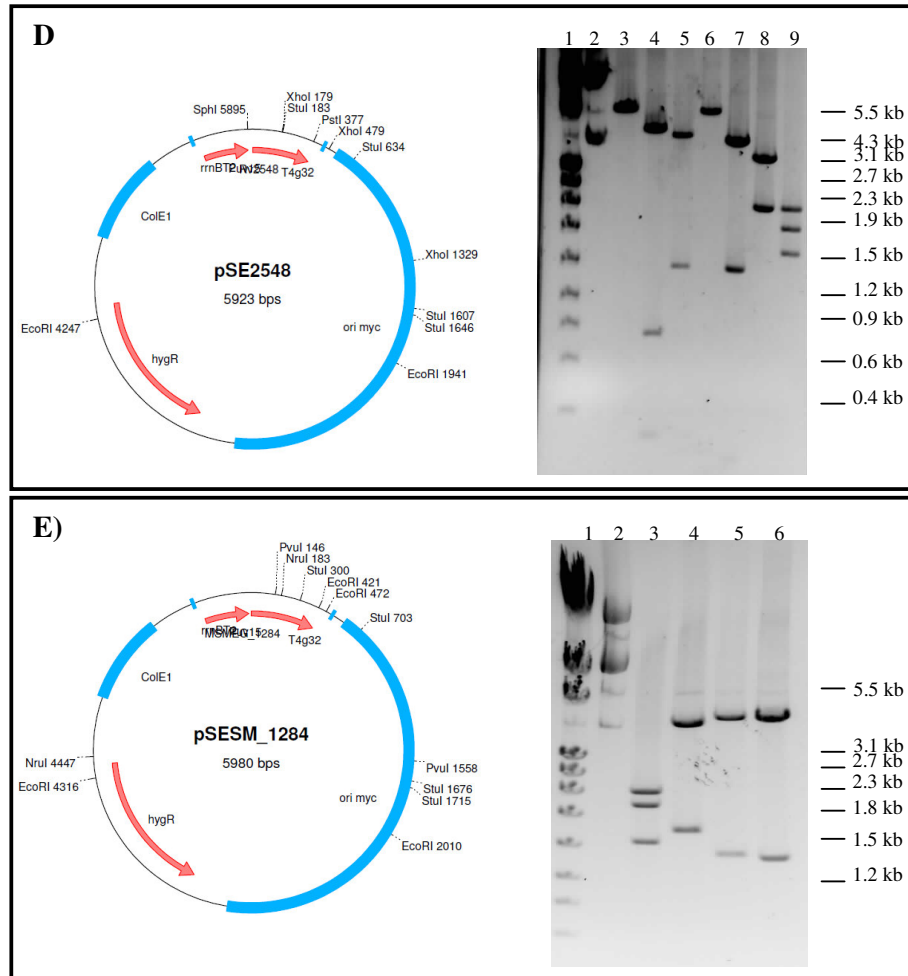
Figure 3.8: Restriction mapping of constructs recovered post-constitutive VapC expression in *M. smegmatis*. In all panels, a schematic representation of the original plasmid is depicted and the position of restriction sites annotated. Also, with the exception of (B), Lane 1 for all gels displays the separation of the molecular weight marker Roche Marker III or IV, with the fragment sizes adjacent to the gel and Lane 2 shows uncut plasmid DNA. **(A) pSE0549c**: Comparison of restriction digests of plasmids for both gels, where Lane 3: *EcoR*V, Lane 4: *BamH*I, Lane 5: *Hind*III, Lane 6: *BamH*I/*Hind*III, Lane 7: *Sal*I and Lane 8: *EcoR*I, showed the expected fragment sizes from a haze-like colony (right gel) but gross plasmid rearrangement in the large colonies (left gel) since none of the expected fragment sizes were detected. **(B) pSE0627**: Here, Lane 7 displays the separation of Roche Marker IV, with the fragment sizes adjacent to the gel. Restriction analysis shows the expected fragment sizes with all enzymes (Lane 2: *Sal*I, Lane 3: *EcoR*I, Lane 4: *Mlu*I, Lane 5: *Pst*I, Lane 6: *Mlu*I/*Pst*I and Lane 7: *Mlu*I/*EcoR*I). **(C) pSE2546**: Restriction analysis shows the expected fragment sizes with all enzymes (Lane 3: *Sal*I, Lane 4: *Sph*I, Lane 5: *Stu*I, Lane 6: *Stu*I/*Sph*I, Lane 7: *EcoR*I and Lane 8: *EcoR*I/*Sph*I). **(D) pSE2548**: Restriction analysis shows the expected fragment sizes with all enzymes (Lane 3: *Pst*I, Lane 4: *Xho*I, Lane 5: *Stu*I, Lane 6: *Sph*I, Lane 7: *Stu*I/*Sph*I Lane 8: *EcoR*I and Lane 9: *EcoR*I/*Sph*I). **(E) pSESM_1284**: Restriction analysis shows the expected fragment sizes with all enzymes (Lane 3: *EcoR*I, Lane 4: *Nru*I, Lane 5: *Pvu*I, Lane 6: *Stu*I).

<u>Effect of constitutive *M. tuberculosis* VapC over-expression on its native host</u>

The effect of the ten selected *M. tuberculosis* VapC proteins was then assessed in wild type *M. tuberculosis*. A major difference between this host strain when compared to *M. smegmatis* is that wild type *M. tuberculosis* carries the cognate VapB antitoxin-encoding gene as part of the corresponding chromosomal *vapBC* module. As such, the consequence of VapC expression may differ in the native host compared to the heterologous *M. smegmatis* host.

The expression constructs for the ten *M. tuberculosis* VapCs were electroporated into *M. tuberculosis* in the absence of a TetR. As above, transformation efficiency was used to assess the effect of constitutive VapC expression, with low efficiencies indicating toxicity. This experiment revealed that pSE0549c, pSE0595c, pSE2549c, pSE2829c and pSE3320c were poorly tolerated in *M. tuberculosis*, as evidenced by $\geq$ 2-$\log_{10}$ lower transformation efficiencies when compared to the empty vector control. In contrast, pSE0627, pSE1953, pSE2010, pSE2546, and pSE2548 conferred no apparent toxicity, displaying transformation efficiencies comparable to that of pSE100 (between 0.5- and 3.2- fold of the transformation efficiency of pSE100) (Table 3.4). Restriction mapping of plasmids recovered from randomly selected transformants revealed the rearrangement of the constructs expressing the toxic VapCs Rv0549c, Rv0595c, Rv2549c, Rv2829c and Rv3320 in the surviving transformants (data not shown). These results mirror those in *M. smegmatis* (Table 3.3) and therefore suggest that the heterologous *M. smegmatis* host was appropriate for assessing VapC toxicity.

Taken together, these data suggest a differentiation in VapC function in mycobacteria, where Rv0627, Rv1953, Rv2010, Rv2546, and Rv2548 are non-toxic whilst Rv0549c, Rv0595c, Rv2549c, Rv2829c and Rv3320c are toxic, with Rv0549c being the least potent of the toxic VapC proteins.

Table 3.4: Toxicity of VapCs in an *M. tuberculosis* H37Rv wild type strain assessed by transformation efficiency of VapC expression vector

VapC	Plasmid	Transformation efficiency (CFU/μg)*
-	pSE100	3.0×10^6
Rv0549c	pSE0549c	1.4×10^4
Rv0595c	pSE0595c	3.3×10^3
Rv0627	pSE0627	8.7×10^6
Rv1953	pSE1953	5.6×10^6
Rv2010	pSE2010	9.7×10^6
Rv2546	pSE2546	1.6×10^6
Rv2548	pSE2548	2.6×10^6
Rv2549c	pSE2549c	8.4×10^2
Rv2829c	pSE2829c	1.0×10^4
Rv3320c	pSE3320c	9.0×10^2

*These data represent the results from one of four independent experiments

3.2.2 Moderate regulation of VapC expression is insufficient to repress toxic VapC proteins in wild type *M. smegmatis*

To probe whether expression of *tetR* under the control of a mycobacterial promoter of intermediate strength (P_{imyc}) could regulate expression of the toxic VapCs, and hence, modulate their toxic effects on *M. smegmatis*, the constructs pSE0549c, pSE0595c, pSE2549c, pSE2829c and pSE3320 were co-electroporated into *M. smegmatis* together with pMC2m to generate *M. smegmatis vapC*::pMC2m strains, which were selected on 7H10 plates containing both hygromycin (Hyg) and kanamycin (Km), but not ATc. Notably, co-electroporation of pMC2m with pSE0549c did not result in the 'haze-like' colony phenotype of pSE0549c observed in the absence of a TetR (Figure 3.7). Here, the resulting transformants were phenotypically similar to the control transformants recovered by co-electroporation of the empty vector, pSE100, with pMC2m.

The co-transformation efficiency of pSE0549c with pMC2m was also similar to that of the *M. smegmatis* pSE100::pMC2m and *M. smegmatis* pSE1953::pMC2m control strains (Table 3.5). This differs from the observations above (Table 3.3), and shows, quite clearly, that Rv0549c toxicity that is evidenced under conditions of maximal, constitutive ectopic expression, can be effectively eliminated when the

expression level of this VapC is dampened by a moderately expressed TetR. In contrast, co-transformation of pSE0595c, pSE2549c and pSE2829c with pMC2m resulted in $\geq$2-$\log_{10}$ lower transformation efficiencies compared to the empty vector control strain, with co-electroporation of pSE3320c with pMC2m yielding no colonies (Table 3.5).

As observed with plasmids recovered from transformants obtained by electroporation of *M. smegmatis* with the VapC expression vectors alone (Figure 3.8), the toxic VapC-expressing episomal plasmids isolated from *M. smegmatis* transformants obtained by co-electroporation with pMC2m had undergone gross plasmid rearrangement, as assessed by restriction mapping (data not shown). This observation convincingly demonstrates that a promoter of intermediate strength does not allow for sufficient TetR expression to repress the expression of these VapCs. In addition, these findings corroborate those in Section 3.2.1 which suggest a differentiation in VapC toxicity, with Rv0549c being the least toxic of the toxic VapCs investigated.

Table 3.5: Toxicity of VapCs in *M. smegmatis* as assessed by co-transformation efficiency of VapC expressing vectors and pMC2m

VapC	Plasmid	Transformation efficiency (CFU/µg)*
-	pSE100	7.2×10^3
Rv0549c	pSE0549c	3.7×10^3
Rv0595c	pSE0595c	2.0×10^1
Rv1953	pSE1953	3.2×10^4
Rv2549c	pSE2549c	2.2×10^1
Rv2829c	pSE2829c	1.0×10^1
Rv3320	pSE3320c	0

*The data represent the results of one of three independent experiments

3.2.3 Tight repression of *tetO* is sufficient for regulation of *M. tuberculosis* VapC toxicity in wild type *M. smegmatis*

To determine whether the strong P_{smyc} promoter was able to drive expression of the TetR to levels sufficient for repression of VapC toxicity, the construct pSE2549c, expressing the toxic VapC Rv2549c, was co-electroporated with pMC1s

into *M. smegmatis*. As controls, the pSE100 vector as well as the two non-toxic constructs pSE2546 and pSE2548 were co-electroporated with pMC1s into *M. smegmatis*. The transformation efficiencies of all transformants, selected on 7H10 plates containing Hyg and Km but not ATc, was similar ($\sim 10^4$ CFU/µg of DNA), thereby suggesting that enough TetR was expressed to repress expression of the *Rv2549c* gene.

To assess the integrity of the VapC expression plasmids, electroductions from the *M. smegmatis* transformants were performed to recover Hyg^R plasmids from the pSE2546, pSE2548 and pSE2549c co-electroporations. Consistent with the constitutive over-expression data (Figure 3.8), restriction mapping and sequencing of the episomal plasmids recovered from pSE2546 and pSE2548 transformants revealed that the plasmids had neither undergone rearrangements nor had they acquired point mutations (data not shown). In the case of transformants recovered from the pSE2549c co-electroporation, the Rv2549c expression vector was stable in the absence of the ATc inducer, as it did not undergo plasmid rearrangement or acquire point mutations (data not shown). This observation therefore establishes that *vapC* expression is sufficiently repressed by the TetR expressed under the control of a strong promoter, to avoid plasmid loss or mutation(s) arising as a result of toxic gene expression.

3.2.4 Effect of conditional *vapC* expression on the growth and viability of *M. smegmatis*

Since pMC1s was able to repress toxic *vapC* expression, its usefulness for conditional toxin expression was determined. To this end, each of the VapC expressing *M. smegmatis* strains, in which *vapC* expression was repressed by the highly expressed TetR carried on pMC1s, were spotted on solid media containing Hyg, Km and varying concentrations of ATc. As reported under Section 3.2.1, Rv2546 and Rv2548 were not toxic when expressed under conditions of maximal de-repression (*i.e.* in the absence of TetR). Consistent with these results, no growth inhibition was observed for strains conditionally expressing Rv2546 and Rv2548 at concentrations of ATc up to 50ng/ml. In contrast, conditional expression of Rv2549c was growth inhibitory to *M. smegmatis*. However, growth inhibition was only observed at ATc concentrations $\geq$ 6.2ng/ml (Figure 3.9).
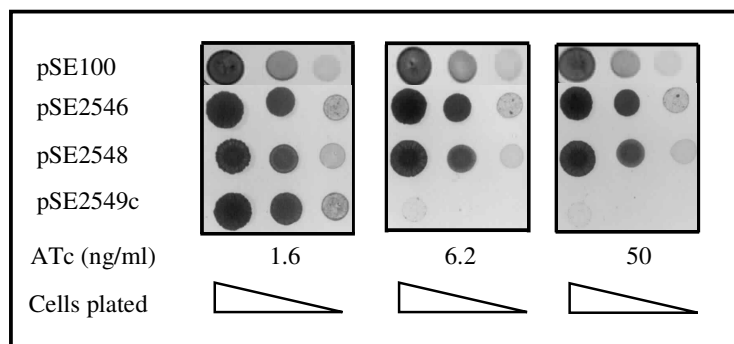
Figure 3.9: The effect of conditional VapC expression on the growth of *M. smegmatis*. Spotting assays in which 10µl of 10-fold serial dilutions of late logarithmic phase cells were spotted on 7H10 agar with increasing concentrations of ATc (1.6, 6.2 and 50ng/ml) and incubated for 24 - 48 h at 37°C before scoring.

The effect of these *M. tuberculosis* VapC proteins on the growth and viability of *M. smegmatis* was also assessed in liquid media. Here, the toxins were induced during early logarithmic growth stages (OD_{600} ~ 0.1) with ATc at a concentration of 25ng/ml, which was sufficiently high to confer growth inhibition on *M. smegmatis* on solid medium (Figure 3.9). The growth and viability of *M. smegmatis* was monitored over a period of up to 25h. The VapC proteins Rv2546 and Rv2548 had no effect on *M. smegmatis* growth, as assessed spectrophotometrically (OD_{600}) and by enumeration of CFUs (Figure 3.10). Restriction mapping and sequence analyses of the episomal plasmids expressing Rv2546 and Rv2548 for up to 24h show that neither construct had undergone plasmid rearrangement or acquired point mutations (data not shown), thus ruling out plasmid instability as a reason for the lack of toxicity in this case.
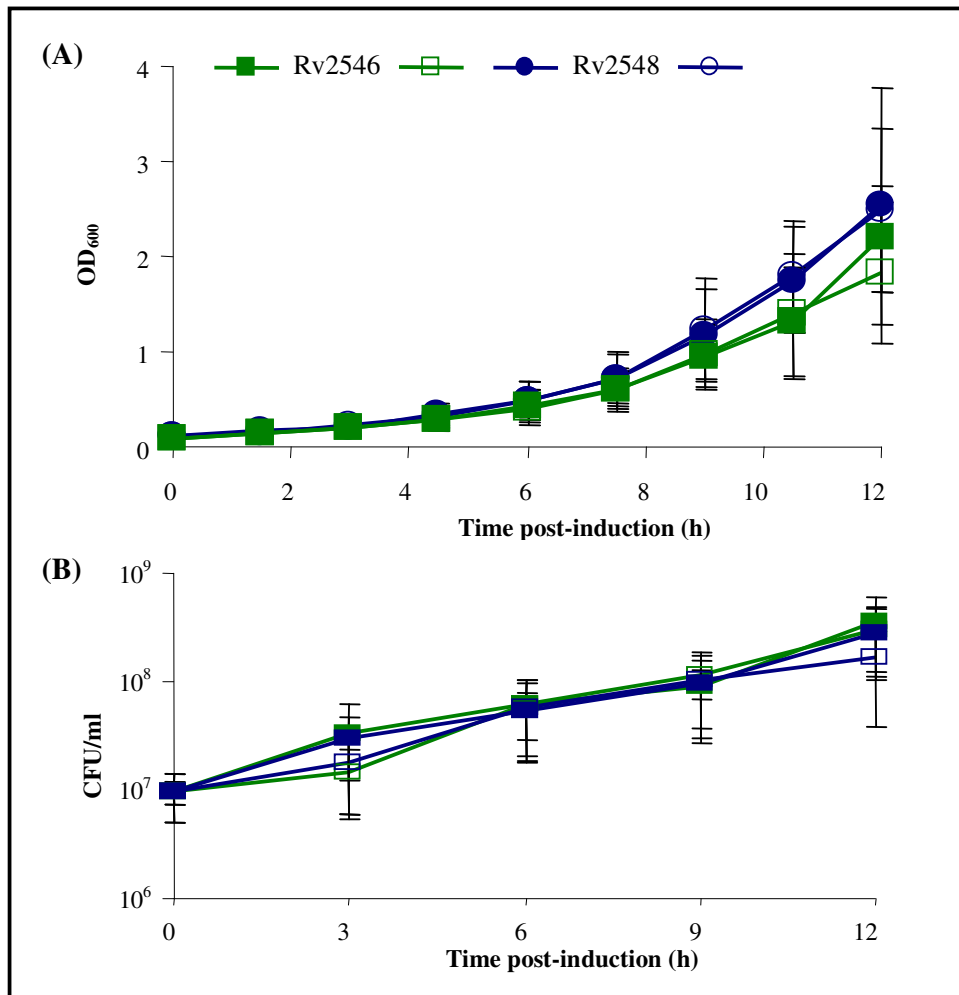
Figure 3.10: Effect of conditional ectopic expression of Rv2546 and Rv2548 on the growth and viability of *M. smegmatis*. **(A)** OD_{600} spectrophotometric measurements were made at 1.5h intervals for 12h. **(B)** CFUs were assessed by plating 100µl of 10-fold serial dilutions of cells every 3h over a 12h period, and plates were scored after 3 - 4 days incubation at 37°C. **Annotation:** Empty symbols represent induced samples and filled in symbols represent uninduced samples

In contrast, Rv2549c was growth inhibitory in liquid media, as assessed by OD_{600} measurements which showed no increase above the starting OD_{600} value over the time period of the experiment (Figure 3.11A). CFU enumeration of samples taken over the 25h time course revealed a 2-$\log_{10}$ decrease in viability within 3h post-induction, which was maintained for the duration of the experiment (Figure 3.11B).
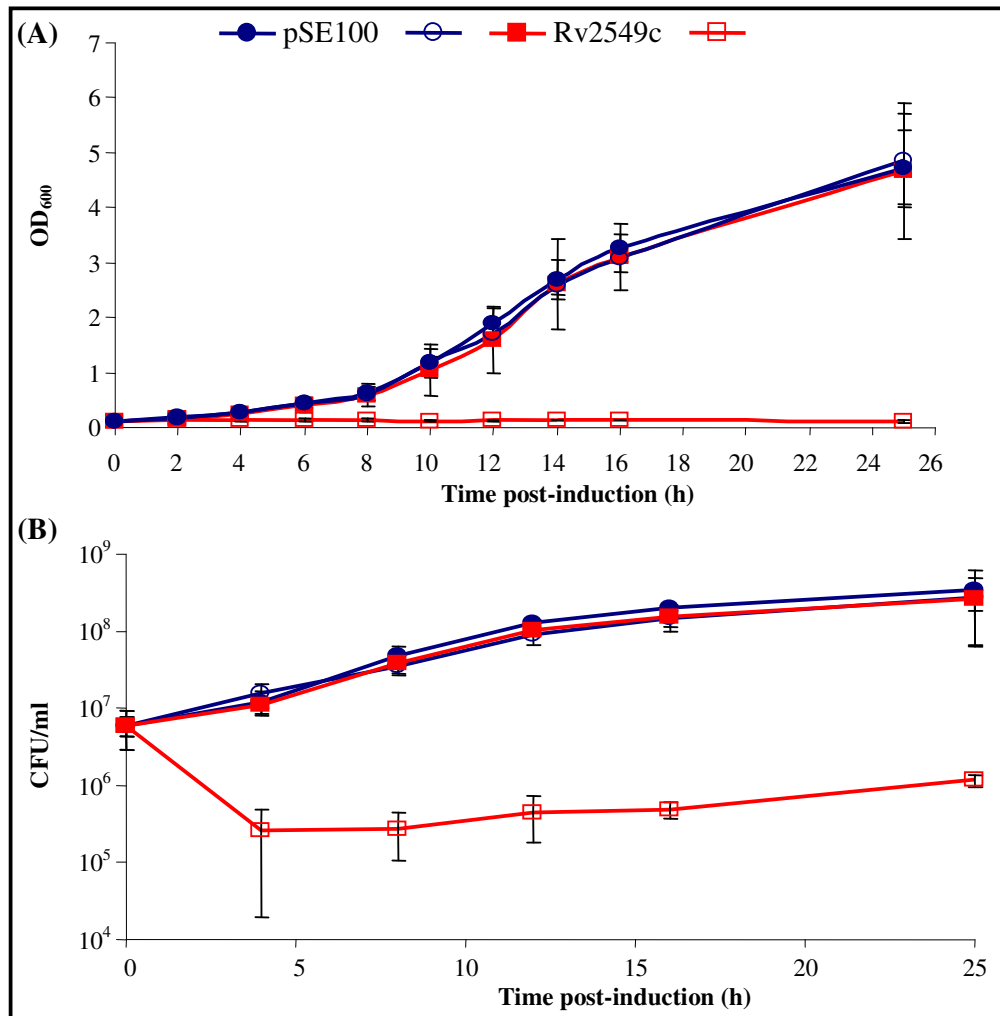
Figure 3.11: Effect of conditional ectopic expression of Rv2549c on the growth and viability of *M. smegmatis*. (A) OD_{600} spectrophotometric readings were taken at 2h intervals for 16h, and then again at 25h post-induction of Rv2549c. (B) CFUs were assessed by plating 100μl of 10-fold serial dilutions of cells every 4h over a 16h period and at 25h post-induction of Rv2549c. Plates were scored after 3 - 4 days incubation at 37°C. **Annotation:** Empty symbols represent induced samples and filled in symbols represent uninduced samples.

To ascertain whether the viable *M. smegmatis* colonies obtained subsequent to Rv2549c induction (Figure 3.11) still retained the intact pSE2549c and pMC1s plasmids, ten colonies from each time point assayed were spotted onto solid 7H10 media containing Km, Hyg and/or ATc. As a control, colonies were recovered from the Rv2549c uninduced sample at the same time points. All of the colonies recovered from the uninduced Rv2549c sample behaved as expected *i.e.* they grew in the presence of Hyg and Km, but not upon induction of the toxin by addition of ATc (Figure 3.12, top panel). This confirmed that the Km[R] pMC1s integrating plasmid was

intact, and that the Hyg^R pSE2549c episomal plasmid was functional since it grew on Hyg and addition of ATc resulted in growth arrest due to Rv2549c expression.
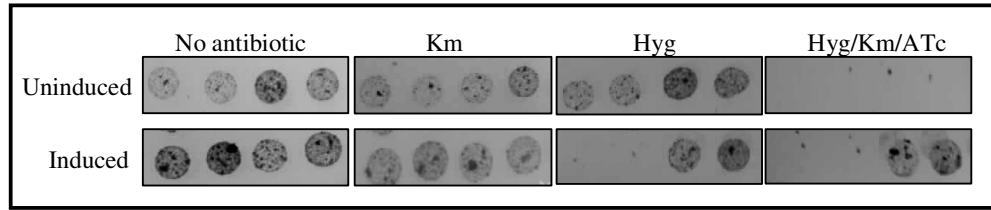
Figure 3.12: Assessing plasmids retained by viable *M. smegmatis* colonies by use of antibiotic markers. Single colonies recovered at varying time-points after 3 - 24h post-induction of Rv2549c were resuspended in 50µl 7H9 media and 10µl was spotted onto 7H10 media containing antibiotics as annotated above.

In contrast, while the *M. smegmatis* colonies recovered after induction of Rv2549c in liquid culture appear to have retained pMC1s since these grew on Km, the episomal plasmid did not remain intact. These episomal plasmids either appeared to have been lost, as evidenced by the failure to grow on Hyg, or to have rearranged, as observed by the ability of the *M. smegmatis* clones to thrive in the presence of ATc (Figure 3.12, bottom panel). These data suggest that within one replication cycle of *M. smegmatis*, either loss or extensive rearrangement of pSE2549c occurs so as to mitigate the growth inhibitory effects of the toxic Rv2549c VapC protein.

To further investigate the molecular basis of these phenotypes, plasmids were recovered from the *M. smegmatis* clones obtained following ATc induction in liquid culture. From the hygromycin sensitive colonies, no episomal plasmid could be recovered, confirming that the pSE2549c plasmid had been lost from these clones. Moreover, analyses of all plasmids recovered from colonies that showed a Hyg^R and ATc^R phenotype showed extensive plasmid rearrangement within the *tetO* and/or the *Rv2549c* ORF, as evidenced by restriction mapping (Figure 3.13). These observations indicate that Rv2549c is extremely toxic to *M. smegmatis*, and to survive, the organism either renders the toxic Rv2549c non-toxic through mutations, or it prevents induction of Rv2549c expression.
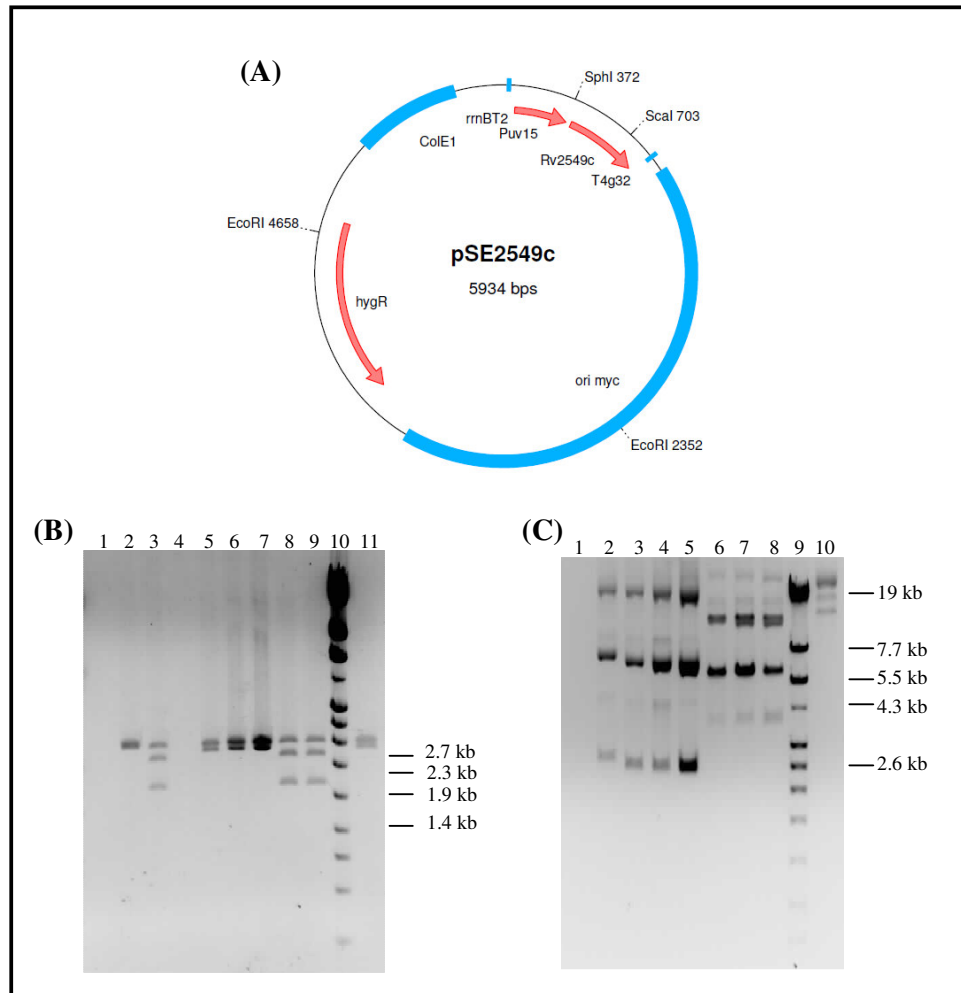
Figure 3.13: Restriction mapping of pSE2549c recovered post-VapC induction in *M. smegmatis*. **(A)** Schematic representation of the original pSE2549c plasmid with the position of the restriction sites annotated. **(B)** For assessment of gross plasmid rearrangement and mutations within the *tetO* region, the 10 clones recovered by electroductions into *E. coli* after induction of VapC expression were digested with *Sph*I and *EcoR*I. Here, only 3 clones retained the expected 1.6 kb, 2.0 kb and 2.3 kb fragment size, thus suggesting no plasmid rearrangement in these cases, but plasmid rearrangement in the remaining 7 clones. **(C)** For assessment of gross mutations within *Rv2549c*, the 9 of the 10 clones recovered by electroduction in (B) were digested with *Sca*I. Here, none of the clones displayed the expected linearized 5.9 kb fragment, confirming rearrangement and/or loss of the *Rv2549c* for all 10 clones. All empty lanes represent colonies from which plasmids were not recovered *i.e.* the plasmids had been lost, and Lane 10 (Gel B) and Lane 9 (Gel C) displays the separation of the molecular weight marker marker IV (Roche), with fragment sizes adjacent to the gels.

3.2.5 <u>Regulated expression of Rv2549c results in bacteriostasis of wild type *M.* *tuberculosis*</u>

To understand the effect of expression of a toxic *M. tuberculosis* VapC on the growth and viability of its native host, pSE2549c was co-electroporated with pMC1s into wild type *M. tuberculosis*. As controls, the constructs pSE2546 and pSE2548, which direct the ectopic over-expression of VapCs that were non-toxic in *M. smegmatis*, were used in addition to the empty vector, pSE100. PCR-based genotyping at the *attB* locus (See Appendix C for strategy) confirmed that pMC1s successfully integrated into the H37Rv chromosome following electroporation of this plasmid (data not shown). In addition, the transformation efficiency of all constructs was similar (~ 10^2 CFU/µg of DNA), thereby confirming that pSE2549c expression was sufficiently repressed by the highly expressed TetR from pMC1s to restrict the growth inhibitory effects of this VapC. Each strain was then grown in liquid media to early logarithmic growth stages ($OD_{600} \sim 0.1$) and the VapCs were induced with ATc at a concentration of 25ng/ml. The effect of Rv2546 and Rv2548 on the viability of *M. tuberculosis* was assessed by scoring CFUs over an 8-day period. Consistent with the transformation efficiency data (Table 3.4), the strains expressing Rv2546 and Rv2548 did not affect the viability of wild type *M. tuberculosis* as these displayed the same growth kinetics as the control strain carrying the empty vector, pSE100 (Figure 3.14).
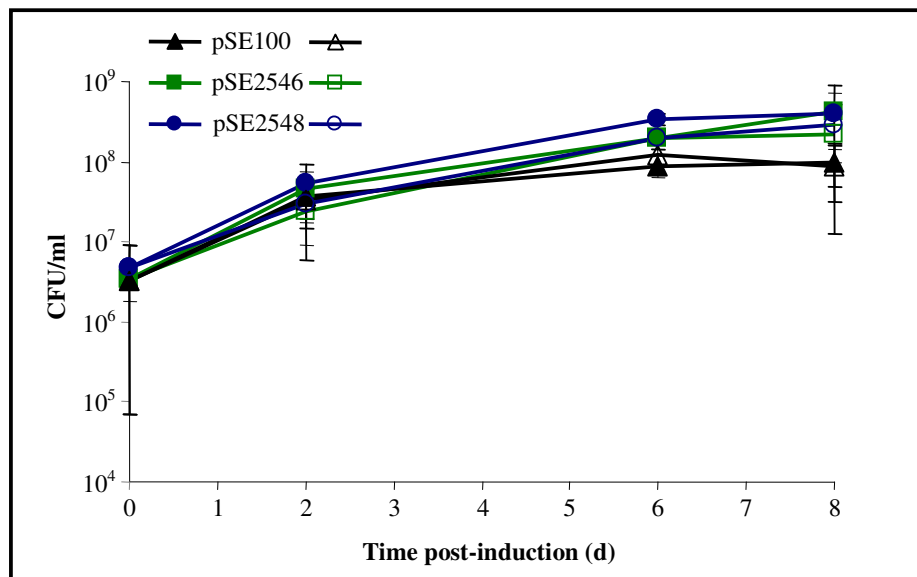
Figure 3.14: Effect of ectopic expression of Rv2546 and Rv2548 on the viability of wild type *M. tuberculosis* H37Rv. Each *M. tuberculosis* transformant was grown in media containing Hyg and Km to mid-logarithmic phase and diluted to OD_{600} 0.04 in 30ml 7H9 media. The cultures were then grown overnight at 37°C standing, and divided the next day into 2 equal aliquots of 10ml each. To one aliquot, ATc was added at a concentration of 25ng/ml to induce the VapC toxin. To determine the effect of toxin over-expression on the viability of *M. tuberculosis*, CFUs were assessed by plating 100µl of 10-fold serial dilutions of cells over an 8-day period post VapC-induction, and plates were scored after 21 - 27 days incubation at 37°C. **Annotation:** Empty symbols represent induced samples and filled in symbols represent uninduced samples

In contrast, regulated expression of Rv2549c in its native host resulted in growth inhibition for at least 2 days, as observed by OD_{600} measurements (Figure 3.15A). Whilst this was similar to the data observed in *M. smegmatis* (Figure 3.11A), regulated expression of Rv2549c appeared to result in bacteriostasis rather than cidality of *M. tuberculosis* during these first 2 days post-induction, as assessed by CFU enumeration (Figure 3.15B). This suggests that the presence of the cognate antitoxin on the chromosome may be able to mitigate, to some extent, the growth inhibitory effects of ectopically expressed Rv2549c. Interestingly, rearrangement or loss of the pSE2549c plasmid occurred after day 2 (data not shown), presumably to ensure that Rv2549c is no longer expressed and thus allowing the cells to overcome the Rv2549c-induced bacteriostasis.
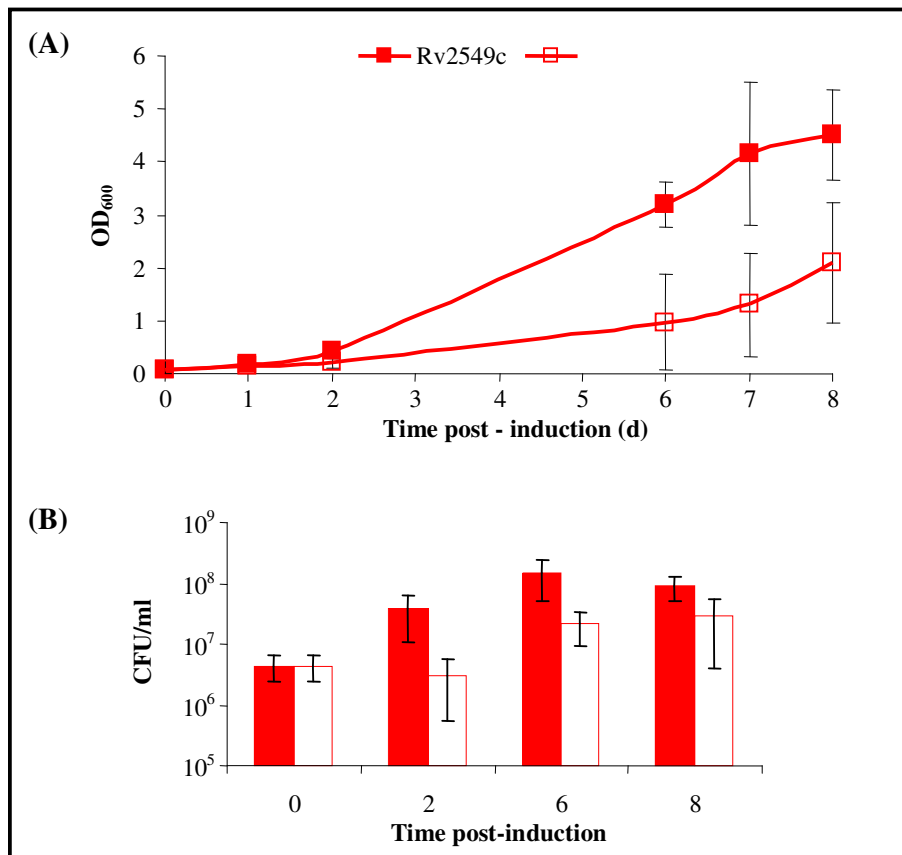
Figure 3.15: Effect of Rv2549c on viability of wild type *M. tuberculosis* H37Rv.
The *M. tuberculosis* transformant containing pSE2549c and pMC1s was grown in media containing Hyg and Km to mid-logarithmic phase and diluted to OD_{600} 0.04 in 30ml 7H9 media. The culture was then grown overnight at 37°C standing, and divided the next day into 2 equal aliquots of 10ml each. To one aliquot, ATc was added at a concentration of 25ng/ml to induce Rv2549c. **(A)** The effect of Rv2549c on the growth of *M. tuberculosis* was assessed by OD_{600} spectrophotometric readings taken over an 8-day period. **(B)** The effect of ectopic expression of Rv2549c on the viability of *M. tuberculosis* was determined by CFU assessment. Here, plating of 100µl of 10-fold serial dilutions of cells over an 8-day period post-induction of Rv2549c was performed, and the plates were scored after 21 - 27 days of incubation at 37°C. **Annotation:** Empty symbols represent induced samples and filled in symbols represent uninduced samples

3.2.6 <u>VapCs are transcribed but not evenly translated in *M. smegmatis*</u>

To assess whether the lack of toxicity of non-toxic VapC proteins might be due to deficient expression of the *vapC*s, semi-quantitative RT-PCR was used to investigate the expression of the *Rv2546* gene upon addition of ATc at a concentration of 25ng/ml, which has been shown not induce Rv2546 toxicity (Figure 3.10 & 3.14). The *sigA* housekeeping gene was used as an internal control, and the *Rv2549c*

transcript was used as a positive control, since expression of this *vapC* causes toxicity in mycobacteria (Figure 3.11 & 3.15). As shown below (Figure 3.16), no amplicon was detected in reactions in which the RNA samples had not been reverse transcribed, thus excluding genomic DNA contamination. As expected, the *Rv2549c* control transcript was detected upon reverse transcription (Figure 3.16A, +ATc; +RT). Interestingly, *Rv2549c* transcript was also detected in the uninduced sample (Figure 3.16A, -ATc; +RT), suggesting that this conditional expression system is leaky. Nonetheless, the level of *Rv2549c* transcript observed after treatment with ATc for a period of 1h, was significantly higher than that in the uninduced control. Similar results were obtained with the non-toxic *vapC*, *Rv2546* (Figure 3.16B). These results therefore confirm that the VapCs Rv2549c and Rv2546 are conditionally expressed by addition of ATc and suggest that the lack of toxicity associated with ectopic expression of Rv2546 in a mycobacterial host is not due to a lack of transcription of the encoding gene.
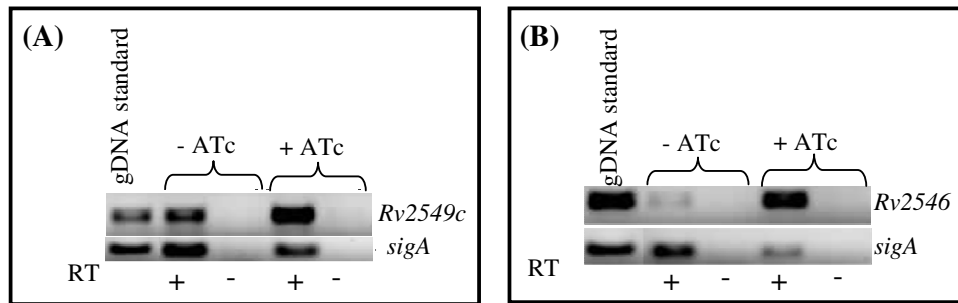
Figure 3.16: Inducible expression of (A) the toxic *Rv2549c vapC* and (B) the non-toxic *Rv2546 vapC*. Cells were grown in a 50ml culture volume to mid-logarithmic phase (OD$_{600}$ ~ 0.4 - 0.7), and divided into 2 equal volumes. To one 25ml aliquot, ATc was added at a concentration of 50ng/ml to induce VapC expression. Both 25ml cultures were then incubated at 37°C for 1h to allow for mRNA expression in the induced samples. Both RNA extraction and reverse transcription were performed as described in Section 2.8, and 10µl of the amplified cDNA was loaded onto a 2% agarose gel.

Since the lack of toxicity of Rv2546 could be as a result of defective post-translational processing, an epitope tagging system was used to detect VapC proteins when conditionally expressed in *M. smegmatis* (Figure 3.17). Here, the gene of interest was amplified by PCR to incorporate the standardized consensus ribosome binding site (GGAAG/A) at the N-terminus in order to optimize the yield of expressed protein. The PCR amplification also incorporated a triple (3×) FLAG sequence at the C-terminus, followed by the native stop codon. This amplicon was cloned into the *BamH*I/*Hind*III

site of pSE100 under the control of the $P_{myc1}tetO$ promoter-operator element. The resulting FLAG-tagged construct, pSEvapC_FLAG, was co-electroporated with pMC1s into *M. smegmatis* to allow for conditional gene expression upon addition of ATc. The supernatants and pellets from whole-cell extracts of ATc-induced *vs.* uninduced *M. smegmatis* strains were run on SDS-PAGE gels, and blotted onto nitrocellulose membranes before detection of the FLAG-tagged fusion protein by an anti-FLAG antibody (Figure 3.17).
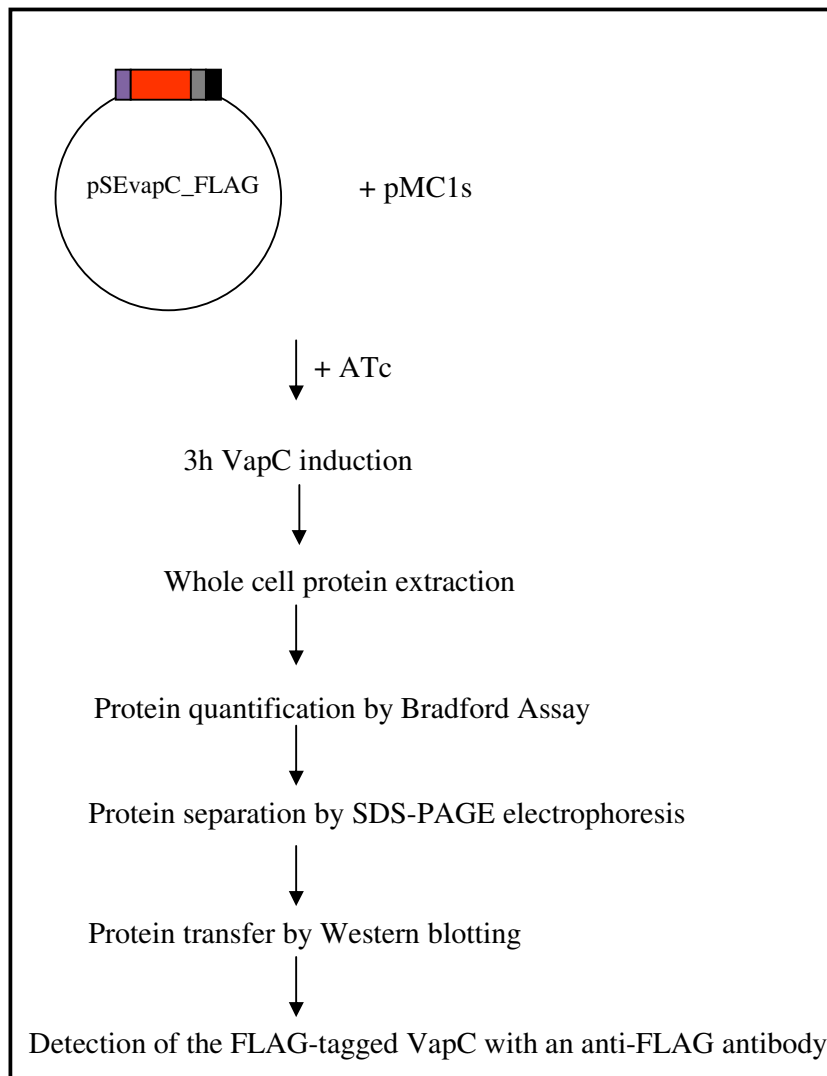
Figure 3.17: Schematic representation of construction, expression and detection of epitope tagged VapC proteins in *M. smegmatis*. Annotation of the episomal construct: The purple box represents the $P_{myc1}tetO$ promoter, the red box represents the VapC with a consensus ribosome binding site, the grey box represents the 3 × FLAG sequence and the black box denotes the stop codon.

As per Figure 3.17, the non-toxic Rv2546 was epitope-tagged and co-electroporated with pMC1s into *M. smegmatis.* After addition of ATc at a concentration of 50ng/ml for 3h to allow for protein expression, detection of the FLAG-tagged fusion protein by an anti-FLAG antibody, revealed the tagged 17.53kDa Rv2546 protein in both the supernatant and pellet fractions of *M. smegmatis*, with more protein observed in the supernatant fractions (Figure 3.18). As observed with the transcription data (Figure 3.16), this gene expression system was leaky since protein was observed even in the absence of the ATC inducer (Figure 3.18). These data conclusively demonstrate that, although insoluble Rv2546 was observed in the pellet fraction, this non-toxic VapC was translated using this system. This therefore excluded defective post-translational processing as a factor for non-toxicity of this VapC.
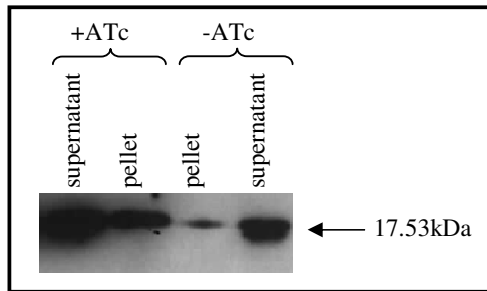
Figure 3.18: Detection of the FLAG-tagged Rv2546 protein. Cells were grown in a 50ml culture volume to early-logarithmic phase (OD$_{600}$ 0.3 - 0.4), and divided into 2 equal volumes. To one 25ml culture aliquot, ATc was added to a concentration of 50ng/ml to induce Rv2546 expression. Both 25ml culture aliquots were then incubated at 37°C for 3h to allow for protein translation in the induced samples. Subsequent to protein extraction, a Bradford assay was performed to ensure equal amounts of total protein (10µg) were loaded into each well of the SDS-PAGE gel. Hybridization and western blotting were performed as previously described (Section 2.9) to detect the flag-tagged protein.

3.2.7 A specific VapC expression threshold appears to be required for toxicity in *M. smegmatis*

The effect of Rv2549c expression on the growth of *M. smegmatis* was responsive to the concentration of ATc (Figures 3.9 & 3.19A), suggesting that the system was titratable. Western blot analysis of *M. smegmatis* cultures expressing Rv2549c carrying a C-terminal 3× FLAG tag (Figure 3.17), that were induced with varying ATc concentrations, revealed that the level of Rv2549c protein was indeed

titratable, with increased amounts of VapC observed when higher ATc concentrations were used for induction (Figure 3.19B).
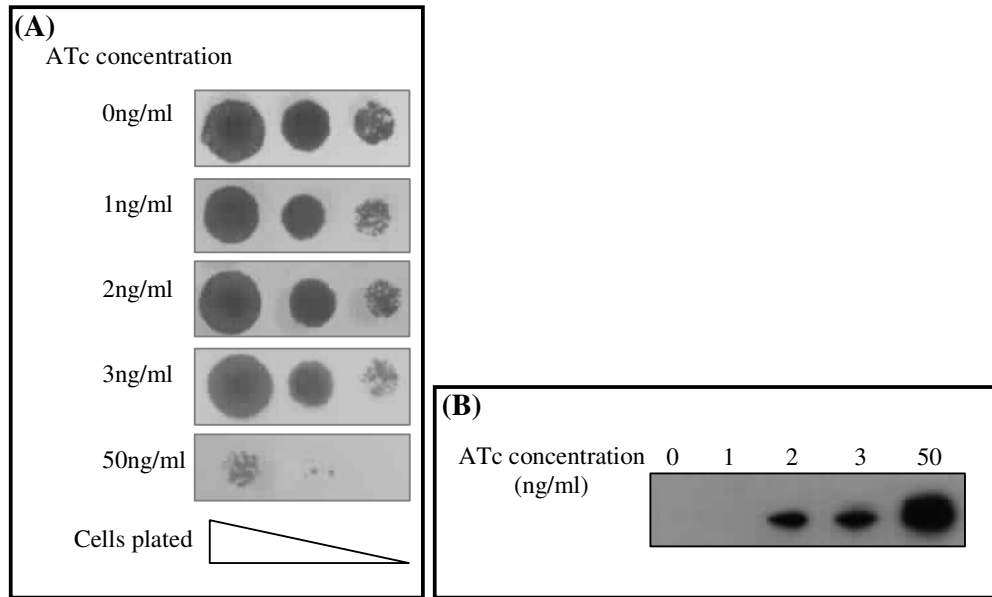
Figure 3.19: The titratable Rv2549c VapC initiates mycobacterial toxicity when its protein levels reach the threshold caused by >3ng/ml ATc. **(A)** Spotting assays in which 10μl of 10-fold serial dilutions of mid-logarithmic phase *M. smegmatis* cells were spotted on 7H10 agar with or without ATc (0 - 50 ng/ml) and incubated for 24 - 48 h at 37°C before scoring. **(B)** To determine Rv2549c concentrations by Western blotting, 25ml cultures induced with varying ATc concentrations were incubated at 37°C for 3h. Extraction, quantification and detection of the Rv2549c protein, was performed as previously described (Section 2.9), with 3μg of protein from each culture loaded into each lane of the SDS-PAGE gel.

Since toxicity of Rv2549c was only observed once a certain threshold of the VapC was present in the cell (Figure 3.19), it is possible that the reason for the non-toxicity attributed to Rv2546 was as a result of insufficient Rv2546 present in the cell. To determine if this was the case, the level of Rv2546 protein produced when constitutively expressed (*i.e.* in the absence of a TetR) was compared to the level of Rv2549c protein when conditionally expressed by induction with ATc at a concentration of 2ng/ml, which is known not to cause mycobacterial toxicity (Figure 3.19). Briefly, the expression vector carrying the C-terminally FLAG-tagged *Rv2546* under the control of P$_{myc1}$*tetO* was electroporated into *M. smegmatis* in the absence of a TetR. An ensuing *M. smegmatis*::pSE2546_FLAG transformant was grown to mid-logarithmic phase and as per Figure 3.17, cellular proteins were extracted, quantified using the Bradford Assay (Section 2.9). Equal amounts of total protein from *M.*

smegmatis::pSE2546_FLAG and *M. smegmatis*::pSE2549c_FLAG obtained when Rv2549c was either uninduced or induced with ATc at a concentration of 2ng/ml were separated by SDS-PAGE electrophoresis. The epitope-tagged Rv2546 and Rv2549c proteins were then detected using an anti-FLAG antibody, as described above (Figure 3.17). This experiment revealed that even when tagged Rv2546 was constitutively expressed, the level of this protein was markedly lower than that of the tagged Rv2549c protein when induced with 2ng/ml ATc (Figure 3.20). The profound difference in VapC protein levels when comparing Rv2546 to Rv2549c (Figure 3.20), could explain their differential effects on mycobacterial growth.
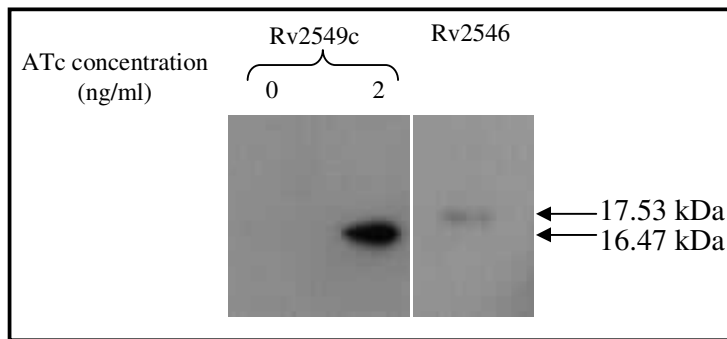
Figure 3.20: Comparison of the relative abundance of unregulated Rv2546 protein vs. Rv2549c induced with 2ng/ml ATc. A 25ml *M. smegmatis* culture constitutively expressing the epitope-tagged Rv2546 was grown to mid-logarithmic phase. Protein was extracted, quantified and 3µg of protein loaded into each lane of an SDS-PAGE gel was detected as previously described (Section 2.9). A 50ml *M. smegmatis*::pSE2549c_FLAG strain was grown to early-logarithmic phase (OD$_{600}$ 0.3 - 0.4), and divided into 2 equal volumes. To one of the 25ml cultures, ATc at a concentration of 2ng/ml was added to induce VapC expression. Both 25ml culture aliquots were then incubated at 37°C for 3h to allow for protein translation in the induced samples. The epitope-tagged VapCs were extracted, quantified and detected as previously described (Section 2.9), with 3µg of protein from each culture loaded onto the SDS-PAGE gel.

3.3 Abrogation of *M. tuberculosis* VapC toxicity

Having established that ectopic expression of Rv2549c was growth inhibitory in *M. smegmatis* and *M. tuberculosis* (Figs. 3.11 and 3.15), this VapC was used as a tool to investigate how VapC toxicity in a mycobacterial host can be neutralized.

3.3.1 <u>Co-expression of the Rv2550c VapB abrogates the growth inhibitory effects of Rv2549c</u>

To assess whether Rv2549c toxicity could be neutralised by its cognate Rv2550c antitoxin when expressed as a bi-cistronic unit, the 746bp *Rv2550c-Rv2549c* operon was amplified by PCR and cloned into the *BamH*I and *Hind*III sites of pSE100, to generate the pSE2550c_49c construct. This construct was co-electroporated with pMC1s into *M. smegmatis*. Integration of the pMC1s plasmid was confirmed by PCR using the *attB* primers and the integrity of pSE2550c_49c was confirmed by restriction analysis and sequencing of plasmid recovered from a *M. smegmatis* transformant by electroduction into *E. coli* (data not shown). Spotting assays on plates containing ATc at a concentration of 50ng/ml revealed that regulated expression of the bi-cistronic unit, *Rv2550c-Rv2549c* had no effect on the growth and viability of *M. smegmatis* (Figure 3.21). Semi-quantitative RT-PCR confirmed the presence of the Rv2549c transcript in ATc-induced cultures of the strain carrying the *Rv2550c-Rv2549c* operon (Figure 3.22). This conclusively demonstrated that co-expression of the Rv2550c antitoxin abrogated the toxicity of its cognate Rv2549c toxin.
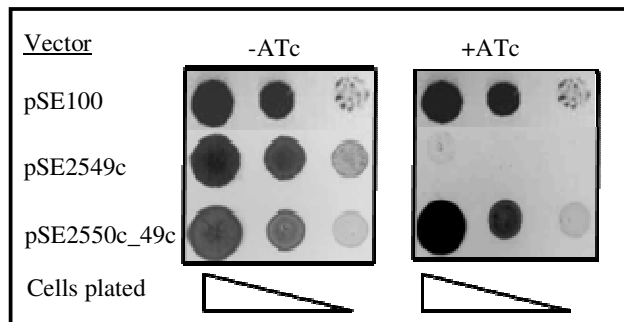
Figure 3.21: Effect of ectopic expression of the *Rv2550c-Rv2549c* operon on the growth of *M. smegmatis*. Induction of *Rv2550c_Rv2549c* has no growth inhibitory effects on *M. smegmatis* as assessed by spotting assays in which 10-fold serial dilutions of late logarithmic phase cells were spotted on 7H10 agar with or without ATc (50ng/ml). The vectors pSE100 and pSE2549c were used as negative and positive controls, respectively.
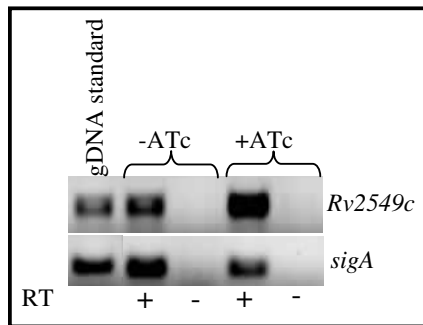
Figure 3.22: Inducible expression of the *Rv2550c-Rv2549c* operon. Cells containing pSE2550c_49c were grown in a 50ml culture volume to mid-logarithmic phase (OD$_{600}$ ~ 0.4 - 0.7), and divided into 2 equal volumes. To one of the 25ml culture aliquots, 50ng/ml ATc was added to induce *vapBC* expression. Both 25ml aliquots were then incubated at 37°C for 1h to allow for mRNA expression in the induced samples. Both RNA extraction and reverse transcription were performed as previously described (Section 2.8), and 10µl of the amplified cDNA, using *Rv2549c* specific primers, was loaded onto a 2% agarose gel.

3.3.2 The toxicity of Rv2549c and Rv0595c can only be abrogated by their respective cognate antitoxins

To assess whether VapC toxicity could also be neutralized by expression of a non-cognate VapB, an uncoupled expression system was developed in which *vapC* and *vapB* genes were expressed under the control of different promoters from different chromosomal loci. In this system, the *vapC* gene was expressed under control of P$_{myc1}$*tetO* on a Tweety-based integrative vector containing a gentamicin resistance cassette as well as the P$_{smyc}$-*tetR* element from pMC1s to allow for ATc-dependent regulation of *vapC* expression (pTTvapC). This Tweety-based integration-proficient vector, pTTvapC, which possesses the *attP-int* region of the *M. smegmatis* mycobacteriophage Tweety, integrates at a tRNA^{Lys} attachment site (223). It is important to note that this uncoupled expression system differs significantly from the system previously used to assess VapC toxicity (Section 3.2), as the *vapC* is cloned in single copy (*i.e.* on an integrative vector) rather than in multi-copy (i.*e.* on an episomal plasmid). The antitoxins, on the other hand, were cloned under the control of the acetamide-inducible acetamidase promoter, P$_{ami}$ on a Km^R, mycobacteriophage L5-based integration vector that integrates at a tRNA^{Gly} attachment site, to generate a pMAPvapB construct (Table 2.4).

Using this expression system, the toxicity of Rv2549c, and the abrogation thereof, was initially assessed. It was imperative to first determine whether sufficient Rv2549c was expressed in this configuration to inhibit *M. smegmatis* growth. To this end, the pTTRv2549c construct was electroporated into *M. smegmatis*, and a resulting transformant was spotted on solid media containing ATc at a concentration of 50ng/ml. In this configuration, the toxicity of Rv2549c was retained (Figure 3.23), thus convincingly demonstrating that even when ATc-dependent expression of Rv2549c was driven from a single-copy integrating vector, growth inhibition was still observed.
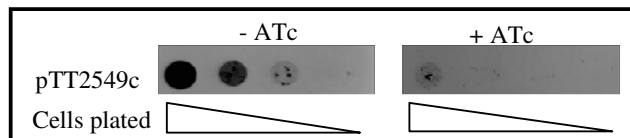
Figure 3.23: Toxicity of Rv2549c when expressed from the Tweety site. Growth was assessed by a spotting assay, where 10µl aliquots of 10-fold serial dilutions of logarithmic phase cells were spotted on 7H10 agar with (50ng/ml) or without ATc.

In contrast to the ATc-dependent regulation of Rv2549c expression observed in this system, Rv2550c expression under the control of the acetamidase promoter was not regulatable by addition of acetamide (Figure 3.24). In accordance with previous observations (135, 214, 216), the acetamidase promoter is non-regulatable and as a result, the antitoxin was expressed even in the absence of acetamide.
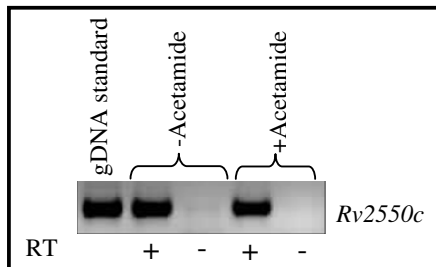
Figure 3.24: Expression of *Rv2550c* from the phage L5 attachment site of *M. smegmatis*. Cells were grown in a 50ml culture volume to mid-logarithmic phase (OD$_{600}$ ~ 0.4 - 0.7), and divided into 2 equal volumes. To one of the 25ml culture aliquots, acetamide was added at a concentration of 2mg/ml to induce *vapB* expression. Both 25ml cultures aliquots were then incubated at 37°C for 1h to allow for mRNA expression in the induced samples. RNA was isolated and quantified as described in Section 2.8.

Having confirmed that Rv2549c expression conferred toxicity and that Rv2550c was expressed, the uncoupled system was then used to determine what effect expression of cognate vs. non-cognate *vapB* expression would have on the growth inhibition of *M. smegmatis* upon ATc-inducible expression of two toxic VapCs, namely Rv2549c and Rv0595c, the latter of which was also toxic in this configuration (data not shown). The pTTRv2549c and pTTRv0595c constructs were co-electroporated with various antitoxin-expressing constructs into *M. smegmatis* (Figure 3.25) (Table 2.4). The transformants were grown to mid-logarithmic phase (OD_{600} ~ 0.4 - 0.7) and then spotted onto plates containing various antibiotics (Figure 3.26). In this configuration, both the Rv2549c and Rv0595c toxicity (Figure 3.26A&B, panel 1) was completely neutralized by expression of the cognate Rv2550c and Rv0596c antitoxins, respectively, when integrated at a chromosomal locus distal from that of the toxin (Figure 3.26A&B, panel 2). In stark contrast, two different non-cognate antitoxins, which previously had been shown to abrogate toxicity of their cognate toxins when co-expressed on an operon (Figure 3.21, and Diane Kuhnert, personal communication), could not alleviate the toxic effects of Rv2549c, and Rv0595c when expressed in a strain of *M. smegmatis* in which the non-cognate toxin is also expressed (Figure 3.26A&B, panels 3&4). These data therefore confirm the specificity of the VapC-VapB interactions for the two cases investigated in this study, namely Rv2549c-Rv2550c, and Rv0595c-Rv0596c.
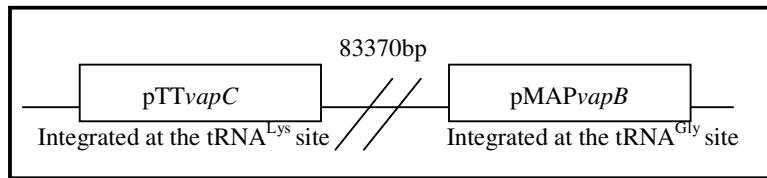
Figure 3.25: Schematic representation of a *M. smegmatis* strain carrying a *M. tuberculosis vapC* gene under the control of $P_{myc1}tetO$ integrated at the phage Tweety attachment site and a *M. tuberculosis vapB* gene (cognate or non-cognate) under the control of the P_{ami} promoter integrated at the phage L5 attachment site in the mycobacterial chromosome.
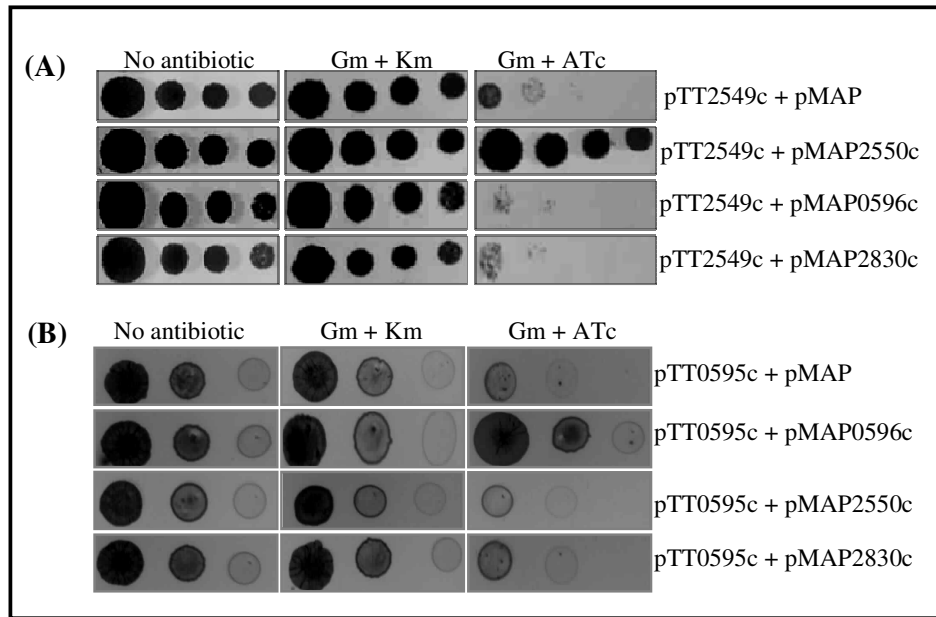
Figure 3.26: VapC toxicity is specifically abrogated by its cognate VapB antitoxin. The *M. smegmatis* strains express: **(A)** *Rv2549c* under the control of P$_{myc1}$*tetO* from the Tweety attachment site and cognate vs. non-cognate *vapB* genes under the control of P$_{ami}$ from the L5 attachment site of the chromosome. **(B)** Rv0595c under the control of P$_{myc1}$*tetO* from the Tweety site and the same *vapB* under the control of P$_{ami}$ from the L5 sites of the chromosome. For induction of *vapC* gene expression, 10µl of 10-fold serial dilutions of cells were spotted on 7H10 agar with or without ATc (50ng/ml).

3.3.3 <u>Can mutation of an aspartic acidic residue conserved in PIN domain proteins also abrogate the growth inhibitory effects of Rv2549c?</u>

To determine whether there was an association between the growth inhibitory effects of VapC function and nuclease activity associated with PIN domain proteins (50, 186), the acidic Asp/Asp/Gln/Asp residues that are conserved in VapCs were first identified by multiple sequence alignment (Figure 3.3). If these residues are required for VapC catalytic function, then mutation of one or more of these residues would be expected to lead to loss of catalytic function, and hence, loss of VapC toxicity. The conserved Asp5 residue in the N-terminal region of Rv2549c was thus mutated to an Ala residue, to produce the Rv2549c^{D5A} mutant. The *Rv2549c^{D5A}* gene was cloned into the pSE100 vector, and the resulting construct, pSE2549cM, was co-electroporated into *M. smegmatis* together with pMC1s. The effect of this mutation on the viability of *M. smegmatis* was assessed alongside the empty vector (negative control), the wild-type Rv2549c (positive control), as well as the Rv2550c-Rv2549c operon negative

control, by spotting serial dilutions of the various cultures on plates containing ATc at a concentration of 50ng/ml. As expected, the empty vector and Rv2550c-Rv2549c controls showed no ATc-dependent *M. smegmatis* growth inhibition, whereas expression of the Rv2549c toxin resulted in growth inhibition. Interestingly, the Asp5→Ala mutation in Rv2549c completely abrogated the growth inhibitory effects resulting from ectopic expression of this VapC (Figure 3.27).
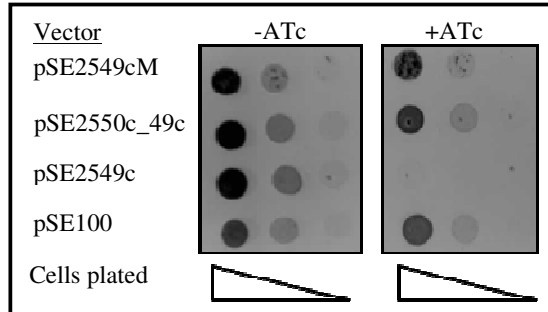
Figure 3.27: Effect of ectopic expression of the Rv2549cM on the growth of *M. smegmatis*. For induction of gene expression 10-fold serial dilutions of logarithmic-phase cells were spotted on 7H10 agar with or without ATc (50ng/ml).

To test whether the expression level of Rv2549c was affected by the Asp5→Ala mutation, a gene encoding a C-terminal, FLAG-tagged version of the mutated VapC, Rv2549c^{D5A}, was generated by PCR and cloned in pSE100. The expression cassette was identical, in all respects, to the FLAG-tagged version of wild type Rv2549c described above (Section 3.2.7), with the exception of the D5A mutation. This expression cassette was cloned into the *BamHI*/*Hind*III site of pSE100 under the control of the P$_{myc1}$*tetO* promoter-operator element. The ensuing FLAG-tagged construct was co-electroporated with pMC1s in *M. smegmatis* and detected using an anti-FLAG antibody post-induction with ATc at a concentration of 50ng/ml, as described previously (Figure 3.17). Western blot analysis revealed that the 16.47kDa Rv2549c^{D5A} VapC was indeed expressed upon addition of ATc at a concentration of 50ng/ml (Figure 3.28A). However, comparison of its expression level to that of the corresponding wild type protein revealed that the relative abundance of Rv2549c^{D5A} was significantly lower than the corresponding wild type protein (Figure 3.28A). Moreover, even when Rv2549c^{D5A} was constitutively expressed in the absence of a TetR, the amount of protein present was significantly less than that of wild type

Rv2549c conditionally expressed at an ATc concentration of 2 ng/ml (Figure 3.28B), which had been shown not to cause toxicity (Figure 3.19).
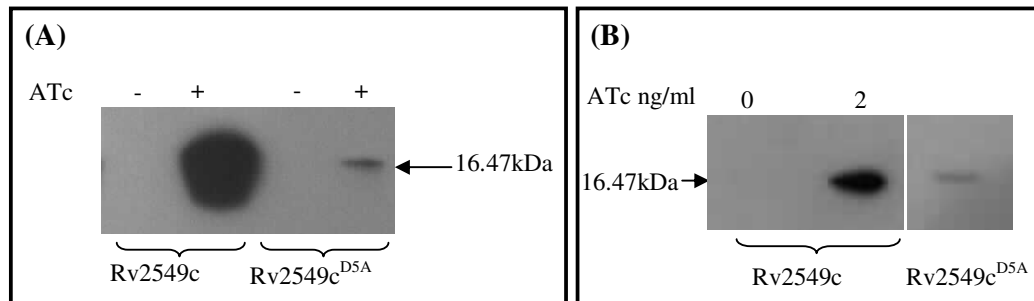
Figure 3.28: Detection of FLAG-tagged Rv2549c and Rv2549cD5A proteins. **(A)** Cells were grown in a 50ml culture volume to early-logarithmic phase (OD$_{600}$ ~ 0.3 - 0.4), and divided into 2 equal volumes. To one 25ml culture aliquot, ATc was added to a concentration of 50ng/ml to induce gene expression. Both 25ml culture aliquots were then incubated at 37°C for 3h to allow for protein translation in the induced samples. Subsequent to protein extraction, a Bradford assay was performed to ensure equal amounts of protein at a concentration of 5µg were loaded onto the SDS-PAGE gel. Hybridization and western blotting were performed as previously described (Section 2.9) to detect the flag-tagged protein. **(B)** A 25ml *M. smegmatis* culture constitutively expressing the epitope tagged Rv2549c^{D5A} was grown to mid-logarithmic, and protein was extracted, quantified and 3µg of loaded protein was detected as previously described (Section 2.9). A 50ml *M. smegmatis*::pSE2549c_FLAG strain was grown to early-logarithmic phase (OD$_{600}$ ~ 0.3 - 0.4), and divided into 2 equal volumes. To one of the 25ml cultures, ATc at a concentration of 2ng/ml was added to induce VapC expression. Both 25ml culture aliquots were then incubated at 37°C for 3h to allow for protein translation in the induced samples. The epitope tagged VapCs were extracted, quantified and detected as previously described (Section 2.9), with 3µg of protein from each culture loaded onto the SDS-PAGE gel.

The Asp5→Ala mutation Rv2549c may have affected the level of protein by destabilizing the mRNA secondary structure and thus decreasing translational efficiency (55, 224, 281), or by destabilizing the N-terminus of the translated protein, resulting in protein degradation (224, 285). To investigate the latter possibility, the structures of both the wild type and mutant proteins were predicted using the PSIPRED protein structure prediction program (26). Interestingly, this analysis revealed a potentially significant difference in the predicted structure of Rv2549c^{D5A} compared to Rv2549c. Specifically, the Asp5→Ala mutation was predicted to have disrupted the first β strand in Rv2549c, resulting in a protein comprised of three instead of four β strands (Figure 3.29). This amino acid substitution in the N-terminal region of Rv2549c may have affected the structure and/or folding of the protein, rendering it more prone to intracellular degradation. Irrespective of the reason underlying the difference in expression level between Rv2549c and Rv2549c^{D5A} in *M.*

smegmatis (Figure 3.28), this finding makes it difficult to ascribe the lack of toxicity observed for Rv2549c^{D5A} to a loss of nuclease activity.

Figure 3.29: Predicted protein structure of (A) Rv2549c and (B) Rv2549c^{D5A} using the PSIPRED protein structure prediction server.

3.3.4 <u>Members of the other type II TA families do not alleviate VapC toxicity in *M. smegmatis*</u>

Members of some type II TA module families have been implicated in regulation of other TA modules either directly or indirectly (91, 138, 304). As such it was important to determine whether VapC function in *M. smegmatis* is modulated, in any way, by the presence of other type II TA modules. To this end, a *M. smegmatis* mc^{2}155 parental strain and a derivative thereof that lacks all three type II TA modules – *vapBC*, *mazEF* and *phd/doc* (Δ*mazEF* Δ*vapBC*::*aphA-3* Δ*phd/doc*::*aph*) were obtained as a generous gift from Professor Gregory Cook (University of Otago, New Zealand). The plasmids expressing each of the ten *M. tuberculosis* VapCs and the sole *M. smegmatis* VapC (MSMEG_1284) (Section 3.2.1) were electroporated into both strains without a *tetR*-expressing vector, and transformation efficiencies determined (Table 3.6). As observed previously (Section 3.2.1), Rv0627, Rv1953, Rv2010, Rv2546, Rv2548 and MSMEG_1284 had no effect on the wild type strain of *M. smegmatis*, as evidenced by the fact that the transformation efficiencies of the expression vectors were similar to that of the empty vector control (0.6 - 3.8 fold change), whereas Rv0549c, Rv0595c, Rv2549c, Rv2829c and Rv3320c were toxic to *M. smegmatis*, as evidenced by $\geq$ 2-log$_{10}$ lower transformation efficiencies (Table 3.6).

As in the wild type *M. smegmatis* strain, the VapCs Rv0549c, Rv0595c, Rv2549c, Rv2829c and Rv3320c were toxic to the Δ*mazEF*Δ*vapBC*::*aphA-3*Δ*phd/doc*::*aph*, as evidenced by $\geq$ 4-log$_{10}$ lower transformation efficiencies (Table 3.6). It was however interesting to note that constitutive ectopic expression of the VapCs Rv0627, Rv1953, Rv2010, Rv2546, Rv2548 and MSMEG_1284 VapCs, had also no effect on the viability of the *M. smegmatis* Δ*mazEF*Δ*vapBC*::*aphA-3*Δ*phd/doc*::*aph* strain (between 0.08 and 6 fold of the transformation efficiency of pSE100) (Table 3.6). Taken together, these data suggest that VapC function in *M. smegmatis* is not modulated by the presence of other, chromosomally encoded type II TA modules in this organism.

Table 3.6: Effect of unregulated mycobacterial VapC expression in an *M. smegmatis* strain devoid of any type II TA modules

VapC	Plasmid	Wild type transformation efficiency (CFU/µg)*	*ΔmazEF ΔvapBC::aphA-3 Δphd/doc::aph* transformation efficiency (CFU/µg)*
-	pSE100	3.4×10^3	1.7×10^5
Rv0549c	pSE0549c	44	2
Rv0595c	pSE0595c	20	4
Rv0627	pSE0627	2.1×10^3	1.0×10^6
Rv1953	pSE1953	6.8×10^3	1.0×10^6
Rv2010	pSE2010	4.1×10^6	3.3×10^5
Rv2546	pSE2546	2.5×10^3	2.9×10^5
Rv2548	pSE2548	1.2×10^4	7.5×10^4
Rv2549c	pSE2549c	30	8
Rv2829c	pSE2829c	12	16
Rv3320c	pSE3320c	2	2
MSMEG_1284	pSESM1284	1.2×10^4	1.3×10^4

*The data are from one of three independent experiments.

3.4 Does the single *vapBC* module play a role in *M. smegmatis* stress physiology?

TA modules have been shown to play a significant role in stress-induced growth regulation (38, 39, 41, 50, 111, 118, 119, 131, 134, 151, 237, 248, 249, 304, 312). The fact that *M. smegmatis* has a highly restricted complement of TA modules, which includes only one *vapBC*, makes this organism an attractive one for investigating the role of TA modules in mycobacterial physiology. To determine if the *M. smegmatis vapBC* plays a role in stress physiology, a deletion mutant of *M. smegmatis* mc²155 in which an internal segment of the *MSMEG_1283-MSMEG_1284* operon was removed by allelic exchange mutagenesis was constructed. The two-step allelic replacement strategy employed for this purpose allows for the replacement of a functional chromosomal gene with a disrupted copy carried on a suicide vector. As described in Section 2.8, the p2ΔSM1283_84KO suicide vector was engineered to carry 932bp of the genomic region upstream of the *vapB* gene *MSMEG_1283*, and 23bp of the 5' end of this gene, as well as 880bp of the genomic region downstream of the *vapC* gene *MSMEG_1284*, and 219bp of the 3' end of this gene. This construct,

which lacks a 428bp segment internal to the *MSMEG_1283-MSMEG_1284* operon and the two of the conserved acidic residues essential for MSMEG_1284 ribonuclease activity *i.e* Asp^5 and Gln^{38}, was electroporated into *M. smegmatis* and plated on media containing Km, Hyg and X-gal to select for a partial merodiploid carrying both the wild type and the deleted operon. After a 3 - 5 day incubation period at 37°C, seven blue, Km^{R-}, Hyg^{R-} colonies were recovered. Two of these putative single cross-over recombinants (SCOs) were subjected to *sacB*-based counter selection, by plating on sucrose and Km, to allow double cross-over (DCO) recombinants to be identified. Ten white, Suc^{R-}, Km^{S-} clones were identified from both SCOs. Genotypic characterization of these recombinants by PCR revealed that two of the ten colonies were wild type revertants, in which the second crossover event occurred on the same side of the deletion mutant as the first, whereas two showed a PCR genotype expected for genuine, allelic exchange mutants. These classes of DCOs were distinguishable by the size of the PCR amplicons obtained (data not shown). The remaining four colonies appeared to be spontaneous *sacB* mutants of the SCO recombinant.

One of the putative allelic exchange mutants was selected for further study. The genotype of this Δ*MSMEG_1283-MSMEG_1284* strain was confirmed by Southern blot analysis (Figure 3.30). Using this strategy, a probe was generated by PCR to hybridize to the 2857bp and 4204bp *EcoR*V fragments of *MSMEG_1283-MSMEG_1284* in the wild type *M. smegmatis*. Successful disruption of the *vapBC* module should result in the deletion of an internal 428bp segment within the operon. Southern blot analyses of the wild type *M. smegmatis* strain revealed that the probe bound to 2857bp and 4204bp *EcoR*V fragments, as expected. This analysis revealed that the two SCOs that had been used to identify DCOs, by *sacB*-based counter-selection, differed in that one was a product of homologous recombination in the upstream region, whereas the other the product of recombination in the downstream region. Importantly, this analysis confirmed the genotype of the Δ*MSMEG_1283-MSMEG_*1284 mutant since a 2429bp cross-hybridizing fragment was observed in place of the wild type 2857bp *EcoR*V fragment, consistent with loss of an internal 428bp fragment within the *MSMEG_1283-MSMEG_1284* operon. Furthermore, this deletion did not affect the integrity of the regions upstream of the *MSMEG_1283-MSMEG1284* operon, with the 4204bp region remaining unaffected (Figure 3.30).
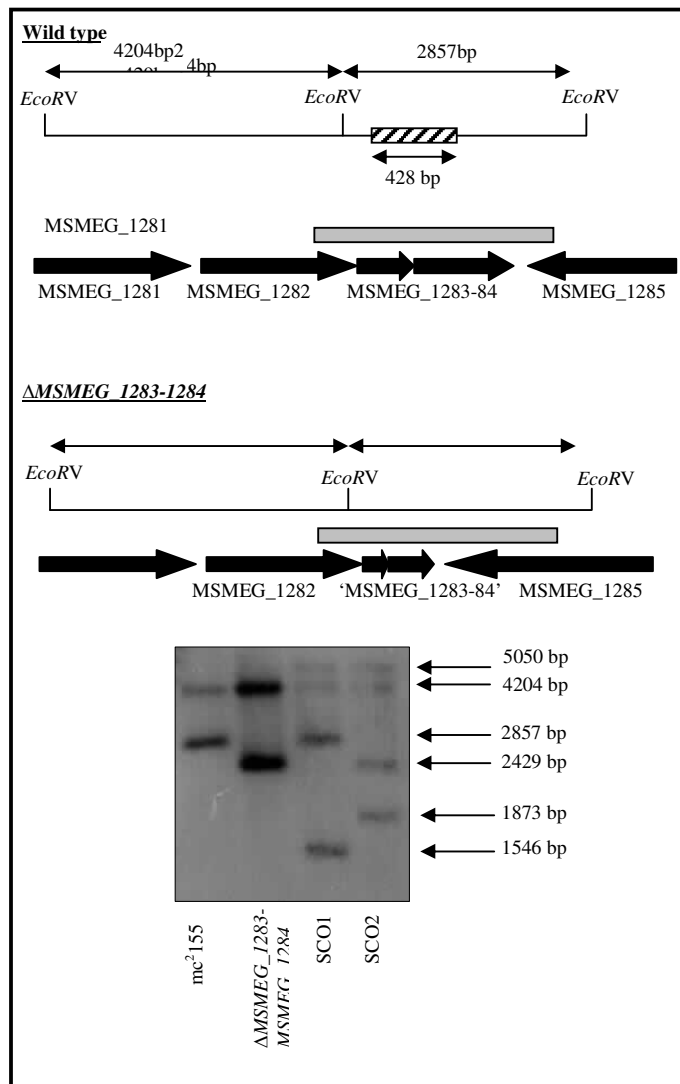
Figure 3.30: Construction and genotypic characterization of *ΔMSMEG_1283-MSMEG_1284* mutant by homologous recombination. The *MSMEG_1283-MSMEG_1284* and flanking genes are shown as solid arrows (Figure not drawn to scale). The hatched box represents the 428bp internal deletion in the Δ*MSMEG_1283-MSMEG_1284* mutant strain. For the Southern blot analysis (below), 1 - 5μg chromosomal DNA was digested with *EcoR*V, which cuts on either side of the deleted region, to produce a common 4204bp fragment in both wild type and mutant strains. This digestion also produces a 2857bp fragment in the wild type strain and a 2429bp fragment in the mutant strain. All fragments were detected using a PCR-generated probe denoted by the grey box.

3.4.1 The sole *vapBC* module is dispensable for growth of *M. smegmatis* in liquid media

To determine whether loss of *vapBC* function affected the growth of *M. smegmatis*, the Δ*MSMEG_1283-MSMEG_1284* strain was compared to its parental wild type when grown into stationary phase in 7H9 media containing glycerol. However, the two strains were indistinguishable in terms of the rate of growth and the maximum cell density achieved in stationary phase (Figure 3.31).
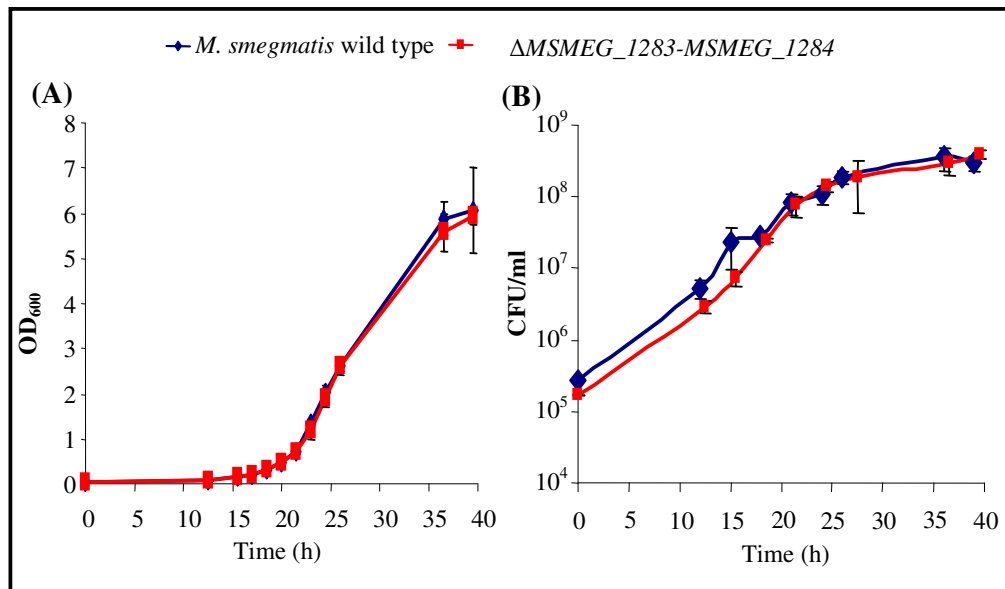
Figure 3.31: Deletion of *MSMEG_1283-MSMEG_1284* has no effect on the growth kinetics of *M. smegmatis*. **(A)** OD_{600} spectrophotometric readings were taken at regular intervals over a 40h period. **(B)** CFUs were assessed by plating 100µl of 10-fold serial dilutions of cells over a 40h period, and scored after 3 - 4 days incubation at 37°C. The data represent the average of 3 independent experiments.

3.4.2 The *M. smegmatis vapBC* module is dispensable for the survival of *M. smegmatis* under conditions of stress

To determine whether the single *M. smegmatis vapBC* module is involved in the response of the organism to nitrosative, genotoxic, cell wall, heat, or antibiotic-mediated stresses, the survival of the Δ*MSMEG_1283-MSMEG_1284* strain was compared to wild type under these stress conditions by monitoring CFUs during the course of the exposure. The mutant and wild type strains behaved identically in all of

the assays, suggesting that the *vapBC* module is dispensable for the survival of *M. smegmatis* under the stress conditions tested (Figure 3.32).
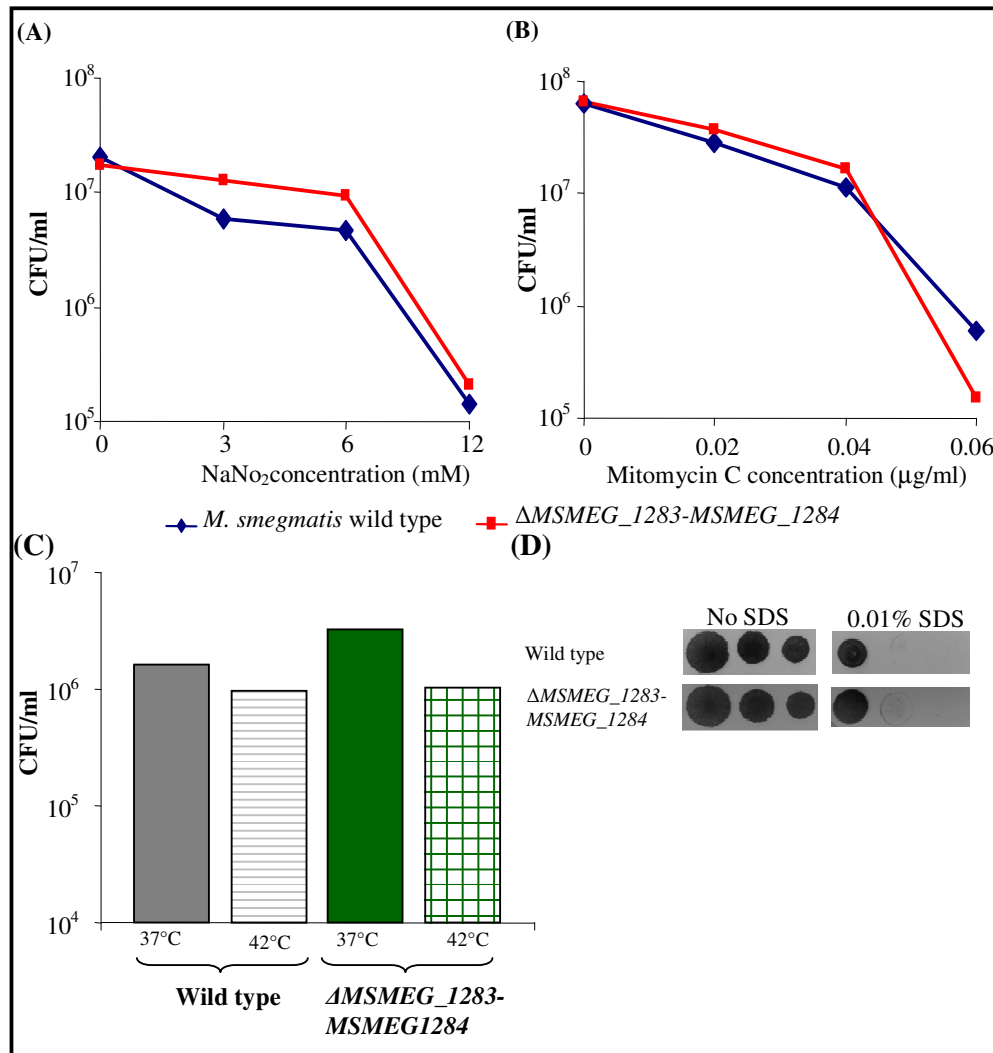
Figure 3.32: Effect of loss of *MSMEG_1283-MSMEG_1284* on the survival of *M. smegmatis* under conditions of (A) Nitrosative, (B) Genotoxic, (C) Heat and (D) Cell wall stress. CFUs were assessed by plating 10-fold serial dilutions of *M. smegmatis* cells exposed to the various stresses as described in Section 2.7. The data panels represent one of three biological replicates.

To then assess whether the *vapBC* module plays a role in the susceptibility of *M. smegmatis* to anti-mycobacterial drugs, the MICs of four drugs were determined for the wild type and Δ*MSMEG_1283-MSMEG_1284* strains by the broth microdilution method (Section 2.10). For both strains, the MICs of ofloxacin, streptomycin and clofazimine fell within the reported range of 0.25 - 4μg/ml, 0.25 -

2μg/ml and 0.12 - 8μg/ml, respectively (233, 271, 294, 295). In contrast, the MIC values of rifampicin differed by < 2- fold of the reported values of 16 - 32μg/ml (43, 229, 271, 295). This is not unexpected as the MIC value of rifampicin against *M. smegmatis* has been shown to be strain-dependent and also dependent on the starting inoculum size (43, 229, 271, 295). Taken together, these data revealed that loss of *vapBC* function had no discernable effect on the MICs of rifampicin, ofloxacin, streptomycin and clofazimine (Table 3.7). In summary, the *vapBC* module, *MSMEG_1283-MSMEG_1284*, was entirely dispensable *M. smegmatis* under all of the stress conditions tested.

Table 3.7: MICs of wild type and ΔMSMEG_1283-MSMEG_1284 M. smegmatis strains to anti-mycobacterial antibiotics

| Antibiotic | Minimal inhibitory concentration (μg/ml) | |
	mc^{2}155	Δ*MSMEG_1283-MSMEG_1284*
Rifampicin	6.25	6.25
Ofloxacin	0.4	0.4
Streptomycin	0.8	0.8
Clofazimine	0.8	0.8

3.5 Role of the cluster of three contiguous *vapBC* modules at the *Rv2545-Rv2550c* locus in *M. tuberculosis*

Given that TA modules have been implicated in the formation of multidrug tolerant persisters (74, 113, 142, 154, 155), and *M. tuberculosis* is intransigent to elimination by antibiotics (162, 165, 203, 206, 278), there is considerable interest in understanding the role of TA modules in *M. tuberculosis*. Based on the results described above, strains with altered expression of the *vapC* genes in the *Rv2545-Rv2550c* region of the *M. tuberculosis* genome were constructed for use in various assays in an attempt to understand the role of this cluster in the physiology of *M. tuberculosis*.

3.5.1 Construction of Δ*Rv2545-Rv2550c*::*hyg* and Δ*Rv2545-Rv2550c* mutants

A classic way to investigate the function of a gene is to determine the effect that loss of its function has on an organism. Whilst individually *Rv2545*, *Rv2546*, *Rv2547*, *Rv2548*, *Rv2549c* and *Rv2550c* are not essential (247), the possibility that that the *Rv2545-Rv2550c* cluster, as a whole, might be essential for growth of *M.*

tuberculosis could not be excluded. As such, strategies for generating both *hyg*-marked and unmarked deletions of the Δ*Rv2545-Rv2550c* cluster were pursued in parallel (103). As described in Section 2.6, the marked and unmarked suicide vectors, p2Δ2545_50cKO::*hyg* and p2Δ2545_50cKO, respectively, were engineered to contain an upstream region of homology generated as a 2052bp amplicon comprising 1921bp of the genomic region upstream of *Rv2545* with 131bp of the 5' end of *Rv2545*, and a downstream region of homology generated as a 1776 bp amplicon comprising 1734bp of the genomic region downstream of *Rv2550c* with 42bp of the 3' end of the *Rv2550c* gene. Both constructs were electroporated into the wild type *M. tuberculosis* H37Rv strain and plated on Km, Hyg and X-gal. After the first cross-over event, five blue Km^R, Hyg^R SCO recombinants were recovered from the electroporation with the p2Δ2545_50cKO::*hyg* vector. Two of these were subjected to *sacB*-based counter-selection by plating on sucrose-containing medium to identify products of second cross-over homologous recombination events. Eleven clones were recovered by counter-selection. These clones were identified as possible DCO mutants by virtue of their Hyg^R, Km^S, Suc^R phenotype and the fact that they formed white colonies when plated on X-gal-containing media and had thus lost the *lacZ* marker. Genotypic characterization of these eleven possible DCOs by PCR revealed that two were spontaneous *sacB* mutants, whereas the remaining nine clones were DCO recombinants with a putative Δ*Rv2545-Rv2550c*::*hyg* genotype (data not shown).

The genotype of these two Δ*Rv2545-Rv2550c*::*hyg* mutants was then further confirmed by Southern blot analysis using the strategy illustrated below (Figure 3.33). Using the *BamH*I restriction enzyme, digestion of wild type *M. tuberculosis* chromosomal DNA should yield a 6039bp fragment that would cross-hybridize to a probe within the *Rv2545-Rv2550c* region. Allelic exchange mutagenesis should result in the deletion of an internal 2426bp segment within the *Rv2545-Rv2550c* region as well as the insertion of a *hyg* cassette, resulting in a 4463bp fragment identifiable by the probe. In addition, this probe would also be able to ascertain the site-specificity of recombination as the *Bam*HI sites are located beyond the upstream and downstream region of homology contained in the suicide vector.

Southern blot analysis of both Δ*Rv2545-Rv2550c*::*hyg* mutants, with the same probe as that used in the wild type stain, identified the expected 4463bp fragment upon

digestion with *Bam*HI (Figure 3.33). This confirmed both the successful deletion of the three contiguous *vapBC* modules as well as the conservation of the integrity of the downstream region surrounding the three *vapBC* modules.
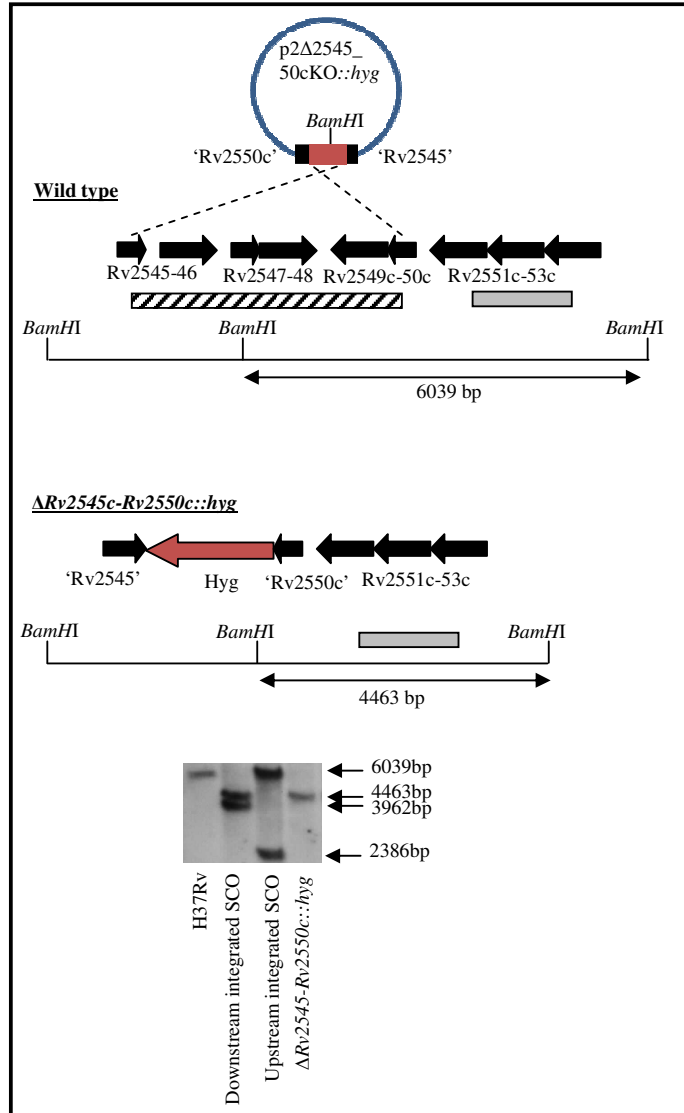
Figure 3.33: Construction and genotypic characterization of the marked Δ*Rv2545-Rv2550c::hyg* mutant by homologous recombination. The *Rv2545-Rv2550c* cluster and flanking genes are shown as solid arrows (Figure not drawn to scale). The hatched box represents the 2426bp internal segment replaced through homologous recombination by the hygromycin resistant cassette (red box) in the Δ*Rv2545-Rv2550c::hyg* strain. For the Southern blot analysis (below), 1 - 5µg chromosomal DNA was digested with *Bam*HI, which cuts on either side of the deleted region, to produce a 6039bp fragment in the wild type strain and a 4463bp fragment in the mutant strain. All fragments were detected using a PCR-generated probe denoted by the grey box.

Electroporation of the p2Δ2545_50cKO suicide vector into *M. tuberculosis* H37Rv, on the other hand, yielded two Km^R, Hyg^R blue colonies. These SCOs were confirmed to be site-specific, and each recombinant integrated either downstream or upstream of the *Rv2545-Rv2550c* cluster (Figure 3.34). These SCOs were then subjected to counter selection, where plating on sucrose and Km yielded eighty four white Suc^R, Km^S putative DCO recombinants. Of these putative DCOs, one was an allelic exchange mutant, whereas the rest were wild type revertants, as confirmed by PCR (data not shown). The genotype of putative allelic exchange mutant was confirmed by Southern blot analysis using the strategy depicted below (Figure 3.34).
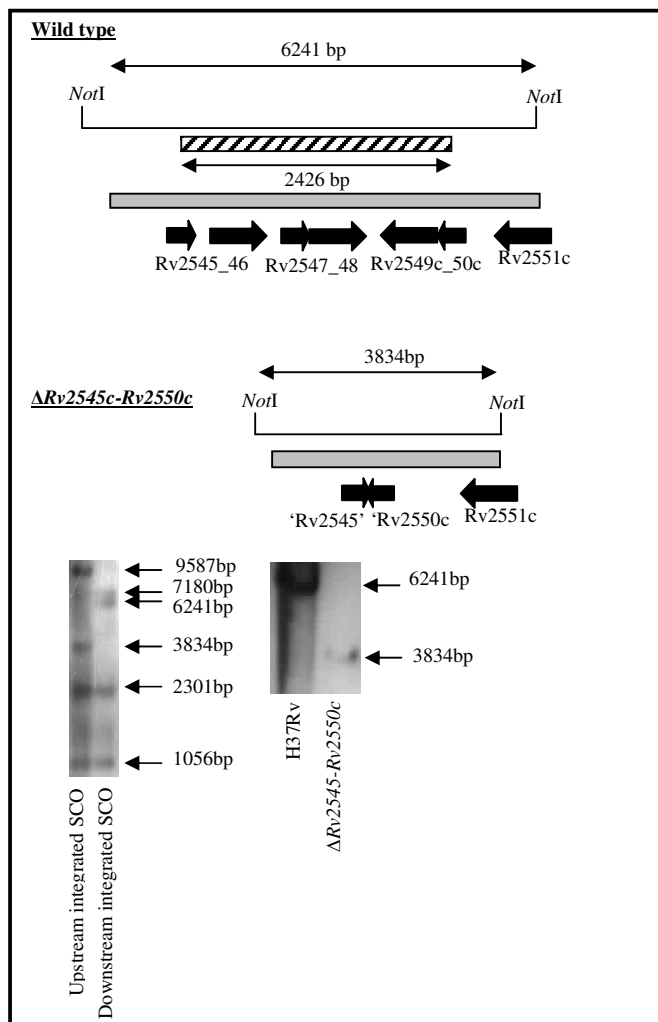
Figure 3.34: Construction and genotypic characterization of *ΔRv2545-Rv2550c* mutant by homologous recombination. The *Rv2545-Rv2550c* and flanking genes are shown as solid arrows (Figure not drawn to scale). The hatched box represents the 2426bp internal deletion in the *ΔRv2545-Rv2550c* mutant strain. For the Southern blot analysis (below), 1 - 5µg of chromosomal DNA was digested with *Not*I, which cuts on either side of

the deleted region, to produce a 6241bp fragment in the wild type strain and a 3834bp fragment in the mutant strain. All fragments were detected using a PCR-generated probe denoted by the grey box.

3.5.2 The *Rv2545-Rv2550c* cluster is dispensable for *M. tuberculosis* growth in both rich and minimal media

The effect of the *vapBC* cluster deletion on the growth of *M. tuberculosis* in axenic culture was investigated using the Δ*Rv2545-Rv2550c*::*hyg* strain. The growth of this strain in rich 7H9 media containing OADC and in Sauton's minimal media was monitored over a period of 14 days and compared to its parental wild type. This analysis revealed that the deletion mutant grew as well as the wild type in both rich and minimal media (Figure 3.35).
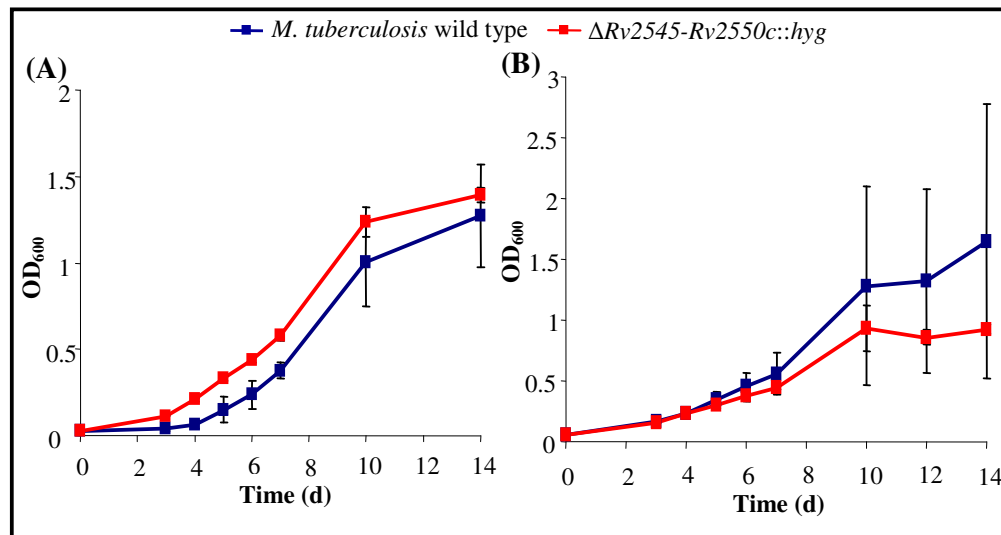
Figure 3.35: Effect of loss of the *Rv2545-Rv2550* region on the growth kinetics of *M. tuberculosis*. OD_{600} spectrophotometric readings of the strains where taken over 14 days when grown in **(A)** 7H9 containing OADC or **(B)** Sauton's minimal media. The data represent the average of 3 independent experiments.

3.5.3 Effect of constitutive, ectopic VapC expression on the viability of the Δ*Rv2545-Rv2550c* deletion mutant strain

To determine the role of constitutive VapC expression in a strain lacking the *Rv2545-Rv2550c* gene cluster, the plasmids expressing each of the three *M. tuberculosis* VapCs Rv2546, Rv2548 and Rv2549c were electroporated into Δ*Rv2545-Rv2550c* in the absence of a TetR, and transformation efficiencies used to score

toxicity of each VapC. Whilst, Rv2549c behaved in a similar manner to when expressed in the wild type H37Rv strain (Table 3.4), unexpectedly too, Rv2546 and Rv2548 whose cognate antitoxins are absent in the mutant, were also non-toxic to this strain with transformation efficiencies comparable to that of pSE100 (Table 3.8). Restriction analyses of pSE2546 showed that the Rv2546 expressing construct had not undergone any plasmid rearrangement. This, coupled with the fact that pSE2549cM had transformation efficiencies comparable to that of pSE100 (Table 3.8), suggests that, like with *M. smegmatis* (Section 3.2.7), the protein threshold required to cause mycobacterial toxicity had not been attained with either pSE2546 or pSE2548.

Table 3.8: Toxicity of VapCs in Δ*Rv2545-Rv2550c* as assessed by transformation efficiency of VapC expressing vectors

VapC	Plasmid	Transformation efficiency (CFU/µg*)
-	pSE100	1.0×10^5
Rv2546	pSE2546	1.0×10^5
Rv2548	pSE2548	1.5×10^4
Rv2549c	pSE2549c	7.1×10^2
Rv2549c^{D5A}	pSE2549cM	1.1×10^6

*This is a representation of one of three reproducible experiments.

3.5.4 <u>Regulated expression of *Rv2549c* is bactericidal in *M. tuberculosis* Δ*Rv2545-Rv2550c*</u>

To determine the effect of regulated expression of a toxic *M. tuberculosis* VapC on its native host in the absence of its cognate antitoxin, the pSE2549c construct was co-electroporated with pMC1s into Δ*Rv2545-Rv2550c*. A Km^R Hyg^R transformant was then grown in liquid media to early logarithmic growth stages (OD$_{600}$ ~ 0.1), and the VapC induced with ATc at a concentration of 25ng/ml. The effect of Rv2549c on the viability of Δ*Rv2545-Rv2550c* was assessed by spectrophotometric readings and CFUs over an 8-day period. Interestingly, although OD$_{600}$ growth assessment was similar to that observed upon Rv2549c expression in wild type *M. tuberculosis*, where no growth was observed (Figure 3.15A), CFU assessments revealed that unlike the observation in wild type *M. tuberculosis* where regulated expression of Rv2549c results in bacteriostasis (Figure 3.15B), regulated expression of Rv2549c in its native

host lacking its cognate antitoxin on the chromosome, results in growth inhibition that leads to a 1-$\log_{10}$ decrease in viability (Figure 3.36). Restriction analyses of plasmids recovered after 2 days of Rv2549c expression show the occurrence of plasmid rearrangement, accounting for the re-growth observed after day 2 (data not shown). This therefore suggests that not only is Rv2549c extremely toxic to *M. tuberculosis* in the absence of its neutralizing cognate antitoxin Rv2550c, but also that the remaining 85 non-cognate type II antitoxins present on the Δ*Rv2545-Rv2550c* chromosome cannot alleviate the toxicity of this VapC.
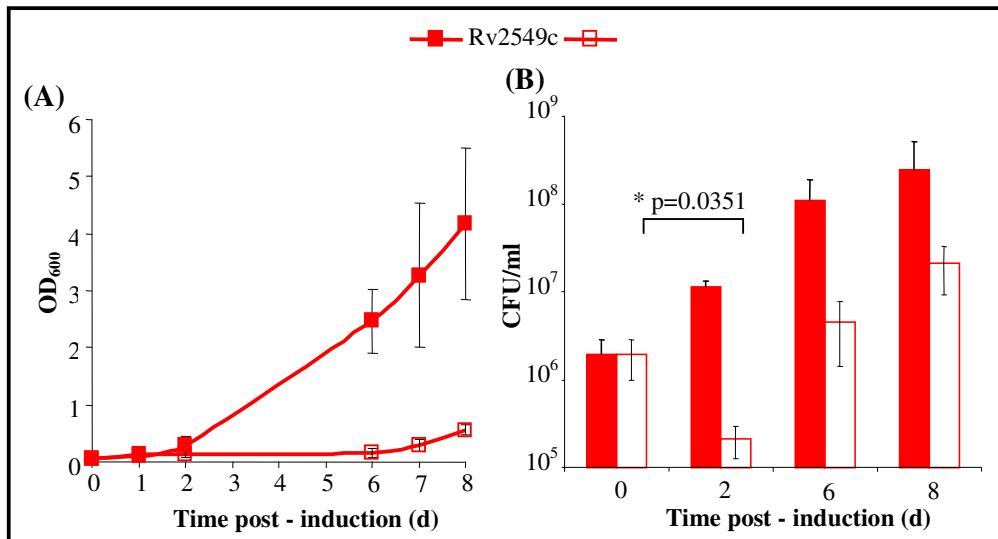
Figure 3.36: Effect of regulated expression of *Rv2549c* on the growth and viability of Δ*Rv2545-Rv2550c*. A culture was grown to mid-logarithmic phase and diluted to OD_{600} 0.04 in 30ml 7H9 media. After growth overnight at 37°C standing, it was divided into 2 equal aliquots of 10ml each. To one aliquot, 25ng/ml ATc was added to induce Rv2549c. **(A)** The effect of Rv2549c on the growth of Δ*Rv2545-Rv2550c* was assessed by OD_{600} spectrophotometric readings taken over an 8-day period. **(B)** The effect of Rv2549c ectopic expression on the viability of Δ*Rv2545-Rv2550c* was determined by CFU assessment. Here, plating of 100µl of 10-fold serial dilutions of cells over an 8-day period post-induction of Rv2549c was performed, and the plates were scored after 21 - 27 days incubation at 37°C. **Annotation:** Empty symbols represent induced samples and filled in symbols represent uninduced samples.

3.6 Effect of VapC expression on ofloxacin tolerance of *M. tuberculosis*

Toxin-antitoxin modules have been widely implicated in the antibiotic tolerance of numerous organisms (74, 113, 142, 154, 155). Whilst deletion of TA modules have no effect on the ability of bacteria to form persisters in the presence of antibiotics (142), over-expression of the toxins HipA, MazF, RelE and TisB all resulted in increased drug tolerant bacterial populations in the presence of antibiotics such as fluoroquinolones (60, 74, 113, 142). It is therefore possible that expression of VapCs might allow for *M. tuberculosis* drug tolerance.

As described above, ectopic expression of certain VapCs was shown to induce bacteriostasis and cidality in *M. tuberculosis* (Figures 3.15 & 3.36). To test whether VapC expression might affect the tolerance of *M. tuberculosis* to anti-tubercular drugs, the fluoroquinolone ofloxacin (OFX), which is employed during the second-line drug regimen of TB, was used for antibiotic treatment. In mycobacteria, fluoroquinolones bind to the two bacterial type II topoisomerase bacterial DNA gyrase which catalyzes the introduction and maintenance of the supercoiling process of DNA (62). During supercoiling, these enzymes decatenate duplex molecules and this process results in transient DNA breaks (123, 124). Fluoroquinolones then trap the topoisomerases on the broken DNA forming a complex which blocks DNA replication and RNA synthesis, resulting in bacteriostasis, and eventually cell death (62, 63).

To determine whether VapCs play a role in *M. tuberculosis* drug tolerance, the *M. tuberculosis*::pSE2829c strain carrying pMC1s, which was available prior to the start of this study, was used. The VapC, Rv2829c, was shown to be toxic to *M. tuberculosis* when constitutively expressed (Table 3.4), and like Rv2549c (Figure 3.15), when conditionally expressed in wild type *M. tuberculosis* this VapC also results in bacteriostasis (Diane Kuhnert, personal communication). Using the experimental protocol described in Figure 3.37, the *M. tuberculosis*::pSE2829c co-electroporated with pMC1s was grown to mid-logarithmic phase and induced with ATc at a concentration of 50ng/ml to allow for Rv2829c expression. After 24h induction, both uninduced and induced cultures were treated with the antibiotic OFX at a concentration of 8μg/ml (10 × MIC). ATc was maintained in the induced culture to allow for continued expression of Rv2829c. After a 6-day exposure to OFX at 37°C,

serial dilutions of the cultures were plated on 7H10 media to score for cells that had survived the drug treatment. It has been reported that at concentrations of 5 - 10 times the MIC value, this fluoroquinolone rapidly kills logarithmic phase *M. tuberculosis* cultures but its activity against stationary phase cultures is significantly reduced (121, 212), possibly due to the fact that stationary phase cells have low metabolic rates and so would not undergo DNA synthesis (212). As such, if Rv2829c plays a role in drug tolerance, an increase in the number of survivors would be observed upon toxin induction, even when the activity of OFX is significantly reduced. As a control, an aliquot of uninduced cells was treated with chloramphenicol (CM). This antibiotic has been reported to induce bacteriostasis via protein synthesis inhibition, and enable increased fluoroquinolone tolerance (176). Since expression of the toxic Rv2829c resulted in bacteriostasis of the wild type *M. tuberculosis* strain (Diane Kuhnert, personal communication), the CM-treated control would ascertain whether any increased ability to tolerate OFX upon VapC induction is analogous to the effects of this bacteriostatic agent on drug tolerance.
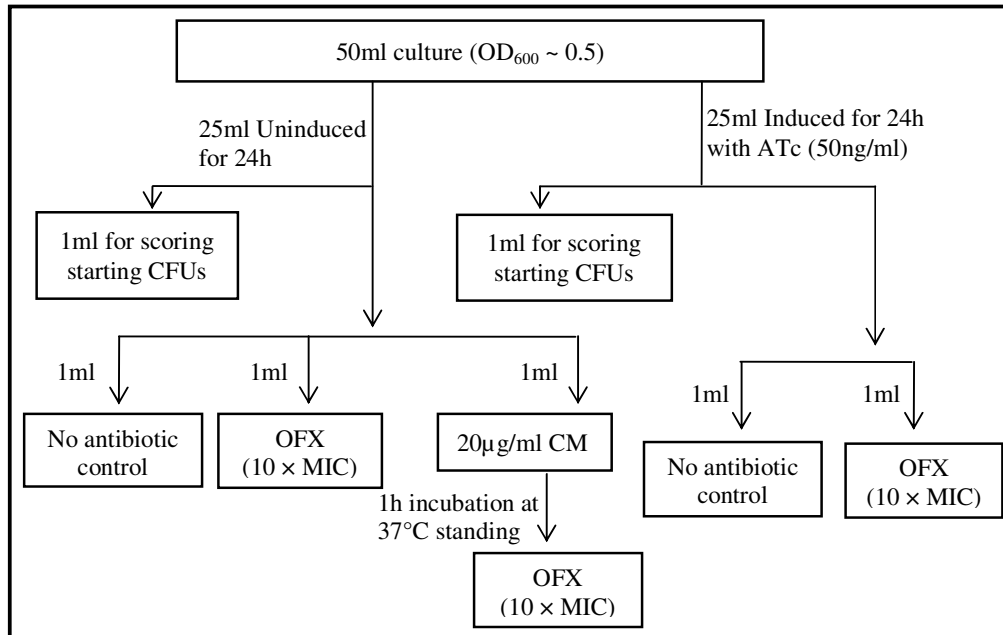
Figure 3.37: Schematic representation of strategy used to assess tolerance of *M. tuberculosis* to ofloxacin. Fifty ml of the *M.tuberculosis*::pSE2829c strain carrying pMC1s was grown with rolling to mid-logarithmic phase. The culture was divided into two equal aliquots, and the toxin in one was induced by addition of ATc for 24h. Both uninduced and induced cultures were grown for 24h with rolling at 37°C. Starting CFUs were assessed by plating 100µl of 10-fold serial dilutions of cells, and the plates were scored after 21 - 27 days incubation at 37°C. **Uninduced culture:** Three 1ml cultures of uninduced samples were aliquoted into 2ml eppendorf tubes. To the untreated control aliquot, no antibiotics were

added. One of the two remaining aliquots was treated with OFX ($10 \times$ MIC) and the last aliquot was first treated with CM for 1h before addition of OFX ($10 \times$ MIC). **Induced culture:** Two 1ml cultures of induced samples were aliquoted into 2ml eppendorf tubes. To the untreated control aliquot, no antibiotics were added and the remaining aliquot was treated with OFX ($10 \times$ MIC), as depicted in the flow diagram. These were grown at 37°C standing for 7 days. CFUs were also assessed by plating 100µl of 10-fold serial dilutions of cells, and the plates were scored after 21 - 27 days incubation at 37°C.

For induction of Rv2829c, ATc was added to a mid-logarithmic *M. tuberculosis*::pSE2829c culture for 24h. The uninduced *M. tuberculosis*::pSE2829c culture, on the other hand, was not treated with ATc, thereby allowing the culture to reach late-logarithmic to early-stationary phases of growth after 24h incubation. The starting cell densities of the uninduced and ATc-induced cultures were 7.4×10^7 CFU/ml and 8.5×10^7 CFU/ml, respectively (Figure 3.38, purple bars). After 6 days' further incubation, both the ATc-induced and uninduced control cultures of *M. tuberculosis*::pSE2829c that were not exposed to OFX remained in late-logarithmic phase (Figure 3.38, red bars). This is possibly due to the fact that the 1ml cultures were grown in 2ml eppendorf tubes, and as such, reduced oxygen availability might have restricted further growth.

Treatment of *M. tuberculosis*::pSE2829c uninduced samples with $10 \times$ MIC OFX for 6 days resulted in a statistically significant reduction of CFU ($p < 0.05$) from 4×10^7 CFU/ml to 2.93×10^6 CFU/ml (Figure 3.38, "uninduced" panel red bar vs. yellow bar). This is in accordance with previously reported data (121, 212), which show that high OFX concentrations reduce the CFU of *M. tuberculosis* stationary phase cultures by about 10-fold (212). Pretreatment of the uninduced *M. tuberculosis*::pSE2829c culture with CM before addition of OFX allowed for little or no killing by the fluoroquinolone ($p > 0.5$) (Figure 3.38, "uninduced" panel red bar vs. green bar). This observation confirmed that the protein synthesis inhibitory properties of CM resulted in increased fluoroquinolone tolerance.

As mentioned above, induction of Rv2829c had no effect on CFUs after 6 days ($p > 0.5$) (Figure 3.38, "induced" panel purple bar vs. red bar). This is possibly due to the fact that the cells, being in late-logarithmic to early-stationary growth phase, were already in a state of growth arrest, presumably as a result of poor aeration, thus making it difficult to discern any Rv2829c-specific effect. OFX-treatment of *M. tuberculosis*::pSE2829c cells after Rv2829c induction resulted in a < 1-log reduction

of viability cell death from 1.6×10^8 CFU/ml to 4.6×10^7 CFU/ml ($p < 0.5$) (Figure 3.38, "induced" panel red bar vs. yellow bar). This observation was similar to when uninduced cells were pre-treated with CM before addition of OFX ($p > 0.5$) (Figure 3.38, "uninduced" panel green bar vs. "induced" panel yellow bar). The increase in the number of OFX-tolerant cells observed in cultures in which Rv2829c expression was induced was also greater than when Rv2829c was not induced ($p < 0.5$) (Figure 3.38, "uninduced" panel yellow bar vs. "induced" panel yellow bar). Taken together, these data suggest that induction of Rv2829c increases the ability of *M. tuberculosis* to form persisters in the presence of OFX in a manner similar to CM.
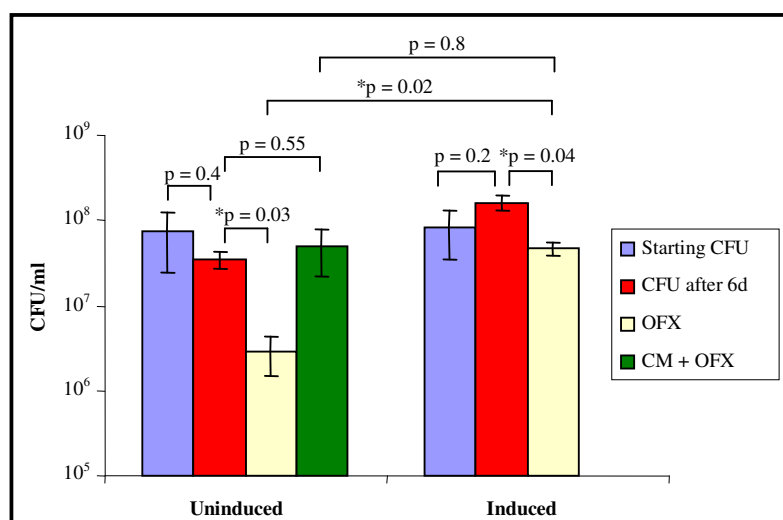
Figure 3.38: Expression of Rv2829c appears to contribute to *M. tuberculosis* tolerance to ofloxacin. CFUs were obtained by plating 100µl of 10-fold serial dilutions of cells obtained subsequent to treatment and incubation at 37°C for 21 - 27 days. The data panels represent the average of 2 biological replicates. All two-tailed p-values were obtained using the Graphpad software as described in Section 2.11. The asterisks represent statistically significant p-values.

To then determine whether VapCs enhance *M. tuberculosis* drug tolerance in the absence of their cognate antitoxins, the effect of conditional expression of Rv2546 with pMC1s and Rv2549c with pMC1s were assessed in the Δ*Rv2545-Rv2550c* strain. In *E. coli*, reduced binding of the HipA7 mutant to HipB antitoxin has been shown to result in a higher probability of persister formation (239). Assuming that analogous situation applies in the case of VapBC modules in *M. tuberculosis* it is possible that a non-toxic VapC drug tolerant phenotype may be unmasked by the absence of its cognate antitoxin. In addition, since the possibility that the mechanism of VapC-

induced mycobacterial toxicity could be different from that of formation of drug-tolerant populations, these experiments would also address the question of whether a toxicity phenotype is linked to drug tolerance.

Using the modified experimental protocol described in Figure 3.39, Δ*Rv2545-Rv2550c*::pSE2546 and Δ*Rv2545-Rv2550c*::pSE2549c strains, both with pMC1s, were grown to early-logarithmic phase and induced with ATc at a concentration of 50ng/ml to allow for VapC expression. After 24h induction, both uninduced and induced cultures were treated with OFX at a concentration of 8µg/ml (10 × MIC). As previously, ATc was maintained in the induced culture for the entire duration of the OFX treatment to ensure continued expression of VapC. However, in contrast to the Rv2829c tolerance experiment (Figure 3.37), the cultures were treated with OFX in 50ml tissue culture flasks to enable the cells to have sufficient oxygen to ensure growth during a 7-day period at 37°C. As per the original protocol, an aliquot of uninduced cells was treated with CM to determine whether any increased ability to tolerate OFX upon induction of the VapCs is similar to this bacteriostatic agent. If ectopic expression of either of the toxins has an effect in OFX tolerance, an increase in the number of survivors would be observed in the presence of OFX upon toxin induction.
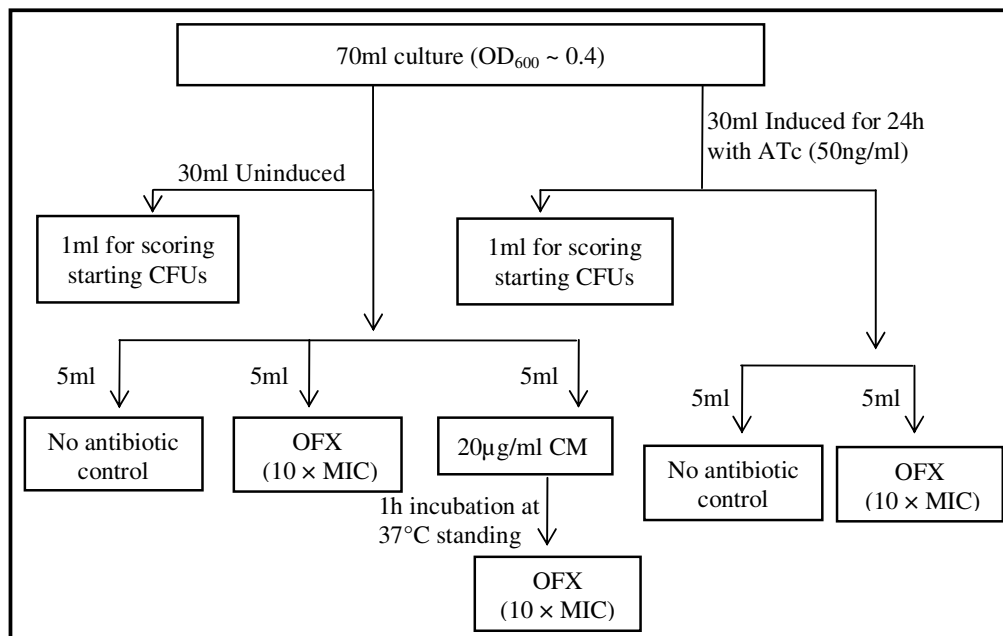
Figure 3.39: Schematic representation of the modified strategy used to assess tolerance of *M. tuberculosis* to ofloxacin. Seventy ml of the Δ*Rv2545-Rv2550c*::pSE2546 and Δ*Rv2545-Rv2550c*::pSE2549c, both carrying pMC1s was grown with rolling to early logarithmic phase. The culture was divided into two equal aliquots, and the toxin in one was induced by addition of ATc for 24h. Both uninduced and induced cultures were grown for 24h with rolling at 37°C. Starting CFUs were assessed by plating 100µl of 10-fold serial dilutions of cells, and the plates were scored after 21 - 27 days incubation at 37°C. **Uninduced culture:** Three 5ml cultures of uninduced samples were aliquoted into 50ml tissue culture flasks. To the untreated control aliquot, no antibiotics were added. One of the two remaining aliquots was treated with ofloxacin (10 × MIC) and the last aliquot was first treated with chloramphenicol (CM) for 1h before addition of ofloxacin (10 × MIC). **Induced culture:** Two 5ml cultures of induced samples were aliquoted into 50ml tissue culture flasks. To the untreated control aliquot, no antibiotics were added and the remaining aliquot was treated with ofloxacin (10 × MIC), as depicted in the flow diagram. These were grown at 37°C standing for 7 days. CFUs were also assessed by plating 100µl of 10-fold serial dilutions of cells, and the plates were scored after 21 - 27 days incubation at 37°C.

After 7 days' incubation, both the ATc-induced and uninduced cultures of Δ*Rv2545-Rv2550c*::pSE2546 grew from a starting cell density of ca. 10^7 CFU/ml to stationary phase, reaching cell densities of ca. 3×10^8 CFU/ml (Figure 3.40, blue and red bars). This improved growth of the untreated OFX controls observed using the modified protocol (Figure 3.39), suggested that limited oxygen availability restricted growth in the original protocol (Figure 3.37). Addition of OFX to the control culture in which Rv2546 was not induced, resulted in a ≥ 6-log reduction in viability of cells *i.e.* from 2×10^8 CFU/ml to 5×10^2 CFU/ml (Figure 3.40, "uninduced" panel, red bar vs. green bar). This massive killing effect, compared to that seen in the Rv2829c

experiment, confirmed that high OFX concentrations reduce the CFU of *M. tuberculosis* logarithmic phase cultures significantly more than stationary phase cultures (121, 212). Importantly, however, pre-treatment of the uninduced culture with CM for 1h before addition of OFX reduced the susceptibility of the cells to OFX-mediated killing by 2-$\log_{10}$ *i.e.* the viable cell count after 7 days' exposure to OFX was 2×10^4 as opposed to 5×10^2 for the sample that had not been pre-treated with CM (Figure 3.40, "uninduced" panel, turquoise bar vs. green bar). These observations are in accordance with previous data which have reported a > 3-$\log_{10}$ reduction in viability of logarithmic phase *M. tuberculosis* cultures when treated with high concentrations of fluoroquinolones, as well as the observation that addition of CM reduces fluoroquinolone lethality (121, 170, 176, 212, 313).

For the $\Delta Rv2545$-$Rv2550c$::pSE2546 cultures where Rv2546 was induced by addition of ATc, the untreated control behaved as expected (Figure 3.14), with the cultures reaching stationary phase after 7 days (Figure 3.40, "induced" panel, red bar). Induction of Rv2546 with ATc followed by treatment with OFX resulted in a ~ 5-$\log_{10}$ reduction in viability of cells *i.e.* from 2×10^8 CFU/ml to 1×10^3 CFU/ml (Figure 3.40, "induced" panel, red bar vs. green bar). Over-expression of Rv2546 appeared to increase the percentage of OFX-tolerant cells in *M. tuberculosis* when compared to the cultures in which this VapC is uninduced (p < 0.05) (Figure 3.40, "uninduced" panel green bar vs. "induced" panel green bar). This statistically significant difference suggests that expression of low levels of VapC contributes to formation of *M. tuberculosis* OFX-tolerant populations, and that VapC toxicity – as assessed using the methods employed in this study, in which toxicity is scored by growth inhibition - is not a requirement for the formation of drug tolerance cells. It is interesting to note that unlike with Rv2829c, induction of Rv2546 did not result in as high a fraction of OFX-tolerant cells as the pre-treated CM cells (p < 0.05) (Figure 3.40, "uninduced" panel turquoise bar vs. "induced" panel green bar). These data therefore suggest that, in the absence of the cognate antitoxin, although Rv2546 increases the percentage of *M. tuberculosis* persisters when treated with OFX, the effect on OFX tolerance is not as profound as that manifested by CM treatment.
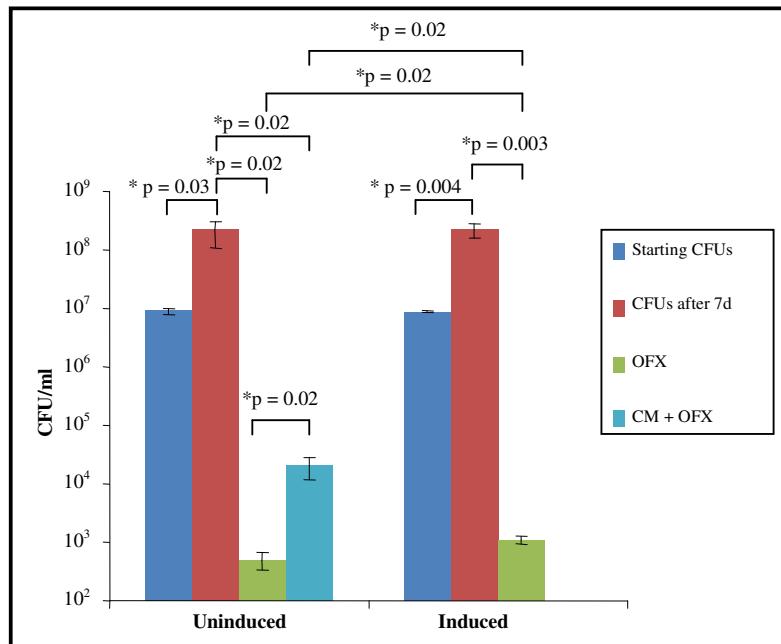
Figure 3.40: Expression of Rv2546 contributes to *M. tuberculosis* tolerance of ofloxacin. CFUs were obtained by plating 100µl of 10-fold serial dilutions of cells obtained subsequent to treatment and incubation at 37°C for 21-27 days. The data panels represent the average of 3 biological replicates. All two-tailed p-values were obtained using the Graphpad software as described in Section 2.11. The asterisks represent statistically significant p-values.

In the case of Δ*Rv2545-Rv2550c*::pSE2549c, although the experiment was performed four times, the results from only one experiment are reported here (Figure 3.41) as most of the plates from the other three experiments were lost to fungal contamination, and due to time constraints, the experiment could not be repeated. The results of the single experiment revealed that, after 7 days' incubation, the ATc-uninduced culture of grew from a starting cell density of 2×10^6 CFU/ml to a cell density of ca. 2×10^7 CFU/ml (Figure 3.41, "uninduced" panel blue and red bars). As expected (121, 212), addition of OFX to this control culture resulted in a > 3-log reduction in viability of cells *i.e.* from 2×10^7 CFU/ml to 6.7×10^2 CFU/ml (Figure 3.41, "uninduced" panel, red bar vs. green bar). As observed with Rv2546 (Figure 3.40), pre-treatment of the uninduced culture with CM for 1h before addition of the fluoroquinolone increased OFX-tolerance of the cells by 2-$\log_{10}$ *i.e.* from 6.7×10^2 to 1.5×10^4 (Figure 3.41, "uninduced" panel, green bar vs. turquoise bar).

However, it was surprising to note that when Rv2549c expression was induced, the culture reached a cell density of 1.5×10^7 CFU/ml (Figure 3.41, blue and red bars).

This result is in contrast with previous observations, which show that induction of the toxic Rv2549c results in a reduction of viability of $\Delta Rv2545$-$Rv2550c$ (Figure 3.36). Since the cultures in this experiment were grown rolling instead of standing, and so had a faster doubling time, it is possible that plasmid rearrangement/ mutation leading to abrogation of Rv2549c toxicity may have occurred at an earlier stage, thereby enabling the "induced" culture to attain cell density levels similar to "uninduced" culture by day 7. The fact that induction of Rv2549c followed by treatment with OFX resulted in a ~ 6-$\log_{10}$ reduction in viability of cells *i.e.* from 1.5×10^7 CFU/ml to 8×10^1 CFU/ml (Figure 3.41, "induced" panel, red bar vs. green bar), instead of the 5-$\log_{10}$ reduction in viability observed with the "uninduced" cells (Figure 3.41, "uninduced" panel, red bar vs. green bar), suggests that the expected 1-$\log_{10}$ reduction in viability upon expression of Rv2549c occurred. Taken together, these data suggest that expression of the toxic Rv2549c in the absence of its cognate Rv2550c antitoxin did not significantly increase the percentage of OFX-tolerant cells. Although this experiment needs to be repeated to confirm these data, this finding contrasts with the findings obtained from the Rv2829c and Rv2546 tolerance experiments, where expression of these latter two VapCs was shown to result in an increase in OFX tolerance in *M. tuberculosis* (Figures 3.38 & 3.40). Like the toxic Rv2549c (Figures 3.11 & 3.15), expression of Rv2829c in the presence of its cognate antitoxin was found to result in bacteriostasis (Diane Kuhnert, personal communication), whilst expression of this toxin in *M. smegmatis*, which lacks a cognate antitoxin resulted in a 2-$\log_{10}$ decrease in viability (Diane Kuhnert, personal communication). It therefore follows that, just as with Rv2549c (Figure 3.15), the presence in *M. tuberculosis* of the cognate antitoxin, Rv2830c, may have dampened the toxic effect of Rv2829c, resulting in low levels of active cellular VapC, and increased persisters (Figure 3.38). This, coupled with the fact that low levels of Rv2546 also resulted in increased OFX-tolerant populations (Figure 3.40), make it highly probable that a specific VapC threshold is required for persister formation, and once this threshold has been breached, toxicity/ cell death ensues.
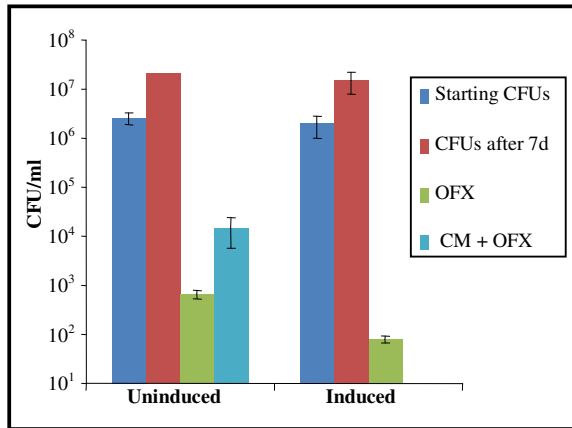
Figure 3.41: Expression of Rv2549c does not contribute to *M. tuberculosis* tolerance to ofloxacin. CFUs were obtained by plating 100µl of 10-fold serial dilutions of cells obtained subsequent to treatment and incubation at 37°C for 21 - 27 days. The vertical bars represent the experimental standard deviation.

4. Discussion

Based on the most recent estimates, the pathogen, *M. tuberculosis*, possesses 88 TA loci on its chromosome, of which 47 belong to the *vapBC* family (230). Despite the fact that this is the largest TA family currently annotated (9, 96, 108, 211, 230), the *vapBC*s have been relatively poorly characterized (9). This study has shown that over-expression of VapCs caused mycobacterial toxicity only once a certain threshold level of protein was attained, and this toxicity was fully alleviated only by the presence of their cognate antitoxins. Whilst VapCs were not found to play a role in stress management of mycobacteria under the conditions tested in this study, the presence of low cellular VapC levels appears to contribute to the formation of ofloxacin-tolerant *M. tuberculosis* populations.

4.1 Are all mycobacterial VapCs functional?

Conditional gene expression is a classic and powerful tool for elucidation of gene function. Several such gene expression systems are available for use in mycobacteria. The first inducible expression system described for use in mycobacteria makes use of the acetamide-inducible *M. smegmatis* acetamidase promoter (213). This promoter is located within the 1.5kb region upstream of the amide-encoding gene (213), which contains four possible open reading frames with mycobacterial codon usage (172), and is regulated by both positive and negative elements (213, 214, 216, 236). Although this promoter has successfully been used for inducible expression of mycobacterial proteins by addition of acetamide (69, 101, 105, 177, 275), this system is unstable and not tightly regulated, as evidenced by the high levels of basal gene expression observed in the absence of inducer (25, 135, 214, 216, 236).

Another mycobacterial gene expression system, the arabinose-inducible system, derived from the *E. coli* arabinose operon, has successfully been demonstrated to express a *M. tuberculosis* MazF toxin in *M. smegmatis* (31). Unlike in *E. coli* where arabinose is the sole inducer of this system, in *M. smegmatis* addition of either arabinose or glucose results in gene expression. The P_{BAD} promoter used in this system is extremely weak, exhibiting low promoter level activities and gene expression was only detectable on solid media and not in liquid media. In addition to these

confounders, a basal level of gene expression is observed even in the absence of the inducer, demonstrating that this system is not tightly repressed (31).

Two novel inducible gene expression systems have recently been described for mycobacteria: the Pip-inducible (81) and nitrile-inducible expression systems (210). The Pip-inducible system, which has already widely been used in eukaryotic cells including plant and mammalian cells, comprises of the *Streptomyces pristinaespiralis* multidrug resistance *ptr* gene promoter-operator region and the *S. coelicor pip* repressor gene which is responsive to the pristinamycin inducer (81). The nitrile-inducible system, on the other hand, comprises of the regulatory *nitR* gene, under the control of a *Rhodococcus rhodochrous nitA* gene promoter, as well as a second *nitA* promoter which regulates the gene of interest (210). Whilst both systems have been used successfully in saprophytic and pathogenic mycobacteria, these were not available at the start of this study.

The most commonly used gene expression systems in mycobacteria are tetracycline-inducible (Tet-inducible) (21, 32, 70, 122, 146). Four Tet-inducible systems have been described to date. In 2005, Carroll and colleagues adapted a *Staphylococcus aureus* Tet-inducible system (17), which made use of Tet regulatory elements from the *E. coli Tn*10 transposable element and the *Bacillus subtilis*-derived P_{xyl} promoter (310) to generate an integrating vector possessing the TetR repressor with two divergent promoters (32). In this system, *tetR* is located downstream of one of these promoters and the gene of interest is cloned downstream of the second divergent promoter. Since the two operator sites to which TetR binds overlaps with these promoters, absence of the Tet inducer guarantees that TetR is bound to its target, thus ensuring no gene expression. Addition of Tet, on the other hand, allows for binding of TetR to the inducer, leading to a conformational change of this protein resulting to its dissociation from the operators, and hence expression of the gene of interest. This system, which makes use of a single-copy integrating plasmid, exhibited a significantly higher gene expression than the acetamide system, and was successfully used to express genes in both the saprophytic *M. smegmatis* and pathogenic *M. tuberculosis* (32).

The second Tet-inducible system described makes use of a *Corynebacterium glutamicum* Tet efflux system (21). Here, the *tetR*-encoded transcriptional regulator, the *tetO* operator region and the *tetA* promoter of the *C. glutamicum tetZ* locus were cloned onto an episomal plasmid, and the gene of interest cloned downstream of *tetRO*. Although this system could be used to regulate *in vitro* and *ex vivo* gene expression in both saprophytic and pathogenic mycobacteria, the *tetA* promoter was significantly weaker than that of the strong mycobacterial *hsp60* promoter used for constitutive expression, and incomplete gene repression was observed in the absence of the inducer (21).

Up until 2006, no mycobacterial inducible gene-expression system had been developed for use in animal models (122). In 2006, Hernandez-Abanto and co-workers developed a mycobacterial Tet-inducible system for use *in vitro* (122). This system made use of a *tcp830* Tet-inducible promoter and a TetR regulator, both of which were obtained from the closely related actinomycete *Streptomyces coelicolor*. The *tetR* was cloned under the control of the acetamidase promoter and the *tcp830* promoter-operator region was optimized to ensure maximal expression of the gene of interest. Whilst this system was shown to regulate gene expression of the saprophytic *M. smegmatis* within an animal model, addition of acetamide is required for control of TetR. Furthermore, gene expression using this system has not been demonstrated in pathogenic mycobacteria suggesting that modification of this system may be required for expression in *M. tuberculosis*.

In this study, the functionality of VapCs in *M. smegmatis* and *M. tuberculosis* was investigated using the uncoupled ATc-dependent (ATc-dependent) mycobacterial conditional gene expression system that was developed by Ehrt, Schnappinger and colleagues (70). This system utilizes the $P_{myc1}tetO$ mycobacterial promoter - a promoter stronger than the mycobacterial *hsp60* promoter - for expression of the gene of interest off an episomal plasmid (70). In addition, this system not only enables efficient regulation of a gene of interest in both fast and slow-growing mycobacteria, but also allows for regulatable expression of the TetR, which is available in both forward and reverse configurations (70, 107), by different strength promoters. Moreover, because the Tet-regulated promoter-operator (*tetO*) and the TetR are carried

on different vectors, the Ehrt and Schnappinger system (70) allows for constitutive and regulatable gene expression over a large dynamic range (Figure 3.5).

Using this system, constitutive VapC expression of the sole *M. smegmatis vapC* and the ten selected *M. tuberculosis vapC*s revealed a similar differentiation in VapC function in both the heterologous *M. smegmatis* and native *M. tuberculosis* hosts (Tables 3.3 & 3.4). In this instance where maximal derepression of VapC is achieved in the absence of a TetR (Figure 3.5), the Rv1953 control, which has only two conserved active site acidic residues (Asp/Glu) (Figure 3.3), was not growth inhibitory to mycobacteria (Tables 3.3 & 3.4). These data are consistent with the notion that cleavage of free RNA by VapCs occurs when the four conserved acidic residues (Asp/Glu/Asp/Asp) form a negatively charged pocket to which divalent metal ions bind, forming the active site required for nuclease degradation (28, 46, 50, 186, 237, 304). It was therefore surprising to observe that the VapC proteins Rv0627, Rv2010, Rv2546, Rv2548 and MSMEG_1284, all of which retain the four highly conserved Asp/Glu/Asp/Asp catalytic residues essential for ribonuclease activity (Figure 3.3) were not growth inhibitory when ectopically expressed in either *M. smegmatis* or *M. tuberculosis*. In fact, mycobacterial growth inhibition only occurred in cells ectopically expressing Rv0549c, Rv0595c, Rv2549c, Rv2829c and Rv3320c, where Rv0549c was the least potent of the toxic VapC proteins (Section 3.2.1). These data therefore suggested a differentiation in VapC function where Rv0627, Rv2010, Rv2546, Rv2548 and MSMEG_1284 are non-toxic and, of the toxic Rv0549c, Rv0595c, Rv2549c, Rv2829c and Rv3320c VapCs, Rv0549c is the least toxic VapC. Differentiation in VapC function has widely been reported, where differences in VapC toxicity in *E. coli*, *M. smegmatis* and *M. tuberculosis* hosts have been observed (Table 4.1) (108, 153, 261, 316). For instance, of the five toxic *M. tuberculosis* VapCs observed in this study, Gupta demonstrated that only expression of Rv0595c and Rv2549c were growth inhibitory to *E. coli* (108). While these discrepancies may have been expected because a non-related host was used to assess growth inhibition, and factors such as G+C content could affect protein expression and hence toxicity, differences in VapC function have also been observed upon expression in *M. smegmatis* (186, 230, 237). Miallau and colleagues reported that Rv0627, which was non-toxic to *M. tuberculosis* when constitutively expressed in this study (Table 3.4),

was extremely toxic when expressed in *M. tuberculosis* (Table 4.1) (186). In addition, while Robson and co-workers observed that conditional expression of MSMEG_1284 resulted in growth inhibition of *M. smegmatis* (Table 4.1) (237), the data reported herein revealed a lack of toxicity of this gene even when constitutively expressed in both wild type *M. smegmatis* (Table 3.3), and in a deletion *M. smegmatis* mutant lacking all type II TA modules (Table 3.7). Furthermore, using *M. smegmatis* as a host to test for toxicity, Ramage and colleagues observed that Rv0595c, Rv2549c and Rv3320c were not growth inhibitory to *M. smegmatis*, while Rv2548 and Rv2010 were growth inhibitory (Table 4.1) (230). These data contrast those reported in this study where both Rv2548 and Rv2010 were non-toxic while Rv0595c, Rv2549c and Rv3320c were growth inhibitory (Table 3.3). It is therefore probable that all the discrepancies in attributing VapC function (Table 4.1) may be due to experimental differences such as use of different conditional gene expression systems, differences in standardized ribosome binding sites - if incorporated, as well as the method used for assaying toxicity, as evidenced by the observation that Rv3320c is only toxic to mycobacteria when constitutively, but not conditionally expressed. .

Table 4.1: General experimental conditions used for assessing VapC toxicity – A comparison

VapC	Host	Conditional expression system	Standardized ribosome binding site	Toxicity assay	Toxicity	Reference
Rv0549c	*E. coli*	Arabinose-inducible	Unknown	Growth by OD_{600} and CFU	Non-toxic	(108)
	M. smegmatis	Acetamide-inducible	Yes	Growth on solid media	Toxic	(230)
	M. smegmatis	ATc-inducible	Yes	Transformation efficiency	Toxic	This study
	M. tuberculosis	ATc-inducible	Yes	Transformation efficiency	Toxic	This study
Rv0595c	*E. coli*	Arabinose-inducible	Unknown	Growth by OD_{600} and CFU	Toxic	(108)
	M. smegmatis	Acetamide-inducible	Yes	Growth on solid media	Non-toxic	(230)
	M. smegmatis	ATc-inducible	Yes	Transformation efficiency	Toxic	This study
	M. tuberculosis	ATc-inducible	Yes	Transformation efficiency	Toxic	This study
Rv0627	*E. coli*	Arabinose-inducible	Unknown	Growth by OD_{600} and CFU	Toxic	(108)
	M. smegmatis	Acetamide-inducible	Yes	Growth on solid media	Non-toxic	(230)
	M. tuberculosis	Unknown	Unknown	Unknown	Toxic	(186)
	M. smegmatis	ATc-inducible	Yes	Transformation efficiency	Non-toxic	This study
	M. tuberculosis	ATc-inducible	Yes	Transformation efficiency	Non-toxic	This study
Rv1953	*E. coli*	Arabinose-inducible	Unknown	Growth by OD_{600} and CFU	Non-toxic	(108)
	M. smegmatis	Acetamide-inducible	Yes	Growth on solid media	Non-toxic	(230)
	M. smegmatis	ATc-inducible	Yes	Transformation efficiency	Non-toxic	This study
	M. tuberculosis	ATc-inducible	Yes	Transformation efficiency	Non-toxic	This study
Rv2010	*E. coli*	Arabinose-inducible	Unknown	Growth by OD_{600} and CFU	Non-toxic	(108)
	M. smegmatis	Acetamide-inducible	Yes	Growth on solid media	Toxic	(230)
	M. smegmatis	ATc-inducible	Yes	Transformation efficiency	Non-toxic	This study
	M. tuberculosis	ATc-inducible	Yes	Transformation efficiency	Non-toxic	This study

Rv2546	*E. coli*	Arabinose-inducible	Unknown	Growth by OD_{600} and CFU	Non-toxic	(108)
	M. smegmatis	Acetamide-inducible	Yes	Growth on solid media	Non-toxic	(230)
	M. smegmatis	ATc-inducible	Yes	Transformation efficiency and growth by OD_{600} and CFU	Non-toxic	This study
	M. tuberculosis	ATc-inducible	Yes	Transformation efficiency and growth by CFU	Non-toxic	This study
Rv2548	*E. coli*	Arabinose-inducible	Unknown	Growth by OD_{600} and CFU	Non-toxic	(108)
	M. smegmatis	Acetamide-inducible	Yes	Growth on solid media	Toxic	(230)
	M. smegmatis	ATc-inducible	Yes	Transformation efficiency and growth by OD_{600} and CFU	Non-toxic	This study
	M. tuberculosis	ATc-inducible	Yes	Transformation efficiency and growth by CFU	Non-toxic	This study
Rv2549c	*E. coli*	Arabinose-inducible	Unknown	Growth by OD_{600} and CFU	Toxic	(108)
	M. smegmatis	Acetamide-inducible	Yes	Growth on solid media	Non-toxic	(230)
	M. smegmatis	ATc-inducible	Yes	Transformation efficiency and growth by OD_{600} and CFU	Toxic	This study
	M. tuberculosis	ATc-inducible	Yes	Transformation efficiency and growth by OD_{600} and CFU	Toxic	This study
Rv2829c	*E. coli*	Arabinose-inducible	Unknown	Growth by OD_{600} and CFU	Non-toxic	(108)
	M. smegmatis	Acetamide-inducible	Yes	Growth on solid media	Toxic	(230)
	M. smegmatis	ATc-inducible	Yes	Transformation efficiency	Toxic	This study
	M. tuberculosis	ATc-inducible	Yes	Transformation efficiency	Toxic	This study
Rv3320c	*E. coli*	Arabinose-inducible	Unknown	Growth by OD_{600} and CFU	Non-toxic	(108)
	M. smegmatis	Acetamide-inducible	Yes	Growth on solid media	Non-toxic	(230)
	M. smegmatis	ATc-inducible	Yes	Transformation efficiency	Toxic	This study
	M. tuberculosis	ATc-inducible	Yes	Transformation efficiency	Toxic	This study
	M. smegmatis	ATc-inducible	Yes	Growth by OD_{600} and CFU	Non-toxic	Diane Kuhnert, MMRU

MSMEG _1284	*M. smegmatis*	*C. glutamicum* Tet- inducible	Yes	CFU	Toxic	(237)
	M. smegmatis	ATc- inducible	Yes	Transformation efficiency	Non- toxic	This study

Prior to this work, all studies in which VapC function was ascertained assumed that since an identical expression system was used for assessment of gene function, all VapCs were expressed at equal levels in the cell (108, 186, 230). In an attempt to understand the molecular basis of the functional differentiation of VapCs, *i.e.* toxic vs. non-toxic, this study was the first to monitor *vap(B)C* expression at both mRNA as well as at protein levels. It was interesting to note that, despite the fact that both a non-toxic and toxic VapC were transcribed when conditionally expressed from the same ATc-inducible system (Figure 3.16), the protein levels of the toxic Rv2549c was significantly higher than that of the non-toxic Rv2546 VapC, even when the latter was constitutively expressed (Figure 3.20). This difference in cellular protein levels may account for the differentiation of VapC function observed in this and other studies (108, 186, 230). The observations that growth inhibition by Rv2549c (Figure 3.19) and HipA – another type II TA toxin (239) – is only observed once a cellular protein threshold is achieved, corroborates this notion.

Over-expression of proteins often results in the formation of inactive insoluble aggregates of the protein referred to as inclusion bodies. More often than not, these inclusion bodies form when the protein does not fold correctly during expression (175, 181, 250, 289, 306). To determine whether VapC proteins became insoluble during expression, the supernatant (soluble) and pellet (insoluble) fractions of *M. smegmatis* strains expressing various VapCs were analyzed. Although in this study there was always significantly more soluble than insoluble VapC protein detected (Figures 3.18 and 3.20), the presence of insoluble aggregates make it possible for the discrepancies observed in variations of functionality between studies (Table 4.1) to be a consequence of differences in the amount of inclusion bodies formed when using different expression systems. If more insoluble aggregates are formed when using a specific conditional expression system, this could result in diminished availability of soluble active VapC, and thus make the readout of VapC functionality "non-toxic".

The presence of these inclusion bodies (Figures 3.18 and 3.20), coupled with the fact that toxicity occurs only once a specific cellular threshold has been achieved (Figure 3.19), suggests that differences in expression vectors and cloning strategies where different promoters, ribosome binding sites and codon usage were employed, may account for the incongruities observed between studies (Table 4.1). It therefore follows that factors affecting processes such as rates of translation and protein solubility greatly influence growth inhibition readout and hence the "functionality" score of a TA module (108, 152, 230, 261, 316). The findings of this study therefore make it imperative for VapC protein levels to be determined before any conclusions *vis-à-vis* (comparative) toxicity of these proteins can be made.

4.2 Are the growth inhibitory effects of Rv2549c associated with nuclease activity of PIN domains?

To probe the association of Rv2549c toxicity with nuclease activity of PIN domains (50, 186), site-directed mutagenesis was used to replace one of the conserved acidic residues (Asp5) by an alanine. The growth inhibitory effects resulting from expression of the mutant VapC were then compared to that of the wild type (Section 3.3.3), and this D5A mutation was observed to abrogate Rv2549c toxicity (Figure 3.27). Comparison of the expression levels of the FLAG-tagged mutant protein to that of the wild type protein, however, revealed that the mutation resulted in a significant reduction of protein present upon expression (Figure 3.28). This finding makes it impossible to conclude that the abrogation of growth inhibitory activity was a direct result of the loss of nuclease activity.

Whilst it is possible that disruption of this acidic residue may have destabilized the transcribed mRNA thereby leading to degradation (175), protein structure prediction analyses revealed a potentially significant difference in the mutant Rv2549c (Figure 3.29). It appears that the mutation of the N-terminal conserved acidic residue may have rendered the protein unstable through disruption of the first β strand. This abnormal protein would then have been targeted for proteolytic degradation by the bacteria (175). Taken together, these data reaffirm that soluble protein expression levels of all VapCs must be quantified before conclusions about toxicity and/or

abrogation thereof may be made, even when single amino acid substitutions are introduced into the VapCs.

4.3 Conditional gene expression of Rv2549c causes bacteriostasis in the presence of its cognate antitoxin but cidality in its absence

Using the ability to conditionally express the toxic Rv2549c in the presence of high TetR levels (Section 3.2.3), the effect of regulated VapC expression in mycobacteria was elucidated. Ectopic expression of Rv2549c was observed to induce bacteriostasis in wild type *M. tuberculosis*, which carries the cognate Rv2550c antitoxin as part of the chromosomal *Rv2550c-Rv2549c* operon, over a period of two days (Figure 3.15). Unlike episomal RelE-induced bacteriostasis which could be prolonged by supplementation of the *M. tuberculosis* culture with more inducer (261), VapC-induced bacteriostasis could not be prolonged in this manner because plasmid rearrangement or loss occurred resulting in the abrogation of toxic VapC expression in *M. tuberculosis* (data not shown). Whilst the mode of action of VapCs remains unknown, these data suggest that although RelE is also growth inhibitory (41, 104, 221, 261) and cleaves mRNA (87), its mode of action of nuclease degradation may be vastly different to that of VapCs.

Upon conditional expression of Rv2549c in the heterologous *M. smegmatis* host - which lacks the cognate *Rv2550c* antitoxin - a "no-growth" phenotype was observed (Figure 3.11A). This was as a result of a rapid initial reduction in viability, as determined by CFU assessment, followed by protracted bacteriostasis (Figure 3.11B). This 2-$\log_{10}$ decrease in viable cell counts was in accordance with previously reported data that demonstrated that expression of MSMEG_1284 in a $\Delta vapBC$ *M. smegmatis* strain (237), and expression of *M. tuberculosis* RelE in *M. smegmatis* – which, incidentally, lacks the *relBE* family (211, 230, 237) - both resulted in a 100-fold decrease in viability followed by protracted bacteriostasis (152). In addition, expression of Rv2549c in the $\Delta Rv2545-Rv2550c$ strain, which lacks the cognate Rv2550c antitoxin, resulted in a 1-$\log_{10}$ reduction in viability of *M. tuberculosis* (Figure 3.36), while bacteriostasis was observed upon expression of the same toxin in wild type *M. tuberculosis* (Figure 3.15). Furthermore, since all survivors expressing Rv2549c had either been lost or had undergone plasmid rearrangement, taken together,

these data confirm that: (i) the effect of toxic VapC expression on mycobacteria is tempered by its cognate antitoxin expressed in the context of its chromosomal operon *i.e.* bacteriostasis *vs.* cidality; and (ii) expression of a toxic VapC has deleterious effects on mycobacteria, which surviving cells overcome by mutations that abrogate VapC expression (Figure 3.16, 3.17, 3.19 & 3.44).

4.4 There is a specificity of interaction between cognate VapBC pairs

Given the plethora of v*apC*s on the *M. tuberculosis* chromosome, which encode related proteins that retain PIN domains, the ability for cross-regulation of the *vapBC*s was assessed. The interaction of cognate VapBC pairs was initially tested by co-expressing the VapC with its cognate antitoxin from a single operon. Expression of the *Rv2550c-Rv2549c* operon was observed to neutralize Rv2549c toxicity (Figure 3.21). This was in accordance with previous findings that demonstrated that in *E. coli* as well as *M. smegmatis*, co-expression of antitoxins from the same operon abrogated the toxicity imposed by their cognate toxins (42, 72, 230, 237). Whilst a number of groups have obtained evidence for cognate and non-cognate TA interactions using biochemical (113, 307, 312) and genetic approaches (41, 104, 134, 190, 220, 230) in which the toxins and antitoxins were both conditionally induced using high copy plasmids, a different genetic approach was employed in this study. Plasmid incompatibility, which occurs when two high copy number plasmids reside within a bacterial, still remains a real problem with eventual loss of plasmid occurring despite the fact that two co-resident episomal plasmids can be stably inherited for a defined period of time (202, 287). Therefore, a modular system was developed such that a toxic VapC was conditionally expressed, in single copy, from one phage integration site, while cognate vs. non-cognate *vapB*s were expressed from a different chromosomal locus using a different promoter (Figure 3.25). Using this system, the toxic Rv2549c as well as Rv0595c were found to be neutralized only by their cognate antitoxins (Figure 3.26). These findings were in agreement with Ramage and colleagues who showed, using high copy plasmids, the specificity of interaction of cognate VapBC pairs (230). In view of the fact that cidality rather than bacteriostasis of a *M. tuberculosis* strain devoid of the cognate *Rv2550c* antitoxin occurred subsequent to Rv2549c induction (Figure 3.36) and that constitutive expression of

toxic VapCs in wild type *M. smegmatis* was observed to have a similar effect to expression of the same VapCs in a *M. smegmatis* strain devoid of all type II TA modules (Table 3.6), these data argue against cross-interaction between the toxin and antitoxin components of different VapBC modules in *M. tuberculosis* for alleviation of growth inhibition.

Even though all antitoxins located upstream of *vapC*s are denoted *vapB*s, the *vapB* antitoxins Rv0599c and Rv2595 have been observed to be more similar to MazE antitoxins (315). Interestingly, these two VapBs have been demonstrated to restore growth of *E. coli* (partially or fully), post induction of the toxic Rv2801c and Rv1991c MazFs (315). Moreover, protein interactions between (i) the VapB antitoxin Rv0599c with the non-cognate toxins Rv2596 (VapC) and Rv1991c (MazF) (315); (ii) the MazE antitoxin Rv1991A with the VapCs Rv0598c and Rv2596 (315); and (iii) both *M. tuberculosis* RelB1 and RelB2 with their non-cognate RelEs (307) have also been established. Despite the findings of this study, the abovementioned observations, together with the fact that some TA modules appear to directly or indirectly regulate other TA loci (91, 138, 304), make it important to probe whether interactions that may not alleviate toxicity may nonetheless be physiologically relevant in *M. tuberculosis* pathogenesis.

4.5 Are *vapBC*s required for mycobacterial survival to cellular stressors?

Numerous type II TA modules have been implicated in genome stabilization and stress-induced growth regulation of bacteria during nutrient starvation, DNA damage, oxidative stress, heat and antibiotic treatment (118, 119, 134, 230, 248, 249), just to name a few. Apart from inferences deduced from transcriptional data (Table 1.2), little, if anything is known about the role of VapCs in stress-induced growth regulation of mycobacteria. Consequently, this study attempted to determine whether VapCs play a role in mycobacterial stress physiology by investigating the effect of loss of TA module function on survival under conditions of stress. The saprophytic mycobacterium *M. smegmatis* has successfully been used to study *M. tuberculosis* pathogenesis (14, 198, 234, 259, 277). This, together with the fact that *M. smegmatis* possesses only one *vapBC* module on its chromosome, and thus, is not complicated by the massive expansion of the VapBC family which would render such an undertaking

in *M. tuberculosis* unfeasible, makes *M. smegmatis* a useful tool for this understanding the role of *vapBC*s in mycobacterial stress physiology. Using a genetic approach, the sole *M. smegmatis vapBC* module was successfully deleted from *M. smegmatis* by homologous recombination (Figure 3.30).The survival of the *M. smegmatis vapBC* deletion mutant following exposure to cell wall, nitrosative, genotoxic, thermal and antibiotic stresses was indistinguishable from its parental wild type strain under all conditions tested, as measured by enumerating CFUs (Figure 3.32 & Table 3.7). Whilst viability measurement by means of CFU assessment is a widely used method for monitoring effect of gene loss, as was the case in this study, it nonetheless remains a crude readout of the response of an organism to cellular stress and subtle differences in survival could be missed. Significantly, whereas Engelberg-Kulka's group demonstrated an association between the stress response of *E. coli* with *mazEF*s (118, 119, 248, 249), this association could not be reproduced by Tsilibaris *et al*. using a quintuple mutant of *E. coli* lacking all five type II TA modules, presumably as a result of the high density of the bacterial culture used (276). These findings suggest that variations in experimental conditions, such as growth phase, can profoundly affect the outcome of stress survival experiments. Therefore, although loss of the sole *M. smegmatis vapBC* did not appear to sensitize *M. smegmatis* to the lethal effects of certain stresses, the possibility that *vapBC* modules may play a role in stress-induced growth regulation of mycobacteria cannot be excluded.

4.6 VapC expression and *M. tuberculosis* drug tolerance

With the overwhelming evidence implicating TA modules in the formation of multidrug tolerant persisters upon treatment with antibiotics (60, 113, 116, 142, 193, 254), and the sheer number of *vapBC* modules on the *M. tuberculosis* chromosome, it was important to determine whether VapC expression results in the tolerance of *M. tuberculosis* to antibiotics. Wild type *M. tuberculosis* ectopically expressing the toxic Rv2829c VapC, was initially used to establish a protocol for testing the effect of VapC expression on the drug tolerance in *M. tuberculosis*. Using this initial protocol (Figure 3.37), over-expression of Rv2829c was observed to increase *M. tuberculosis* OFX-tolerance of late-logarithmic to early-stationary phase *M. tuberculosis* cells (Figure 3.38). However, limited oxygen availability not only restricted *M. tuberculosis* growth,

but also hindered the ability to discern any bacteriostatic effect that the VapC might have on the culture (Figure 3.38). As such, it was not possible to conclude that this was akin to the increase in OFX tolerance mediated by the protein synthesis inhibitor, CM. Therefore, the protocol was modified to ensure availability of oxygen-rich environments, maximal growth of *M. tuberculosis* cells and maximal killing by OFX for the duration of the experiment (Figure 3.39). Since Rotem and colleagues had demonstrated, using the mutant HipA7 toxin/ HipB antitoxin pair, that weakened binding between a toxin and its antitoxin resulted in a higher probability for persister formation in *E. coli* (239), the Δ*Rv2545-Rv2550c* strain which lacks both cognate antitoxins to bind the VapCs, was used in place of the wild type *M. tuberculosis* to increase the likelihood that even marginal changes in the ability of *M. tuberculosis* to tolerate OFX might be detected.

Upon implementation of these modifications, treatment of Δ*Rv2545-Rv2550c* cells expressing Rv2549c with OFX revealed a 1-$\log_{10}$ reduction in OFX-tolerance (Figure 3.41), similar to the 1-$\log_{10}$ reduction in viability observed upon Rv2549c expression in the absence of antibiotics (Figure 3.36). Although the expected 1-$\log_{10}$ decrease in viability of *M. tuberculosis* upon Rv2549c expression (Figure 3.36) was not observed in the absence of OFX in this experiment (Figure 3.41), the faster doubling time of the cells, as a result of being grown as rolling rather than standing cultures, probably allowed for earlier and faster plasmid loss or rearrangement, and hence a more rapid outgrowth of cells. This notwithstanding, the data suggested that expression of a toxic VapC in the absence of its cognate-antitoxin plays no role in *M. tuberculosis* OFX-tolerance. However, induction of Rv2546, which from previous observations yield lower cellular levels compared to Rv2549c (Figure 3.20), resulted in increased *M. tuberculosis* OFX-tolerance (Figure 3.40).

Therefore, to summarise the data obtained from three different VapCs: (i) the toxic Rv2829c expressed in the presence of its cognate antitoxin carried on the chromosome as part of the endogenous TA module - which effectively reduced the total amount of Rv2829c in the cell - increased *M. tuberculosis* OFX-tolerance; (ii) ectopic expression of Rv2546, with its low protein cellular levels, increased *M. tuberculosis* OFX-tolerance; and (iii) over-expression Rv2549c, whose high cellular

protein levels resulted in loss of viability in the absence of its cognate antitoxin, had no effect on *M. tuberculosis* OFX-tolerance. These data, together with the fact that ectopic expression of (i) the three toxic *M. tuberculosis* RelEs (261); and (ii) the toxic Rv1102c MazF (113), also increase mycobacterial persister populations using a variety of different antibiotics, including fluoroquinolones (113, 261), strongly suggest that OFX treatment of cells with low cellular VapC levels results in drug tolerance, but once high cellular VapC levels are reached, toxicity ensues. This may potentially explain why *M. tuberculosis* has undergone a massive expansion of this family. The availability of so many of these modules on its chromosome may act as a fail-safe mechanism to ensure that under conditions of stress, expression of these VapCs in the presence of their cognate antitoxins reduce the levels of the toxin in the cell, thereby allowing the cells to persist within the stressful environments.

4.7 Concluding Remarks

The work presented here has highlighted numerous challenges - plasmid instability and variations in VapC functionality readout when using different expression systems, to name but a few - encountered during elucidation of the role of mycobacterial VapCs. It is therefore imperative that future studies address these challenges before assigning absolute and comparative functionality to these proteins. Moreover, whilst VapC proteins do not appear to play a role in stress management of mycobacteria *in vitro* under the conditions tested, it would be interesting to assess the role of VapCs in various *ex vivo* and *in vivo* models, as well as analyzing and comparing transcriptome data obtained from *M. tuberculosis* exposed to a variety of stress conditions.

Given that low levels of VapC appear to result in increased drug tolerance, and comparatively high levels of VapC are required in order to see growth inhibitory effects in a mycobacterial host, it is likely that lower levels of VapCs that are induced as a result of stochastic and/or environmentally-induced *vapBC* expression might have a significant effect on the physiology of mycobacteria, without necessarily affecting growth. The presence of this large ribonuclease family in *M. tuberculosis* may also ensure abundant nuclease activity under specific conditions, which would likely have a profound effect on the physiology of the organism. Unlike MazF toxins which have

been characterized as sequence-specific ribonucleases (314, 316), very little is known about the nuclease activity of VapC proteins or their cellular target(s) (8, 50, 186, 230, 304). Studies are therefore required to identify the mechanism(s) of action as well as the cellular target(s) of VapCs, and to shed further light on their role in *M. tuberculosis* physiology and pathogenesis.

5. Appendices

Appendix A: List of Abbreviations

AAP	Antarctic Alkaline Phosphatase
Amp	Ampicillin
aph	Gene encoding aminoglycoside phosphotransferase
ATc	Anhydrotetracycline
ATCC	American Type Culture Collection
BCP	bromo-3-chloropropane
bp	Base pairs
BSA	Bovine serum albumin
CDC	Centres for Disease Control and Prevention
CFU	Colony forming unit
CM	Chloramphenicol
CSPD	Disodium 2-chloro-5-(4-methoxyspiro (2-dioxetane-3,2 (2-dioxetane-3,2'-(5'-chloro)-tricyclo[3.3.1.1. 3, 7.]decan)-. 4-yl)-1-phenyl phosphate
CTAB	Cetyltrimethylammonium bromide
d	Days
DCO	Double cross over
DIG	Digoxigenin
DMSO	Dimethylsulphoxide
DNA	Deoxyribonucleic acid
DNTPs	Deoxynucleotide triphosphate
DOTS	Directly Observed Therapy – Short Course
DTT	Dithiothreitol
EDTA	Ethylenediaminetetraacetic acid
g	Gravitational force
Gm	Gentamicin

h	Hours
HAART	Highly Active Antiretroviral Therapy
HCl	Hydrochloric acid
HIV	Human Immunodeficiency Virus
hyg	Gene conferring resistance to hygromycin B
Hyg	Hygromycin
IPTG	Isopropyl-beta-D-thiogalactopyranoside
IRIS	Immune Reconstitution Inflammatory Syndrome
kb	Kilo base pair
Km	Kanamycin
kPA	Kilo Pascal
LA	Luria-Bertani agar
lacZ	Gene encoding β-galactosidase
LB	Luria-Bertani broth
LTBI	Latent tuberculosis infection
MDR-TB	Multidrug-Resistant Tuberculosis
MIC	Minimum inhibitory concentration
min	Minutes
ml	Mililitre
MTBC	*Mycobacterium tuberculosis* complex
NaCl	Sodium chloride
$NaNO_2$	Sodium nitrite
NaOH	Sodium hydroxide
OADC	Oleic acid-albumin-dextrose-catalase
OD_{600}	Optical density at 600 nanometre wavelength
OFX	Ofloxacin
ORF	Open reading frame
PCR	Polymerase Chain Reaction

ppGpp	Guanosine 3'-5'-Bispyrophosphate
R	Resistant
RNA	Ribonucleic acid
RT	Reverse transcription/transcriptase
s	Seconds
sacB	Gene encoding levansucrase
SAP	Shrimp Alkaline Phosphatase
SCO	Single cross over
sdH$_2$0	Sterile distilled water
SDS	Sodium dodecylsulphate
Suc	Sucrose
TB	Tuberculosis
TDR-TB	Totally Drug Resistant Tuberculosis
TE	Tris-EDTA
tmRNA	Transfer messenger RNA
Tris	Tris(hydroxymethyl)aminomethane
Tween	Polyoxyethylene sorbitan monooleate
U	Units
XDR-TB	Extensively Drug Resistant Tuberculosis
v/v	Volume per volume
w/v	Weight per volume
WHO	World Health Organization
X-gal	5-bromo-4-chloro-3-indolyl-α-D-thiogalactopyranoside

Appendix B: Culture media and solutions

Culture media

All media was made up in one litre de-ionized water and except otherwise stated sterilized by autoclaving (121°C for 20 mins).

Luria-Bertani Broth (LB)

5g yeast, 10g tryptone, 10g sodium chloride

Luria-Bertani Agar (LA)

5g yeast, 10g tryptone, 10g sodium chloride, 15g agar

2TY

5g sodium chloride, 10g yeast extract, 16g tryptone

Middlebrook 7H9

2ml glycerol, 4.7g Difco^TM Middlebrook 7H9 broth

Middlebrook 7H10

5ml glycerol, 19g Difco^TM Middlebrook 7H10 agar

Sauton's minimal media (pH 7.2)

4 g asparagine, 0.5 g magnesium sulphate, 2 g citric acid, 0.5 g potassium dihydrogen orthophosphate, 0.05 g ammonium ferric citrate, 48ml glycerol. Sterilized by filtration.

Solutions

20× SSC

8.82% sodium citrate, 17.53% NaCl; pH to 7.0 with HCl

50× Denhardt's Reagent

1% Ficoll (Type 400), 1% polyvinylpyrrolidone, 1% BSA

Appendix C: *attB* PCR strategy
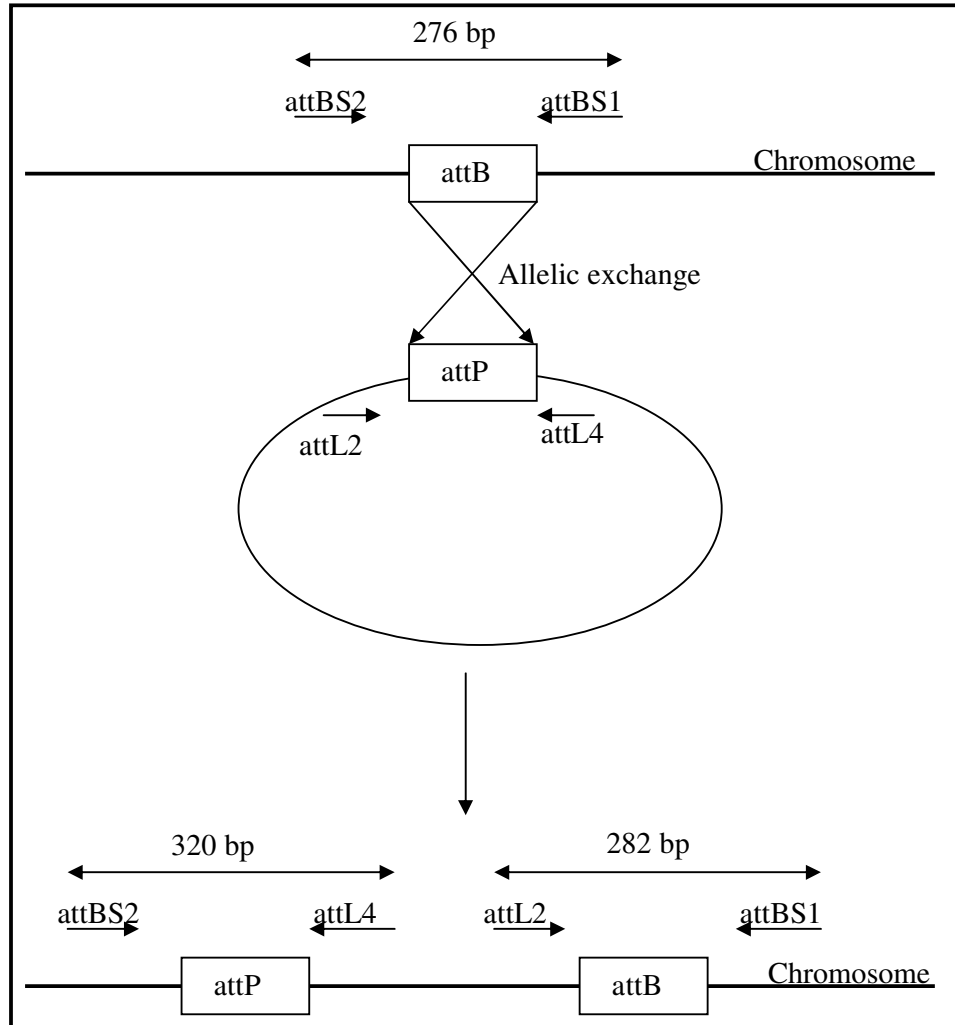
Schematic representation of the PCR strategy used to confirm successful integration at the tRNA[Gly] **attachment site following allelic exchange**

Appendix D: Lamda DNA molecular weight markers

Marker		Marker IV		Marker V	
bp	ng/4 μl	bp	ng/4 μl	bp	ng/4 μl
21226	438	19329	374	587	135
5148	106	7743	150	540	124
4973	103	5526	107	504	116
4268	88	4254	82	458	105
3530	73	3140	61	434	99
2027	42	2690	52	267	61
1904	39	2322	45	234	54
1584	33	1882	36	213	49
1375	28	1489	29	192	44
947	19	1150	22	184	42
831	17	925	18	124/123	28/28
564	12	697	14	104	24
		421	8	89/80	20/18
				64/75/51/21/18/11/8	15/13/12/5/4/3/2
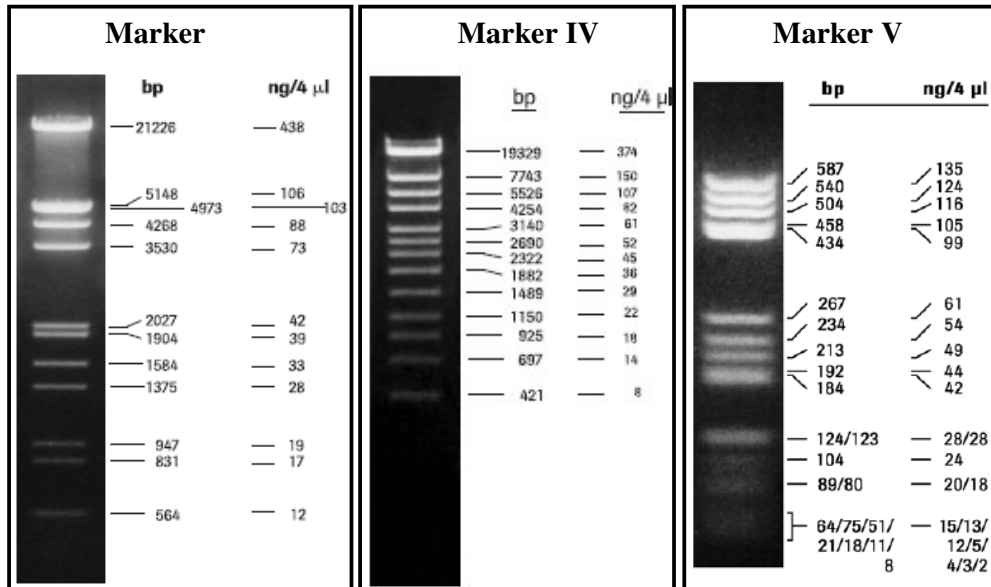
The above DNA molecular weight markers III, IV and V used in this study were supplied by Roche Applied Science.

6. References

1. **Afif, H., N. Allali, M. Couturier, and L. Van Melderen.** 2001. The ratio between CcdA and CcdB modulates the transcriptional repression of the *ccd* poison-antidote system. Mol Microbiol **41:**73-82.

2. **Aizenman, E., H. Engelberg-Kulka, and G. Glaser.** 1996. An *Escherichia coli* chromosomal "addiction module" regulated by guanosine [corrected] 3',5'-bispyrophosphate: a model for programmed bacterial cell death. Proc Natl Acad Sci USA **93:**6059-63.

3. **Amitai, S., I. Kolodkin-Gal, M. Hananya-Meltabashi, A. Sacher, and H. Engelberg-Kulka.** 2009. *Escherichia coli* MazF leads to the simultaneous selective synthesis of both "death proteins" and "survival proteins". PLoS Genet **5:**e1000390.

4. **Amitai, S., Y. Yassin, and H. Engelberg-Kulka.** 2004. MazF-mediated cell death in *Escherichia coli*: a point of no return. J Bacteriol **186:**8295-300.

5. **Anantharaman, V., and L. Aravind.** 2003. New connections in the prokaryotic toxin-antitoxin network: relationship with the eukaryotic nonsense-mediated RNA decay system. Genome Biol **4:**R81.

6. **Anon.** 2006. Emergence of Mycobacterium tuberculosis with extensive resistance to second-line drugs-worldwide, 2000-2004. MMWR Morb Mortal Wkly Rep **55:**301-5.

7. **Anon.** 2006. The Global Plan to Stop TB, 2006-2015. Actions for life: towards a world free of tuberculosis. Int J Tuberc Lung Dis **10:**240-1.

8. **Arcus, V. L., K. Backbro, A. Roos, E. L. Daniel, and E. N. Baker.** 2004. Distant structural homology leads to the functional characterization of an archaeal PIN domain as an exonuclease. J Biol Chem **279:**16471-8.

9. **Arcus, V. L., J. L. McKenzie, J. Robson, and G. M. Cook.** 2010. The PIN-domain ribonucleases and the prokaryotic VapBC toxin-antitoxin array. Protein Eng Des Sel.

10. **Arcus, V. L., P. B. Rainey, and S. J. Turner.** 2005. The PIN-domain toxin-antitoxin array in mycobacteria. Trends Microbiol **13:**360-5.

11. **Bahassi, E. M., M. H. O'Dea, N. Allali, J. Messens, M. Gellert, and M. Couturier.** 1999. Interactions of CcdB with DNA gyrase. Inactivation of GyrA, poisoning of the gyrase-DNA complex, and the antidote action of CcdA. J Biol Chem **274:**10936-44.

12. **Balaban, N. Q., J. Merrin, R. Chait, L. Kowalik, and S. Leibler.** 2004. Bacterial persistence as a phenotypic switch. Science **305:**1622-5.

13. **Baleta, A.** 2008. Trial finds simultaneous HIV/tuberculosis treatment beneficial. Lancet Infect Dis **8:**669.

14. **Barry, C. E.** 2001. *Mycobacterium smegmatis*: an absurd model for tuberculosis? Response from Barry, III. Trends Microbiol **9:**473-4.

15. **Barry, C. E., 3rd, and J. S. Blanchard.** 2010. The chemical biology of new drugs in the development for tuberculosis. Curr Opin Chem Biol **14:**456-466.

16. **Barry, C. E., 3rd, H. I. Boshoff, V. Dartois, T. Dick, S. Ehrt, J. Flynn, D. Schnappinger, R. J. Wilkinson, and D. Young.** 2009. The spectrum of latent tuberculosis: rethinking the biology and intervention strategies. Nat Rev Microbiol **7:**845-55.

17. **Bateman, B. T., N. P. Donegan, T. M. Jarry, M. Palma, and A. L. Cheung.** 2001. Evaluation of a tetracycline-inducible promoter in *Staphylococcus aureus* in vitro and in vivo and its application in demonstrating the role of sigB in microcolony formation. Infect Immun **69:**7851-7.

18. **Betts, J. C., P. T. Lukey, L. C. Robb, R. A. McAdam, and K. Duncan.** 2002. Evaluation of a nutrient starvation model of *Mycobacterium tuberculosis* persistence by gene and protein expression profiling. Mol Microbiol **43:**717-31.

19. **Bigger, J. W.** 1944. Treatment of staphylococcal infections with penicillin. Lancet **244:**497-500.

20. **Billington, O. J., T. D. McHugh, and S. H. Gillespie.** 1999. Physiological cost of rifampin resistance induced in vitro in *Mycobacterium tuberculosis*. Antimicrob Agents Chemother **43:**1866-9.

21. **Blokpoel, M. C., H. N. Murphy, R. O'Toole, S. Wiles, E. S. Runn, G. R. Stewart, D. B. Young, and B. D. Robertson.** 2005. Tetracycline-inducible gene regulation in mycobacteria. Nucleic Acids Res **33:**e22.

22. **Blondelet-Rouault, M. H., J. Weiser, A. Lebrihi, P. Branny, and J. L. Pernodet.** 1997. Antibiotic resistance gene cassettes derived from the omega interposon for use in *E. coli* and *Streptomyces*. Gene **190:**315-7.

23. **Bloom, B. R. (ed.).** 1994. Tuberculosis: pathogenesis, protection, and control. American Society for Microbiology Press, Washington, DC.

24. **Blower, T. R., P. C. Fineran, M. J. Johnson, I. K. Toth, D. P. Humphreys, and G. P. Salmond.** 2009. Mutagenesis and functional characterization of the RNA and protein components of the toxIN abortive infection and toxin-antitoxin locus of Erwinia. J Bacteriol **191:**6029-39.

25. **Brown, A. C., and T. Parish.** 2006. Instability of the acetamide-inducible expression vector pJAM2 in *Mycobacterium tuberculosis*. Plasmid **55:**81-6.

26. **Bryson, K., L. J. McGuffin, R. L. Marsden, J. J. Ward, J. S. Sodhi, and D. T. Jones.** 2005. Protein structure prediction servers at University College London. Nucleic Acids Res **33:**W36-8.

27. **Budde, P. P., B. M. Davis, J. Yuan, and M. K. Waldor.** 2007. Characterization of a *higBA* toxin-antitoxin locus in *Vibrio cholerae*. J Bacteriol **189:**491-500.

28. **Bunker, R. D., J. L. McKenzie, E. N. Baker, and V. L. Arcus.** 2008. Crystal structure of PAE0151 from *Pyrobaculum aerophilum*, a PIN-domain (VapC) protein from a toxin-antitoxin operon. Proteins **72:**510-8.

29. **Buts, L., J. Lah, M. H. Dao-Thi, L. Wyns, and R. Loris.** 2005. Toxin-antitoxin modules as bacterial metabolic stress managers. Trends Biochem Sci **30:**672-9.

30. **Calver, A. D., A. A. Falmer, M. Murray, O. J. Strauss, E. M. Streicher, M. Hanekom, T. Liversage, M. Masibi, P. D. van Helden, R. M. Warren, and T. C. Victor.** 2010. Emergence of increased resistance and extensively drug-resistant tuberculosis despite treatment adherence, South Africa. Emerg Infect Dis **16:**264-71.

31. **Carroll, P., A. C. Brown, A. R. Hartridge, and T. Parish.** 2007. Expression of *Mycobacterium tuberculosis* Rv1991c using an arabinose-inducible promoter demonstrates its role as a toxin. FEMS Microbiol Lett **274:**73-82.

32. **Carroll, P., D. G. Muttucumaru, and T. Parish.** 2005. Use of a tetracycline-inducible system for conditional expression in *Mycobacterium tuberculosis* and *Mycobacterium smegmatis*. Appl Environ Microbiol **71:**3077-84.

33. **Carter, G., M. Wu, D. C. Drummond, and L. E. Bermudez.** 2003. Characterization of biofilm formation by clinical isolates of *Mycobacterium avium*. J Med Microbiol **52:**747-52.

34. **Caws, M., G. Thwaites, S. Dunstan, T. R. Hawn, N. T. Lan, N. T. Thuong, K. Stepniewska, M. N. Huyen, N. D. Bang, T. H. Loc, S. Gagneux, D. van Soolingen, K. Kremer, M. van der Sande, P. Small, P. T. Anh, N. T. Chinh, H. T. Quy, N. T. Duyen, D. Q. Tho, N. T. Hieu, E. Torok, T. T. Hien, N. H. Dung, N. T. Nhu, P. M. Duy, N. van Vinh Chau, and J. Farrar.** 2008. The influence of host and bacterial genotype on the development of disseminated disease with *Mycobacterium tuberculosis*. PLoS Pathog **4:**e1000034.

35. **Caws, M., G. Thwaites, K. Stepniewska, T. N. Nguyen, T. H. Nguyen, T. P. Nguyen, N. T. Mai, M. D. Phan, H. L. Tran, T. H. Tran, D. van Soolingen, K. Kremer, V. V. Nguyen, T. C. Nguyen, and J. Farrar.** 2006. Beijing genotype of *Mycobacterium tuberculosis* is significantly associated with human immunodeficiency virus infection and multidrug resistance in cases of tuberculous meningitis. J Clin Microbiol **44:**3934-9.

36. **Chao, M. C., and E. J. Rubin.** 2010. Letting sleeping *dos* lie: Does dormancy play a role in tuberculosis. Annual Review Microbiology**:**293 - 311.

37. **Cherny, I., L. Rockah, and E. Gazit.** 2005. The YoeB toxin is a folded protein that forms a physical complex with the unfolded YefM antitoxin. Implications for a structural-based differential stability of toxin-antitoxin systems. J Biol Chem **280:**30063-72.

38. **Christensen-Dalsgaard, M., and K. Gerdes.** 2006. Two *higBA* loci in the *Vibrio cholerae* superintegron encode mRNA cleaving enzymes and can stabilize plasmids. Mol Microbiol **62:**397-411.

39. **Christensen-Dalsgaard, M., M. G. Jorgensen, and K. Gerdes.** 2010. Three new RelE-homologous mRNA interferases of *Escherichia coli* differentially induced by environmental stresses. Mol Microbiol **75:**333-48.

40. **Christensen, S. K., G. Maenhaut-Michel, N. Mine, S. Gottesman, K. Gerdes, and L. Van Melderen.** 2004. Overproduction of the Lon protease triggers inhibition of translation in *Escherichia coli*: involvement of the *yefM-yoeB* toxin-antitoxin system. Mol Microbiol **51:**1705-17.

41. **Christensen, S. K., M. Mikkelsen, K. Pedersen, and K. Gerdes.** 2001. RelE, a global inhibitor of translation, is activated during nutritional stress. Proc Natl Acad Sci USA **98:**14328-33.

42. **Christensen, S. K., K. Pedersen, F. G. Hansen, and K. Gerdes.** 2003. Toxin-antitoxin loci as stress-response-elements: ChpAK/MazF and ChpBK cleave translated RNAs and are counteracted by tmRNA. J Mol Biol **332:**809-19.

43. **Chung, G. A., Z. Aktar, S. Jackson, and K. Duncan.** 1995. High-throughput screen for detecting antimycobacterial agents. Antimicrob Agents Chemother **39:**2235-8.

44. **Clissold, P. M., and C. P. Ponting.** 2000. PIN domains in nonsense-mediated mRNA decay and RNAi. Curr Biol **10:**R888-90.

45.   **Cohen, T., M. Murray, K. Wallengren, G. G. Alvarez, E. Y. Samuel, and D. Wilson.** 2010. The prevalence and drug sensitivity of tuberculosis among patients dying in hospital in KwaZulu-Natal, South Africa: a postmortem study. PLoS Med **7:**e1000296.

46.   **Cooper, C. R., A. J. Daugherty, S. Tachdjian, P. H. Blum, and R. M. Kelly.** 2009. Role of *vapBC* toxin-antitoxin loci in the thermal stress response of *Sulfolobus solfataricus*. Biochem Soc Trans **37:**123-6.

47.   **Correia, F. F., A. D'Onofrio, T. Rejtar, L. Li, B. L. Karger, K. Makarova, E. V. Koonin, and K. Lewis.** 2006. Kinase activity of overexpressed HipA is required for growth arrest and multidrug tolerance in *Escherichia coli*. J Bacteriol **188:**8360-7.

48.   **Cosma, C. L., D. R. Sherman, and L. Ramakrishnan.** 2003. The secret lives of the pathogenic mycobacteria. Annu Rev Microbiol **57:**641-76.

49.   **Dahl, J. L., C. N. Kraus, H. I. Boshoff, B. Doan, K. Foley, D. Avarbock, G. Kaplan, V. Mizrahi, H. Rubin, and C. E. Barry, 3rd.** 2003. The role of RelMtb-mediated adaptation to stationary phase in long-term persistence of *Mycobacterium tuberculosis* in mice. Proc Natl Acad Sci USA **100:**10026-31.

50.   **Daines, D. A., M. H. Wu, and S. Y. Yuan.** 2007. VapC-1 of nontypeable *Haemophilus influenzae* is a ribonuclease. J Bacteriol **189:**5041-8.

51.   **Danelishvili, L., Y. Yamazaki, J. Selker, and L. E. Bermudez.** 2010. Secreted *Mycobacterium tuberculosis* Rv3654c and Rv3655c Proteins Participate in the Suppression of Macrophage Apoptosis. PLoS One **5:**e10474.

52.   **Dao-Thi, M. H., L. Van Melderen, E. De Genst, H. Afif, L. Buts, L. Wyns, and R. Loris.** 2005. Molecular basis of gyrase poisoning by the addiction toxin CcdB. J Mol Biol **348:**1091-102.

53.   **Darwin, K. H., S. Ehrt, J. C. Gutierrez-Ramos, N. Weich, and C. F. Nathan.** 2003. The proteasome of *Mycobacterium tuberculosis* is required for resistance to nitric oxide. Science **302:**1963-6.

54.   **De Groote, V. N., N. Verstraeten, M. Fauvart, C. I. Kint, A. M. Verbeeck, S. Beullens, P. Cornelis, and J. Michiels.** 2009. Novel persistence genes in *Pseudomonas aeruginosa* identified by high-throughput screening. FEMS Microbiol Lett **297:**73-9.

55.   **de Smit, M. H., and J. van Duin.** 1990. Secondary structure of the ribosome binding site determines translational efficiency: a quantitative analysis. Proc Natl Acad Sci USA **87:**7668-72.

56.   **Dhar, N., and J. D. McKinney.** 2007. Microbial phenotypic heterogeneity and antibiotic tolerance. Curr Opin Microbiol **10:**30-8.

57.   **Dhar, N., and J. D. McKinney.** 2010. *Mycobacterium tuberculosis* persistence mutants identified by screening in isoniazid-treated mice. Proc Natl Acad Sci USA **107:**12275-80.

58.   **Domenech, P., M. B. Reed, and C. E. Barry, 3rd.** 2005. Contribution of the *Mycobacterium tuberculosis* MmpL protein family to virulence and drug resistance. Infect Immun **73:**3492-501.

59.   **Dorr, T., K. Lewis, and M. Vulic.** 2009. SOS response induces persistence to fluoroquinolones in *Escherichia coli*. PLoS Genet **5:**e1000760.

60.   **Dorr, T., M. Vulic, and K. Lewis.** 2010. Ciprofloxacin causes persister formation by inducing the TisB toxin in *Escherichia coli*. PLoS Biol **8:**e1000317.

61. **Downing, K. J., J. C. Betts, D. I. Young, R. A. McAdam, F. Kelly, M. Young, and V. Mizrahi.** 2004. Global expression profiling of strains harbouring null mutations reveals that the five rpf-like genes of *Mycobacterium tuberculosis* show functional redundancy. Tuberculosis (Edinb) **84:**167-79.

62. **Drlica, K., H. Hiasa, R. Kerns, M. Malik, A. Mustaev, and X. Zhao.** 2009. Quinolones: action and resistance updated. Curr Top Med Chem **9:**981-98.

63. **Drlica, K., C. Xu, J. Y. Wang, R. M. Burger, and M. Malik.** 1996. Fluoroquinolone action in mycobacteria: similarity with effects in *Escherichia coli* and detection by cell lysate viscosity. Antimicrob Agents Chemother **40:**1594-9.

64. **Drobniewski, F., Y. Balabanova, V. Nikolayevsky, M. Ruddy, S. Kuznetzov, S. Zakharova, A. Melentyev, and I. Fedorin.** 2005. Drug-resistant tuberculosis, clinical virulence, and the dominance of the Beijing strain family in Russia. Jama **293:**2726-31.

65. **Dubnau, E., P. Fontan, R. Manganelli, S. Soares-Appel, and I. Smith.** 2002. *Mycobacterium tuberculosis* genes induced during infection of human macrophages. Infect Immun **70:**2787-95.

66. **Dutta, N. K., S. Mehra, P. J. Didier, C. J. Roy, L. A. Doyle, X. Alvarez, M. Ratterree, N. A. Be, G. Lamichhane, S. K. Jain, M. R. Lacey, A. A. Lackner, and D. Kaushal.** 2010. Genetic requirements for the survival of tubercle bacilli in primates. J Infect Dis **201:**1743-52.

67. **Dye, C., and B. G. Williams.** 2010. The population dynamics and control of tuberculosis. Science **328:**856-61.

68. **Dye, C., B. G. Williams, M. A. Espinal, and M. C. Raviglione.** 2002. Erasing the world's slow stain: strategies to beat multidrug-resistant tuberculosis. Science **295:**2042-6.

69. **Dziadek, J., S. A. Rutherford, M. V. Madiraju, M. A. Atkinson, and M. Rajagopalan.** 2003. Conditional expression of *Mycobacterium smegmatis ftsZ*, an essential cell division gene. Microbiology **149:**1593-603.

70. **Ehrt, S., X. V. Guo, C. M. Hickey, M. Ryou, M. Monteleone, L. W. Riley, and D. Schnappinger.** 2005. Controlling gene expression in mycobacteria with anhydrotetracycline and Tet repressor. Nucleic Acids Res **33:**e21.

71. **Ehrt, S., and D. Schnappinger.** 2009. Mycobacterial survival strategies in the phagosome: defence against host stresses. Cell Microbiol **11:**1170-8.

72. **Engelberg-Kulka, H., R. Hazan, and S. Amitai.** 2005. *mazEF*: a chromosomal toxin-antitoxin module that triggers programmed cell death in bacteria. J Cell Sci **118:**4327-32.

73. **Engelberg-Kulka, H., M. Reches, S. Narasimhan, R. Schoulaker-Schwarz, Y. Klemes, E. Aizenman, and G. Glaser.** 1998. *rexB* of bacteriophage lambda is an anti-cell death gene. Proc Natl Acad Sci USA **95:**15481-6.

74. **Falla, T. J., and I. Chopra.** 1998. Joint tolerance to beta-lactam and fluoroquinolone antibiotics in *Escherichia coli* results from overexpression of *hipA*. Antimicrob Agents Chemother **42:**3282-4.

75. **Fenner, L., M. Egger, and S. Gagneux.** 2009. Annie Darwin's death, the evolution of tuberculosis and the need for systems epidemiology. Int J Epidemiol **38:**1425-8.

76. **Fineran, P. C., T. R. Blower, I. J. Foulds, D. P. Humphreys, K. S. Lilley, and G. P. Salmond.** 2009. The phage abortive infection system, ToxIN, functions as a protein-RNA toxin-antitoxin pair. Proc Natl Acad Sci U S A **106:**894-9.

77. **Firmani, M. A., and L. W. Riley.** 2002. Reactive nitrogen intermediates have a bacteriostatic effect on *Mycobacterium tuberculosis* in vitro. J Clin Microbiol **40:**3162-6.

78. **Fisher, M. A., B. B. Plikaytis, and T. M. Shinnick.** 2002. Microarray analysis of the *Mycobacterium tuberculosis* transcriptional response to the acidic conditions found in phagosomes. J Bacteriol **184:**4025-32.

79. **Fivian-Hughes, A. S., and E. O. Davis.** 2010. Analysing the Regulatory Role of the HigA Antitoxin within *Mycobacterium tuberculosis*. J Bacteriol.

80. **Fontan, P., V. Aris, S. Ghanny, P. Soteropoulos, and I. Smith.** 2008. Global transcriptional profile of *Mycobacterium tuberculosis* during THP-1 human macrophage infection. Infect Immun **76:**717-25.

81. **Forti, F., A. Crosta, and D. Ghisotti.** 2009. Pristinamycin-inducible gene regulation in mycobacteria. J Biotechnol **140:**270-7.

82. **Fozo, E. M., M. R. Hemm, and G. Storz.** 2008. Small toxic proteins and the antisense RNAs that repress them. Microbiol Mol Biol Rev **72:**579-89.

83. **Fozo, E. M., M. Kawano, F. Fontaine, Y. Kaya, K. S. Mendieta, K. L. Jones, A. Ocampo, K. E. Rudd, and G. Storz.** 2008. Repression of small toxic protein synthesis by the Sib and OhsC small RNAs. Mol Microbiol **70:**1076-93.

84. **Fozo, E. M., K. S. Makarova, S. A. Shabalina, N. Yutin, E. V. Koonin, and G. Storz.** 2010. Abundance of type I toxin-antitoxin systems in bacteria: searches for new candidates and discovery of novel families. Nucleic Acids Res.

85. **Gagneux, S., M. V. Burgos, K. DeRiemer, A. Encisco, S. Munoz, P. C. Hopewell, P. M. Small, and A. S. Pym.** 2006. Impact of bacterial genetics on the transmission of isoniazid-resistant *Mycobacterium tuberculosis*. PLoS Pathog **2:**e61.

86. **Gagneux, S., C. D. Long, P. M. Small, T. Van, G. K. Schoolnik, and B. J. Bohannan.** 2006. The competitive cost of antibiotic resistance in *Mycobacterium tuberculosis*. Science **312:**1944-6.

87. **Galvani, C., J. Terry, and E. E. Ishiguro.** 2001. Purification of the RelB and RelE proteins of *Escherichia coli*: RelE binds to RelB and to ribosomes. J Bacteriol **183:**2700-3.

88. **Gandhi, N. R., A. Moll, A. W. Sturm, R. Pawinski, T. Govender, U. Lalloo, K. Zeller, J. Andrews, and G. Friedland.** 2006. Extensively drug-resistant tuberculosis as a cause of death in patients co-infected with tuberculosis and HIV in a rural area of South Africa. Lancet **368:**1575-80.

89. **Gandotra, S., M. B. Lebron, and S. Ehrt.** 2010. The *Mycobacterium tuberculosis* proteasome active site threonine is essential for persistence yet dispensable for replication and resistance to nitric oxide. PLoS Pathog **6**.

90. **Gandotra, S., D. Schnappinger, M. Monteleone, W. Hillen, and S. Ehrt.** 2007. In vivo gene silencing identifies the *Mycobacterium tuberculosis* proteasome as essential for the bacteria to persist in mice. Nat Med **13:**1515-20.

91. **Garcia-Pino, A., M. Christensen-Dalsgaard, L. Wyns, M. Yarmolinsky, R. D. Magnuson, K. Gerdes, and R. Loris.** 2008. Doc of prophage P1 is inhibited by its antitoxin partner Phd through fold complementation. J Biol Chem **283:**30821-7.

92. **Garton, N. J., S. J. Waddell, A. L. Sherratt, S. M. Lee, R. J. Smith, C. Senner, J. Hinds, K. Rajakumar, R. A. Adegbola, G. S. Besra, P. D. Butcher, and M. R. Barer.** 2008. Cytological and transcript analyses reveal fat and lazy persister-like bacilli in tuberculous sputum. PLoS Med **5:**e75.

93. **Gefen, O., and N. Q. Balaban.** 2009. The importance of being persistent: heterogeneity of bacterial populations under antibiotic stress. FEMS Microbiol Rev **33:**704-17.

94. **Gefen, O., C. Gabay, M. Mumcuoglu, G. Engel, and N. Q. Balaban.** 2008. Single-cell protein induction dynamics reveals a period of vulnerability to antibiotics in persister bacteria. Proc Natl Acad Sci USA **105:**6145-9.

95. **Gerdes, K.** 2000. Toxin-antitoxin modules may regulate synthesis of macromolecules during nutritional stress. J Bacteriol **182:**561-72.

96. **Gerdes, K., S. K. Christensen, and A. Lobner-Olesen.** 2005. Prokaryotic toxin-antitoxin stress response loci. Nat Rev Microbiol **3:**371-82.

97. **Gerdes, K., A. P. Gultyaev, T. Franch, K. Pedersen, and N. D. Mikkelsen.** 1997. Antisense RNA-regulated programmed cell death. Annu Rev Genet **31:**1-31.

98. **Gerdes, K., and E. G. Wagner.** 2007. RNA antitoxins. Curr Opin Microbiol **10:**117-24.

99. **Gill, W. P., N. S. Harik, M. R. Whiddon, R. P. Liao, J. E. Mittler, and D. R. Sherman.** 2009. A replication clock for *Mycobacterium tuberculosis*. Nat Med **15:**211-4.

100. **Glavan, F., I. Behm-Ansmant, E. Izaurralde, and E. Conti.** 2006. Structures of the PIN domains of SMG6 and SMG5 reveal a nuclease within the mRNA surveillance complex. EMBO J **25:**5117-25.

101. **Gomez, J. E., and W. R. Bishai.** 2000. *whmD* is an essential mycobacterial gene required for proper septation and cell division. Proc Natl Acad Sci U S A **97:**8554-9.

102. **Gonzalez Barrios, A. F., R. Zuo, Y. Hashimoto, L. Yang, W. E. Bentley, and T. K. Wood.** 2006. Autoinducer 2 controls biofilm formation in *Escherichia coli* through a novel motility quorum-sensing regulator (MqsR, B3022). J Bacteriol **188:**305-16.

103. **Gordhan, B. G., and T. Parish.** 2001. Gene replacement using pre-treated DNA. Methods in Molecular Medicine **54:**77-92.

104. **Gotfredsen, M., and K. Gerdes.** 1998. The *Escherichia coli relBE* genes belong to a new toxin-antitoxin gene family. Mol Microbiol **29:**1065-76.

105. **Greendyke, R., M. Rajagopalan, T. Parish, and M. V. Madiraju.** 2002. Conditional expression of *Mycobacterium smegmatis dnaA*, an essential DNA replication gene. Microbiology **148:**3887-900.

106. **Gross, M., I. Marianovsky, and G. Glaser.** 2006. MazG - a regulator of programmed cell death in *Escherichia coli*. Mol Microbiol **59:**590-601.

107. **Guo, X. V., M. Monteleone, M. Klotzsche, A. Kamionka, W. Hillen, M. Braunstein, S. Ehrt, and D. Schnappinger.** 2007. Silencing *Mycobacterium smegmatis* by using tetracycline repressors. J Bacteriol **189:**4614-23.

108. **Gupta, A.** 2009. Killing activity and rescue function of genome-wide toxin-antitoxin loci of *Mycobacterium tuberculosis*. FEMS Microbiol Lett **290:**45-53.

109. **Hall-Stoodley, L., J. W. Costerton, and P. Stoodley.** 2004. Bacterial biofilms: from the natural environment to infectious diseases. Nat Rev Microbiol **2:**95-108.

110. **Hall-Stoodley, L., and P. Stoodley.** 2009. Evolving concepts in biofilm infections. Cell Microbiol **11:**1034-43.

111. **Hallez, R., D. Geeraerts, Y. Sterckx, N. Mine, R. Loris, and L. Van Melderen.** 2010. New toxins homologous to ParE belonging to three-component toxin-antitoxin systems in *Escherichia coli* O157:H7. Mol Microbiol **76:**719-32.

112. **Hampshire, T., S. Soneji, J. Bacon, B. W. James, J. Hinds, K. Laing, R. A. Stabler, P. D. Marsh, and P. D. Butcher.** 2004. Stationary phase gene expression of *Mycobacterium tuberculosis* following a progressive nutrient depletion: a model for persistent organisms? Tuberculosis (Edinb) **84:**228-38.

113. **Han, J. S., J. J. Lee, T. Anandan, M. Zeng, S. Sripathi, W. J. Jahng, S. H. Lee, J. W. Suh, and C. M. Kang.** 2010. Characterization of a chromosomal toxin-antitoxin, Rv1102c-Rv1103c system in *Mycobacterium tuberculosis*. Biochem Biophys Res Commun.

114. **Hanekom, M., G. D. van der Spuy, E. Streicher, S. L. Ndabambi, C. R. McEvoy, M. Kidd, N. Beyers, T. C. Victor, P. D. van Helden, and R. M. Warren.** 2007. A recently evolved sublineage of the *Mycobacterium tuberculosis* Beijing strain family is associated with an increased ability to spread and cause disease. J Clin Microbiol **45:**1483-90.

115. **Hansen, S., K. Lewis, and M. Vulic.** 2008. Role of global regulators and nucleotide metabolism in antibiotic tolerance in *Escherichia coli*. Antimicrob Agents Chemother **52:**2718-26.

116. **Harrison, J. J., W. D. Wade, S. Akierman, C. Vacchi-Suzzi, C. A. Stremick, R. J. Turner, and H. Ceri.** 2009. The chromosomal toxin gene *yafQ* is a determinant of multidrug tolerance for *Escherichia coli* growing in a biofilm. Antimicrob Agents Chemother **53:**2253-8.

117. **Hayes, F.** 2003. Toxins-antitoxins: plasmid maintenance, programmed cell death, and cell cycle arrest. Science **301:**1496-9.

118. **Hazan, R., and H. Engelberg-Kulka.** 2004. *Escherichia coli mazEF*-mediated cell death as a defense mechanism that inhibits the spread of phage P1. Mol Genet Genomics **272:**227-34.

119. **Hazan, R., B. Sat, and H. Engelberg-Kulka.** 2004. *Escherichia coli mazEF*-mediated cell death is triggered by various stressful conditions. J Bacteriol **186:**3663-9.

120. **Hazan, R., B. Sat, M. Reches, and H. Engelberg-Kulka.** 2001. Postsegregational killing mediated by the P1 phage "addiction module" *phd-doc* requires the *Escherichia coli* programmed cell death system *mazEF*. J Bacteriol **183:**2046-50.

121. **Herbert, D., C. N. Paramasivan, P. Venkatesan, G. Kubendiran, R. Prabhakar, and D. A. Mitchison.** 1996. Bactericidal action of ofloxacin, sulbactam-ampicillin, rifampin, and isoniazid on logarithmic- and stationary-

phase cultures of *Mycobacterium tuberculosis*. Antimicrob Agents Chemother **40:**2296-9.

122. **Hernandez-Abanto, S. M., S. C. Woolwine, S. K. Jain, and W. R. Bishai.** 2006. Tetracycline-inducible gene expression in mycobacteria within an animal host using modified *Streptomyces tcp830* regulatory elements. Arch Microbiol **186:**459-64.

123. **Hiasa, H., and K. J. Marians.** 1994. Topoisomerase III, but not topoisomerase I, can support nascent chain elongation during theta-type DNA replication. J Biol Chem **269:**32655-9.

124. **Hiasa, H., and K. J. Marians.** 1994. Topoisomerase IV can support oriC DNA replication *in vitro*. J Biol Chem **269:**16371-5.

125. **Homolka, S., S. Niemann, D. G. Russell, and K. H. Rohde.** 2010. Functional genetic diversity among *Mycobacterium tuberculosis* complex clinical isolates: delineation of conserved core and lineage-specific transcriptomes during intracellular survival. PLoS Pathog **6:**e1000988.

126. **Hu, Y., and A. R. Coates.** 2005. Transposon mutagenesis identifies genes which control antimicrobial drug tolerance in stationary-phase *Escherichia coli*. FEMS Microbiol Lett **243:**117-24.

127. **Hurley, J. M., and N. A. Woychik.** 2009. Bacterial toxin HigB associates with ribosomes and mediates translation-dependent mRNA cleavage at A-rich sites. J Biol Chem **284:**18605-13.

128. **Hussain, S., M. Malik, L. Shi, M. L. Gennaro, and K. Drlica.** 2009. In vitro model of mycobacterial growth arrest using nitric oxide with limited air. Antimicrob Agents Chemother **53:**157-61.

129. **Ioerger, T. R., S. Koo, E. G. No, X. Chen, M. H. Larsen, W. R. Jacobs, Jr., M. Pillay, A. W. Sturm, and J. C. Sacchettini.** 2009. Genome analysis of multi- and extensively-drug-resistant tuberculosis from KwaZulu-Natal, South Africa. PLoS One **4:**e7778.

130. **Jensen, R. B., and K. Gerdes.** 1995. Programmed cell death in bacteria: proteic plasmid stabilization systems. Mol Microbiol **17:**205-10.

131. **Jiang, Y., J. Pogliano, D. R. Helinski, and I. Konieczny.** 2002. ParE toxin encoded by the broad-host-range plasmid RK2 is an inhibitor of *Escherichia coli* gyrase. Mol Microbiol **44:**971-9.

132. **Joers, A., N. Kaldalu, and T. Tenson.** 2010. The frequency of persisters in *Escherichia coli* reflects the kinetics of wake-up from dormancy. J Bacteriol.

133. **Johnson, R., R. M. Warren, G. D. van der Spuy, N. C. Gey van Pittius, D. Theron, E. M. Streicher, M. Bosman, G. J. Coetzee, P. D. van Helden, and T. C. Victor.** 2010. Drug-resistant tuberculosis epidemic in the Western Cape driven by a virulent Beijing genotype strain. Int J Tuberc Lung Dis **14:**119-21.

134. **Jorgensen, M. G., D. P. Pandey, M. Jaskolska, and K. Gerdes.** 2009. HicA of *Escherichia coli* defines a novel family of translation-independent mRNA interferases in bacteria and archaea. J Bacteriol **191:**1191-9.

135. **Kana, B. D., G. L. Abrahams, N. Sung, D. F. Warner, B. G. Gordhan, E. E. Machowski, L. Tsenova, J. C. Sacchettini, N. G. Stoker, G. Kaplan, and V. Mizrahi.** 2010. Role of the DinB homologs Rv1537 and Rv3056 in *Mycobacterium tuberculosis*. J Bacteriol **192:**2220-7.

136. **Kana, B. D., B. G. Gordhan, K. J. Downing, N. Sung, G. Vostroktunova, E. E. Machowski, L. Tsenova, M. Young, A. Kaprelyants, G. Kaplan, and**

V. Mizrahi. 2008. The resuscitation-promoting factors of *Mycobacterium tuberculosis* are required for virulence and resuscitation from dormancy but are collectively dispensable for growth in vitro. Mol Microbiol **67:**672-84.

137. **Kana, B. D., E. A. Weinstein, D. Avarbock, S. S. Dawes, H. Rubin, and V. Mizrahi.** 2001. Characterization of the cydAB-encoded cytochrome bd oxidase from *Mycobacterium smegmatis*. J Bacteriol **183:**7076-86.

138. **Kasari, V., K. Kurg, T. Margus, T. Tenson, and N. Kaldalu.** 2010. The *Escherichia coli mqsR* and *ygiT* genes encode a new toxin-antitoxin pair. J Bacteriol **192:**2908-19.

139. **Kawano, H., Y. Hirokawa, and H. Mori.** 2009. Long-term survival of *Escherichia coli* lacking the *hipBA* toxin-antitoxin system during prolonged cultivation. Biosci Biotechnol Biochem **73:**117-23.

140. **Kawano, M., L. Aravind, and G. Storz.** 2007. An antisense RNA controls synthesis of an SOS-induced toxin evolved from an antitoxin. Mol Microbiol **64:**738-54.

141. **Kawano, M., T. Oshima, H. Kasai, and H. Mori.** 2002. Molecular characterization of long direct repeat (LDR) sequences expressing a stable mRNA encoding for a 35-amino-acid cell-killing peptide and a cis-encoded small antisense RNA in *Escherichia coli*. Mol Microbiol **45:**333-49.

142. **Keren, I., D. Shah, A. Spoering, N. Kaldalu, and K. Lewis.** 2004. Specialized persister cells and the mechanism of multidrug tolerance in *Escherichia coli*. J Bacteriol **186:**8172-80.

143. **Kim, Y., X. Wang, Q. Ma, X. S. Zhang, and T. K. Wood.** 2009. Toxin-antitoxin systems in *Escherichia coli* influence biofilm formation through YjgK (TabA) and fimbriae. J Bacteriol **191:**1258-67.

144. **Kim, Y., X. Wang, X. S. Zhang, S. Grigoriu, R. Page, W. Peti, and T. K. Wood.** 2010. *Escherichia coli* toxin/antitoxin pair MqsR/MqsA regulate toxin CspD. Environ Microbiol **12:**1105-21.

145. **Kim, Y., and T. K. Wood.** 2009. Toxins Hha and CspD and small RNA regulator Hfq are involved in persister cell formation through MqsR in *Escherichia coli*. Biochem Biophys Res Commun **391:**209-13.

146. **Klotzsche, M., S. Ehrt, and D. Schnappinger.** 2009. Improved tetracycline repressors for gene silencing in mycobacteria. Nucleic Acids Res **37:**1778-88.

147. **Kolodkin-Gal, I., and H. Engelberg-Kulka.** 2008. The extracellular death factor: physiological and genetic factors influencing its production and response in *Escherichia coli*. J Bacteriol **190:**3169-75.

148. **Kolodkin-Gal, I., and H. Engelberg-Kulka.** 2006. Induction of *Escherichia coli* chromosomal *mazEF* by stressful conditions causes an irreversible loss of viability. J Bacteriol **188:**3420-3.

149. **Kolodkin-Gal, I., and H. Engelberg-Kulka.** 2009. The stationary-phase sigma factor sigma(S) is responsible for the resistance of *Escherichia coli* stationary-phase cells to *mazEF*-mediated cell death. J Bacteriol **191:**3177-82.

150. **Kolodkin-Gal, I., R. Hazan, A. Gaathon, S. Carmeli, and H. Engelberg-Kulka.** 2007. A linear pentapeptide is a quorum-sensing factor required for *mazEF*-mediated cell death in *Escherichia coli*. Science **318:**652-5.

151. **Kolodkin-Gal, I., R. Verdiger, A. Shlosberg-Fedida, and H. Engelberg-Kulka.** 2009. A differential effect of *E. coli* toxin-antitoxin systems on cell death in liquid media and biofilm formation. PLoS One **4:**e6785.

152. **Korch, S. B., H. Contreras, and J. E. Clark-Curtiss.** 2009. Three *Mycobacterium tuberculosis* Rel toxin-antitoxin modules inhibit mycobacterial growth and are expressed in infected human macrophages. J Bacteriol **191:**1618-30.

153. **Korch, S. B., H. Contreras, and J. E. Clark-Curtiss.** 2008. Three *Mycobacterium tuberculosis* Rel toxin:antitoxin modules inhibit mycobacterial growth and are expressed in human-infected macrophages. J Bacteriol.

154. **Korch, S. B., T. A. Henderson, and T. M. Hill.** 2003. Characterization of the *hipA7* allele of *Escherichia coli* and evidence that high persistence is governed by (p)ppGpp synthesis. Mol Microbiol **50:**1199-213.

155. **Korch, S. B., and T. M. Hill.** 2006. Ectopic overexpression of wild-type and mutant *hipA* genes in *Escherichia coli*: effects on macromolecular synthesis and persister formation. J Bacteriol **188:**3826-36.

156. **Kruh, N. A., J. Troudt, A. Izzo, J. Prenni, and K. M. Dobos.** 2010. Portrait of a pathogen: The *Mycobacterium tuberculosis* proteome in vivo. PLoS One **5:**e13938.

157. **Kussell, E., R. Kishony, N. Q. Balaban, and S. Leibler.** 2005. Bacterial persistence: a model of survival in changing environments. Genetics **169:**1807-14.

158. **Labes, M., A. Puhler, and R. Simon.** 1990. A new family of RSF1010-derived expression and lac-fusion broad-host-range vectors for gram-negative bacteria. Gene **89:**37-46.

159. **Lamichhane, G., M. Zignol, N. J. Blades, D. E. Geiman, A. Dougherty, J. Grosset, K. W. Broman, and W. R. Bishai.** 2003. A postgenomic method for predicting essential genes at subsaturation levels of mutagenesis: application to *Mycobacterium tuberculosis*. Proc Natl Acad Sci USA **100:**7213-8.

160. **Larsen, M. H.** 2000. Appendix 1, p. 313-320. *In* G. F. Hatful and J. W. R. Jacobs (ed.), Molecular genetics of mycobacteria. ASM Press, Washington, D.C.

161. **Lehnherr, H., and M. B. Yarmolinsky.** 1995. Addiction protein Phd of plasmid prophage P1 is a substrate of the ClpXP serine protease of Escherichia coli. Proc Natl Acad Sci U S A **92:**3274-7.

162. **Lenaerts, A. J., V. Gruppo, K. S. Marietta, C. M. Johnson, D. K. Driscoll, N. M. Tompkins, J. D. Rose, R. C. Reynolds, and I. M. Orme.** 2005. Preclinical testing of the nitroimidazopyran PA-824 for activity against *Mycobacterium tuberculosis* in a series of *in vitro* and *in vivo* models. Antimicrob Agents Chemother **49:**2294-301.

163. **Lenaerts, A. J., D. Hoff, S. Aly, S. Ehlers, K. Andries, L. Cantarero, I. M. Orme, and R. J. Basaraba.** 2007. Location of persisting mycobacteria in a guinea pig model of tuberculosis revealed by r207910. Antimicrob Agents Chemother **51:**3338-45.

164. **Levin, B. R., and D. E. Rozen.** 2006. Non-inherited antibiotic resistance. Nat Rev Microbiol **4:**556-62.

165. **Lewis, K.** 2010. Persister Cells. Annual Review Microbiology **64:**357-372.

166. **Lewis, K.** 2007. Persister cells, dormancy and infectious disease. Nat Rev Microbiol **5:**48-56.

167. **Li, G. Y., Y. Zhang, M. Inouye, and M. Ikura.** 2009. Inhibitory mechanism of *Escherichia coli* RelE-RelB toxin-antitoxin module involves a helix

displacement near an mRNA interferase active site. J Biol Chem **284:**14628-36.

168. **Li, Y., and Y. Zhang.** 2007. PhoU is a persistence switch involved in persister formation and tolerance to multiple antibiotics and stresses in *Escherichia coli*. Antimicrob Agents Chemother **51:**2092-9.

169. **Liu, M., Y. Zhang, M. Inouye, and N. A. Woychik.** 2008. Bacterial addiction module toxin Doc inhibits translation elongation through its association with the 30S ribosomal subunit. Proc Natl Acad Sci USA **105:**5885-90.

170. **Lu, T., and K. Drlica.** 2003. In vitro activity of C-8-methoxy fluoroquinolones against mycobacteria when combined with anti-tuberculosis agents. J Antimicrob Chemother **52:**1025-8.

171. **Ma, Z., C. Lienhardt, H. McIlleron, A. J. Nunn, and X. Wang.** 2010. Global tuberculosis drug development pipeline: the need and the reality. Lancet **375:**2100-9.

172. **Mahenthiralingam, E., P. Draper, E. O. Davis, and M. J. Colston.** 1993. Cloning and sequencing of the gene which encodes the highly inducible acetamidase of Mycobacterium smegmatis. J Gen Microbiol **139:**575-83.

173. **Makarova, K. S., N. V. Grishin, and E. V. Koonin.** 2006. The HicAB cassette, a putative novel, RNA-targeting toxin-antitoxin system in archaea and bacteria. Bioinformatics **22:**2581-4.

174. **Makarova, K. S., Y. I. Wolf, and E. V. Koonin.** 2009. Comprehensive comparative-genomic analysis of type 2 toxin-antitoxin systems and related mobile stress response systems in prokaryotes. Biol Direct **4:**19.

175. **Makrides, S. C.** 1996. Strategies for achieving high-level expression of genes in *Escherichia coli*. Microbiol Rev **60:**512-38.

176. **Malik, M., and K. Drlica.** 2006. Moxifloxacin lethality against *Mycobacterium tuberculosis* in the presence and absence of chloramphenicol. Antimicrob Agents Chemother **50:**2842-4.

177. **Manabe, Y. C., J. M. Chen, C. G. Ko, P. Chen, and W. R. Bishai.** 1999. Conditional sigma factor expression, using the inducible acetamidase promoter, reveals that the *Mycobacterium tuberculosis sigF* gene modulates expression of the 16-kilodalton alpha-crystallin homologue. J Bacteriol **181:**7629-33.

178. **Manganelli, R., M. I. Voskuil, G. K. Schoolnik, E. Dubnau, M. Gomez, and I. Smith.** 2002. Role of the extracytoplasmic-function sigma factor sigma(H) in Mycobacterium tuberculosis global gene expression. Mol Microbiol **45:**365-74.

179. **Manganelli, R., M. I. Voskuil, G. K. Schoolnik, and I. Smith.** 2001. The *Mycobacterium tuberculosis* ECF sigma factor sigmaE: role in global gene expression and survival in macrophages. Mol Microbiol **41:**423-37.

180. **Mariam, D. H., Y. Mengistu, S. E. Hoffner, and D. I. Andersson.** 2004. Effect of *rpoB* mutations conferring rifampin resistance on fitness of *Mycobacterium tuberculosis*. Antimicrob Agents Chemother **48:**1289-94.

181. **Markossian, K. A., I. K. Yudin, and B. I. Kurganov.** 2009. Mechanism of suppression of protein aggregation by alpha-crystallin. Int J Mol Sci **10:**1314-45.

182. **Martinez, A., S. Torello, and R. Kolter.** 1999. Sliding motility in mycobacteria. J Bacteriol **181:**7331-8.

183.   **McKinley, J. E., and R. D. Magnuson.** 2005. Characterization of the Phd repressor-antitoxin boundary. J Bacteriol **187:**765-70.

184.   **McKinney, J. D., K. Honer zu Bentrup, E. J. Munoz-Elias, A. Miczak, B. Chen, W. T. Chan, D. Swenson, J. C. Sacchettini, W. R. Jacobs, Jr., and D. G. Russell.** 2000. Persistence of *Mycobacterium tuberculosis* in macrophages and mice requires the glyoxylate shunt enzyme isocitrate lyase. Nature **406:**735-8.

185.   **Meintjes, G., S. D. Lawn, F. Scano, G. Maartens, M. A. French, W. Worodria, J. H. Elliott, D. Murdoch, R. J. Wilkinson, C. Seyler, L. John, M. S. van der Loeff, P. Reiss, L. Lynen, E. N. Janoff, C. Gilks, and R. Colebunders.** 2008. Tuberculosis-associated immune reconstitution inflammatory syndrome: case definitions for use in resource-limited settings. Lancet Infect Dis **8:**516-23.

186.   **Miallau, L., M. Faller, J. Chiang, M. Arbing, F. Guo, D. Cascio, and D. Eisenberg.** 2009. Structure and proposed activity of a member of the VapBC family of toxin-antitoxin systems. VapBC-5 from *Mycobacterium tuberculosis*. J Biol Chem **284:**276-83.

187.   **Miller, C., L. E. Thomsen, C. Gaggero, R. Mosseri, H. Ingmer, and S. N. Cohen.** 2004. SOS response induction by beta-lactams and bacterial defense against antibiotic lethality. Science **305:**1629-31.

188.   **Mizrahi, V., and S. J. Andersen.** 1998. DNA repair in *Mycobacterium tuberculosis*. What have we learnt from the genome sequence? Mol Microbiol **29:**1331-9.

189.   **Mizrahi, V., S. S. Dawes, and H. Rubin.** 2000. DNA replication, p. 159-172. *In* G. F. Hatful and J. W. R. Jacobs (ed.), Molecular Genetics of Mycobacteria. ASM Press, Washington.

190.   **Motiejunaite, R., J. Armalyte, A. Markuckas, and E. Suziedeliene.** 2007. *Escherichia coli dinJ-yafQ* genes act as a toxin-antitoxin module. FEMS Microbiol Lett **268:**112-9.

191.   **Motiwala, A. S., Y. Dai, E. C. Jones-Lopez, S. H. Hwang, J. S. Lee, S. N. Cho, L. E. Via, C. E. Barry, and D. Alland.** 2010. Mutations in extensively drug-resistant *Mycobacterium tuberculosis* that do not code for known drug-resistance mechanisms. J Infect Dis **201:**881-8.

192.   **Mowa, M. B., D. F. Warner, G. Kaplan, B. D. Kana, and V. Mizrahi.** 2009. Function and regulation of class I ribonucleotide reductase-encoding genes in mycobacteria. J Bacteriol **191:**985-95.

193.   **Moyed, H. S., and K. P. Bertrand.** 1983. *hipA*, a newly recognized gene of *Escherichia coli* K-12 that affects frequency of persistence after inhibition of murein synthesis. J Bacteriol **155:**768-75.

194.   **Moyed, H. S., and S. H. Broderick.** 1986. Molecular cloning and expression of *hipA*, a gene of *Escherichia coli* K-12 that affects frequency of persistence after inhibition of murein synthesis. J Bacteriol **166:**399-403.

195.   **Munoz-Elias, E. J., and J. D. McKinney.** 2005. *Mycobacterium tuberculosis* isocitrate lyases 1 and 2 are jointly required for in vivo growth and virulence. Nat Med **11:**638-44.

196.   **Munoz-Gomez, A. J., S. Santos-Sierra, A. Berzal-Herranz, M. Lemonnier, and R. Diaz-Orejas.** 2004. Insights into the specificity of RNA cleavage by the *Escherichia coli* MazF toxin. FEBS Lett **567:**316-20.

197. **Murakami, K., T. Ono, D. Viducic, S. Kayama, M. Mori, K. Hirota, K. Nemoto, and Y. Miyake.** 2005. Role for rpoS gene of *Pseudomonas aeruginosa* in antibiotic tolerance. FEMS Microbiol Lett **242:**161-7.

198. **Murry, J. P., and E. J. Rubin.** 2005. New genetic approaches shed light on TB virulence. Trends Microbiol **13:**366-72.

199. **Muttucumaru, D. G., G. Roberts, J. Hinds, R. A. Stabler, and T. Parish.** 2004. Gene expression profile of *Mycobacterium tuberculosis* in a non-replicating state. Tuberculosis (Edinb) **84:**239-46.

200. **Newton, S. M., R. J. Smith, K. A. Wilkinson, M. P. Nicol, N. J. Garton, K. J. Staples, G. R. Stewart, J. R. Wain, A. R. Martineau, S. Fandrich, T. Smallie, B. Foxwell, A. Al-Obaidi, J. Shafi, K. Rajakumar, B. Kampmann, P. W. Andrew, L. Ziegler-Heitbrock, M. R. Barer, and R. J. Wilkinson.** 2006. A deletion defining a common Asian lineage of *Mycobacterium tuberculosis* associates with immune subversion. Proc Natl Acad Sci USA **103:**15594-8.

201. **Nieto, C., I. Cherny, S. K. Khoo, M. G. de Lacoba, W. T. Chan, C. C. Yeo, E. Gazit, and M. Espinosa.** 2007. The *yefM-yoeB* toxin-antitoxin systems of *Escherichia coli* and *Streptococcus pneumoniae*: functional and structural correlation. J Bacteriol **189:**1266-78.

202. **Novick, R. P.** 1987. Plasmid incompatibility. Microbiol Rev **51:**381-95.

203. **Nuermberger, E. L., T. Yoshimatsu, S. Tyagi, R. J. O'Brien, A. N. Vernon, R. E. Chaisson, W. R. Bishai, and J. H. Grosset.** 2004. Moxifloxacin-containing regimen greatly reduces time to culture conversion in murine tuberculosis. Am J Respir Crit Care Med **169:**421-6.

204. **O'Gaora, P., S. Barnin, C. Hayward, E. Filley, G. Rook, D. Young, and J. Thole.** 1997. Mycobacteria as immunogens: development of expression vectors for use in multiple mycobacterial species. Medical Principles and Practice **6:**91-96.

205. **Ojha, A., M. Anand, A. Bhatt, L. Kremer, W. R. Jacobs, Jr., and G. F. Hatfull.** 2005. GroEL1: a dedicated chaperone involved in mycolic acid biosynthesis during biofilm formation in mycobacteria. Cell **123:**861-73.

206. **Ojha, A. K., A. D. Baughn, D. Sambandan, T. Hsu, X. Trivelli, Y. Guerardel, A. Alahari, L. Kremer, W. R. Jacobs, Jr., and G. F. Hatfull.** 2008. Growth of *Mycobacterium tuberculosis* biofilms containing free mycolic acids and harbouring drug-tolerant bacteria. Mol Microbiol **69:**164-74.

207. **Ojha, A. K., X. Trivelli, Y. Guerardel, L. Kremer, and G. F. Hatfull.** 2010. Enzymatic hydrolysis of trehalose dimycolate releases free mycolic acids during mycobacterial growth in biofilms. J Biol Chem **285:**17380-9.

208. **Overgaard, M., J. Borch, and K. Gerdes.** 2009. RelB and RelE of *Escherichia coli* form a tight complex that represses transcription via the ribbon-helix-helix motif in RelB. J Mol Biol **394:**183-96.

209. **Overgaard, M., J. Borch, M. G. Jorgensen, and K. Gerdes.** 2008. Messenger RNA interferase RelE controls relBE transcription by conditional cooperativity. Mol Microbiol **69:**841-57.

210. **Pandey, A. K., S. Raman, R. Proff, S. Joshi, C. M. Kang, E. J. Rubin, R. N. Husson, and C. M. Sassetti.** 2009. Nitrile-inducible gene expression in mycobacteria. Tuberculosis (Edinb) **89:**12-6.

211. **Pandey, D. P., and K. Gerdes.** 2005. Toxin-antitoxin loci are highly abundant in free-living but lost from host-associated prokaryotes. Nucleic Acids Res **33:**966-76.

212. **Paramasivan, C. N., S. Sulochana, G. Kubendiran, P. Venkatesan, and D. A. Mitchison.** 2005. Bactericidal action of gatifloxacin, rifampin, and isoniazid on logarithmic- and stationary-phase cultures of *Mycobacterium tuberculosis*. Antimicrob Agents Chemother **49:**627-31.

213. **Parish, T., E. Mahenthiralingam, P. Draper, E. O. Davis, and M. J. Colston.** 1997. Regulation of the inducible acetamidase gene of *Mycobacterium smegmatis*. Microbiology **143 (Pt 7):**2267-76.

214. **Parish, T., and N. G. Stoker.** 1997. Development and use of a conditional antisense mutagenesis system in mycobacteria. FEMS Microbiol Lett **154:**151-7.

215. **Parish, T., and N. G. Stoker.** 2000. Use of a flexible cassette method to generate a double unmarked *Mycobacterium tuberculosis tlyA plcABC* mutant by gene replacement. Microbiology **146 (Pt 8):**1969-75.

216. **Parish, T., J. Turner, and N. G. Stoker.** 2001. amiA is a negative regulator of acetamidase expression in Mycobacterium smegmatis. BMC Microbiol **1:**19.

217. **Park, H. D., K. M. Guinn, M. I. Harrell, R. Liao, M. I. Voskuil, M. Tompa, G. K. Schoolnik, and D. R. Sherman.** 2003. Rv3133c/dosR is a transcription factor that mediates the hypoxic response of *Mycobacterium tuberculosis*. Mol Microbiol **48:**833-43.

218. **Parrish, N. M., J. D. Dick, and W. R. Bishai.** 1998. Mechanisms of latency in *Mycobacterium tuberculosis*. Trends Microbiol **6:**107-12.

219. **Patel, S., and K. E. Weaver.** 2006. Addiction toxin Fst has unique effects on chromosome segregation and cell division in *Enterococcus faecalis* and *Bacillus subtilis*. J Bacteriol **188:**5374-84.

220. **Pedersen, K., S. K. Christensen, and K. Gerdes.** 2002. Rapid induction and reversal of a bacteriostatic condition by controlled expression of toxins and antitoxins. Mol Microbiol **45:**501-10.

221. **Pedersen, K., A. V. Zavialov, M. Y. Pavlov, J. Elf, K. Gerdes, and M. Ehrenberg.** 2003. The bacterial toxin RelE displays codon-specific cleavage of mRNAs in the ribosomal A site. Cell **112:**131-40.

222. **Pei, J., B. H. Kim, and N. V. Grishin.** 2008. PROMALS3D: a tool for multiple protein sequence and structure alignments. Nucleic Acids Res **36:**2295-300.

223. **Pham, T. T., D. Jacobs-Sera, M. L. Pedulla, R. W. Hendrix, and G. F. Hatfull.** 2007. Comparative genomic analysis of mycobacteriophage Tweety: evolutionary insights and construction of compatible site-specific integration vectors for mycobacteria. Microbiology **153:**2711-23.

224. **Picard, F., C. Dressaire, L. Girbal, and M. Cocaign-Bousquet.** 2009. Examination of post-transcriptional regulations in prokaryotes by integrative biology. C R Biol **332:**958-73.

225. **Pillay, M., and A. W. Sturm.** 2007. Evolution of the extensively drug-resistant F15/LAM4/KZN strain of *Mycobacterium tuberculosis* in KwaZulu-Natal, South Africa. Clin Infect Dis **45:**1409-14.

226. **Primm, T. P., S. J. Andersen, V. Mizrahi, D. Avarbock, H. Rubin, and C. E. Barry, 3rd.** 2000. The stringent response of *Mycobacterium tuberculosis* is required for long-term survival. J Bacteriol **182:**4889-98.

227. **Provvedi, R., F. Boldrin, F. Falciani, G. Palu, and R. Manganelli.** 2009. Global transcriptional response to vancomycin in *Mycobacterium tuberculosis*. *Microbiology* **155:**1093-102.

228. **Prysak, M. H., C. J. Mozdzierz, A. M. Cook, L. Zhu, Y. Zhang, M. Inouye, and N. A. Woychik.** 2009. Bacterial toxin YafQ is an endoribonuclease that associates with the ribosome and blocks translation elongation through sequence-specific and frame-dependent mRNA cleavage. Mol Microbiol **71:**1071-87.

229. **Quan, S., H. Venter, and E. R. Dabbs.** 1997. Ribosylative inactivation of rifampin by *Mycobacterium smegmatis* is a principal contributor to its low susceptibility to this antibiotic. Antimicrob Agents Chemother **41:**2456-60.

230. **Ramage, H. R., L. E. Connolly, and J. S. Cox.** 2009. Comprehensive functional analysis of *Mycobacterium tuberculosis* toxin-antitoxin systems: implications for pathogenesis, stress responses, and evolution. PLoS Genet **5:**e1000767.

231. **Ramaswamy, S., and J. M. Musser.** 1998. Molecular genetic basis of antimicrobial agent resistance in *Mycobacterium tuberculosis*: 1998 update. Tuber Lung Dis **79:**3-29.

232. **Recht, J., A. Martinez, S. Torello, and R. Kolter.** 2000. Genetic analysis of sliding motility in *Mycobacterium smegmatis*. J Bacteriol **182:**4348-51.

233. **Revel, V., E. Cambau, V. Jarlier, and W. Sougakoff.** 1994. Characterization of mutations in *Mycobacterium smegmatis* involved in resistance to fluoroquinolones. Antimicrob Agents Chemother **38:**1991-6.

234. **Reyrat, J. M., and D. Kahn.** 2001. *Mycobacterium smegmatis*: an absurd model for tuberculosis? Trends Microbiol **9:**472-4.

235. **Rifat, D., W. R. Bishai, and P. C. Karakousis.** 2009. Phosphate depletion: a novel trigger for *Mycobacterium tuberculosis* persistence. J Infect Dis **200:**1126-35.

236. **Roberts, G., D. G. Muttucumaru, and T. Parish.** 2003. Control of the acetamidase gene of *Mycobacterium smegmatis* by multiple regulators. FEMS Microbiol Lett **221:**131-6.

237. **Robson, J., J. L. McKenzie, R. Cursons, G. M. Cook, and V. L. Arcus.** 2009. The *vapBC* operon from *Mycobacterium smegmatis* is an autoregulated toxin-antitoxin module that controls growth via inhibition of translation. J Mol Biol **390:**353-67.

238. **Rodriguez, G. M., M. I. Voskuil, B. Gold, G. K. Schoolnik, and I. Smith.** 2002. *ideR*, An essential gene in *Mycobacterium tuberculosis*: role of IdeR in iron-dependent gene expression, iron metabolism, and oxidative stress response. Infect Immun **70:**3371-81.

239. **Rotem, E., A. Loinger, I. Ronin, I. Levin-Reisman, C. Gabay, N. Shoresh, O. Biham, and N. Q. Balaban.** 2010. Regulation of phenotypic variability by a threshold-based mechanism underlies bacterial persistence. Proc Natl Acad Sci USA **107:**12541-6.

240. **Russell, D. G., C. E. Barry, 3rd, and J. L. Flynn.** 2010. Tuberculosis: what we don't know can, and does, hurt us. Science **328:**852-6.

241. **Russell, D. G., B. C. VanderVen, W. Lee, R. B. Abramovitch, M. J. Kim, S. Homolka, S. Niemann, and K. H. Rohde.** 2010. *Mycobacterium tuberculosis* wears what it eats. Cell Host Microbe **8:**68-76.

242. **Sacchettini, J. C., E. J. Rubin, and J. S. Freundlich.** 2008. Drugs versus bugs: in pursuit of the persistent predator *Mycobacterium tuberculosis*. Nat Rev Microbiol **6:**41-52.

243. **Sala, C., N. Dhar, R. C. Hartkoorn, M. Zhang, Y. H. Ha, P. Schneider, and S. T. Cole.** 2010. A simple model for testing drugs against non-replicating *Mycobacterium tuberculosis*. Antimicrob Agents Chemother.

244. **Salomon, J. A., J. O. Lloyd-Smith, W. M. Getz, S. Resch, M. S. Sanchez, T. C. Porco, and M. W. Borgdorff.** 2006. Prospects for advancing tuberculosis control efforts through novel therapies. PLoS Med **3:**e273.

245. **Sambrook, J., E. F. Fritsch, and T. Maniatis.** 1989. Molecular Cloning. A laboratory manual. Second Edition. Cold Spring Harbour Laboratory Press, Cold Spring Harbour, New York.

246. **Sambrook, J., and D. W. Russell.** 2001. Molecular Cloning. A laboratory manual. Third Edition. Cold Spring Harbour Laboratory Press, Cold Spring Harbour, New York.

247. **Sassetti, C. M., D. H. Boyd, and E. J. Rubin.** 2003. Genes required for mycobacterial growth defined by high density mutagenesis. Mol Microbiol **48:**77-84.

248. **Sat, B., R. Hazan, T. Fisher, H. Khaner, G. Glaser, and H. Engelberg-Kulka.** 2001. Programmed cell death in *Escherichia coli*: some antibiotics can trigger *mazEF* lethality. J Bacteriol **183:**2041-5.

249. **Sat, B., M. Reches, and H. Engelberg-Kulka.** 2003. The *Escherichia coli mazEF* suicide module mediates thymineless death. J Bacteriol **185:**1803-7.

250. **Schein, C. H.** 1991. Optimizing protein folding to the native state in bacteria. Curr Opin Biotechnol **2:**746-50.

251. **Scherrer, R., and H. S. Moyed.** 1988. Conditional impairment of cell division and altered lethality in *hipA* mutants of *Escherichia coli* K-12. J Bacteriol **170:**3321-6.

252. **Schnappinger, D., S. Ehrt, M. I. Voskuil, Y. Liu, J. A. Mangan, I. M. Monahan, G. Dolganov, B. Efron, P. D. Butcher, C. Nathan, and G. K. Schoolnik.** 2003. Transcriptional adaptation of *Mycobacterium tuberculosis* within macrophages: Insights into the phagosomal environment. J Exp Med **198:**693-704.

253. **Schumacher, M. A., K. M. Piro, W. Xu, S. Hansen, K. Lewis, and R. G. Brennan.** 2009. Molecular mechanisms of HipA-mediated multidrug tolerance and its neutralization by HipB. Science **323:**396-401.

254. **Shah, D., Z. Zhang, A. Khodursky, N. Kaldalu, K. Kurg, and K. Lewis.** 2006. Persisters: a distinct physiological state of *E. coli*. BMC Microbiol **6:**53.

255. **Shelburne, S. A., 3rd, and R. J. Hamill.** 2003. The immune reconstitution inflammatory syndrome. AIDS Rev **5:**67-79.

256. **Sherman, D. R., M. Voskuil, D. Schnappinger, R. Liao, M. I. Harrell, and G. K. Schoolnik.** 2001. Regulation of the *Mycobacterium tuberculosis* hypoxic response gene encoding alpha -crystallin. Proc Natl Acad Sci USA **98:**7534-9.

257. **Shi, L., C. D. Sohaskey, B. D. Kana, S. Dawes, R. J. North, V. Mizrahi, and M. L. Gennaro.** 2005. Changes in energy metabolism of *Mycobacterium*

tuberculosis in mouse lung and under in vitro conditions affecting aerobic respiration. Proc Natl Acad Sci USA **102:**15629-34.

258. **Shi, W., and Y. Zhang.** 2010. PhoY2 but not PhoY1 is the PhoU homologue involved in persisters in *Mycobacterium tuberculosis*. J Antimicrob Chemother.

259. **Shiloh, M. U., and P. A. DiGiuseppe Champion.** 2010. To catch a killer. What can mycobacterial models teach us about *Mycobacterium tuberculosis* pathogenesis? Curr Opin Microbiol **13:**86-92.

260. **Silvaggi, J. M., J. B. Perkins, and R. Losick.** 2005. Small untranslated RNA antitoxin in *Bacillus subtilis*. J Bacteriol **187:**6641-50.

261. **Singh, R., C. E. Barry, 3rd, and H. I. Boshoff.** 2010. The three RelE homologs of *Mycobacterium tuberculosis* have individual, drug-specific effects on bacterial antibiotic tolerance. J Bacteriol **192:**1279-91.

262. **Smith, A. M., and K. P. Klugman.** 1997. "Megaprimer" method of PCR-based mutagenesis: the concentration of megaprimer is a critical factor. Biotechniques **22:**438, 442.

263. **Smith, J. A., and R. D. Magnuson.** 2004. Modular organization of the Phd repressor/antitoxin protein. J Bacteriol **186:**2692-8.

264. **Smollett, K. L., A. S. Fivian-Hughes, J. E. Smith, A. Chang, T. Rao, and E. O. Davis.** 2009. Experimental determination of translational start sites resolves uncertainties in genomic open reading frame predictions - application to *Mycobacterium tuberculosis*. Microbiology **155:**186-97.

265. **Snapper, S. B., R. E. Melton, S. Mustafa, T. Kieser, and W. R. Jacobs, Jr.** 1990. Isolation and characterization of efficient plasmid transformation mutants of *Mycobacterium smegmatis*. Mol Microbiol **4:**1911-9.

266. **Spoering, A. L., M. Vulic, and K. Lewis.** 2006. GlpD and PlsB participate in persister cell formation in *Escherichia coli*. J Bacteriol **188:**5136-44.

267. **Stallings, C. L., and M. S. Glickman.** 2010. Is *Mycobacterium tuberculosis* stressed out? A critical assessment of the genetic evidence. Microbes Infect.

268. **Stewart, G. R., J. Patel, B. D. Robertson, A. Rae, and D. B. Young.** 2005. Mycobacterial mutants with defective control of phagosomal acidification. PLoS Pathog **1:**269-78.

269. **Stewart, G. R., B. D. Robertson, and D. B. Young.** 2003. Tuberculosis: a problem with persistence. Nat Rev Microbiol **1:**97-105.

270. **Stewart, G. R., L. Wernisch, R. Stabler, J. A. Mangan, J. Hinds, K. G. Laing, D. B. Young, and P. D. Butcher.** 2002. Dissection of the heat-shock response in *Mycobacterium tuberculosis* using mutants and microarrays. Microbiology **148:**3129-38.

271. **Systems, T. D.** SENSITITRE (R) Broth microdilution method: For rapidly growing mycobacteria (RGM), slowly growing nontuberculosis mycobacteria, norcadia and other aerobic actinomycetes.

272. **Szekeres, S., M. Dauti, C. Wilde, D. Mazel, and D. A. Rowe-Magnus.** 2007. Chromosomal toxin-antitoxin loci can diminish large-scale genome reductions in the absence of selection. Mol Microbiol **63:**1588-605.

273. **Talaat, A. M., R. Lyons, S. T. Howard, and S. A. Johnston.** 2004. The temporal expression profile of *Mycobacterium tuberculosis* infection in mice. Proc Natl Acad Sci USA **101:**4602-7.

274. **Tischler, A. D., and J. D. McKinney.** 2009. Contrasting persistence strategies in *Salmonella* and *Mycobacterium*. Curr Opin Microbiol **13:**93-9.

275. **Triccas, J. A., T. Parish, W. J. Britton, and B. Gicquel.** 1998. An inducible expression system permitting the efficient purification of a recombinant antigen from *Mycobacterium smegmatis*. FEMS Microbiol Lett **167:**151-6.

276. **Tsilibaris, V., G. Maenhaut-Michel, N. Mine, and L. Van Melderen.** 2007. What is the benefit to *Escherichia coli* of having multiple toxin-antitoxin systems in its genome? J Bacteriol **189:**6101-8.

277. **Tyagi, J. S., and D. Sharma.** 2002. *Mycobacterium smegmatis* and tuberculosis. Trends Microbiol **10:**68-9.

278. **Tyagi, S., E. Nuermberger, T. Yoshimatsu, K. Williams, I. Rosenthal, N. Lounis, W. Bishai, and J. Grosset.** 2005. Bactericidal activity of the nitroimidazopyran PA-824 in a murine model of tuberculosis. Antimicrob Agents Chemother **49:**2289-93.

279. **UNAIDS, and WHO.** 2009. AIDS Epidemic Update.

280. **Unoson, C., and E. G. Wagner.** 2008. A small SOS-induced toxin is targeted against the inner membrane in *Escherichia coli*. Mol Microbiol **70:**258-70.

281. **van de Guchte, M., T. van der Lende, J. Kok, and G. Venema.** 1991. A possible contribution of mRNA secondary structure to translation initiation efficiency in *Lactococcus lactis*. FEMS Microbiol Lett **65:**201-8.

282. **Van Melderen, L., and M. Saavedra De Bast.** 2009. Bacterial toxin-antitoxin systems: more than selfish entities? PLoS Genet **5:**e1000437.

283. **Van Melderen, L., M. H. Thi, P. Lecchi, S. Gottesman, M. Couturier, and M. R. Maurizi.** 1996. ATP-dependent degradation of CcdA by Lon protease. Effects of secondary structure and heterologous subunit interactions. J Biol Chem **271:**27730-8.

284. **Vandal, O. H., J. A. Roberts, T. Odaira, D. Schnappinger, C. F. Nathan, and S. Ehrt.** 2009. Acid-susceptible mutants of *Mycobacterium tuberculosis* share hypersusceptibility to cell wall and oxidative stress and to the host environment. J Bacteriol **191:**625-31.

285. **Varshavsky, A.** 1996. The N-end rule: functions, mysteries, uses. Proc Natl Acad Sci USA **93:**12142-9.

286. **Vazquez-Laslop, N., H. Lee, and A. A. Neyfakh.** 2006. Increased persistence in *Escherichia coli* caused by controlled expression of toxins or other unrelated proteins. J Bacteriol **188:**3494-7.

287. **Velappan, N., D. Sblattero, L. Chasteen, P. Pavlik, and A. R. Bradbury.** 2007. Plasmid incompatibility: more compatible than previously thought? Protein Eng Des Sel **20:**309-13.

288. **Velayati, A. A., M. R. Masjedi, P. Farnia, P. Tabarsi, J. Ghanavi, A. H. Ziazarifi, and S. E. Hoffner.** 2009. Emergence of new forms of totally drug-resistant tuberculosis bacilli: super extensively drug-resistant tuberculosis or totally drug-resistant strains in iran. Chest **136:**420-5.

289. **Ventura, S.** 2005. Sequence determinants of protein aggregation: tools to increase protein solubility. Microb Cell Fact **4:**11.

290. **Via, L. E., P. L. Lin, S. M. Ray, J. Carrillo, S. S. Allen, S. Y. Eum, K. Taylor, E. Klein, U. Manjunatha, J. Gonzales, E. G. Lee, S. K. Park, J. A. Raleigh, S. N. Cho, D. N. McMurray, J. L. Flynn, and C. E. Barry, 3rd.**

2008. Tuberculous granulomas are hypoxic in guinea pigs, rabbits, and nonhuman primates. Infect Immun **76:**2333-40.

291. **Volkman, H. E., T. C. Pozos, J. Zheng, J. M. Davis, J. F. Rawls, and L. Ramakrishnan.** 2010. Tuberculous granuloma induction via interaction of a bacterial secreted protein with host epithelium. Science **327:**466-9.

292. **Voskuil, M. I., D. Schnappinger, K. C. Visconti, M. I. Harrell, G. M. Dolganov, D. R. Sherman, and G. K. Schoolnik.** 2003. Inhibition of respiration by nitric oxide induces a *Mycobacterium tuberculosis* dormancy program. J Exp Med **198:**705-13.

293. **Waddell, S. J., R. A. Stabler, K. Laing, L. Kremer, R. C. Reynolds, and G. S. Besra.** 2004. The use of microarray analysis to determine the gene expression profiles of *Mycobacterium tuberculosis* in response to anti-bacterial compounds. Tuberculosis (Edinb) **84:**263-74.

294. **Wallace, R. J., Jr., G. Bedsole, G. Sumter, C. V. Sanders, L. C. Steele, B. A. Brown, J. Smith, and D. R. Graham.** 1990. Activities of ciprofloxacin and ofloxacin against rapidly growing mycobacteria with demonstration of acquired resistance following single-drug therapy. Antimicrob Agents Chemother **34:**65-70.

295. **Wallace, R. J., Jr., D. R. Nash, L. C. Steele, and V. Steingrube.** 1986. Susceptibility testing of slowly growing mycobacteria by a microdilution MIC method with 7H9 broth. J Clin Microbiol **24:**976-81.

296. **Walters, S. B., E. Dubnau, I. Kolesnikova, F. Laval, M. Daffe, and I. Smith.** 2006. The *Mycobacterium tuberculosis* PhoPR two-component system regulates genes essential for virulence and complex lipid biosynthesis. Mol Microbiol **60:**312-30.

297. **Warner, D. F., and V. Mizrahi.** 2007. The survival kit of *Mycobacterium tuberculosis*. Nat Med **13:**282-4.

298. **Warner, D. F., and V. Mizrahi.** 2006. Tuberculosis chemotherapy: the influence of bacillary stress and damage response pathways on drug efficacy. Clin Microbiol Rev **19:**558-70.

299. **Wayne, L. G., and C. D. Sohaskey.** 2001. Nonreplicating persistence of *Mycobacterium tuberculosis*. Annu Rev Microbiol **55:**139-63.

300. **Weaver, K. E., K. D. Walz, and M. S. Heine.** 1998. Isolation of a derivative of *Escherichia coli-Enterococcus faecalis* shuttle vector pAM401 temperature sensitive for maintenance in *E. faecalis* and its use in evaluating the mechanism of pAD1 par-dependent plasmid stabilization. Plasmid **40:**225-32.

301. **Weaver, K. E., D. M. Weaver, C. L. Wells, C. M. Waters, M. E. Gardner, and E. A. Ehli.** 2003. *Enterococcus faecalis* plasmid pAD1-encoded Fst toxin affects membrane permeability and alters cellular responses to lantibiotics. J Bacteriol **185:**2169-77.

302. **WHO.** 2009. Global TB Control Report.

303. **WHO.** 2006. The Stop TB Strategy.

304. **Winther, K. S., and K. Gerdes.** 2009. Ectopic production of VapCs from *Enterobacteria* inhibits translation and *trans*-activates YoeB mRNA interferase. Mol Microbiol **72:**918-30.

305. **Yamaguchi, Y., J. H. Park, and M. Inouye.** 2009. MqsR, a crucial regulator for quorum sensing and biofilm formation, is a GCU-specific mRNA interferase in *Escherichia coli*. J Biol Chem **284:**28746-53.

306. **Yang, J. K., M. S. Park, G. S. Waldo, and S. W. Suh.** 2003. Directed evolution approach to a structural genomics project: Rv2002 from *Mycobacterium tuberculosis*. Proc Natl Acad Sci USA **100:**455-60.

307. **Yang, M., C. Gao, Y. Wang, H. Zhang, and Z. G. He.** 2010. Characterization of the interaction and cross-regulation of three *Mycobacterium tuberculosis* RelBE modules. PLoS One **5:**e10672.

308. **Yoshizumi, S., Y. Zhang, Y. Yamaguchi, L. Chen, B. N. Kreiswirth, and M. Inouye.** 2009. *Staphylococcus aureus* YoeB homologues inhibit translation initiation. J Bacteriol **191:**5868-72.

309. **Zhang, J., Y. Zhang, and M. Inouye.** 2003. Characterization of the interactions within the mazEF addiction module of *Escherichia coli*. J Biol Chem **278:**32300-6.

310. **Zhang, L., F. Fan, L. M. Palmer, M. A. Lonetto, C. Petit, L. L. Voelker, A. St John, B. Bankosky, M. Rosenberg, and D. McDevitt.** 2000. Regulated gene expression in *Staphylococcus aureus* for identifying conditional lethal phenotypes and antibiotic mode of action. Gene **255:**297-305.

311. **Zhang, Y., and M. Inouye.** 2009. The inhibitory mechanism of protein synthesis by YoeB, an *Escherichia coli* toxin. J Biol Chem **284:**6627-38.

312. **Zhang, Y. X., J. Li, X. K. Guo, C. Wu, B. Bi, S. X. Ren, C. F. Wu, and G. P. Zhao.** 2004. Characterization of a novel toxin-antitoxin module, VapBC, encoded by *Leptospira interrogans* chromosome. Cell Res **14:**208-16.

313. **Zhao, B. Y., R. Pine, J. Domagala, and K. Drlica.** 1999. Fluoroquinolone action against clinical isolates of *Mycobacterium tuberculosis*: effects of a C-8 methoxyl group on survival in liquid media and in human macrophages. Antimicrob Agents Chemother **43:**661-6.

314. **Zhu, L., S. Phadtare, H. Nariya, M. Ouyang, R. N. Husson, and M. Inouye.** 2008. The mRNA interferases, MazF-mt3 and MazF-mt7 from *Mycobacterium tuberculosis* target unique pentad sequences in single-stranded RNA. Mol Microbiol **69:**559-69.

315. **Zhu, L., J. D. Sharp, H. Kobayashi, N. A. Woychik, and M. Inouye.** 2010. Noncognate *Mycobacterium tuberculosis* toxin-antitoxins can physically and functionally interact. Journal of Biological Chemistry.

316. **Zhu, L., Y. Zhang, J. S. Teh, J. Zhang, N. Connell, H. Rubin, and M. Inouye.** 2006. Characterization of mRNA interferases from *Mycobacterium tuberculosis*. J Biol Chem **281:**18638-43.